

**Dissertation zur Erlangung des Doktorgrades
der Fakultät für Chemie und Pharmazie
der Ludwig-Maximilians-Universität München**

**Characterization of the Human Adenovirus 19a E3/49K Protein:
A Secreted Lymphocyte Binding Factor with an
Immunomodulatory Function**

**vorgelegt von
Mark Windheim
aus Stadthagen
April 2002**

Erklärung

Diese Dissertation wurde im Sinne von §13 Abs. 3 bzw. 4 der Promotionsordnung vom 29. Januar 1998 von Prof. Dr. Ernst-Ludwig Winnacker betreut.

Ehrenwörtliche Versicherung

Diese Dissertation wurde selbstständig, ohne unerlaubte Hilfe erarbeitet.

München, am 22.04.2002

Mark Windheim

Dissertation eingereicht am

1. Gutachter: Prof. Dr. Ernst-Ludwig Winnacker
2. Gutachter: Prof. Dr. Karl-Klaus Conzelmann

Mündliche Prüfung am 04.06.2002

An dieser Stelle möchte ich mich bei all denen bedanken, ohne die diese Doktorarbeit nicht möglich gewesen wäre.

Mein Dank gilt insbesondere PD Dr. Hans-Gerhard Burgert für die Überlassung des Themas und die Betreuung meiner Doktorarbeit am Max-von-Pettenkofer Institut, Genzentrum der LMU München. Prof. Dr. Ernst-Ludwig Winnacker danke ich dafür, meine Doktorarbeit gegenüber der Fakultät für Chemie und Pharmazie zu vertreten. Prof. Dr. Karl-Klaus Conzelmann danke ich für die Bereitschaft, als Gutachter zu fungieren.

Für Unterstützung und ertragreiche Diskussionen danke ich Annette Hilgendorf, Susanne Obermeier, Andrea Osterlehner und Zsolt Ruzsics. Für die Einführung in die Methodik bedanke ich mich bei Andreas Elsing.

Mein Dank gilt ferner den Mitarbeitern des Max-von-Pettenkofer Instituts am Genzentrum für die angenehme Arbeitsatmosphäre. Insbesondere Walter Muranyi danke ich für die Einführung in die Immunfluoreszenz.

Dr. Elisabeth Kremmer danke ich für die Herstellung monoklonaler Antikörper, Dr. Stefan Höning für die Durchführung der „surface plasmon resonance“-Analyse. Ferner gilt mein Dank Christine Falk für die Durchführung von „Killer-Assays“ und die Bereitstellung von Zelllinien für Bindungsstudien.

Anja Gutermann danke ich für ihre Unterstützung und Anregungen beim Verfassen dieser Arbeit.

Meiner Familie, insbesondere meinen Eltern, ohne die es definitiv nicht so weit hätte kommen können, gilt mein Dank für viele Dinge, die hier alle zu erwähnen zu weit führen würde.

TABLE OF CONTENTS

1	INTRODUCTION	1
1.1	Adenoviruses and pathogenesis	1
1.2	Adenovirus particle	3
1.3	Adenovirus infectious cycle	4
1.4	Adenoviruses and antiviral defense mechanism: Viral immune evasion	7
1.5	Adenoviruses and the innate immune defense	8
1.6	Adenoviruses and the adaptive immune defense	9
1.6.1	Cellular immune response	9
1.6.2	Humoral immune response	10
1.7	Adenovirus early transcription unit 3 and its role in immune evasion	10
1.8	Intracellular trafficking and cellular sorting	13
1.8.1	Overview of vesicular transport in the eukaryotic cell	13
1.8.2	Sorting in the endoplasmatic reticulum and the Golgi apparatus	15
1.8.3	Sorting at the TGN and within the endosomal/lysosomal system	16
1.8.3.1	Adaptor complexes and sorting motifs	16
1.8.3.2	YXX Φ and LL motifs	18
1.9	Adenovirus E3 proteins and cellular sorting	21
1.10	The Ad19a E3/49K protein of subgenus D adenoviruses	21
1.11	Aim of this study	24
2	MATERIALS AND METHODS	25
2.1	Materials	25
2.1.1	Equipment	25
2.1.2	Chemicals	26
2.1.3	Additional materials	28

2.1.4	Cell lines	28
2.1.5	Viruses	28
2.1.6	Bacterial strains	29
2.1.7	Plasmids	29
2.1.8	Oligonucleotides	29
2.1.9	Molecular weight markers	29
2.1.10	Kits	30
2.1.11	Antibodies	30
2.1.11.1	Primary antibodies	30
2.1.11.2	Secondary antibodies	30
2.1.12	Enzymes	31
2.2	Methods	31
2.2.1	Bacterial cell culture	31
2.2.1.1	Cultivation and conservation of bacteria	31
2.2.1.2	Preparation of competent bacteria	32
2.2.1.3	Transformation	32
2.2.2	DNA techniques	32
2.2.2.1	Purification of plasmid DNA	32
2.2.2.2	Determination of DNA concentration	32
2.2.2.3	Restriction endonuclease digestion	33
2.2.2.4	5'-Dephosphorylation reaction	33
2.2.2.5	Polymerase chain reaction (PCR)	33
2.2.2.6	Isolation of DNA fragments	34
2.2.2.7	Phenol/chloroform extraction and ethanol precipitation	34
2.2.2.8	Ligation	34
2.2.2.9	DNA sequencing	34
2.2.2.9.1	PCR	34
2.2.2.9.2	Polyacrylamide gel electrophoresis	35
2.2.2.10	Agarose gel electrophoresis	35
2.2.3	Tissue culture	36
2.2.3.1	Cultivation and cryoconservation	36
2.2.3.2	Calcium phosphate transfection	36
2.2.3.3	Adenovirus infection	37
2.2.3.4	Preparation of adenovirus stocks	37

2.2.3.5	Plaque assay	37
2.2.3.6	Immunofluorescence	38
2.2.3.7	Flow cytometry analysis	38
2.2.3.8	Flow-cytometry-based 49K binding assay	39
2.2.3.9	NK cell-mediated lysis	39
2.2.4	Protein techniques	39
2.2.4.1	Metabolic labeling and immunoprecipitation	39
2.2.4.2	Glycosidase digestions	41
2.2.4.3	SDS PAGE	41
2.2.4.3.1	Maxigel	41
2.2.4.3.2	Minigel	42
2.2.4.4	Western blotting	43
2.2.4.4.1	Preparation of cell lysate	43
2.2.4.4.2	Protein blotting and detection	43
2.2.4.5	Surface plasmon resonance	44
2.2.4.6	Purification and refolding of recombinant HisTag-fusion protein	44
2.2.4.7	Production of rabbit polyclonal and rat monoclonal antibodies	46
2.2.4.7.1	Rabbit polyclonal antibodies	46
2.2.4.7.2	Rat monoclonal antibodies	46
2.2.4.8	Purification of secreted E3/49K	46
2.2.4.8.1	Coupling of antibody to the protein G-Sepharose column	46
2.2.4.8.2	Purification protocol	47
2.2.4.9	Silver staining	48
2.2.4.10	Coomassie blue staining	48
3	RESULTS	49
3.1	Time course of Ad19a E3/49K synthesis during infection	49
3.2	Carbohydrate processing of E3/49K early and late during infection	50
3.3	E3/49K expression in 293 and A549 cell lines	53
3.4	Expression of the N-terminal ectodomain of Ad19a E3/49K as a HisTag-fusion protein in E.coli	54

3.5	Production of polyclonal and monoclonal antibodies directed against the N-terminal domain of E3/49K	56
3.6	Proteolytic processing and secretion of E3/49K	58
3.7	Fully processed E3/49K proteins contain high-mannose and/or hybrid in addition to complex N-glycans	61
3.8	Only 12-13 of the 14 predicted N-glycosylation sites of E3/49K are utilized	63
3.9	Evidence for O-glycosylation of E3/49K	64
3.10	Kinetics of E3/49K processing	67
3.11	E3/49K contains intramolecular disulfide bonds	69
3.12	Intracellular staining patterns detected with antibodies directed against the N- and the C-terminus of E3/49K early during infection are indistinguishable	70
3.13	E3/49K localizes to the Golgi/trans-Golgi-network (TGN) and early endosomal vesicles early during infection	71
3.14	Cytoplasmic tail fragments of E3/49K accumulate in late endosomes/lysosomes during the course of Ad19a infection	74
3.15	Intracellular localization of E3/49K is influenced by acidotropic agents	76
3.16	Evidence for E3/49K recycling to the TGN	78
3.17	Processing of E3/49K is influenced by agents affecting glycosylation, acidification, lysosomal proteases and intracellular trafficking	80
3.18	Function of the potential endosomal/lysosomal sorting motifs in the cytoplasmic tail of E3/49K	84
3.18.1	Surface plasmon resonance analysis	84
3.18.2	Increased cell surface expression of E3/49K proteins with mutated cytoplasmic tails	85
3.18.3	Increased secretion of E3/49K proteins with mutated cytoplasmic tails	87
3.18.4	Decreased internalization of mutated E3/49K proteins and accumulation of mutated cytoplasmic tail fragments at the cell surface	90

3.19 High stability of E3/49K in the supernatant of Ad19a-infected and E3/49K-transfected cells	93
3.20 Purification of secreted E3/49K	95
3.21 E3/49K is a lymphocyte binding factor	96
3.22 Jurkat specific 49K-binding proteins coprecipitate with E3/49K	97
3.23 E3/49K inhibits NK cell-mediated lysis	99
4 DISCUSSION	101
4.1 Ad19a E3/49K expression during the time course of infection	101
4.2 Posttranslational modifications of Ad19a E3/49K: N- and O-glycosylation, disulfide bonds	101
4.3 Posttranslational modifications of Ad19 a E3/49K: Proteolytic processing and secretion	104
4.4 Intracellular trafficking and secretion of Ad19a E3/49K directed by sorting motifs in the cytoplasmic tail	108
4.5 Binding of secreted 49K to lymphocyte cell lines and coprecipitation of 49K-binding protein(s)	114
4.6 Inhibition of NK cell-mediated target cell lysis	118
4.7 Conclusion and outlook	119
5 SUMMARY	120
6 REFERENCES	121
7 ABBREVIATIONS	136
8 PUBLICATIONS	139
9 CURRICULUM VITAE	140

1 INTRODUCTION

1.1 Adenoviruses and pathogenesis

Adenoviruses (Ads) were initially isolated as infectious agents from adenoid tissues in the early 1950s (Hillemann and Werner, 1954; Rowe et al., 1953). The family of Adenoviridae is subdivided into two genera according to serological criteria, genome organization and host range: Mastadenovirus and Aviadenovirus. Mastadenoviruses infect mammals, Aviadenoviruses birds. In addition, several unassigned adenoviruses are considered to be assigned to a third genus, Atadenovirus (Benkő et al., 1999). The natural host range of adenoviruses is mostly confined to one species or to closely related species. So far, 51 different human adenovirus serotypes have been described, which are classified into 6 subgenera A-F based on hemagglutination properties, DNA homology and oncogenicity in rodents (Bailey and Mautner, 1994; Benkő et al., 1999; De Jong et al., 1999; Shenk T., 1996) (Tab. 1). Interestingly, the subgenus D harbors more than half (ca. 56%) of all described Ad serotypes. Remarkably, most Ads isolated from human immunodeficiency virus (HIV) infected individuals belong to subgenus D. In a recent study, 84% of 183 HIV-associated Ad isolates belonged to subgenus D, 3% to subgenus C, whereas only 5% of Ad serotypes isolated from healthy individuals belonged to subgenus D and 49% to subgenus C (De Jong et al., 1999). Many of these Ads are rarely or never isolated from immunocompetent individuals for reasons that are not understood. Eight out of the nine most recently described Ad serotypes (Ad43-49, 51) belong to subgenus D and were isolated from HIV-infected individuals (De Jong et al., 1999; Hierholzer et al., 1988; Schnurr and Dondero, 1993).

Tab. 1: Human adenovirus subgenera and serotypes

Subgenus	Serotypes
A	12, 18, 31
B	3, 7, 11, 14, 16, 21, 34, 35, 50
C	1, 2, 5, 6
D	8, 9, 10, 13, 15, 17, 19, 20, 22-30, 32, 33, 36-39, 42-49, 51
E	4
F	40, 41

Ads cause acute as well as persistent infections (Horwitz, 1996), although little is known how Ads establish persistence. Diseases induced by Ads are in general mild or even subclinical, but can be severe or even fatal, especially in immunocompromised patients (Horwitz, 1996). Ads are frequently isolated from patients worldwide and were responsible for ~13% (17771 cases) of respiratory diseases reported to the WHO from 1967 to 1976 (Wadell, 1984). In total, approximately 25000 Ad isolates were reported during that time period (Schmitz et al., 1983).

59.2% of the isolates belonged to subgenus C (mainly Ad1, Ad2 and Ad5), 33.7% to subgenus B (mainly Ad3 and Ad7) and only 4.1% to subgenus D, 2.4% to subgenus E and 0.6% to subgenus A. The prevalence of Ad specific antibodies is generally very high worldwide, although differences exist between different populations with regard to the prevalence of antibodies against specific Ad serotypes. More than 85% of adults have been exposed to common subgenus C Ads. Antibodies against Ad3 were found in 50% of adults in the USA, but in 90% in Japan. 15% of Germans were found to be positive for Ad19, whereas in Zaire the number was 85%. Thus, Ads of all subgenera are constantly maintained and spread in the human population.

The pattern of disease differs depending on the subgenus (Tab. 2). The molecular basis of the distinct pathogenesis of different Ad serotypes is poorly understood. Ads of subgenus A and F cause gastrointestinal diseases. Subgenus B and C Ads are mainly associated with acute respiratory diseases. Subgenus B Ads also induce infections of the urinary tract. Ad4, the only member of subgenus E, is known for its capacity to cause epidemics of an acute respiratory disease in military recruits.

Tab. 2: Diseases associated with adenovirus infections (modified from Lukashok and Horwitz, 1998)

Disease	Individuals Most at Risk	Principal serotypes
Acute febrile pharyngitis	Infants, young children	1-3, 5-7
Pharyngoconjunctival fever	School-age children	3, 7, 14
Acute respiratory disease	Military recruits	3, 4, 7, 14, 21
Pneumonia	Infants, young children	1-3, 7
Pneumonia	Military recruits	4, 7
Epidemic keratoconjunctivitis	Any age group	8, 11, 19a, 37
Pertussis-like syndrome	Infants, young children	40, 41
Acute hemorrhagic cystitis	Young children	11, 21
Gastroenteritis	Infants, young children	40, 41
Meningoencephalitis	Children and immuno-compromised hosts	7, 12, 32
Hepatitis	Infants and children with liver transplants	1, 2, 5
Persistence of virus in the urinary tract	Bone marrow transplant recipients, patients with acquired or immunodeficiency or other immunosuppression	9, 11, 19, 20, 22, 23, 26, 27, 34, 35, 43, 44, 45, 48, 49

Adenoviral conjunctivitis may be caused by several Ads of subgenera B, C, D and E, but mainly few Ads of subgenus D, Ad8, Ad19a and Ad37, are associated with a particularly severe and extremely contagious form of conjunctivitis, the epidemic keratoconjunctivitis (EKC) (Lukashok and Horwitz, 1998). In EKC, conjunctivitis is combined with epithelial and stromal keratitis.

Subepithelial infiltrates of immunopathological origin are found that fade gradually over weeks or months but may persist for years. In general, the disease is self-limiting and does not produce permanent corneal damage. Symptoms are red eye, severe pain, discomfort from glare, blurry vision, photophobia, foreign body sensation and excessive tearing. Disease can last up to four weeks, but most frequently resolves after 1-3 weeks. The incubation time is 2-14 days and persons remain infectious for 10-14 days. Spreading often occurs by the ophthalmologist's hand or contaminated instruments. So far, no efficient treatment is available.

1.2 Adenovirus particle

Adenoviruses (Ads) are non-enveloped viruses with a linear double-stranded (ds) DNA genome of 26-45 kbp flanked by inverted terminal repeats of 43-369 bp. A virus-encoded terminal protein (TP) is covalently attached to the 5'-end of each strand. The viral DNA associates with the highly basic protein VII, a small peptide termed mu and the protein V that seems to link the core of the virion to the capsid via interaction with protein VI. The icosahedral capsid consists of the three major proteins, hexon (II), penton base (III) and a knobbed fiber (IV), and of several minor proteins, VI, VIII, IX, IIIa and IVa2 (Fig. 1) (Russell, 2000; Shenk T., 1996). The capsid diameter is 70-90 nm.

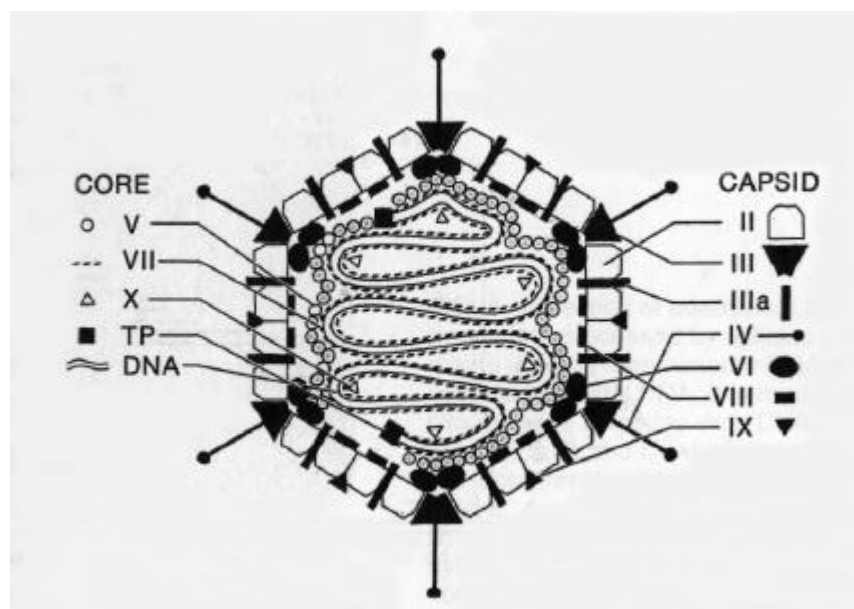


FIG. 1: The adenovirus particle. Schematic model of an adenovirus particle adapted from Stewart et al., 1991. Virion components are designated by their polypeptide numbers with exception of the terminal protein (TP).

1.3 Adenovirus infectious cycle

The Ad infectious cycle is divided into the early and the late phase of infection. The early phase encompasses the viral entry and the expression of early genes, which modulate cellular functions to prepare the cell for the replication of the viral DNA and the expression of late genes in the late phase of infection. The duration of the early phase depends on the cell type and takes about 6-8 h in HeLa cells, but can last much longer, e.g. in primary cells.

The Ad infectious cycle starts with the binding of virus particles to receptor(s) on the target cells via the knob portion of fiber. Ads of all subgenera with the exception of subgenus B can bind to the host cell via the „coxsackie adenovirus receptor“, CAR, a 46 kDa protein which is expressed in most tissues *in vivo* (Bergelson et al., 1998; Bewley et al., 1999; Nemerow, 2000; Roelvink et al., 1998; Tomko et al., 1997). In addition, it was proposed that the Ad5 fiber knob binds with low affinity to the MHC class I $\alpha 2$ domain (Davison et al., 1999; Hong et al., 1997). The subgenus D Ads Ad9, Ad15 and Ad19p can also bind to CAR (Roelvink et al., 1998; Roelvink et al., 1999), whereas the EKC causing members Ad8, Ad19a and Ad37 seem to utilize $\alpha(2\rightarrow 3)$ -linked sialic acid but not CAR (Arnberg et al., 2000a; Arnberg et al., 2000b). Interestingly, Ad19a and Ad37 have identical fiber proteins (Arnberg et al., 1997). Although it is striking that EKC-causing Ads seem to use sialic acid as a receptor, this fact cannot explain the distinct pathogenesis of these viruses, since sialic acid is expressed on virtually all cell types. The same is true for the MHC class I $\alpha 2$ moiety. Therefore, other unknown receptors, which are subgenus specific, have to be postulated or other events following the attachment might be decisive. Experiments with human airway epithelia and primary central nervous system cells substantiate the former hypothesis (Chillon et al., 1999; Zabner et al., 1999). With both cell types differences in viral attachment and infection efficiency depending on the Ad subgenus were observed. Interestingly, subgenus D Ads proved to be much better in the transduction of these cells than Ad2 and Ad5 of subgenus C, which are commonly used in gene therapy approaches. The attachment to these cells and the transduction efficiency could be increased by transferring the fiber of Ad17 (subgenus D) to Ad2 (subgenus C). It is currently unknown whether this increase is solely due to the different fiber proteins or is also partly based on subgenus-specific processes at the postattachment level. After the initial receptor binding an exposed RGD motif of the penton base interacts with cellular $\alpha_v\beta 3$ or $\alpha_v\beta 5$ integrins on the host cell and triggers clathrin-mediated endocytosis involving dynamin (Nemerow, 2000). These initial events activate the phosphoinositide-3-OH-kinase (PI-3K) and Rho GTPases triggering reorganization of actin cytoskeleton and the Raf/mitogen-activated protein (MAPK) kinase pathway inducing IL-8 production (Nemerow, 2000; Russell, 2000). The endocytosis of virus particles is accompanied by a partial disassembly assisted by the

viral cysteine protease (p23). The capsids penetrate by inducing acid-enhanced lysis of the endosomal membrane. The viruses utilize dynein to migrate along microtubules to the nuclear pore complex (NPC) (Leopold et al., 2000; Suomalainen et al., 1999). Ad2 particles dock to the NPC-filament protein CAN/Nup214 of the NPC (Trotman et al., 2001). The subsequent disassembly of the Ad2 particle, which is necessary to penetrate the nuclear pore with a diameter of <40 nm, requires histone H1 and the H1 import factors Imp β and Imp7.

In summary, the Ad capsid disassembles stepwise by processes induced by receptor interactions, exposure to acidic pH, re-entry into a reducing milieu and by interactions with the NPC. Finally, the viral DNA is imported into the nucleus, where the genome is targeted to the nuclear matrix via the interaction of TP with the cellular CAD (carbamoyl phosphate synthetase, aspartate transcarbamoylase, dihydroorotase) pyrimidine synthesis enzyme (Russell, 2000). Subsequently, early gene transcription starts.

Virus infection induces an early shut-down of host DNA synthesis and later also of host RNA and protein synthesis. About 40 different polypeptides are encoded by the adenoviral genome. Almost one third of these are structural proteins. Transcription by the host RNA polymerase II involves both DNA strands and initiates from five early (E1A, E1B, E2, E3, E4), two intermediate promoters and one major late promoter (MLP) (Fig. 2). All primary transcripts are capped and polyadenylated. Families of adenoviral mRNAs are produced by complex splicing processes. VA (virus-associated) RNAs, which inhibit the antiviral interferon response, are transcribed by host RNA polymerase III.

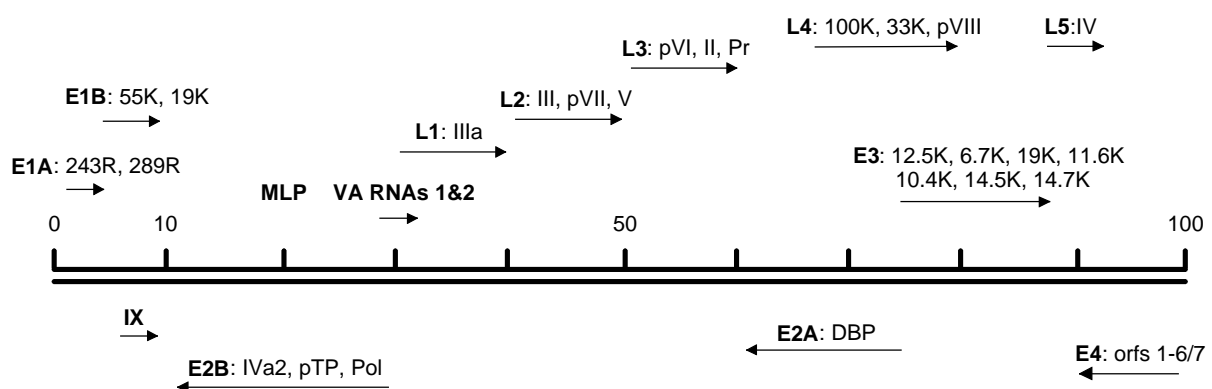


FIG. 2: Transcription of the adenovirus genome (subgenus C). Early transcription units are designated E, late transcription units L. The proteins encoded by each transcription unit are indicated by thin line characters. Most late mRNAs originate from the major late promoter (MLP). For details see text.

In the early phase of infection, viral mRNAs are derived from the E1A, E1B, E2, E3 and E4 regions (Fig. 2). E1A encodes two major proteins termed 289R (13S) and 243R (12S), which differ in the number of amino acid residues (and mRNA sedimentation coefficient). The E1A proteins create a favorable environment for viral DNA replication in the late phase. Numerous

activities of E1A proteins have been reported frequently based on *in vitro* studies. Most notably, E1A proteins can activate transcription by binding to a variety of different cellular transcription factors and regulatory proteins (Gallimore and Turnell, 2001; Russell, 2000). Of major importance is the interaction with proteins of the Rb/p130 family, which induces the release of the transcription factor E2F that directs the transcription of a variety of genes functionally related to DNA synthesis. E2F and E2F released from Rb, on the other hand, induce the p53 dependent pathway of apoptosis by two major mechanisms: 1) They directly induce transcription of p53. 2) They induce transcription of the p19^{arf} gene and thereby synthesis of the corresponding protein which inhibits mdm2-mediated induction of p53 proteolysis. Thus, E1A actions stabilize p53 and thereby trigger apoptosis. In addition, E1A proteins induce apoptosis independently of p53 (Putzer et al., 2000). E1A activates also the transcription of the early transcription units E1B, E2, E3 and E4. Two gene products of the E1B region, E1B-19K and E1B-55K, turn off the intrinsic apoptosis program that is triggered by E1A. E1B-19K is homologous to the cellular protein Bcl-2 and seems to inhibit the mitochondrial pathway of apoptosis mainly by inactivating with the pro-apoptotic proteins Bax and Bak (White, 2001). E1B-55K directly binds to p53 and represses p53-dependent transcriptional activation. In cooperation with E4orf6, E1B-55K enforces the degradation of p53 (Tauber and Dobner, 2001). In addition, E1B-55K and E4orf6 seem to be required for the preferential export and cytoplasmic accumulation of late viral mRNAs. The E2 region is subdivided into E2A (DNA bending protein (DBP)) and E2B (pTP and Pol). The corresponding gene products are required for the replication of viral DNA and transcription of late genes. The proteins encoded in the E3 region seem to be mainly involved in Ad subversion of the immune system and are discussed in detail in chapter 1.7. Gene products of the E4 region, termed orf 1-6/7, are involved in mRNA metabolism and transport, DNA replication and host shutoff (Leppard, 1997). E4orf4 and E4orf6/7 have recently been implicated in the inhibition of lysis of infected cells by cytotoxic T lymphocytes (CTLs) (Kaplan et al., 1999). E4orf6/7 was also reported to functionally compensate for E1A via induction of E2F (O'Connor and Hearing, 2000).

The late phase of infection starts with the onset of viral DNA replication. Thereafter, the five late transcription units (L1-5) are transcribed. Transcription is driven by the major late promoter (MLP), which is not active in the early phase of infection. The polycistronic primary transcript is processed by differential splicing. The late transcripts encode mainly structural components of virus particles or proteins involved in assembly. In addition, Ad assembly protein L4-100K has recently been shown to inhibit granzyme B-induced apoptosis (Andrade et al., 2001). Ad DNA replication occurs by strand displacement using a protein priming mechanism involving the terminal protein together with the virus-encoded DNA polymerase and DNA-bending protein in

concert with cellular factors. Virions are assembled in the nucleus. Late in this assembly process the L3-encoded viral cysteine proteinase cleaves several virion proteins generating mature and infectious Ad particles (Shenk T., 1996). Finally, permeabilization of the nuclear envelope and the disintegration of the plasma membrane facilitate the release of virus particles from the cell by so far poorly defined mechanisms.

1.4 Adenoviruses and antiviral defense mechanism: Viral immune evasion

Adenoviruses induce cellular and humoral immune responses. These were frequently investigated with recombinant Ad vectors with deletions in the viral genomes and/or with transgene insertions in animal, mainly mouse models, but rarely in humans. In animal models human Ads do not establish productive infection, and Ads with deletions, e.g. in the E3 region which encodes proteins with immunomodulatory functions (see below), most likely differ in the elicited immune responses from wild type (WT) Ads. Therefore, the significance of these results for Ad infections of humans remains to be clarified. Immune responses against Ads include an immediate inflammatory response mediated predominantly by neutrophils, macrophages and natural killer (NK) cells followed by CD4⁺ and CD8⁺ T cell-mediated mechanisms and neutralizing antibodies (Molnar-Kimber et al., 1998, and references therein). Remarkably, even in the absence of any viral gene expression chemokine induction, interferon and an anti-adenoviral CTL response were detected (Kafri et al., 1998; Muruve et al., 1999; Reich et al., 1988). Data from investigations of preexisting immunity to Ad5 indicate that also WT Ads induce a long-lasting humoral as well as cellular immune response in humans (Chirmule et al., 1999; Molnar-Kimber et al., 1998).

Two arms of the immune system, the innate and the adaptive immune response, act in concert to eliminate viruses from the organism. The mechanisms employed by the immune system frequently induce apoptosis in infected cells by extracellular stimuli. In addition, programmed cell death leading to apoptosis may be induced in infected cells by changes in the intracellular environment associated with Ad infection.

Whereas the E1B gene products seem to target intrinsic apoptosis programs (chapter 1.3, Fig. 4), proteins of the E3 region appear to counteract the induction of apoptosis programs induced by extracellular signals (Fig. 4), such as tumor necrosis factor α (TNF α), tumor necrosis factor-related apoptosis-inducing ligand (TRAIL) and Fas ligand (FasL). The latter are discussed in the context of the other E3 functions (chapter 1.7). However, E1B-19K was also reported to inhibit the apoptosis pathways induced by the proapoptotic factors TNF α , TRAIL and anti-Fas antibody (White, 2001).

1.5 Adenoviruses and the innate immune defense

An immediate inflammatory response is elicited by Ad infection mediated predominantly by neutrophils, macrophages, natural killer (NK) and NKT cells. The mechanisms how infected cells are recognized by these immune cells are only partly understood. The adenoviral E1A protein was shown to induce susceptibility to NK cell lysis (Cook et al., 1987; Routes and Cook, 1995). But no increased susceptibility was detected after Ad2/5 infection indicating a viral immune escape mechanism (Routes and Cook, 1989). NK cells monitor MHC class I expression on the cell surface and kill cells with decreased MHC class I levels (Biron et al., 1999). Such changes are commonly induced by viruses to reduce the presentation of viral peptides by MHC class I complexes in order to escape CTL recognition. Recently, also receptors triggering NK cell lysis have been identified (Moretta et al., 2001). Their regulation during Ad infection is unknown. Immune cells and infected cells secrete a number of cytokines and interferons with antiviral activities.

Some of these cytokines like $\text{TNF}\alpha$, FasL or TRAIL have pro-apoptotic activities. E1A also sensitizes cells to $\text{TNF}\alpha$ -, FasL- and TRAIL-induced apoptosis (White, 2001). $\text{TNF}\alpha$ -induced apoptosis is counteracted by E3/10.4K-14.5K, E3-14.7K and E1B-19K. $\text{TNF}\alpha$ and $\text{IFN}\gamma$ are also able to mediate non-cytopathological elimination of viruses (Guidotti and Chisari, 2001). It is unknown whether these mechanisms are also involved in the control of Ad infection. Other cytokines induce the recruitment of cells of the innate and adaptive immune response. Nuclear Factor κB ($\text{NF}\kappa\text{B}$) is frequently induced early after viral infection by intracellular processes as well as by extracellular stimuli, e.g. $\text{TNF}\alpha$. $\text{NF}\kappa\text{B}$ is a potent inducer of a number of cytokines and usually induces a pro-inflammatory, anti-apoptotic response. Ad E1A can inhibit $\text{NF}\kappa\text{B}$ activation (Shao et al., 1997; Shao et al., 1999). Nevertheless, $\text{TNF}\alpha$ induced activation of $\text{NF}\kappa\text{B}$ increases the expression of Ad E3 proteins mediated by $\text{NF}\kappa\text{B}$ binding sites within the E3 promoter (Deryckere et al., 1995; Koerner et al., 1992).

In addition, interferons and defensins counteract Ad infection. Defensins are 3-4 kDa antimicrobial peptides, which are released by some epithelial cells and were reported to reduce the Ad infection efficiency (Gropp et al., 1999). Interferons are subdivided into two main classes, type I (containing interferons α and β) and type II (interferon γ). Type I interferons can be synthesized by most cell types upon infection, whereas type II interferons are produced by NK cells and effector T cells. Interferons are induced by Ad particles even in the absence of viral protein synthesis (Reich et al., 1988). Interferon receptor signaling activates the Jak/STAT pathway and induces the transcription of several genes such as dsRNA induced kinase (PKR) and

2'-5' oligoadenylate synthetase, which have antiviral activities and block or at least impair virus replication (Goodbourn et al., 2000).

Adenovirus E1A proteins interfere with interferon signaling. They decrease the levels of STAT1 and p48, which are part of a heterotrimeric ISRE (IFN-stimulated response element) binding complex including STAT2. In addition, E1A sequesters the transcriptional co-activator CBP/p300 and directly binds STAT1 thereby disrupting transcriptional responses to IFN- α/β and IFN- γ . Ad VA RNAs are transcribed by cellular RNA polymerase III in the late phase of infection and form a highly ordered secondary structure that binds to the dsRNA-binding site on PKR and acts as a competitive inhibitor.

Strikingly, in experiments with a recombinant Ad5 with E1A, partial E1B and partial E3 deletions 90% of viral DNA was cleared within 24 h most likely involving the innate immune response (Worgall et al., 1997). Thus, innate immunity may play an important role in the control of Ad infection.

1.6 Adenoviruses and the adaptive immune defense

1.6.1 Cellular immune response

The cellular immune response aims to detect and eliminate virus-infected cells. CD8⁺ CTLs recognize viral peptides generated by the proteasome and presented by MHC class I complexes on the cell surface of infected cells. Subsequently, CTLs release lytic granules with perforin and granzymes or other proapoptotic factors. In addition, the interaction of FasL with Fas can induce the death of the infected cell (Harty et al., 2000; Trapani et al., 2000). The E1A protein was shown to sensitize infected cells to CTL-induced apoptosis independently of p53 (Cook et al., 1999). Three Ad E3 proteins are known to counteract lysis by CTLs: E3/19K and E3/10.4K-14.5K (see below). The Ad12 E1A protein interferes with the transcription of several proteins that are involved in antigen presentation: MHC class I complexes, the peptide transporter subunits TAP1 and TAP2 and LMP2 and LMP7, which are part of the immune proteasome (Gallimore and Turnell, 2001). Moreover, E1A was reported to regulate the 26S proteasome, which might have implications for the generation of viral peptides for the presentation by MHC class I molecules (Gallimore and Turnell, 2001). In addition, E4orf4 and E4orf6/7 have been implicated in the inhibition of CTL lysis (Kaplan et al., 1999) which is difficult to reconcile with reports that both proteins induce apoptosis (Branton and Roopchand, 2001; Yamano et al., 1999). Recently, the Ad assembly protein L4-100K was shown to inhibit granzyme B-induced apoptosis (Andrade et al., 2001).

1.6.2 Humoral immune response

The humoral immune response is based on the release of specific immunoglobulins of various classes, which bind to viral antigens and abrogate the ability of virions to infect cells. Neutralizing antibodies elicited upon Ad infection are mainly directed against the capsid components penton, fiber, hexon and core protein V (Molnar-Kimber et al., 1998).

1.7 Adenovirus early transcription unit 3 and its role in immune evasion

Ad proteins with immunomodulatory functions seem to be mainly encoded by the early transcription unit 3 (E3). Although the E3 region is not required for Ad replication *in vitro*, it is present in all human Ads and seems to encode proteins with immunomodulatory functions. This might be the basis for immune evasion and establishment of persistent infections (Burgert et al., 2002; Burgert and Blusch, 2000; Mahr and Gooding, 1999; Wold et al., 1995).

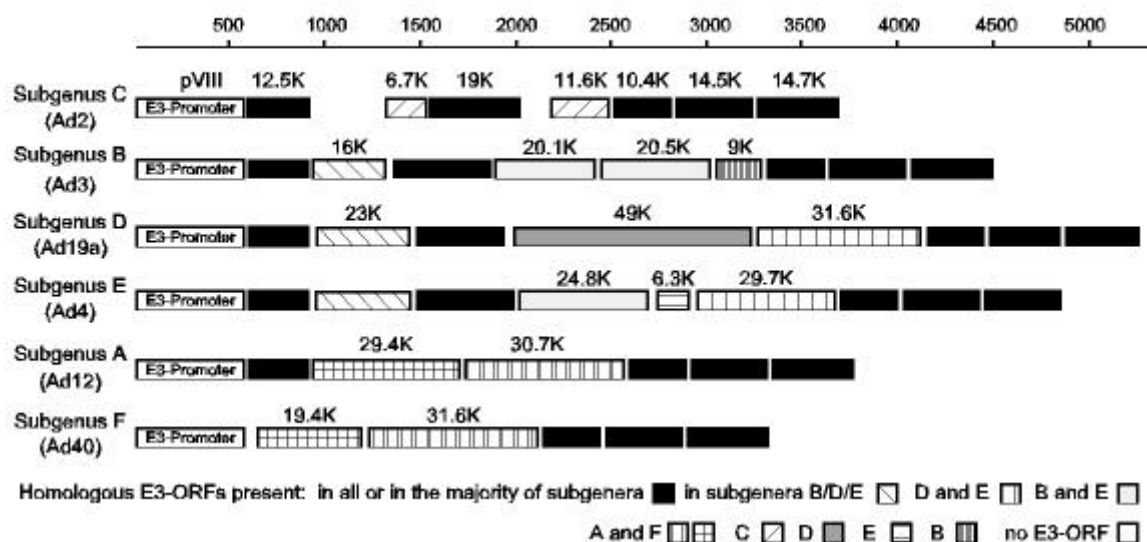


FIG. 3: Organization of E3 region in different adenovirus subgenera. Coding capacity of the E3 region of representative members of subgenus C (Ad2), B (Ad3), D (Ad19a), E (Ad4), A (Ad12) and F (Ad40) (adapted from Burgert and Blusch, 2000). The line on the top denotes the size in bp. Open reading frames (ORFs) are indicated as bars and drawn to scale. The size/name of common ORFs is only given once. The shading code is depicted below the figure. Significant overall homology (similarity > 25 %) is indicated by identical shading. Homology to a portion of a protein was neglected. pVIII is not an E3 protein, but part of its sequence overlaps with the E3 promoter.

Interestingly, the size and composition of the E3 regions of adenoviruses show significant subgenus specific variations (Fig. 3). Whereas in subgenus F (Ad40/41) about 3 kb encode five open reading frames (ORFs), in subgenus D (e.g. Ad19a) approximately 5200 bp encode eight ORFs. Some genes (e.g. 10.4K, 14.5K and 14.7K) are found in all subgenera, others in many (e.g. 19K in subgenera B-E), whereas some genes seem to be unique to a particular subgenus (Fig. 3), e.g. 11.6K of subgenus C or 49K of subgenus D (Burgert and Blusch, 2000). The E3, more precisely the E3A region (exclusive of 10.4K, 14.5K and 14.7K), is the region of the highest variability in the Ad genome in a comparison of different subgenera (Bailey and Mautner, 1994).

Therefore, it seems likely that the E3 regions of different Ads contribute to the subgenus-specific pathogenesis (Tab. 2), especially since differential utilization of receptors for virus adsorption based on the receptors identified so far cannot explain the subgenus-specific differences in pathogenesis (chapter 1.3).

Studies on E3 proteins, primarily of Ad2 and Ad5 of subgenus C, revealed several molecular mechanisms that are employed to escape recognition and elimination of Ad-infected cells by the host immune system (Fig. 4). For example, E3/19K retains MHC class I molecules in the ER and thereby prevents the presentation of viral peptides to and lysis of infected cells by cytotoxic T-lymphocytes (Burgert and Kvist, 1985; Burgert, 1996). The E3/14.7K protein can protect infected cells from TNF α -induced cell death (Burgert and Blusch, 2000; Horwitz, 2001; Mahr and Gooding, 1999; Wold et al., 1999). The complex of the E3 proteins 10.4K and 14.5K has also been implicated in conferring resistance against cytolysis mediated by TNF α and down-regulates the epidermal growth factor receptor from the cell surface (Burgert and Blusch, 2000; Wold et al., 1999). In addition, these proteins dramatically reduce the expression of the apoptosis receptor Fas on the cell surface of infected cells by inducing its internalization and degradation in lysosomes (Elsing and Burgert, 1998; Shisler et al., 1997; Tollefson et al., 1998). Furthermore, data have been presented suggesting that the 10.4K-14.5K complex works in concert with 6.7K to down-regulate TRAIL receptor 1 and 2, death receptors possibly involved in the induction of apoptosis in infected cells mediated by immune effector cells (Benedict et al., 2001; Tollefson et al., 2001). 10.4K-14.5K also down-modulate the receptors for epidermal growth factor and to some extent insulin and insulin-like growth factor from the cell surface (Kuivinen et al., 1993). In addition, 14.7K was reported to inhibit TRAIL-R1-induced apoptosis (Tollefson et al., 2001) and was also reported to interact with FLICE/caspase 8 to inhibit FasL-induced apoptosis (Chen et al., 1998). The latter could not be confirmed by other studies (Elsing and Burgert, 1998; Tollefson et al., 1998).

So far, no functions have been assigned to E3 proteins of Ads of other subgenera than C. Some of them have been characterized biochemically and were shown to be transmembrane proteins, which are frequently glycosylated, e.g. Ad3 16K (Hawkins et al., 1995) and 20.5K (Hawkins and Wold, 1995a; Hawkins and Wold, 1995b) of subgenus B and Ad4 30K of subgenus E (Li and Wold, 2000). Interestingly, many of them contain potential endosomal/lysosomal sorting motifs (YXX Φ or LL motifs, chapter 1.8.3.2) (Windheim et al., 2002).

In summary, Ad E3 proteins are not required for the basic process of replication but rather for virus replication *in vivo* in the presence of an antiviral immune response that seeks to abrogate virus replication and spreading by inducing apoptosis or lysis of the infected host cell, mainly executed by CD8⁺ CTLs and NK cells (Biron et al., 1999; Harty et al., 2000).

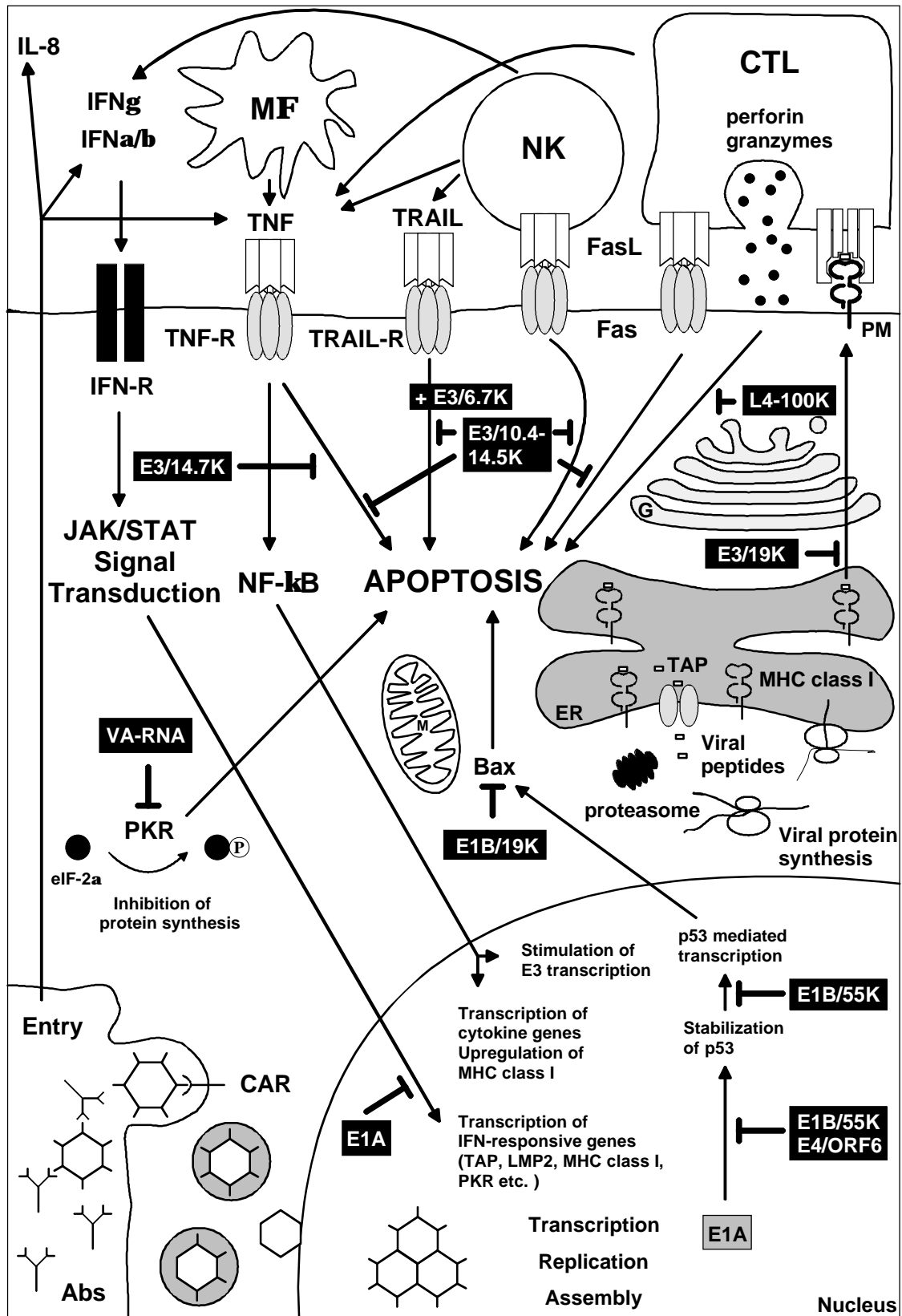


FIG. 4: Adenoviral immune evasion mechanisms. Adenoviruses encode a variety of proteins and virus associated (VA) RNAs with immunomodulatory functions. Adenoviral factors (proteins and VA RNAs) are indicated by boxed characters. For detailed description see text. Abbreviations not explained in the text are: MΦ, macrophages; Abs, antibodies; PM, plasma membrane; G, Golgi; M, mitochondrium.

1.8 Intracellular trafficking and cellular sorting

1.8.1 Overview of vesicular transport in the eukaryotic cell

Viruses have evolved mechanisms to exploit almost every cellular function to achieve successful replication. Therefore, it is not surprising that Ads, like other viruses, utilize membrane-bounded compartments and exploit the cellular trafficking machinery of eukaryotic cells. Findings from other viral proteins, e.g. MCMV gp40 (m154), gp48 (m06) or HIV (e.g. nef), demonstrate the importance of the exploitation of the cellular sorting machinery in the virus-host interaction (Greenway et al., 2000; Reusch et al., 1999; Ziegler et al., 2000). In case of adenoviruses, the capacity to utilize membrane-bounded compartments is mainly confined to E3 proteins. The Ad E3 region is the only part of the Ad genome that harbors transmembrane proteins. Interestingly, 19 out of the 22 different proteins (12.5K, 19K, 10.4K, 14.5K counted only once) in the E3 regions of different subgenera (Fig. 3), i.e. about 86%, are predicted to be transmembrane proteins (Windheim et al., 2002). Although no functions have been assigned to many of these proteins, it seems likely that their function depends on the cellular sorting machinery. This has been demonstrated for E3/19K and 10.4K-14.5K and the down-regulation of MHC class I molecules and Fas/EGFR respectively. Therefore, in the following the intracellular trafficking and the cellular sorting machinery as well as sorting motifs with potential relevance for Ad proteins are introduced.

Most transport processes between the membranous compartments of a eukaryotic cell involve vesicles. Vesicular transport connects the organelles of the secretory pathway (the endoplasmic reticulum, the ER-Golgi intermediate compartment (ERGIC), the Golgi complex, the trans-Golgi-network, secretory vesicles, plasma membrane) as well as those of the endocytic pathway (plasma membrane, clathrin coated vesicles, early and late endosomes, lysosomes) (Fig. 5). Distinct sets of coat proteins select the cargo molecules of the transport vesicles by direct or indirect interaction (Mellman and Warren, 2000). Intrinsic sorting signals determine whether proteins are actively packaged (export) or are excluded (retention) from export vesicles, or are randomly incorporated into export vesicles (default) (Rothman and Wieland, 1996). Resident proteins of a particular compartment can contain retention signals or retrieval signals which efficiently return proteins transported to the acceptor compartment to the donor membrane. Cargo proteins may be transported by export signals or by default ("bulk flow").

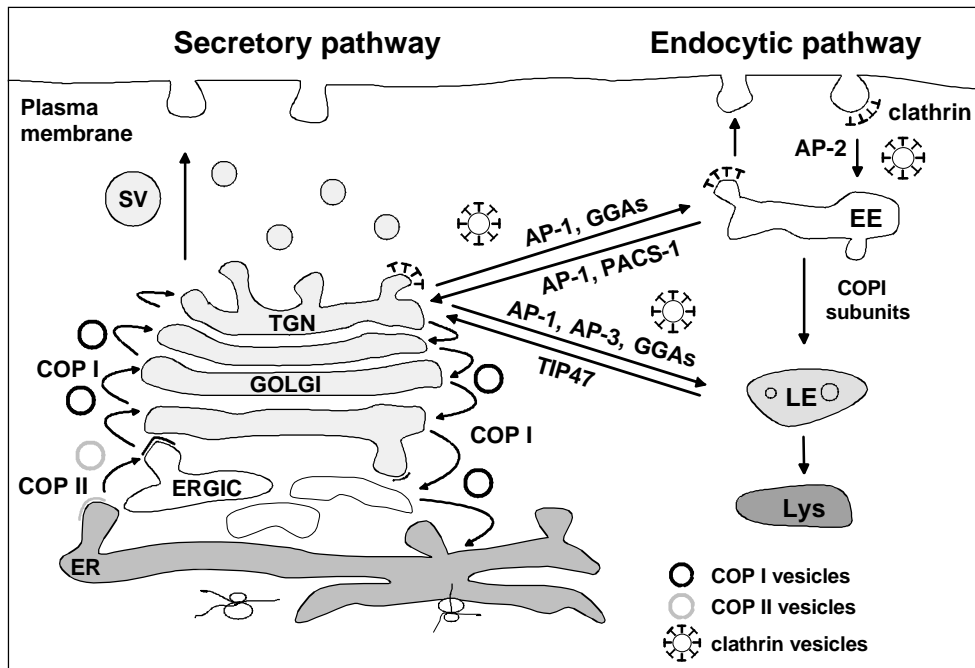


FIG. 5: Overview of intracellular trafficking in the secretory and the endocytic pathway. Export from the ER to the ERGIC occurs in COPII coated vesicles. Transport from the ERGIC to the cis-Golgi, through the Golgi and retrograde to the ER is mediated by COPI coated vesicles. From the TGN proteins can be exported to the plasma membrane in secretory vesicles or to early (EE) or late (LE) endosomes, presumably, by clathrin coated vesicles involving the clathrin adaptor complexes AP-1, AP-3 and the GGAs. In addition, early endosomes can be reached via endocytosis from the plasma membrane, which involves the clathrin adaptor complex AP-2 and clathrin. Exit from early endosomes may occur in three different directions: 1. Recycling to the cell surface; 2. Recycling to the TGN most likely by clathrin-coated vesicles involving AP-1 and PACS-1; 3. Export to late endosomes by a transport process that seems to require COPI subunits. From late endosomes proteins are either delivered to lysosomes (Lys) for degradation or to fulfill their function as lysosomal residents or are recycled to the TGN. The latter pathway seems to be mediated by TIP47. For details and references see text.

Three major types of coat complexes have been identified to play a role in vesicular transport processes: Clathrin, COPI and COPII (Kirchhausen, 2000b). Coats are derived from soluble, cytosolic precursors and are specifically recruited to organelle membranes. Small GTP binding proteins (Rab and Sar1p/Arf proteins) play a crucial role in the regulation of processes such as budding, uncoating, tethering, docking and fusion of vesicles (Takai et al., 2001). The specific docking to the acceptor membrane is thought to be controlled by the pairing of SNAREs (soluble N-ethylmaleimide-sensitive factor attachment protein receptors), v-SNAREs on vesicles and t-SNAREs on target membranes (Chen and Scheller, 2001). *In vivo*, Rab proteins regulate the formation of SNARE complexes (Zerial and McBride, 2001). But SNAREs are not the sole determinants of vesicle targeting. Also, the so-called tethering factors confer targeting specificity to vesicles and work upstream of SNAREs, e.g. p115 in the intra-Golgi transport and EEA-1 in endosomal fusion (Pfeffer, 1999).

1.8.2 Sorting in the endoplasmic reticulum and the Golgi apparatus

To enter the secretory pathway in mammalian cells most proteins contain a N-terminal signal sequence that is recognized by the signal recognition particle (SRP) (Corsi and Schekman, 1996). Proteins are then translocated co-translationally into the ER as soluble proteins or anchored to the membrane by their transmembrane region. Trafficking between the ER, ERGIC and the Golgi/TGN complex is mainly accomplished by COPI and COPII coats (Mellman and Warren, 2000) (Fig. 5). COPII vesicles are thought to be the main players in the anterograde transport between the ER and the ERGIC. Budding of COPII vesicles requires the small GTP-binding protein Sar1p and occurs at specific ER exit sites. In addition, COPI coated vesicles function in the anterograde transport of proteins from the ERGIC to the Golgi and in the retrograde transport from the Golgi to the ERGIC and the ER (Fig. 5). The small GTP-binding protein Arf1 recruits COPI to membranes and initiates the budding of COPI coated vesicles. Sorting motifs implicated in COPI binding and retrograde transport to the ER are C-terminal KKXX and KXXXX sequences, where K is lysine and X is any amino acid (Teasdale and Jackson, 1996). Several other mechanisms related to quality control may also mediate ER retention (Ellgaard et al., 1999). On the other hand, cargo proteins seem to be concentrated in COPII vesicles suggesting that they contain ER export signals (Gorelick and Shugrue, 2001; Hong, 1998).

The ER-Golgi intermediate compartment (ERGIC) is supposed to be a major site for cargo concentration and for sorting of proteins for anterograde transport to the Golgi from those that must be returned to the ER (Martinez-Menarguez et al., 1999).

From the ERGIC, proteins are delivered to the *cis* face of the Golgi complex. Transit through the Golgi complex involves the sequential passage through 3-5 stacks (*cis*, *medial*, *trans*). Transport of cargo proteins through the Golgi/TGN is supposed to follow a default pathway ("bulk flow") (Mellman and Warren, 2000). In contrast to the ER, there are no soluble residents of the Golgi lumen, but instead all Golgi proteins are either integral membrane proteins or peripheral membrane proteins on the cytoplasmic side of the Golgi (Munro, 1998). Glycosyltransferases, SNARE proteins and some viral proteins are targeted to the Golgi by their transmembrane domain (TMD), which is on average five residues shorter than that of plasma membrane proteins (Munro, 1998).

Sorting motifs of TGN proteins will be discussed in the following chapter because the TGN seems to be closely connected to the endosomal/lysosomal system and similar sorting motifs are utilized (Ktiskakis and Roth, 1996).

1.8.3 Sorting at the TGN and within the endosomal/lysosomal system

1.8.3.1 Adaptor complexes and sorting motifs

The TGN serves as a sorting station, where proteins destined for the different cellular compartments are separated (Traub and Kornfeld, 1997). The steady-state localization of TGN proteins like TGN38 and furin was shown to depend on YXX Φ motifs (see below) in their cytoplasmic tails, which are required for the retrieval of these proteins from the cell surface (Tab. 3). In addition, the TGN38 TMD mediates TGN retention (Banting and Ponnambalam, 1997). For the TGN localization of furin an acidic cluster motif with a casein kinase II phosphorylation site is important (Molloy et al., 1999). In non-polarized cells trafficking from the TGN to the cell surface is believed to be mainly a default pathway, whereas in polarized cells proteins are targeted to the apical or basolateral membrane by sorting motifs which seem to be interpreted at the TGN (Keller et al., 2001). Also in polarized cells a default pathway exists that delivers proteins lacking a specific sorting motif to the apical and the basolateral membrane. In general, transport from the TGN to the cell surface is assumed to be mediated directly by secretory vesicles without involving any intermediate organelles. In few cases it was proposed that plasma membrane proteins take an indirect route to the cell surface via an intracellular, most likely endosomal, compartment (Laird and Spiess, 2000, and references therein). In non-polarized cells, coat proteins of secretory vesicles have not been identified yet. In polarized cells, clathrin-coated vesicles have been implicated in the basolateral sorting, whereas the coats for apical transport and default pathways are still unknown. In the formation of clathrin-coated vesicles, members of a class of so-called clathrin adaptor protein (AP) complexes connect cargo proteins to the clathrin coat. AP complexes are tetramers (two large subunits $\gamma/\alpha/\delta/\epsilon$ and $\beta 1-4$, 90-130 kDa, one medium subunit, $\mu 1-4$, ~50 kDa, and a small subunit, $\sigma 1-4$, ~20 kDa) with a molecular mass of about 250-300 kDa and with a similar architecture (AP-1: $\gamma\beta 1\sigma 1\mu 1$, AP-2: $\alpha\beta 2\sigma 2\mu 2$, AP-3: $\delta\beta 3\sigma 3\mu 3$, AP-4: $\epsilon\beta 4\sigma 4\mu 4$) (Boehm and Bonifacino, 2001; Kirchhausen, 1999; Robinson and Bonifacino, 2001). For several subunits different isoforms have been identified. AP-1 localizes to the TGN. AP-3 is found at the TGN and peripheral endosomal structures. Both have been implicated in the sorting and trafficking between the TGN and the endosomal/lysosomal system and to the basolateral membrane. AP-2 localizes to the plasma membrane and directs endocytosis (Fig. 5). AP-2 might also participate in the budding of clathrin-coated vesicles in a retrograde trafficking pathway out of the lysosomal compartment (Traub et al., 1996). AP-1 with its epithelial cell specific subunit $\mu 1B$ directs basolateral targeting (Folsch et al., 1999). The function of AP-1 in TGN-endosome trafficking has recently been challenged, when it was shown that GGAs (Golgi associated, γ ear containing, ARF binding proteins) bind cargo proteins (MPRs,

sortilin) via a sorting motif consisting of an acidic stretch and an LL motif and mediate TGN export (Nielsen et al., 2001; Puertollano et al., 2001a; Zhu et al., 2001). Three GGAs are expressed in mammals and localize to the TGN. They are supposed to be involved in TGN-endosome trafficking and also seem to work as adaptors for clathrin-coated vesicles (Puertollano et al., 2001b). Different recycling pathways exist between the endosomal/lysosomal system and the TGN (Rohn et al., 2000). AP-1 might rather be implicated in transport processes between early/recycling endosomes or late endosomes and the TGN or might be implicated in another trafficking pathway between the TGN and endosomes in addition to that one involving GGAs (Black and Pelham, 2001; Meyer et al., 2000) (Fig. 5). AP-1 has been detected on endosomal membranes and was found to bind to immature secretory granules (Dittie et al., 1996; Futter et al., 1998). AP-3 seems to be involved in the transport of proteins from the TGN to lysosomes (Dell'Angelica et al., 1999; Le Borgne et al., 1998). For AP-1 and AP-2 the association with clathrin-coated vesicles was demonstrated. For AP-3 clathrin association is controversial. AP-4 localizes to non-clathrin-coated vesicles in the area of the TGN (Hirst et al., 1999). The contact site between the heterotetrameric AP complexes and clathrin has been mapped to the so-called "clathrin-box", a sequence of five aa, which is found in several proteins interacting with clathrin. This sequence is found in AP-1 β 1, AP-2 β 2 and AP-3 β 3, but not in AP-4 β 4 consistent with the view that AP-4 does not bind to clathrin (Kirchhausen, 2000a). AP complexes are believed to be recruited to specific membranes through clathrin-independent docking mechanisms. The small GTP-binding protein Arf-1 is essential for TGN membrane association of AP-1 and GGA-3 (Dell'Angelica et al., 2000) as well as membrane association of AP-3 (Faundez et al., 1998; Ooi et al., 1998). No related small GTP binding protein has been found for AP-2 docking. The formation of clathrin-coated vesicles at the plasma membrane involving AP-2 is controlled by a number of proteins and lipids that are connected in a complex network of interactions (Kirchhausen, 2000a). Coated vesicle detachment from the plasma membrane requires dynamin (Hinshaw, 2000).

The AP complexes seem to participate in cargo selection mediated by direct binding of their subunits to sorting motifs in the cytoplasmic tails of transmembrane proteins. Two major sorting motifs for sorting in the TGN and the endosomal/lysosomal system have been identified: YXX Φ and LL (Tab. 3) (Heilker et al., 1999), where Φ represents a bulky hydrophobic aa (L, V, I, F, M) and X can be any aa. In most LL motifs indeed a pair of leucines is found, but one leucine might also be substituted by another bulky hydrophobic aa (M, V, I, F). In the following the term LL motif is used in both cases. The YXX Φ motif has also been described as a YPP Φ motif, where P represents a polar residue (Kirchhausen, 1999). Interestingly, many proteins contain more than one motif and frequently combinations of different signals, e.g. the mannose-

6-phosphate receptors (MPRs). The YXX Φ and LL motifs will be discussed in detail in the following chapter (see below). Several other sorting signals have been demonstrated to play a role in the trafficking pathways between the TGN, the plasma membrane and the endosomal/lysosomal system. These pathways involve proteins like TIP47 and PACS-1 (Fig. 5). TIP47 has recently been shown to interact with Rab9-GTP on endosomal membranes, which seems to play a role in the generation of transport vesicles in endosomes destined for the TGN (Carroll et al., 2001). PACS-1 was shown to bind to AP-1 and AP-3 but not AP-2 complexes and overexpression of a dominant negative PACS-1 mutant redistributed furin and cation-independent mannose-6-phosphate receptor (CI-MPR) from the TGN to a vesicular, most likely endosomal compartment (Crump et al., 2001). Furthermore, COPI subunits have been implicated in the trafficking in the endosomal/lysosomal system (Gu and Gruenberg, 1999) and have been proposed to be crucial for the biogenesis of so-called endocytic carrier vesicles (ECV), which are thought to transport proteins from early to late endosomes (Fig. 5).

1.8.3.2 YXXF and LL motifs

YXX Φ and LL motifs are the most frequent sorting motifs found in the cytoplasmic tails of transmembrane proteins that direct trafficking in the TGN/endosomal/lysosomal system (Tab. 3). YXX Φ motifs bind to the μ 1-4 subunits of the AP complexes (Aguilar et al., 2001; Ohno et al., 1998). It is still a matter of debate whether the LL motifs interact with the β subunits (Rapoport et al., 1998) or the μ subunits (Bremnes et al., 1998; Rodionov and Bakke, 1998) of AP complexes. Crystal structures of the sorting motif binding domain of μ 2 and a peptide containing the YXX Φ motifs of TGN38 and EGF receptor (Owen and Evans, 1998) revealed that the peptide was bound in an extended conformation and not in a tight turn structure as earlier suggested (Collawn et al., 1990).

Strikingly, both YXX Φ and LL motifs in cytoplasmic tails of transmembrane proteins control sorting processes between the TGN and endosomes/lysosomes and the MHC class II compartment as well as targeting from the TGN and endosomes to the basolateral surface of polarized cells. In addition, YXX Φ and LL motifs direct the endocytosis from clathrin-coated pits at the plasma membrane (Tab. 3). Therefore, proteins have to contain information in addition to the basic YXX Φ and LL motifs for the fine-tuning of their specific trafficking and localization information. The difficulties the cellular sorting machinery has to handle are exemplified by the sorting at the TGN. Here, proteins with YXX Φ or LL motifs interacting with AP-1 or AP-3 for targeting to endosomal/lysosomal compartments and proteins that reach the plasma membrane via secretory vesicles but contain YXX Φ or LL motifs for AP-2 mediated

endocytosis have to be distinguished. An example for the latter is the transferrin receptor which contains a YTRF sorting signal that interacts with $\mu 2$ but not $\mu 1$ (Ohno et al., 1995). LL motifs of limp-II and tyrosinase bind with a higher affinity to AP-3 than AP-1 and AP-2 (Honing et al., 1998). For the fine-tuning of YXX Φ and LL motifs the residues surrounding the motif might play an important role.

Tab. 3: TGN and endosomal/lysosomal sorting motifs

Sorting signal or motif	Protein	Destination	Adaptor binding	Ref.
YXXF motifs				
GGEPLSYTRF	transferrin receptor	E ¹ EE ² B ³	AP-2	1
KRSHAGYQTI	lamp-1	E Lys ⁴ B	AP-1,-2,-3	1
RAGHSSYTPL	HLA-DM β	E MIIC ⁵	AP-1,-2	1
RPKASDYQRL	TGN38/46	E TGN B	AP-1,-2	2
LL motifs				
EAENTITYSLLKH	FcRII-B2 (mouse)	E B		3
EGTADERAPLIRT	limp-II	E Lys B	AP-3	1
MDDQRDLISN LISNNEQLPMLGR	Invariant Chain	E MIIC B	AP-1,-2	1
VTSEPKHSLLVG	Menkes disease protein	E TGN		4
Other sorting signals				
Acidic cluster	e.g. HIV-1 nef, furin	E TGN	PACS-1	5
Ubiquitin	e.g. EGFR	E		6
KKFF KRFY	ERGIC-53 VIP36	E		7
FW	CI- and CD-MPR	TGN	TIP47	8
Palmitoylation	CD-MPR			9
Man-6-P	Lysosomal hydrolases	Lys		10

¹E (endocytosis), ²EE (early endosomes), ³B (basolateral sorting), ⁴Lys (Lysosomes), ⁵MIIC (MHC II compartment). For other abbreviations and details see text. References: (1) (Heilker et al., 1999) (2) (Banting and Ponnambalam, 1997) (3) (Hunziker and Fumey, 1994) (4) (Francis et al., 1999; Petris et al., 1998) (5) (Piguet et al., 2000; Voorhees et al., 1995) (6) (Hicke, 1999) (7) (Hauri et al., 2000) (8) (Carroll et al., 2001) (9) (Schweizer et al., 1996) (10) (Roberts et al., 1998)

For the LL motifs a consensus motif (-)(2-4)xLL was proposed where x is usually a polar residue and (-) a negatively charged residue (aspartic or glutamic acid or phospho-serine) (Kirchhausen, 1999). In part, this was confirmed by investigating the surrounding amino acids of 35 functional LL motifs in 31 proteins (Windheim et al., 2002). A preference for acidic residues (E, D) or serine was evident at position -4 and -5. In position -1 proline was found in about 23 % of all LL motifs. In order to investigate the sequence requirements of YXX Φ motifs for their interaction with AP complexes combinatorial peptide libraries and the yeast-two-hybrid system have been applied. For the interaction with $\mu 2$, a YXRL consensus motif was found in a combinatorial library approach (Boll et al., 1996). No preference for surrounding residues was

observed. In another study the yeast-two-hybrid system was applied to reveal that the interactions of the YXX Φ motif of TGN38 with μ 1 and μ 2 were differentially affected by mutations in the SDYQRL sequence (Ohno et al., 1996), demonstrating that the surrounding residues are important determinants of the interaction between YXX Φ motifs and different AP complexes. A combinatorial XXXYXX Φ library was used in the yeast-two-hybrid system to investigate the interactions with μ 1, μ 2, μ 3 and μ 4 and revealed similar and divergent sequence requirements (Aguilar et al., 2001; Ohno et al., 1998). By investigating the surrounding residues of 48 functional YXX Φ motifs in 45 proteins preferences for certain aa were found, although less striking than in case of the LL motifs (Windheim et al., 2002). These findings indicate that, although similar sorting motifs are recognized by the different AP complexes, there are differences in the sequences they recognize, which are possibly the basis for different trafficking pathways of proteins containing YXX Φ and LL motifs.

In accord with this concept, some studies show that sorting motifs that specify different sorting events, e.g. for internalization and basolateral localization, overlap but are not identical (Lin et al., 1997; Matter et al., 1994; Odorizzi and Trowbridge, 1997).

Moreover, the recognition of some YXX Φ and LL motifs seems to be regulated by phosphorylation. Interestingly, recognition of LL motifs seems to be positively regulated by serine phosphorylation, e.g. CD4 (Shin et al., 1991), CD3 γ (Dietrich et al., 1994), whereas YXX Φ motifs are inactivated by tyrosine phosphorylation, e.g. CTLA-4 (Bradshaw et al., 1997; Shiratori et al., 1997), TGN38 (Stephens and Banting, 1997).

The distance of functionally active YXX Φ and LL motifs to the putative transmembrane domain in the primary sequence varies, although these motifs tend to be localized in relative proximity to the TMD and are frequently found in proteins with very short cytoplasmic tails. Both type I transmembrane proteins as well as type II proteins (e.g. transferrin receptor, ASGP receptor, invariant chain and IRAP), contain such motifs. In case of the YTRF motif of transferrin receptor (type II) at least 7 aa between the F and the transmembrane domain were required for function (Collawn et al., 1990) but rather large deletions in the cytoplasmic tail moving the motif closer to the TMD were tolerated without affecting the internalization rate (Girones et al., 1991). In contrast, for the YQTI of lamp-1 7 aa acid spacing as in WT was obligatory and changing that distance to 6 or 12 aa changed the internalization rate and even more dramatically the lysosomal targeting (Rohrer et al., 1996). For the function of the phosphorylation-dependent LL motif (SDKQTLL) of CD3 γ at least 7 aa spacing from the TMD was required, whereas for the phosphorylation-independent LL motif (DKQTLL) at least 6 aa were obligatory (Geisler et al., 1998). Thus, there seems to be a minimal distance between a sorting motif and the membrane,

which might depend on the motif itself and the protein. Changes in the distance between the motif and the plasma membrane seem to be differentially tolerated by different proteins. Notably, also artificial YXX Φ motifs mediating endocytosis could be introduced to hemagglutinin (HA) and glycoporphin A by site directed mutagenesis (Ktistakis et al., 1990; Lazarovits and Roth, 1988; Zwart et al., 1996). In summary, sequence and positional requirements exist for the function of YXX Φ and LL motifs in different trafficking pathways.

1.9 Adenovirus E3 proteins and cellular sorting

Most proteins encoded by Ad E3 regions are transmembrane proteins. Strikingly, many of them contain potential sorting motifs in their cytoplasmic tails (Windheim et al., 2002). For some of them functionality has been demonstrated: The E3/19K protein contains a KKXX or KKKXX motif in the cytoplasmic tail depending on the subgenus. This motif interacts with COPI and is important for the retrieval of E3/19K from the cis-Golgi/ERGIC to the ER and thereby contributes to the ER localization of E3/19K (Windheim et al., 2002). Interestingly, in addition to the retrieval signal, E3/19K contains a retention signal that is localized in the transmembrane region of the protein (Sester et al., in preparation). Therefore, cellular retrieval and retention motifs seem to cooperate to mediate ER localization of E3/19K. The specific interaction of E3/19K with MHC class I complexes results in their retention in the ER, whereby the recognition of infected cells by CTLs through MHC class I-mediated presentation of viral peptides is impaired.

The 10.4K and 14.5K proteins contain LL and YXX Φ motifs, respectively. Both motifs were demonstrated to be crucial for the down-modulation of Fas from the cell surface by the 10.4K-14.5K complex (Hilgendorf et al., in preparation; Windheim et al., 2000).

About most other E3 proteins little, if any data about trafficking as well as function have been gained. Most E3 proteins are postulated to be transmembrane proteins and many of them contain potential sorting motifs, particularly YXX Φ and LL motifs in their cytoplasmic domains (Windheim et al., 2002). The functionality of these motifs remains to be demonstrated and also the functions of these proteins have to be addressed to get insight into the role of Ad exploitation of the host sorting machinery in immune evasion.

1.10 The Ad19a E3/49K protein of subgenus D adenoviruses

A novel E3 gene, E3/49K, was identified recently in the genome of Ad19a, an adenovirus of subgenus D causing epidemic keratoconjunctivitis (EKC) (Deryckere and Burgert, 1996). Subsequently, it was shown that the E3/49K ORF is present in all subgenus D Ads tested, but not in Ads of other subgenera (Fig. 3) (Blusch et al., 2002). In addition, it could be shown that

the corresponding E3/49K protein is expressed by all subgenus D Ads examined. Thus, E3/49K may be implicated in illnesses characteristically caused by subgenus D Ads, which exhibit a tropism for the eye. The sequence predicts a type I transmembrane protein with an N-terminal signal sequence (Fig. 6). The ORF encodes a protein of the calculated molecular weight of 48,984 (46,915 without signal peptide). The short cytoplasmic tail contains two motifs, YXX Φ and LL, that are known to be implicated in endosomal/lysosomal targeting (chapter 1.8.3.2). Both motifs are conserved among 49K proteins of all subgenus D Ad serotypes (Blusch et al., 2002). Remarkably, the E3/49K sequence predicts 14 potential N-glycosylation sites and three potential O-glycosylation sites.

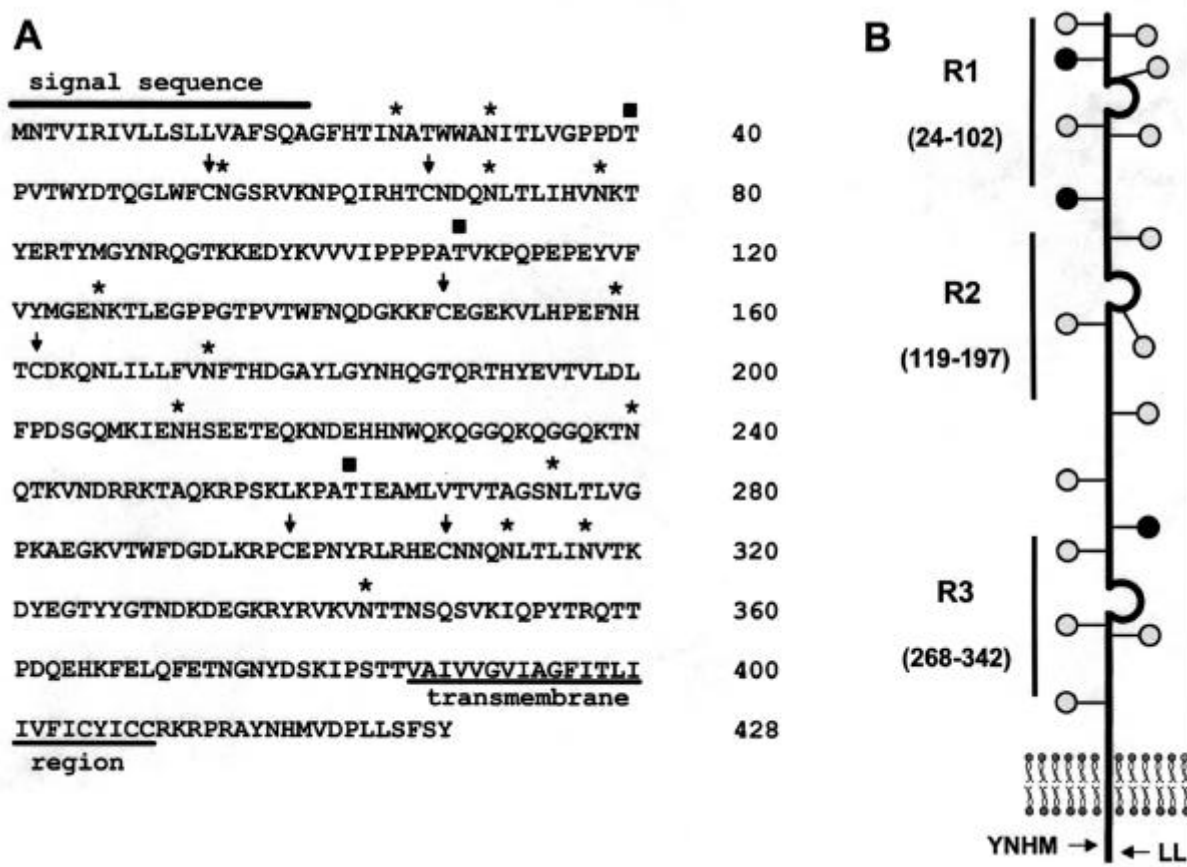


FIG. 6: Primary sequence and structural model of E3/49K. (A) Amino acid sequence of the Ad19a E3/49K protein. The putative signal sequence, the transmembrane region, the predicted N-glycosylation sites (*), O-glycosylation sites (■; (Hansen et al., 1998)) and cysteine residues possibly involved in disulfide bonds (↓) are indicated. (B) Structural model of the Ad19a E3/49K protein. The luminal part is suggested to contain three domains with one disulfide bond each. The previously noted repeat structures R1-R3 with the respective amino acid positions in brackets are marked as black bars (Deryckere and Burgert, 1996). Predicted N- and O-glycosylation sites are indicated as grey and black circles, respectively. Proposed disulfide bonded loops are shown as open circles.

The extracellular domain contains three regions with internal homology (R1-3, Fig. 6, 7), which show limited similarity (<25%) to the 20.1K and 20.5K proteins of Ad3 of subgenus B (Fig. 7A) (Deryckere and Burgert, 1996). Each region encompasses ~80 amino acids and contains two cysteine residues, which may be involved in disulfide bonding (Fig. 6). The R3 domain was found

to show some similarity to immunoglobulin-like domains (Fig. 7C). Based on the similarities between R1, R2 and R3, a similar fold might be postulated for all three domains. Also, the cytoplasmic tails of Ad19a 49K and Ad3 20.1K and 20.5K show some homologies (Fig. 7B). Interestingly, the LL motif is found in all of these proteins.

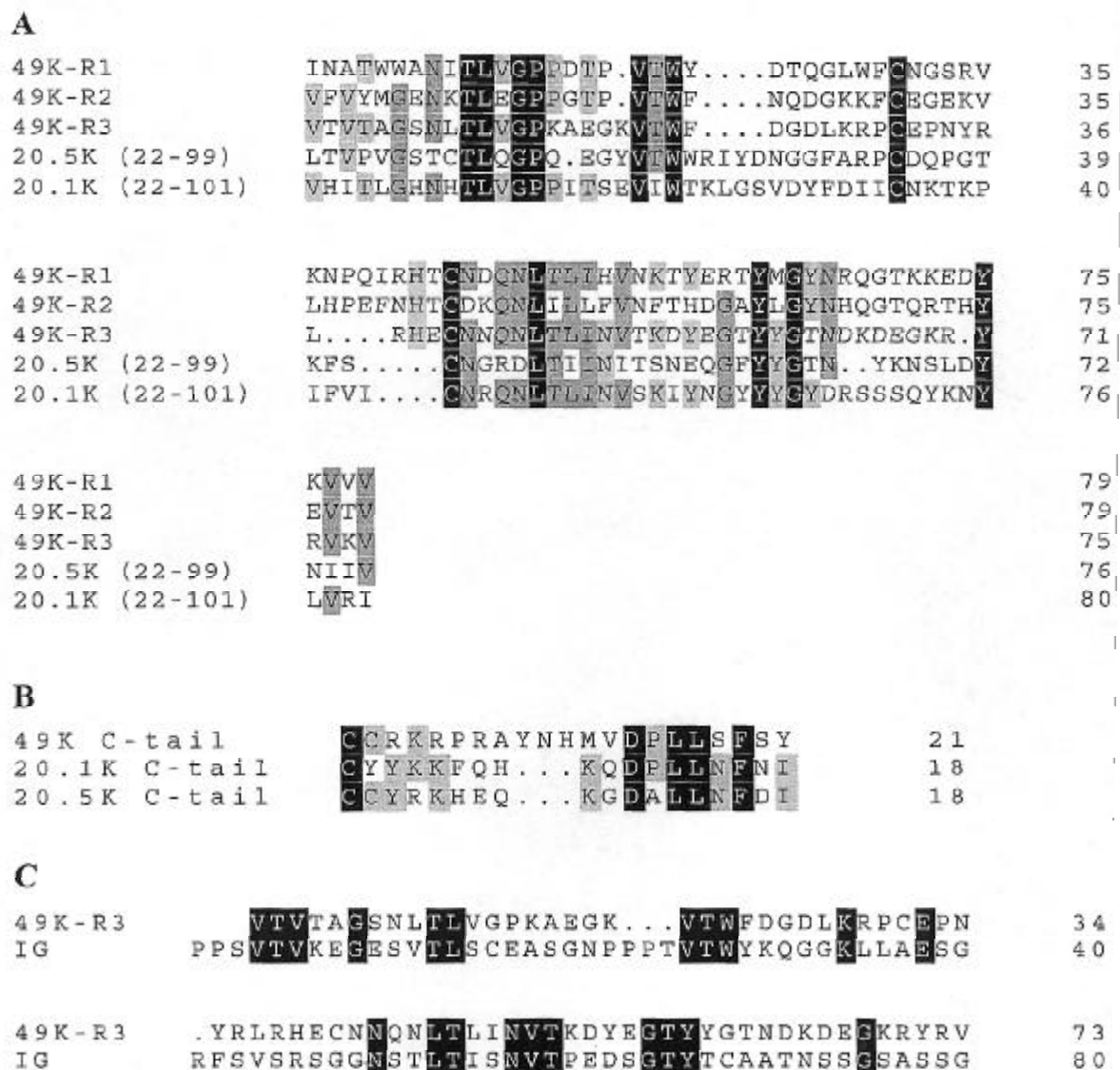


FIG. 7: Homologies between repeat regions (R1-R3) and the cytoplasmic tail of Ad19a E3/49K with Ad3 20.1K and 20.5K and immunoglobulin-like domains. All alignments were performed with DNAMAN 4.20 (Lynnan BioSoft). (A) Alignment of 49K repeat regions R1-R3 with Ad3 20.5K (22-99) and 20.1K (22-101). Different degrees of homology are indicated by different shadings (100% black, >75% dark grey, >50% grey). (B) Alignment of the cytoplasmic tails of 49K and Ad3 20.1K and 20.5K. Shadings are as described above. (C) Alignment of 49K R3 region with immunoglobulin-like domain consensus sequence smart00409 (Schultz et al., 2000).

1.11 Aim of this study

The Ad E3 region most likely contributes to subgenus-specific pathogenesis (chapter 1.1, 1.3, 1.7). However, most studies so far concentrated on subgenus C Ad E3 proteins, and no functional data of Ad E3 proteins not present in subgenus C have been gained. However, such investigations are required to understand the mechanisms that determine subgenus-specific pathogenesis. Subgenus D Ads have the tendency to cause diseases of the eye. The E3/49K protein, which is unique to subgenus D Ads, might play a role in this respect. Few subgenus D Ads, Ad19a, Ad37 and Ad8, cause a severe eye disease, the epidemic keratoconjunctivitis. 49K proteins of different subgenus D Ads may have differential activities that are relevant for serotype-specific pathogenesis, e.g. for the disease pattern characteristic to the epidemic keratoconjunctivitis.

The aim of this work was to study the biochemistry and cell biology of the Ad19a E3/49K protein and to get insight into its function. First, predicted and unexpected posttranslational modifications were examined. Second, the intracellular trafficking of E3/49K was investigated, and particularly the importance of the potential endosomal/lysosomal sorting motifs was addressed. Third, initial data indicative of the function of E3/49K were obtained. The implications of these data for subgenus- or serotype-specific pathogenesis are discussed.

2 MATERIALS AND METHODS

2.1 Materials

2.1.1 Equipment

ABI PRISM System (DNA Sequencing)	Perkin Elmer, Applied Biosystems Division, Foster City, USA
Bacterial Shaker	B.Braun, Melsungen, Germany
Balances	Sartorius, Göttingen, Germany
β -Counter LS6000TA	Beckman, Fullerton, USA
Centrifuge GP	Beckman, Palo Alto, USA
Centrifuge J2-21	Beckman, Palo Alto, USA
Centrifuge Varifuge 3.0R	Heraeus, Hanau, Germany
Centrifuge, refrigerated and non-refrigerated	Heraeus, Hanau, Germany
Chromatography column C10/10	Amersham-Pharmacia, Freiburg, Germany
Confocal laser scanning microscope	Leitz DM IRB Wetzlar, Germany
Confocal laser scanner	Leica TCS NT, Heerbrugg, Switzerland
Eagle eye	Stratagene, Amsterdam, The Netherlands
FACSCalibur	Becton Dickinson, Heidelberg, Germany
Film developing machine Optimax Typ TR	MS Laborgeräte, Heidelberg, Germany
Fluorescence-/light microscope Axiovert 35	Zeiss, Oberkochen, Germany
Fridge (4°C)	Liebherr, Ochsenhausen, Germany
Freezer (-20°C)	Liebherr, Ochsenhausen, Germany
Freezer (-80°C)	Forma Scientific, Inc., Marietta, Ohio, USA
Cryo 1°C Freezing Container	Nalgene Nunc, Wiesbaden, Germany
γ -Counter (COBRA, Auto-Gamma)	Packard, Groningen, The Netherlands
Gel dryer	Bio-Rad, Munich, Germany
GelAir drying system	Bio-Rad, Munich, Germany
Gradient former	Gibco BRL, Karlsruhe, Germany
Incubators for cell culture (37°C)	Heraeus, Hanau, Germany
Inverted microscope Axiovert 25	Zeiss, Oberkochen, Germany
Laminar Flow Hood Lamin Air	BDK, Sonnenbühl-Genkingen, Germany
Magnetic stirrer with heating block	Janke & Kunkel, Staufen, Germany
Microwave	AEG, Berlin, Germany
Multichannel pipette	ICN Flow, Costa Mesa, USA
Optimax Typ TR X-Ray film processor	MS Laborgeräte, Heidelberg, Germany
PCR Thermal Cycler 480	Perkin Elmer, Weiterstadt, Germany
Peristaltic pump P-1	Amersham-Pharmacia, Freiburg, Germany
pH-Meter	WTW, Weilheim, Germany
Phosphorimager (Storm 860 Molecular Imager)	Molecular Dynamics, Sunnyvale, USA
Phosphorimager screens	Molecular Dynamics, Sunnyvale, USA
Photometer Gene Quant II	Pharmacia/LKB, Freiburg, Germany
Pipettes	Gilson, Villies Le Bel, France;
	Eppendorf, Hamburg, Germany
Pipetting aid	Technomara, Zürich, Switzerland
Pipette stepper	Eppendorf, Hamburg, Germany
Electrophoresis Power supply EPS600	Amersham-Pharmacia, Freiburg, Germany
Overhead mixer	Heidolph, Schwabach, Germany
Sonifier 450	Branson Ultrasonics Corp., Danbury, USA
Speed vac concentrator	Savant, Farmingdale, USA
Thermomixer	Eppendorf, Hamburg, Germany

Tissue homogenizer (S)	B.Braun, Melsungen, Germany
Trans-Blot SD Semidry Transfer Cell	Bio-Rad, Munich, Germany
UV-transilluminator (366 nm)	Vetter, Wiesloch, Germany
(254 nm)	Konrad Benda, Wiesloch, Germany
Vortex mixer	Janke & Kunkel, Staufen, Germany
Water bath	Köttermann, Hängsingen, Germany

2.1.2 Chemicals

Acetic Acid	Roth, Karlsruhe, Germany
Acrylamide/Bisacrylamide 29:1 (Protogel)	National Diagnostics, Atlanta, USA
Agar for plates	Gibco BRL, Karlsruhe, Germany
Agarose (low melting point, SeaPlaque)	Biozym, Hess. Oldendorf, Germany
Agarose type I	Sigma, Munich, Germany
Ammonium chloride	Merck, Darmstadt, Germany
Ammonium persulfate (APS)	Sigma, Munich, Germany
Ampicillin	Roche Diagnostics, Mannheim, Germany
Bacto yeast extract	Gibco BRL, Karlsruhe, Germany
Bacto trypton	Difco Lab., Detroit, USA
Bafilomycin A ₁	Sigma, Munich, Germany
Bestatin	Calbiochem, Bad Soden, Germany
β-mercaptoethanol	Merck, Darmstadt, Germany
Blue Dextran/ EDTA	Perkin Elmer, Applied Biosystems Division, Foster City, USA
Boric acid	Roth, Karlsruhe, Germany
Brefeldin A	Sigma, Munich, Germany
Bromophenol blue	Serva, Heidelberg, Germany
BSA (bovine serum albumin)	Sigma, Munich, Germany
Calcium chloride	Merck, Darmstadt, Germany
Chloroform	Merck, Darmstadt, Germany
Chloroquine	Sigma, Munich, Germany
Coomassie brilliant blue R-250	Bio-Rad, Munich, Germany
Cycloheximide	Calbiochem, Bad Soden, Germany
Dimethylpimelimidate	Amersham-Pharmacia, Freiburg, Germany
Dimethylsulfoxid (DMSO)	Merck, Darmstadt, Germany
Dithiothreitol (DTT)	Roth, Karlsruhe, Germany
dNTPs	Amersham-Pharmacia, Freiburg, Germany
Dulbecco's modified Eagle's medium (DMEM)	Gibco BRL, Karlsruhe, Germany
Ethanol (EtOH)	Riedel-de Haën, Seelze, Germany
Ethidium bromide	Sigma, Munich, Germany
Ethylendiamintetraacetate disodium salt (EDTA)	Roth, Karlsruhe, Germany
Fetal calf serum (FCS)	Roche Diagnostics, Mannheim, Germany
Ficoll (type 400)	Amersham-Pharmacia, Freiburg, Germany
Formamide	Sigma, Munich, Germany
Geneticin disulfate salt (G418)	Sigma, Munich, Germany
Glucose	Merck, Darmstadt, Germany
Glycerol	Roth, Karlsruhe, Germany
Glycine	Serva, Heidelberg, Germany
Guanidine hydrochloride	Sigma, Munich, Germany
Histogel	Linaris, Wertheim-Bettingen, Germany
Hydrochloric acid (HCl)	Merck, Darmstadt, Germany
Igepal CA-630	Sigma, Munich, Germany

Imidazole	Fluka, Seelze, Germany
Iodacetamide	Sigma, Munich, Germany
Isopropanol	Riedel-de Haën, Seelze, Germany
Isopropylthio- β -D-galactosid (IPTG)	Roth, Karlsruhe, Germany
Kanamycin	Serva, Heidelberg, Germany
Leupeptin	Sigma, Munich, Germany
L-glutamine	Gibco BRL, Karlsruhe, Germany
L-glutathione (reduced)	Merck, Darmstadt, Germany
L-glutathione (oxidized)	Fluka, Seelze, Germany
Magnesium chloride	Merck, Darmstadt, Germany
Magnesium sulfate	Merck, Darmstadt, Germany
Methanol	Merck, Darmstadt, Germany
Eagle's minimal essential medium (MEM)	Gibco BRL, Karlsruhe, Germany
Eagle's minimal essential medium (MEM) without methionine	Gibco BRL, Karlsruhe, Germany
Paraformaldehyde	J.T.Baker B.V., Deventer, Holland
Pefabloc	Roche Diagnostics, Mannheim, Germany
Penicillin-Streptomycin	Gibco BRL, Karlsruhe, Germany
Pepstatin A	Calbiochem, Bad Soden, Germany
Phenol/ chloroform	Roth, Karlsruhe, Germany
Phenylmethylsulfonfluoride (PMSF)	Roche Diagnostics, Mannheim, Germany
Phosphate buffered saline (PBS) Dulbecco's (liquid)	Gibco BRL, Karlsruhe, Germany
Phosphate buffered saline (powder)	Biochrom KG, Berlin, Germany
Ponceau S	Sigma, Munich, Germany
Potassium acetate	Riedel-de Haën, Seelze, Germany
Potassium chloride	Merck, Darmstadt, Germany
Potassium phosphate salts	Merck, Darmstadt, Germany
Protein A Sepharose CL-4B	Amersham-Pharmacia, Freiburg, Germany
Protein G Sepharose Fast Flow	Amersham-Pharmacia, Freiburg, Germany
RPMI1640	Gibco BRL, Karlsruhe, Germany
RPMI1640 w/o Cys/Met	Gibco BRL, Karlsruhe, Germany
Saponin	Calbiochem, Bad Soden, Germany
Scintillator cocktail (Aquasafe 300 plus)	Zinsser, Frankfurt, Germany
[³⁵ S]-cysteine/methionine (Promix)	Amersham-Pharmacia, Freiburg, Germany
[³⁵ S]-methionine	Amersham-Pharmacia, Freiburg, Germany
SeaPlaque agarose	FMC bioproducts, Rockland, Maine, USA
Skim milk powder	Merck, Darmstadt, Germany
Sodium acetate	Riedel-de Haën, Seelze, Germany
Sodium azide	Serva, Heidelberg, Germany
Sodium borate	Merck, Darmstadt, Germany
Sodium chloride	Riedel-de Haën, Seelze, Germany
Sodium thiosulfate	Merck, Darmstadt, Germany
Sodium dodecylsulfat (SDS)	Merck, Darmstadt, Germany
Sodium carbonate	Merck, Darmstadt, Germany
Sodium hydroxid	J.T.Baker B.V., Deventer, Holland
Sodium phosphate salts	Merck, Darmstadt, Germany
Sucrose	Sigma, Munich, Germany
Tetramethylethyldiamin (TEMED)	Amersham-Pharmacia, Freiburg, Germany
Thimerosal (Merthiolate)	USB, Cleveland, USA
Trichloroacetic acid	Sigma, Munich, Germany
Triton X-100	Serva, Heidelberg, Germany

Trypsin	Gibco BRL, Karlsruhe, Germany
Trypsin inhibitor	Sigma, Munich, Germany
Tunicamycin	Sigma, Munich, Germany
Tween 20	Merck, Darmstadt, Germany
Urea	Roth, Karlsruhe, Germany
Xylene cyanol FF	Fluka, Seelze, Germany

2.1.3 Additional materials

Autoradiography films BIOMAX-MR	Eastman-Kodak, Rochester, USA
Cell culture plastic ware	Greiner, Nürtingen, Germany Nunc, Wiesbaden, Germany Falcon/Becton Dickinson, Heidelberg, Germany
Filter paper (3 mm)	Whatman Ltd., Maidstone, England
Glass plates (round, 12 mm Ø)	Roth, Karlsruhe, Germany
Glass slides for IF	Marienfeld, Bad Mergentheim, Germany
Hybond ECL Nitrocellulose membranes	Amersham-Pharmacia, Freiburg, Germany
Sterile filter units	Millipore

2.1.4 Cell lines

A549	human lung epithelial carcinoma (American Type Culture Collection (ATCC): CCL-185)
293	human embryonal kidney cell line (ATCC: CRL-1573)
SeBu	primary foreskin fibroblasts (Elsing and Burgert, 1998)
LoVo	human colorectal adenocarcinoma (ATCC: CCL-229)
Jurkat J77 (clone SVT35)	T cell leukemia (Ting et al., 1996)
Jurkat E6.1	T cell leukemia (ATCC: TIB-152)
NKL	human natural killer cell leukemia (Robertson et al., 1996), kindly provided by Christine Falk, GSF, Munich, Germany
B.3 NK	kindly provided by Christine Falk, GSF, Munich, Germany (Falk et al., 2000)
CD4 ⁺ CTL (234)	kindly provided by Christine Falk, GSF, Munich, Germany (Besser and Wank, 1999)
B.3 CD4	kindly provided by Christine Falk, GSF, Munich, Germany (Falk et al., 2000)
DS LCL	EBV-transformed B lymphocyte cell line, kindly provided by Christine Falk, GSF, Munich, Germany
BW LCL	EBV-transformed B lymphocyte cell line, kindly provided by Christine Falk, GSF, Munich, Germany
L721.221	Variant of the EBV-transformed human lymphoblastoid cell line L721 (Shimizu and DeMars, 1989), kindly provided by Christine Falk, GSF, Munich, Germany
L721.112	Variant of the EBV-transformed human lymphoblastoid cell line L721 (Shimizu and DeMars, 1989), kindly provided by Christine Falk, GSF, Munich, Germany
Daudi	Burkitt's lymphoma (B lymphoblast, ATCC: CCL-213)
K562	erythroleukemia (ATCC: CCL-243)
HeLa	human cervix carcinoma (ATCC :CCL-2)

2.1.5 Viruses

Ad19a	kind gift of Göran Wadell, Department of Virology, University of
-------	--

Ad19a-49K(-) Umea, Sweden
kindly provided by Zsolt Ruzsics, Max-von-Pettenkofer Institute,
Gene center, Munich

2.1.6 Bacterial strains

DH5 α Gibco BRL, Karlsruhe, Germany
XL1-blue Stratagene, Amsterdam, The Netherlands
M15 [pREP4] Qiagen, Hilden, Germany

2.1.7 Plasmids

pSG5 Stratagene, Amsterdam, The Netherlands
pSG5-E3/49K kindly provided by Jürgen Blusch und Kerstin Siedler
pQE-60 Qiagen, Hilden, Germany
pSV2-neo^r (Koerner et al., 1992)
pQE-60-N49K this study
pSG5-E3/49K-YA/LLAA this study
pSG5-E3/49K-LLAA this study
pSG5-E3/49K-YA this study
pSG5-E3/49K- Δ CT this study

2.1.8 Oligonucleotides

template	name	orientation	Restriction site	sequence (5'® 3')
E3/49K	49K5'NCO	sense	NcoI	gagcgccatgggatttcatactatcaatgctac
E3/49K	49K3'BAM	antisense	BamHI	cgcgggatccgggaatTTTgaatcataatttc
E3/49K	49KdelCT	antisense	BglII	gtccagatctggatccgtcttaacgcttgcggcagcagatgtagc
E3/49K	49KYLLAAA	antisense	BglII	gtccagatctggatccgtcttagtaagagaagctggctgctgggt ctaccatagattggctgcctgggacgctt
E3/49K	49KYA	antisense	BglII	gtccagatctggatccgtcttagtaagagaagctgagtagt ggctaccatagattggctgcctgggacgctt
E3/49K	49KLLAA	antisense	BglII	gtccagatctggatccgtcttagtaagagaagctggctgctgggt ctaccata
pSG5	pSG549K2497rev	antisense	BglII	ggacaaaccacaactagaatgcag
E3/49K	49K1000rev	antisense	BglII	gtaccatagtaagttcctcataatc
E3/49K	49K1000sense	sense	BglII	ttatgaggaacttactatggtagc
E3/49K	49K340rev	antisense	BglII	ggttttacagtagcaggaggaggtgg
E3/49K	49KUSER546	sense		ggtacaatcatcaaggaaccagag
E3/49K	19.20	antisense		tgttcacatggatcaa
E3/49K	19.21	sense		ttgatccatgtgaaca
E3/49K	19.24	antisense		atagtgtgttctctg
E3/49K	21	sense		ggttggacctaaagcagaagg
E3/49K	22	antisense		Ccttctgctttagtccaacc

The oligonucleotides were obtained from metabion (Martinsried, Germany).

2.1.9 Molecular weight markers

DNA Molecular Weight Marker X (0.07-12.2 kbp) Roche Diagnostics, Mannheim, Germany
Protein marker Dalton VII-L (14000-70000) Sigma, Munich, German
[¹⁴C] methylated protein marker (14300-220000) Amersham-Pharmacia, Freiburg, Germany

2.1.10 Kits

BigDye RR Terminator Amplitaq FS Kit	Perkin Elmer, Applied Biosystems Division, Foster City, USA
BCA Protein Assay	Pierce, Rockford, USA
ECL western blotting detection system	Amersham-Pharmacia, Freiburg, Germany
Nucleobond Kit	Macherey-Nagel, Düren, Germany
Pharmacia GFX Micro Plasmid Kit	Amersham-Pharmacia, Freiburg, Germany
Protein Assay	Bio-Rad, Munich, Germany
QIAex II Agarose Gel Extraction Kit	Qiagen, Hilden, Germany
QIAquick PCR Purification Kit	Qiagen, Hilden, Germany
Qiagen Plasmid Maxi Kit	Qiagen, Hilden, Germany

2.1.11 Antibodies**2.1.11.1 Primary antibodies**

anti-Ad19a E3/49K (C-terminus)	R25050, R25044, polyclonal rabbit antisera raised against the C-terminal 15 amino acids of E3/49K, a cysteine was added to the N-terminus for directed coupling to KLH or ovalbumin (Blusch et al., 2002)
anti-Ad19a E3/19K	polyclonal rabbit antisera (Deryckere and Burgert, 1996)
anti- Ad2 hexon	mouse mAb, 2Hx-2, ATCC HB-8117
anti-TGN46	sheep and rabbit serum, kindly provided by S. Ponnambalam, University of Dundee, Scotland
anti- β 1 \rightarrow 4-Galactosyltransferase	mouse mAb, GTL2, (Kawano et al., 1994)
anti-GM130	mouse mAb, clone 35, Transduction Laboratories, Lexington, USA
anti-lamp-2	2D5, mouse mAb (Diettrich et al., 1996)
anti-lamp-1	polyclonal rabbit serum, 931-A, kindly provided by S. Carlson, University of Umea, Sweden
anti-lysobisphosphatidic acid	6C4, mouse mAb (Kobayashi et al., 1998)
anti-transferrin receptor	mouse mAb, clone number L01.1, Becton Dickinson, Heidelberg, Germany, and 5E9C11, ATCC HB-21
anti-EEA1	mouse mAb, clone 14, Transduction Laboratories, Lexington, USA
anti-CD46	mouse mAb, J4-48, Dianova, Hamburg, Germany
anti-AP1	mouse mAb, 100/3, Sigma, Munich, Germany
anti-HLA-A, -B, and -C	mouse mAb, W6/32, ATCC HB95
anti-E1B 19K	rat mAb, Oncogene Science, Manhasset, NY, USA
anti-E1B 55K	rat mAb, Oncogene Science, Manhasset, NY, USA
anti-Ad19a E3/49K (N-terminus)	polyclonal rabbit antiserum directed against the N-terminal part of 49K: R48-1B to R48-8B, R47-1B to R47-10B; this study
anti-Ad19a E3/49K (N-terminus)	rat mAb, directed against the N-terminal part of 49K: 4D1, 1E6, 1F4, 1H8, 5A7, 5D3, 6C12, 6C9, 7H10, 10A11; this study

2.1.11.2 Secondary antibodies

Fluoresceine (FITC)- conjugated:	
Goat anti-Mouse IgG (Cat.No. F2012)	Sigma, Munich, Germany
Goat anti-Mouse IgG (Cat.No. 115-095-146)	Dianova, Hamburg, Germany

Rabbit anti-Rat IgG (Cat.No. FI-4000)	Vector Laboratories, Burlingame, CA, USA
Goat anti-Rabbit IgG (Cat.No. 111-095-144)	Dianova, Hamburg, Germany
Donkey anti-Rabbit IgG (Cat.No. 711-095-152)	Dianova, Hamburg, Germany
Donkey anti-Mouse IgG (Cat.No. 715-095-151)	Dianova, Hamburg, Germany
Rhodamine-, Cy3 or Texas-Red-conjugated:	
Goat anti-Mouse IgG (Cat.No. 115-165-068)	Dianova, Hamburg, Germany
Goat anti-Rat IgG (Cat.No. 112-295-143)	Dianova, Hamburg, Germany
Goat anti-Rabbit IgG (Cat.No. 111-295-045)	Dianova, Hamburg, Germany
Donkey anti-Sheep IgG (Cat.No. 713-295-147)	Dianova, Hamburg, Germany
Donkey anti-Rat IgG (Cat.No. 712-075-153)	Dianova, Hamburg, Germany
Peroxidase conjugated:	
Goat anti-Rat IgG (Cat.No. 112-035-062)	Dianova, Hamburg, Germany
Goat anti-Rabbit IgG (Cat.No. 111-035-144)	Dianova, Hamburg, Germany
Not modified:	
Anti-rat IgG (Cat.No. R3756)	Sigma, Munich, Germany
Anti-mouse IgG (Cat.No. M7023)	Sigma, Munich, Germany

2.1.12 Enzymes

Lysozyme	Roche Diagnostics, Mannheim, Germany
T4 DNA Ligase	MBI Fermentas, St. Leon-Rot, Germany
Phosphatase, alkaline, shrimp (SAP)	Roche Diagnostics, Mannheim, Germany
Proteinase K	Sigma, Munich, Germany
Pwo DNA Polymerase	Roche Diagnostics, Mannheim, Germany
Restriction Endonucleases	MBI Fermentas, St. Leon-Rot, Germany
	Roche Diagnostics, Mannheim, Germany
	New England Biolabs, Beverly, USA
N-glycosidase F (PNGase F)	Roche Diagnostics, Mannheim, Germany
Neuraminidase (Arthrobacter ureafaciens)	Roche Diagnostics, Mannheim, Germany
Endoglycosidase H (Streptomyces plicatus)	Roche Diagnostics, Mannheim, Germany
O-glycosidase (Diplococcus pneumoniae)	Roche Diagnostics, Mannheim, Germany

2.2 Methods

2.2.1 Bacterial cell culture

2.2.1.1 Cultivation and conservation of bacteria

E. coli bacteria were grown in LB medium or on LB agar plates. Incubation was performed at 37°C with constant shaking. For conservation 500 µl aliquots of a bacterial culture in the exponential growth phase obtained after inoculation from single colonies were mixed with 500 µl of LB/30% glycerol, frozen in liquid nitrogen and stored at -70°C.

LB medium (1 l):	10 g Bacto tryptone
	5 g Bacto yeast extract
	5 g NaCl

LB agar:	LB medium with 1.5-2 % agar
Selection medium:	LB medium with 100 µg/ml ampicillin and/or 25 µg/ml kanamycin

2.2.1.2 Preparation of competent bacteria

For preparation of competent bacteria a single clone DH5 α was picked and grown o/n in 5 ml LB at 37°C. 1 ml of the bacterial culture was then transferred to 100 ml LB and incubated 3 h at 37°C until the OD_{600nm} was 0.35-0.49. The following incubations were all performed at 4°C or on ice. The bacteria were distributed to two 50 ml tubes and centrifuged 5 min at 3500 rpm (Heraeus Varifuge 3.0R). The supernatants were discarded and the pellets were resuspended in 15 ml ice-cold Tfb I. After 40-50 min incubation on ice, the bacteria were centrifuged 10 min at 2500 rpm (Heraeus Varifuge 3.0R). The supernatants were discarded and the pellets were resuspended in 4 ml ice-cold Tfb II. Aliquots of 0.2 ml were added to precilled 1.5 ml reaction tubes and stored at -80°C.

Tfb I:	Tfb II:
100 mM RbCl ₂	10 mM MOPS pH 7.0
50 mM MnCl ₂	10 mM RbCl ₂
30 mM KAc	75 mM CaCl ₂
10 mM CaCl	15% (v/v) glycerol
15% (v/v) glycerol	
pH adjusted to 5.8 with 0.2 M HAc	
both buffers sterilized by filtration (Ø0.2 µm) and stored at 4°C	

2.2.1.3 Transformation

Different volumes of the ligation reaction mixture (2, 5, 10 µl) were added to 100 µl competent bacteria and incubated 30 min on ice. After the heat shock, 2 min 42°C, 1 ml LB medium was added and bacteria were cultivated for 1 h at 37°C. Then 100 µl were taken and plated on LB agar plates with antibiotic(s). The residual bacteria were centrifuged (4000 g, 5 min), resuspended and plated the same way. The plates were incubated o/n at 37°C.

2.2.2 DNA techniques

2.2.2.1 Purification of plasmid DNA

Plasmid DNA was purified with the Pharmacia GFX Micro Plasmid Kit in small scale and the Qiagen Plasmid Maxi Kit or the Nucleobond Kit in large scale according to the manufacturer's instructions.

2.2.2.2 Determination of DNA concentration

The concentration and purity of the purified DNA was determined by measuring the UV absorbance at 260 and 280 nm. The DNA concentration was calculated with the OD_{260nm}

(1 OD_{260nm} = 50 µg/ml dsDNA or 33 µg/ml ssDNA). The purity was estimated with the OD_{260nm}/OD_{280nm} ratio, with a ratio of ca. 1.8 indicating a low degree of protein contamination.

2.2.2.3 Restriction endonuclease digestion

Restriction endonuclease reactions were performed according to the manufacturer's recommendations. In general, 1 µg DNA was digested for 1 h at 37°C with 1-3 U enzyme. Efficacy of the cleavage reaction was controlled by agarose gel electrophoresis.

2.2.2.4 5'-Dephosphorylation reaction

5'-dephosphorylation reaction of plasmid vector DNA after restriction endonuclease cleavage was performed with the shrimp alkaline phosphatase (SAP). 2 U SAP were added to about 2 µg restriction enzyme digested plasmid DNA. After 30 min incubation at 37 °C the phosphatase was inactivated by heating to 65°C for 15 min and the DNA was isolated by phenol/chloroform extraction and ethanol precipitation (see below).

2.2.2.5 Polymerase chain reaction (PCR)

Polymerase Chain Reaction (PCR) was performed with the Pwo DNA polymerase from *Pyrococcus woesei* with a 3'→5' exonuclease proofreading activity.

The reaction mixture contained:

10 µl 10x PCR Puffer (100 mM Tris-HCl pH 8.85, 250 mM KCl, 50 mM (NH₄)₂SO₄, 20 mM MgSO₄)
2 µl 10 mM dNTPs (200 µM each)
2 µl 10 µM sense primer (200 nM)
2 µl 10 µM antisense primer (200 nM)
0.5 µl Pwo (2.5U)
83.5 µl H₂O
+ 0.1 µg template DNA

The following cycles were performed:

a) Amplification of the region encoding the N-terminal part of E3/49K for the cloning of the His-Tag-fusion construct:

1. 94°C 5 min
2. 94°C 1 min
3. 55°C 1 min
4. 72°C 2 min
5. 72°C 10 min

} 25x

b) Amplification of the region encoding the C-terminal part of E3/49K and site-directed mutagenesis:

1. 94°C 5 min
 2. 94 °C 1 min
 3. 62°C 2 min
 4. 72°C 2 min
 5. 72°C min 10 min
- } 12x with a decrease of 1°C per cycle down to 50°C (touchdown), then 15x

2.2.2.6 Isolation of DNA fragments

DNA fragments were separated by agarose gel electrophoresis, stained with ethidium bromide and detected with UV light (366 nm). The gel slice containing the DNA fragments was cut out and the DNA was isolated using the QIAex II Agarose Gel Extraction Kit according to the manufacturer's instructions. Alternatively, DNA fragments from PCR reactions were purified using the QIAquick PCR Purification Kit according to the manufacturer's instructions.

2.2.2.7 Phenol/chloroform extraction and ethanol precipitation

Proteins were removed from DNA preparations by extracting twice with 1x volume phenol/chloroform and once with 1x volume chloroform. After vigorous vortexing for 10 s the solution was centrifuged at 14000 rpm (microcentrifuge) for 1 min and the upper DNA containing phase was recovered. Then 0.1x volume 3 M NaAc pH 5.2 and 3x volume 100% EtOH (cold) were added, and incubation at -20°C was performed for 1-12 h. The precipitated DNA was centrifuged down at 14000 rpm for 30 min (4°C). Then the pellet was washed once with 70% EtOH (cold). After another centrifugation step (14000 rpm, 15 min, 4°C, microcentrifuge) the EtOH was carefully removed, the pellet air-dried at RT and finally resuspended in H₂O or 10 mM Tris pH 8.0.

2.2.2.8 Ligation

For ligation about 100-200 ng vector DNA was used with a molar ration of vector/insert of about 1:1. The reaction was performed in a total volume of 20 µl 1x reaction buffer (MBI Fermentas) with 2 U T4 DNA Ligase (MBI Fermentas).

In the first step vector and insert were mixed in reaction buffer and incubated 5 min at 45°C and put on ice. Then the ligase was added. After incubation at 1 h 22°C the ligase was inactivated by heating 10 min at 65 °C.

2.2.2.9 DNA sequencing

2.2.2.9.1 PCR

DNA sequencing was performed using the BigDye RR Terminator Amplitaq FS Kit. The reaction mixture contained 8 µl Premix, 1 µg dsDNA template and 10 pmol primer in a total

volume of 20 μ l.

Then the PCR was performed:

96°C 10 s
50°C 5 s
60°C 4 min } 25x

The product was precipitated by adding 30 μ l H₂O, 5 μ l 3 M NaAc pH 5.2 and 135 μ l EtOH (RT). After 15 min centrifugation at 15000 rpm the pellet was washed with 280 μ l 70% EtOH (RT). Then it was centrifuged for 10 min at 14000 rpm (microcentrifuge), the EtOH was removed and the pellet air-dried.

2.2.2.9.2 Polyacrylamide gel electrophoresis

A 5% polyacrylamide gel (8 M urea, 200 x 560 x 0.3 mm) was prepared as follows:

30 g urea
10 ml 30% acrylamide/bisacrylamide (29:1)
6 ml 10x TBE buffer
22 ml H₂O

10x TBE buffer (1l): 108 g Tris base
55 g Boric acid
7.4 g EDTA

The solution was incubated at 37°C until the urea was dissolved. Then the solution was filtered with a 0.2 μ m filter and degassed for 10 min. 20 μ l TEMED and 350 μ l 10% APS solution were added and the gel was poured and polymerized horizontally for 4 h.

The precipitated DNA from the PCR reaction was resuspended in 2 μ l Blue Dextran/EDTA (50 mg/ml Blue Dextran, 25 mM EDTA pH 8) and 8 μ l formamide and heated for 10 min at 95°C. Then the samples were put on ice for 5 min. After 1 min centrifugation at 14000 rpm (microcentrifuge) 4 μ l of the solution was loaded on the gel. The gel run was performed with 1x TBE buffer at 37 Watt for 18 h (prerun 30 min). Sequencing data were analyzed using the ABI PRISM software.

2.2.2.10 Agarose gel electrophoresis

Analysis of DNA fragments and plasmids was performed by agarose gel electrophoresis in 1x TAE. In general, agarose concentration was between 1 and 2 % in 1x TAE. The agarose was solubilized by heating in a microwave oven. Ethidium bromide was added to a final concentration of 0.1 μ g/ml (1 μ l stock to 100 ml) just before pouring the gel. Probes were mixed with 0.17x volume loading buffer. Gels (6.5 x 9.5 cm) were run horizontally at 80-120 V. DNA was detected with UV light, λ =254 nm or λ =366 nm to cut out specific fragments.

Loading buffer (6x in water):	0.25% bromophenol blue 0.25% xylene cyanol FF 15% Ficoll (type 400)
20x TAE:	800 mM Tris 400 mM NaAc 40 mM EDTA adjusted to pH 7.8 with acetic acid
Ethidium bromide (stock):	10 mg/ml

2.2.3 Tissue culture

2.2.3.1 Cultivation and cryoconservation

A549, 293, SeBu and HeLa cells were maintained in Dulbecco's modified Eagle's medium (DMEM) supplemented with 100 U/ml penicillin, 0.1 mg/ml streptomycin and 10% fetal calf serum at 37°C and 5% CO₂. Jurkat J77 (SVT 35) cells were maintained in RPMI medium supplemented with 100 U/ml penicillin, 0.1 mg/ml streptomycin and 10% fetal calf serum.

For cryoconservation cells were detached with trypsin and centrifuged at 300 g for 5 min at 4°C. Then the cells were resuspended in 1 ml 25% FCS/10% DMSO/65% DMEM (4°C) with a final concentration of 0.5-1x10⁷ cells/ml and transferred to cryovials which were cooled to -70°C in a "Cryo 1°C Freezing Container". From there the vials were transferred to liquid nitrogen for long-term storage. Frozen aliquots were quickly thawed at 37°C in a waterbath, 1x volume DMEM was added and the suspension was carefully pipetted onto a FCS cushion. After centrifugation at 300 g for 5 min the supernatant was removed, cells were resuspended in complete medium and transferred to cell culture dishes.

2.2.3.2 Calcium phosphate transfection

For transient transfection cells were grown on 6 cm Ø dishes to 60-70% confluency. 4 h prior to the transfection the medium was changed. 250 µl of 2x HBS pH 7.05 was added to a 1.5 ml reaction tube. In another tube 6-8 µg DNA was combined with H₂O to a total volume of 225 µl, followed by the addition of 25 µl 2.5 M CaCl₂. The tube with the 2x HBS was vortexed with 800 rpm while the DNA/CaCl₂ solution was added dropwise. The solution was incubated at RT for 15-20 min to allow the formation of the Calcium-DNA precipitate. Subsequently, the suspension was added directly to the medium of the cells. The next day, the medium was changed and 36-48h later protein expression was assessed by immunofluorescence. To generate transfectants stably expressing the E3/49K protein cells were transfected with 20 µg pSG5-E3/49K and 2 µg pSV2-neo^r, the latter conferring G418 resistance, per 10 cm Ø dishes. After two days cells were split 1:4 or 1:8 and cultivated in medium containing 200 µg/ml (293) or 1 mg/ml G418 (A549).

After 10-14 days clones were trypsinized using cloning cylinders and transferred to 3 cm \varnothing dishes. Usually, 20-30 clones were obtained per 10 cm \varnothing dish.

2x HBS pH 7.05: 50 mM HEPES
 1.5 mM Na₂HPO₄ x 2 H₂O
 280 mM NaCl
 12 mM glucose

2.2.3.3 Adenovirus infection

Cells were grown to 80-90% confluency and washed once with DMEM without FCS. In general, 5-10 plaque forming units (pfu) were applied per cell in 1 ml DMEM without FCS. Dishes were incubated for 1-1.5 h in the incubator and were shaken every 10-15 min. Then the virus containing medium was removed, and DMEM with 2.5% FCS was added. This time point was defined as the start of infection. Virus containing solutions were inactivated by disposing them in solutions with >1% SDS.

2.2.3.4 Preparation of adenovirus stocks

To prepare virus stocks A549 cells were grown in T175-flasks to 80-90% confluency. The cells were washed 1x with 30 ml DMEM without FCS. Then 8 ml DMEM without FCS containing $1-4 \times 10^7$ PFUs virus were added and incubated 3 h in the incubator with shaking every 10 min. Then the medium was removed, 35 ml DMEM/1.5% FCS were added and cells were incubated until the cytopathic effect (CPE) reached 100%, which generally took 4-5 days. If necessary additional 15 ml DMEM/1.5% FCS were added after 3 days. Infected cells were detached by shaking the flasks heavily. Then the cells were transferred to 50 ml plastic tubes and centrifuged 10 min at 300 g and 4°C. Infected cells were resuspended in 2 ml PBS (per flask) and viruses were released by 3-4 freeze/thaw cycles: Cells were frozen at -70°C (>30 min) and thawed at 37°C in a water bath. Finally, the samples were centrifuged 10 min at 3500 rpm (Heraeus Varifuge 3.0R) to remove cell debris and the supernatant was split into aliquots of 0.5-1 ml and stored at -70°C. Usually 7-10 T175 flasks were harvested for one virus stock.

2.2.3.5 Plaque assay

Ad19a virus stocks were quantified by plaque assays (Mittereder et al., 1996). Virus stocks were diluted $1:10^9$, 10^8 , 10^7 , 10^6 in DMEM without FCS. A549 cells were grown to 95% confluency and washed once with DMEM without FCS. Then 1 ml DMEM containing different virus dilutions was added and incubated 1.5 h in the incubator shaking every 10 min. 2% sterile low melting point agarose (SeaPlaque, in H₂O) was solubilized in the microwave and a sufficient volume was kept at 37°C together with 2x DMEM. At the end of the adsorption time the DMEM containing virus was removed. 2% low melting point agarose was mixed 1:1 with 2x DMEM and 5 ml was

added to each dish. The dishes were left 10 min at RT (lids partly off) until the agarose hardened. Then the dishes were transferred to the incubator. Cells metabolize approximately 1 ml medium per day. When the medium became yellow, i.e. acidic, indicating depletion of nutrition 3 ml DMEM/1% agarose was added. At around 15-17 days plaques appeared and were counted every day. The final PFU was determined when the PFU count was constant for 2-3 days.

2.2.3.6 Immunofluorescence

Subconfluent layers of A549 or SeBu cells were grown on sterile glass coverslips. Cells were rinsed with PBS and fixed with 3% (w/v) paraformaldehyde in PBS for 20 min. After quenching aldehyde groups with 50 mM NH₄Cl and 20 mM glycine in PBS for 10 min, cells were permeabilized with 0.2% saponin in PBS with 5% FCS to block non-specific binding for 10 min. The cells were incubated with the primary antibody diluted in 0.2% saponin/ 5% FCS in PBS for 1 h, washed four times with 1 ml 0.2% saponin in PBS and incubated with the secondary antibody (fluorescein- or rhodamine-conjugated goat or donkey anti-mouse, anti-rabbit or anti-sheep IgG, respectively, dilution 1:50) for 1 h. After four washing steps with 1 ml 0.2% saponin in PBS, the coverslips were mounted on glass slides with Histogel. The mounted cells were analyzed with a laser scanning confocal microscope.

Antibody	dilution
rabbit anti-49K Carboxy-terminus (R25050)	1:300
rabbit anti-49K N-terminal domain (R48-7/8B)	1:300
rat mAb anti-49K N-terminal domain (supernatant)	undiluted
mouse mAb anti-lamp-2 (2D5, supernatant)	1:10
mouse mAb anti-Calnexin (AF8)	1:100
mouse mAb anti-Galactosyltransferase (GTL2)	1:200
mouse mAb anti-LBPA (6C4)	1:100
mouse mAb anti- γ -adaptin	1:50
mouse mAb anti-EEA1	1:50
mouse mAb anti-transferrin-receptor (5E9C11, supernatant)	undiluted
mouse mAb anti-GM130	1:100
sheep anti-TGN46	1:100
rabbit anti-TGN46	1:100

2.2.3.7 Flow cytometry analysis

For flow cytometry analysis cells were washed once with PBS and detached with 1 mM EDTA in PBS. Cells were centrifuged (300 g, 5 min) and resuspended in FACS (fluorescence activated cell sorter) buffer. 30 μ l with 300000-500000 cells were added to 70 μ l FACS buffer containing the first antibody (ca. 1 μ g purified antibody or undiluted hybridoma supernatant) in a well of a 96-well plate. In the negative control no or isotype control antibody was added. After incubation for 45 min at 4°C, cells were washed 3x with 190 μ l FACS buffer and 50 μ l of secondary antibody

solution (Sigma 1:50, Vector 1:300) was added. Subsequently, it was incubated for 40 min at 4°C in the dark. After three washing steps with 190 µl FACS buffer the cells were resuspended in 100 µl FACS buffer and transferred to plastic tubes with 400 µl FACS buffer and 5000 cells were analyzed in a FACSCalibur flow cytometer.

FACS buffer for cell surface staining:

3% (v/v) FCS
0.02% (w/v) NaN₃
in PBS

FACS buffer for intracellular staining:

0.1% (w/v) saponin
3% (v/v) FCS
0.02% (w/v) NaN₃
in PBS

2.2.3.8 Flow-cytometry-based 49K binding assay

For the investigation of 49K binding to the cell surface of different cell lines a modified flow cytometry protocol was applied. In variation from the standard protocol as described, cells were incubated 1 h with ca. 200 ng purified secreted 49K at 4°C prior to the incubation with the anti-49K antibody (4D1, supernatant, undiluted). In the following, flow cytometry analysis was performed as described.

2.2.3.9 NK cell-mediated lysis

NK cell-mediated lysis was quantified in a standard chromium-51 assay as described (Schendel et al., 1979). Spontaneous release was determined by incubating target cells alone in complete medium. Total release was determined by directly counting an aliquot of labeled cells. The percent cytotoxicity was calculated according to the formula: lysis [%] = (experimental cpm - spontaneous cpm / total cpm - spontaneous cpm) x 100. Total volume was 100 µl. Purified secreted 49K and controls were diluted and 25 µl were combined with Killer cells (NKL, clone 234) in total volume of 50 µl. Preincubation, 30 min at RT to allow binding to receptor(s), was followed by addition of chromium-51 labeled target cells in 50 µl and a standard chromium-51 assay.

2.2.4 Protein techniques

2.2.4.1 Metabolic labeling and immunoprecipitation

A549 or 293 cells were grown on 6 cm Ø culture dishes to 80-90% confluency. After washing once with 5 ml MEM without methionine (and cysteine), cells were incubated with 2 ml MEM without methionine (and cysteine) for 1 h to deplete the intracellular levels of methionine (and

cysteine). Then cells were metabolically labeled with 100 or 200 μCi [^{35}S]-methionine or a mixture of [^{35}S]-methionine and [^{35}S]-cysteine for different time periods. In pulse/chase experiments, subsequently, the cells were washed with DMEM containing unlabeled methionine (and cysteine) and chased for different times with the same medium. Finally, the cells were washed once with cold DMEM and once with cold PBS. The cells were lysed with 1 ml IP-lysis buffer containing freshly added protease inhibitors at 4°C for 10 min. The supernatant was transferred to 1.5 ml tubes. After 15 min centrifugation at 14000 rpm (4°C, cooled microcentrifuge) the supernatants were transferred to new 1.5 ml tubes. To monitor the incorporation of radioactive label 5 μl lysate were added to 1 ml scintillation cocktail and the amount of radioactivity was measured with a β -counter. All further incubations were performed at 4°C. After adding 5 μl preserum (rabbit) to the rest of the lysate, it was incubated for 45 min rotating in an overhead mixer. Preequilibrated protein A-Sepharose was washed 3x with buffer B and a 50% slurry was prepared. 50 μl of the 50% slurry was added to each sample, followed by another incubation for 45 min rotating in an overhead mixer. The protein A-Sepharose beads were centrifuged for 30 s at 14000 rpm (microcentrifuge). The lysate was transferred to 5 μl specific serum (rabbit) in a new 1.5 ml tube and incubated for 45 min rotating in an overhead mixer. 50 μl of a 50% protein A-Sepharose slurry was added followed by another incubation for 45 min rotating in an overhead mixer. The protein A-Sepharose beads were centrifuged for 30 s at 14000 rpm (microcentrifuge). The pellet was washed 3x with 1 ml buffer B, 2x with 1 ml buffer C and 1x with 1 ml 10 mM Tris pH 8. Finally, the pellet was centrifuged for 2 min at 14000 rpm (microcentrifuge). The supernatant was completely removed and the samples were either directly resuspended in SDS sample buffer and analyzed by SDS-PAGE or were stored at -70°C.

Redivue™ L-[^{35}S]-methionine: 10 mCi/ml, specific activity >1000 Ci/mmol

Promix™: 70% L-[^{35}S]-methionine, 30% [^{35}S]-cysteine, 14.3 mCi/ml, specific activity >1000 Ci/mmol

IP-lysis buffer:	1% Triton X-100 140 mM NaCl 5 mM MgCl ₂ 20 mM Tris pH 7.6	Buffer B:	0.2% Triton X-100 150 mM NaCl pH 8.0 2 mM EDTA 10 mM Tris pH 7.6
added freshly from stock:	8 $\mu\text{g}/\text{ml}$ PMSF 10 $\mu\text{g}/\text{ml}$ trypsin inhibitor 0.5 $\mu\text{g}/\text{ml}$ leupeptin	Buffer C:	0.2% Triton X-100 500 mM NaCl 2 mM EDTA pH 8.0 10 mM Tris pH 7.6

Equilibration of protein A-Sepharose:

1.5 g protein A-Sepharose CL-4B was washed 3x with 5 ml 100 mM Tris pH 8.0, 2x with 5 ml 50 mM Tris pH 8.0, 1x with 5 ml 10 mM Tris pH 8.0. Finally, the protein A-Sepharose was resuspended in 10 mM Tris pH 8.0 to obtain a 50% slurry.

2.2.4.2 Glycosidase digestions

For endoglycosidase H (Endo H) treatment the protein A-Sepharose pellet with the immunoprecipitated protein was resuspended in 50 μ l reaction buffer (0.1 M sodium citrate pH 5.5) and incubated for 24 h at 37°C with 5 mU of Endo H from *Streptomyces plicatus*. The mock treated samples were incubated under the same conditions without Endo H. In the partial digestion experiment (Fig. 17) only 2 mU Endo H were used for each reaction and the incubation time was shortened to the times indicated. Treatment with neuraminidase, O-glycosidase and peptide-N-glycosidase F (PNGase F) was carried out sequentially: The protein A-Sepharose pellet with the immunoprecipitated protein was first resuspended in 50 μ l reaction buffer (50 mM sodium phosphate pH 7.2) and incubated for 6 h at 37°C with 20 mU neuraminidase from *Arthrobacter ureafaciens* and/or 2 mU O-glycosidase from *Diplococcus pneumoniae*. Subsequently, the pellets were washed once with 1 ml 10 mM Tris pH 8.0 and resuspended in 12.5 μ l 0.1 M β -mercaptoethanol/0.5% SDS and incubated at 95°C for 5 min. 12.5 μ l buffer including 1 U PNGase F of *Flavobacterium meningosepticum* was added to give final concentrations of 0.2 M Tris pH 8, 0.02 M EDTA, 2% IGEPAL and the sample was incubated for 20 h at 37°C. The mock treated samples were incubated under the same conditions without PNGase F.

2.2.4.3 SDS PAGE

2.2.4.3.1 Maxigel

Gel electrophoresis was performed using 11.5 % or 7.5 % to 13.5 % gradient gels (200 x 300 x 1 mm) (Laemmli, 1970). The two solutions for generating the separation gel were mixed in a gradient former and after pouring the gel, it was overlaid with isopropanol. After polymerization the isopropanol was removed by washing with H₂O. The stacking gel solution was poured on top of the separation gel and a comb (20 wells, 0.8 cm wide) was fixed. After polymerization the glass plates containing the gel were assembled in the gel electrophoresis apparatus. Samples or pellets from immunoprecipitation were resuspended in 25 μ l sample buffer and heated for 5 min to 95°C. After cooling to RT 5 μ l 0.5 M iodacetamide was added and samples were incubated for 15 min at RT. Then the samples were centrifuged for 2 min at 14000 rpm (microcentrifuge) and loaded on the gel. ¹⁴C-methylated proteins were used as molecular weight markers. Separation was performed at 18-25 mA constant current for 12-18 h. Then the gel was fixed in fixing solution for 45 min, transferred to Whatman paper, covered with plastic foil and dried for 2 h at

80°C under vacuum in a gel dryer. Dried gels were exposed to BioMaxMR films at -70° C or phosphorimager screens at RT. Radioactive bands were quantified using a Storm 860 Molecular Imager. Films were developed using an automatic film developing machine.

<u>Separation gel :</u>	<u>7.5%</u>	<u>11.5%</u>	<u>13.5%</u>
Acrylamide/Bisacrylamide (29 :1)	10 ml	15.3 ml	18 ml
2 M Tris pH 8.8	8.4 ml	8.4 ml	8.4 ml
20 % SDS	0.2 ml	0.2 ml	0.2 ml
H ₂ O	21.4 ml	16.1 ml	3.4 ml
60% sucrose	-	-	10 ml
10 % APS	120 µl	120 µl	120 µl
TEMED	20 µl	20 µl	20 µl

<u>Stacking gel:</u>	<u>5%</u>
Acrylamide/Bisacrylamide (29:1)	5 ml
0.5 M Tris pH 6.8	4 ml
20 % SDS	0.15 ml
H ₂ O	14 ml
60% sucrose	7 ml
10 % APS	150 µl
TEMED	15 µl

Sample buffer (complete):	1 ml sample buffer pH 8.8 100 µl 0.5 M DTT (38.5 mg/500 µl) 200 µl 20% SDS
Sample buffer pH 8.8 (stock):	10 ml 2 M Tris pH8.8 57.14 ml 60% sucrose 1 ml 500 mM EDTA 0.01 g bromophenolblue
Fixing solution (1 l):	10% acetic acid 30% methanol
Electrophoresis buffer (5 x):	0.28 g/l Tris 150.14 g/l glycine 0.5% SDS (added just before use, final conc.: 0.1%)

2.2.4.3.2 Minigel

Gel electrophoresis with minigels was performed using the Protean II system (Bio-Rad) with 10% gels (80 x 50 x 1 mm). In general, the samples were mixed with 15 µl sample buffer (1:1) and the same procedure as described for maxigels was applied.

<u>Separation Gel :</u>	<u>10%</u>
Acrylamide/ Bisacrylamide (29:1)	1.665 ml
2 M Tris pH 8.8	1.05 ml
20 % SDS	0.2 ml
H ₂ O	2.24 ml
10 % APS	20 µl
TEMED	2.25 µl

<u>Stacking gel:</u>	5%
Acrylamide/ Bisacrylamide (29:1)	1.35 ml
0.5 M Tris pH 6.8	0.7 ml
20 % SDS	25 μ l
H ₂ O	14 ml
10 % APS	25 μ l
TEMED	5 μ l
 Electrophoresis buffer (10 x):	 30.28 g/l Tris 150.14 g/l glycine 1% SDS (added just before use, final conc.: 0.1%)

2.2.4.4 Western blotting

2.2.4.4.1 Preparation of cell lysate

Cells were grown to 80-90% confluency in 6 cm \varnothing culture dishes, washed with PBS and lysed with 100 μ l IP-lysis buffer. Cells were scraped from the dish with a rubber policeman, transferred to a 1.5 ml tube and incubated for 20 min on ice. After 15 min centrifugation at 14000 rpm (microcentrifuge) the supernatant was transferred to a new 1.5 ml tube and, if not used immediately, stored at -80°C . Protein concentration was determined using the Pierce BCA Kit. 10 μ g protein was loaded per lane on a minigel and SDS-PAGE analysis was performed prior to blotting.

2.2.4.4.2 Protein blotting and detection

Proteins were blotted on nitrocellulose membranes using the Trans-Blot SD Semidry Transfer Cell (Bio-Rad). A piece of nitrocellulose membrane and eight pieces of filter paper of the same size as the gel were soaked with transfer buffer. Four pieces of filter paper, the nitrocellulose membrane, the gel and another four pieces of filter paper were packed with the nitrocellulose facing the anode. Subsequently, air bubbles were removed and blotting was performed with 0.8 mA/cm² for 1.25 h. Proteins were detected after 2 min incubation in Ponceau staining solution. The position of marker proteins was labeled and the membrane was washed several times to remove the Ponceau staining solution. Unspecific binding sites were blocked by incubation in PBS, 0.05% Tween 20, 5% skim milk powder, 0.02% NaN₃ o/n. Then incubation with the first antibody was performed in 5-10 ml PBS, 0.05% Tween 20 (used also in the following washing and incubation steps). After five washing steps of 15 min with ca. 200 ml buffer each incubation with the secondary antibody coupled to peroxidase was performed in 25 ml buffer followed by washing 5x 10 min and 1x 30 min in 200 ml buffer. Then the blotted proteins were detected using the ECL Western blotting detection system (Amersham-Pharmacia) according to the manufacturer's instructions. The membrane was exposed to BIOMAX-MR autoradiography films for different time periods.

Transfer buffer (1l):		Ponceau solution (100 ml):	
Tris base	5.8 g	Ponceau S	0.5 g
Glycine	2.9 g	Glacial acetic acid	1 ml
SDS	0.37 g	H ₂ O	98.5 ml
Methanol	200 ml		
H ₂ O	to 1l		

Antibody	dilution
rabbit anti-49K Carboxy-terminus (R25050)	1:1000
rabbit anti-49K N-terminal domain (R48-7/8B)	1:1000
rat mAb anti-49K N-terminal domain (supernatant)	1:10
rat mAb anti-E1B-19K	1:100
rat mAb anti E1B-55K	1:100
goat anti-rabbit peroxidase coupled	1:10000 – 1:20000
goat anti-rat peroxidase coupled	1:5000

2.2.4.5 Surface plasmon resonance

In order to test the *in vitro* binding of the clathrin adaptor complexes AP-1 and AP-2 an interaction analysis was performed by Stefan Höning, University of Göttingen, Göttingen, Germany (Honing et al., 1997). Peptides representing the cytoplasmic tail of 49K and with mutations of the potential endosomal/lysosomal sorting signal that might be crucial for the interaction with the adaptor complexes were coupled to a CM5 sensor chip. Interaction was analyzed using a BIAcore 2000 (BIAcore AB). Purified AP-1 and AP-2 were used at 100 nM in buffer A and injected at a flow rate of 20 μ l/min. Association (2 min) was followed by dissociation (2 min) during which buffer A was perfused. The equilibrium constant (K_D) was determined as described (Honing et al., 1997).

Analyzed peptides:	Buffer A:	20 mM HEPES pH 7.0
WT: CRKRPRAYNHMVDPLLSFSY		150 mM NaCl
YA: CRKRPRAAANHMVDPLLSFSY		10 mM KCl
LLAA: CRKRPRAYNHMVDPAASFSY		2 mM MgCl
YA/LLAA: CRKRPRAAANHMVDPAASFSY		0.2 mM dithiothreitol

2.2.4.6 Purification and refolding of recombinant HisTag-fusion protein

10 ml of an o/n culture of M15 [pREP4] containing the pQE-60-49K construct were added to 200 ml of prewarmed selection medium (LB with 25 μ g/ml kanamycin, 100 μ g/ml ampicillin) and grown at 37°C to an OD_{600nm} of 0.5-0.7. 1 ml medium was taken and after centrifugation the bacterial pellet was resuspended in 50 μ l 2x Sample Buffer. 200 μ l 1 M IPTG was added to the remaining medium followed by an 4 h incubation at 37°C. 1 ml medium was taken and after centrifugation the pellet was resuspended in 50 μ l 2x Sample Buffer. The remaining bacteria were pelleted by centrifugation at 4000 g for 20 min and resuspended in 5 ml buffer (0.1 M sodium phosphate, 0.01 M Tris, pH 8 including 10 μ M leupeptin, 1 μ M pepstatin, 500 μ M pefabloc, 10

μ M bestatin) at 4°C. 1.5 mg lysozyme was added per g bacteria and after incubation for 30 min on ice bacteria were sonicated 6x for 10 s (output control level 7, 100 %) with a Branson Sonifier 450. 0.5x volume buffer (0.1 M sodium phosphate, 0.01 M Tris, pH 8, 6% Triton X-100, 1.5 M NaCl) including protease inhibitors was added, and after 30 min incubation at 4°C inclusion bodies (IBs) were pelleted by 30 min centrifugation at 31000 g. The pellet was resuspended in 20 ml 0.1 M sodium phosphate, 0.01 M Tris, pH 8 including protease inhibitors with a Dounce tissue homogenizer and centrifuged again. Then the IB pellet was resuspended in 5 ml buffer (6 M guanidine hydrochloride, 0.1 M sodium phosphate, 0.01 M Tris, pH 8, 5 mM β -mercaptoethanol) using the Dounce tissue homogenizer. After incubation for 2 h at 25°C, debris was pelleted by centrifugation (10000 g) for 30 min at 4°C. The protein concentration was determined using the Bio-Rad protein assay kit (according to Bradford). 1 ml Ni-agarose beads slurry was mixed with 0.5-1 mg protein in 5 ml buffer (6 M guanidine hydrochloride, 0.1 M sodium phosphate, 0.01 M Tris pH 8, 5 mM β -mercaptoethanol) and incubated 1 h at RT. The suspension was transferred to a column. The beads were washed two times with 5 ml buffer (6 M guanidine hydrochloride, 0.1 M sodium phosphate, 0.01 M Tris, pH 7, 5 mM β -mercaptoethanol) and were resuspended rapidly in 30 ml degassed refolding buffer (0.1 M sodium phosphate, 0.01 M Tris, pH 7.6, 0.3 mM GSSG, 3 mM GSH, 50 mM NaCl including protease inhibitors) and incubated rotating overnight at 4°C. Subsequently, the suspension was transferred to a column and washed twice with 5 ml buffer (0.1 M sodium phosphate, 0.01 M Tris, pH 7.6, 150 mM NaCl, 0.2 mM β -mercaptoethanol) after a frit had been assembled on top of the beads. Then the HisTag-fusion protein was eluted with 16x 0.5 ml elution buffer (0.1 M sodium phosphate, 0.01 M Tris, pH 7.6, 150 mM NaCl, 0.2 mM β -mercaptoethanol, 250 mM imidazol). Eluted fractions were analyzed by SDS-PAGE. Protein concentration was determined by OD_{280nm}. After washing two times with 5 ml buffer (0.1 M sodium phosphate, 0.01 M Tris, pH 7.6, 150 mM NaCl, 5 mM β -mercaptoethanol) and incubation for 1 h at RT in 5 ml buffer (6 M guanidine hydrochloride, 0.1 M sodium phosphate, 0.01 M Tris, pH 8, 5 mM β -mercaptoethanol) the beads were regenerated by elution with 16x 0.5 ml buffer (6 M guanidine hydrochloride, 0.1 M sodium phosphate, 0.01 M Tris, pH 4.5, 5 mM β -mercaptoethanol) and washing with 2x 10 ml buffer (0.1 M sodium phosphate, 0.01 M Tris, pH 8). For SDS-PAGE analysis of fractions containing guanidine hydrochloride, protein was precipitated with 1x volume 10% trichloroacetic acid and during 20 min incubation on ice. After centrifugation at 14000 rpm (4°C, cooled microcentrifuge) for 15 min the pellet was washed with cold 100% EtOH followed by centrifugation for another 5 min. Then the supernatant was carefully removed, the pellet air-dried and resuspended in sample buffer for analysis.

2.2.4.7 Production of rabbit polyclonal and rat monoclonal antibodies

2.2.4.7.1 Rabbit polyclonal antibodies

Rabbits were immunized with approximately 250 µg 49K-HisTag-fusion protein in 500 µl buffer mixed with 500 µl complete Freund's adjuvant by subcutaneous (s.c.) injection. Boosts were performed in the same way ca. every 2-3 weeks but with incomplete Freund's adjuvant replacing the complete Freund's adjuvant. About 20 ml blood were recovered usually ca. 10 days after boosting. Serum was recovered by incubation at RT for several hours, 30 min incubation at 37°C and o/n at 4°C. Finally, the blood was centrifuged for 15 min at 3000 rpm (Heraeus Varifuge 3.0R) and serum aliquots of 0.5-1 ml were prepared and stored at -70°C.

The course of the antibody development was followed by immunoprecipitation experiments, and the rabbit was sacrificed when the specific activity of the antibodies remained constant.

2.2.4.7.2 Rat monoclonal antibodies

Rat monoclonal antibodies were generated by Elisabeth Kremmer, GSF, Munich, Germany (Kremmer et al., 1995). Lou/C rats were immunized 3x with 50 µg N49K-HisTag-fusion protein in intervals of three weeks. The first injection was done with complete Freund's adjuvant, the second with incomplete Freund's adjuvant both intraperitoneally and subcutaneously and the third without adjuvant intraperitoneally. Fusion of rat immune spleen cells with the myeloma cell line P3X63Ag8.653 was performed following the protocol of Köhler and Milstein 3 days after the final boost (Kohler and Milstein, 1992). Supernatants from hybridoma cells were tested for the presence of anti-49K antibodies by an enzyme-linked immunosorbent assay (ELISA). Microtiter plates were coated with approximately 0.5 µg/well N49K-Histag-fusion protein by incubation in 0.2 M sodium carbonate buffer pH 9.5 o/n. Hybridoma supernatants were added and incubated 30 min with constant shaking followed by 30 min incubation with peroxidase-coupled goat anti-rat antibody. Finally, bound antibody was detected using the chromogen o-phenylenediamine in a peroxidase reaction. ELISA positive supernatants were tested in immunofluorescence for the detection of native 49K. Hybridoma cells producing antibodies recognizing native 49K (4D1, 1E6) were subcloned at least twice by limiting dilution. The immunoglobulin-isotyps were determined by ELISA.

2.2.4.8 Purification of secreted E3/49K

2.2.4.8.1 Coupling of antibody to the protein G-Sepharose column

5 ml 1 M Tris pH 7.4 was added to 50 ml of hybridoma supernatant containing anti-E3/49K rat monoclonal antibodies (4D1) in a concentration of about 40 µg/ml (total 2 mg). 1 ml protein G-

Sepharose beads was washed three times with 10 ml 0.1 M Tris pH 7.4 and added to the hybridoma supernatant. After incubation for 2 h at RT and gentle mixing, the beads were washed three times with 0.2 M sodium borate pH 9.0 (centrifugation: 3000 g for 5 min) and then resuspended in 10 ml 0.2 M sodium borate. 100 μ l of slurry was removed for analysis. 50 mg dimethyl pimelimidate (DMP) were added to give a final concentration of about 20 mM. Incubation was performed at RT with gentle mixing for 45 min. 100 μ l of slurry was removed for analysis. The reaction was stopped by washing the beads once in 0.2 M ethanolamine pH 8 followed by incubation for 2 h at RT in 0.2 M ethanolamine pH 8 with gentle mixing. Then the beads were washed three times with PBS and stored in PBS/0.01% merthiolate (thimerosal) at 4°C. Efficiency of coupling was tested by SDS-PAGE with beads taken before and after the coupling reaction in order to evaluate the elution of antibody.

2.2.4.8.2 Purification protocol

Secreted E3/49K was purified from medium of cell lines stably expressing the E3/49K protein. In general, cells were grown in 150-175 cm² (T175) plastic flasks to 80-90% confluency and washed once with DMEM without FCS. Thereafter, about 35 ml DMEM without FCS was added and cells were cultivated for 7-9 days. The medium was collected and contaminating cells were removed from the medium by centrifugation (500 g, 5 min). The medium was transferred to another tube and stored at 4 °C. 1/10x volume of 10x PBS and 1/100x volume 2% NaN₃ were added as well as the protease inhibitors PMSF, trypsin inhibitor, leupeptin in the same concentrations as used in immunoprecipitation (chapter 2.2.4.1). To remove antibodies or other proteins binding to the protein G-Sepharose specifically or unspecifically the medium was preabsorbed on a protein G-Sepharose column with 2 ml beads: At first, the column was washed with 20 ml PBS. Then the medium was transferred to the column with a flow rate of 10-15 ml/h using a peristaltic pump. The column was washed with 20 ml PBS and 20 ml 10 mM sodium phosphate buffer pH 6.8. Bound protein was eluted with 10 ml glycine buffer pH 2.5 and 1 ml fractions were collected and neutralized with 100 μ l 1 M Tris pH 8. For reconstitution, the protein G-Sepharose column was washed with 20 ml PBS and stored in PBS/0.01% merthiolate at 4°C. Prior to transferring the medium to the column with protein G-Sepharose coupled to the E3/49K specific antibodies, the column was washed with 20 ml PBS. The flow rate was adapted to approximately 5 ml/h using a peristaltic pump. After loading, the column was washed with 20 ml PBS and 20 ml 10 mM sodium phosphate buffer pH 6.8. Then bound E3/49K was eluted with 8x 0.45 ml 0.1 M glycine buffer pH 3.0 and collected in tubes containing 75 μ l 1 M Tris pH 8.0. For reconstitution the column was washed with 20 ml PBS and then stored in PBS/0.01% merthiolate at 4°C. E3/49K in the eluted fractions was detected by Western blotting and silver staining.

2.2.4.9 Silver staining

For silver staining (Blum et al., 1987), polyacrylamide gels were fixed in 30% methanol/10% acetic acid for at least 2 h and subsequently washed 3x for 30 min with 30% ethanol. Then the gels were transferred for 1 min to a 0.22 g $\text{Na}_2\text{S}_2\text{O}_3 \times 5 \text{H}_2\text{O}$ /l solution followed by washing with H_2O 3x for 1 min. Subsequently, the gels were incubated with 2 g AgNO_3 /l, 0.025 % paraformaldehyde for 20-30 min, washed 3x with H_2O for 1 min followed by the reduction step in 60 g Na_2CO_3 /l, 0.0185 % paraformaldehyde, 4 mg $\text{Na}_2\text{S}_2\text{O}_3 \times 5 \text{H}_2\text{O}$ /l for 1-10 min. Paraformaldehyde was added from a freshly thawed 16% stock solution stored at -20°C . Then the gels were washed 3x for 5 min with H_2O and the reaction was stopped by a 10 min incubation in 30% methanol/10% acetic acid. Finally, the gels were incubated for more than 30 min in 30% methanol and dried using Bio-Rad GelAir drying system.

2.2.4.10 Coomassie blue staining

For Coomassie blue staining of proteins, SDS-PAGE gels were incubated in Coomassie blue staining solution for 1-12 h and destained with 30% methanol/10% acetic acid by changing the destaining solution until the desired protein staining was visible.

Coomassie blue staining solution: 0.25% Coomassie brilliant blue R-250
 45% methanol
 10% acetic acid

3 RESULTS

3.1 Time course of Ad19a E3/49K synthesis during infection

E3/49K was identified as a novel gene within the E3 region of the epidemic keratoconjunctivitis (EKC) causing Ad strain Ad19a (Deryckere and Burgert, 1996) and was recently shown to be specific for subgenus D Ads (Blusch et al., 2002). As E3/49K is encoded by the early transcription unit 3, it is supposed to be an early protein. However, some E3 proteins are only poorly expressed early but their expression is greatly amplified at late times (Li and Wold, 2000; Tollefson et al., 1992). Therefore, the expression of E3/49K during the course of infection was monitored in comparison to E3/19K, another early protein, and hexon, a late protein (Fig. 8).

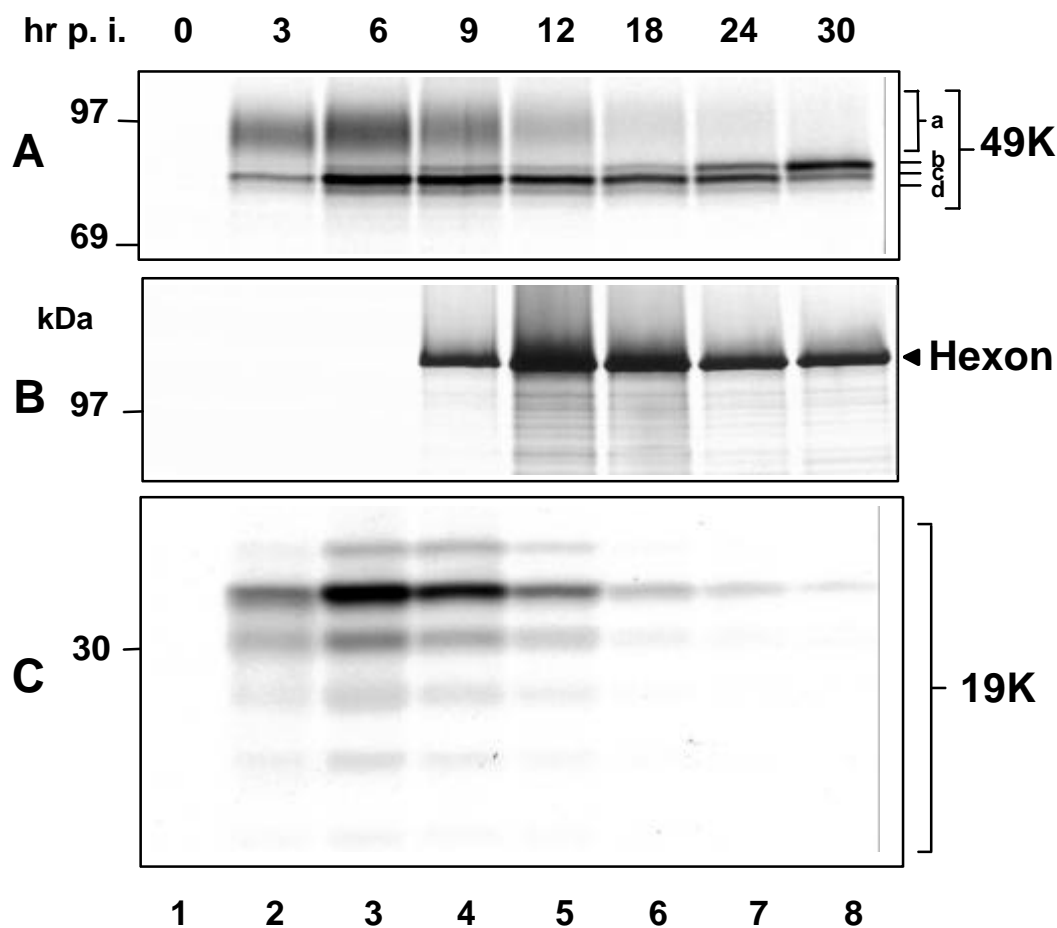


FIG. 8. Time course of Ad19a E3/49K synthesis during infection. A549 cells were labeled with [³⁵S]-methionine at different time points postinfection (p.i.). The start of infection was defined as the end of the 1 h adsorption period. The indicated times given on top of the figure correspond to the start of the 1 h labeling period. Lysates with equal amounts of radioactivity were used for immunoprecipitation. E3/49K (A), E3/19K (C), another early protein, and hexon (B), a late protein, were immunoprecipitated sequentially from the same lysates using the antibodies given in Materials and Methods. E3/49K is visualized by three defined bands with apparent molecular masses of 77-83 kDa, designated b, c, and d, and a diffuse band of 87-100 kDa, designated a. E3/19K is represented by six bands differing in the number of N-glycans attached.

A549 cells were labeled for 1 h with [³⁵S]-methionine at different time points postinfection (p.i.) and after immunoprecipitation, proteins were analyzed by SDS-PAGE. Several bands representing different forms of E3/49K could be visualized: Defined bands representing proteins with the apparent molecular mass of about 77-83 kDa (b-d) and a diffuse band representing proteins of about 87-100 kDa (a). Expression of E3/49K and E3/19K was first detected at 3 h p.i. and reached a maximum at 6 h p.i. In contrast to E3/19K expression that declines rapidly, E3/49K was still expressed late during infection. Interestingly, the glycosylation pattern of E3/49K seemed to change during the course of infection. The intensity of the diffuse band (a) decreased and concomitantly the intensity of one of the lower bands (b) increased in the late phase of infection.

3.2 Carbohydrate processing of E3/49K early and late during infection

To investigate whether this differential appearance, particularly the absence of the diffuse band late during infection (Fig. 8), was due to an impaired carbohydrate processing a pulse/chase analysis was performed early (6 h p.i., Fig. 9, lanes 1-7) and late (30 h p.i., Fig. 9, lanes 8-14) during infection. In the early phase of infection the E3/49K species represented by the defined lower bands b-d (Fig. 9, lane 1) were converted to the E3/49K forms represented by the diffuse upper band a (Fig. 9, lanes 2-7), presumably representing terminally glycosylated products. Late during infection this processing of the protein was severely impaired (Fig. 9, lanes 8-14). Interestingly, low molecular weight fragments were detected in the chased samples (60-240 min) early during infection indicating proteolytic processing (h, lanes 4-7). These were absent late during infection. Thus, carbohydrate as well as proteolytic processing was impaired late during infection. The half-life of Ad19a E3/49K was determined to be only ~2 h in the early phase of infection (6 h p.i.). In the late phase of infection (30 h p.i.) the half-life was significantly prolonged to more than 4 h. The half-life was defined by the time period after which half of the initial protein labeling could still be detected.

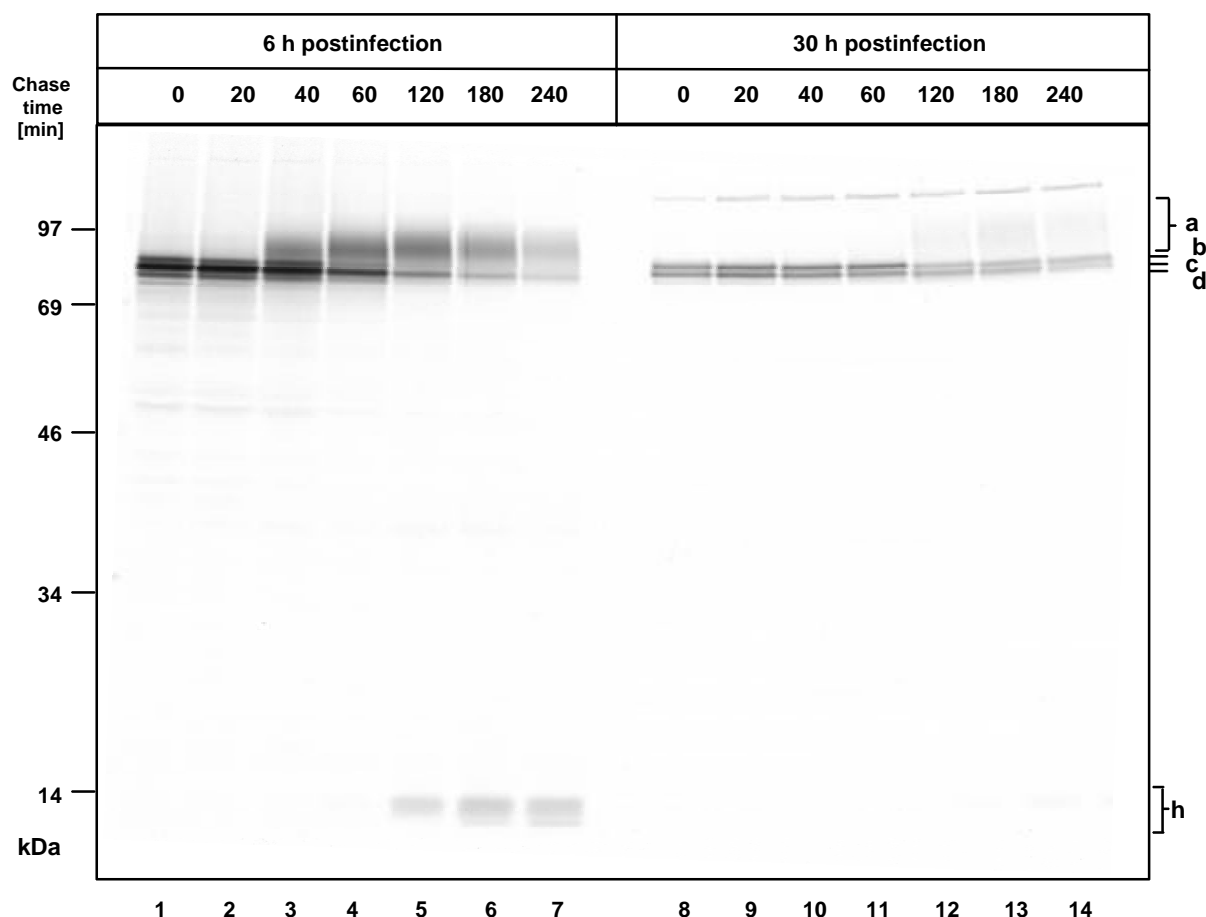
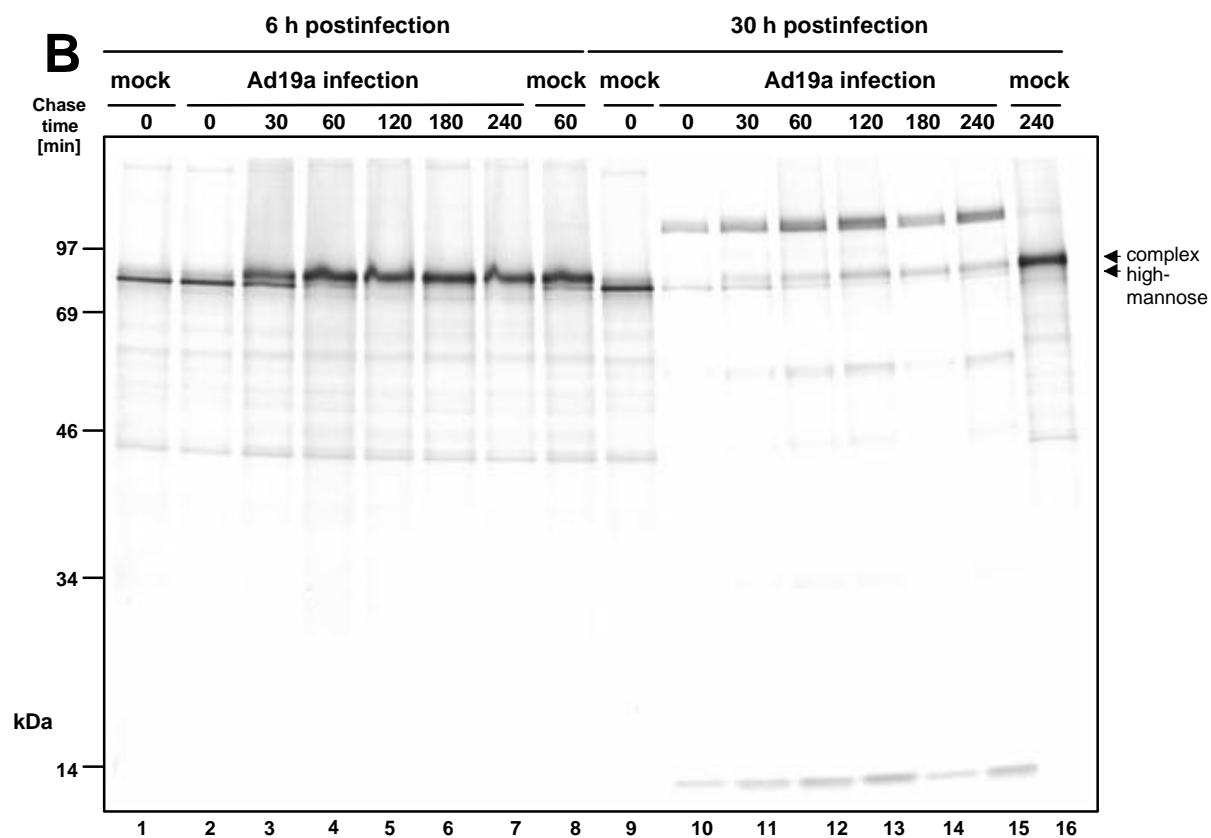
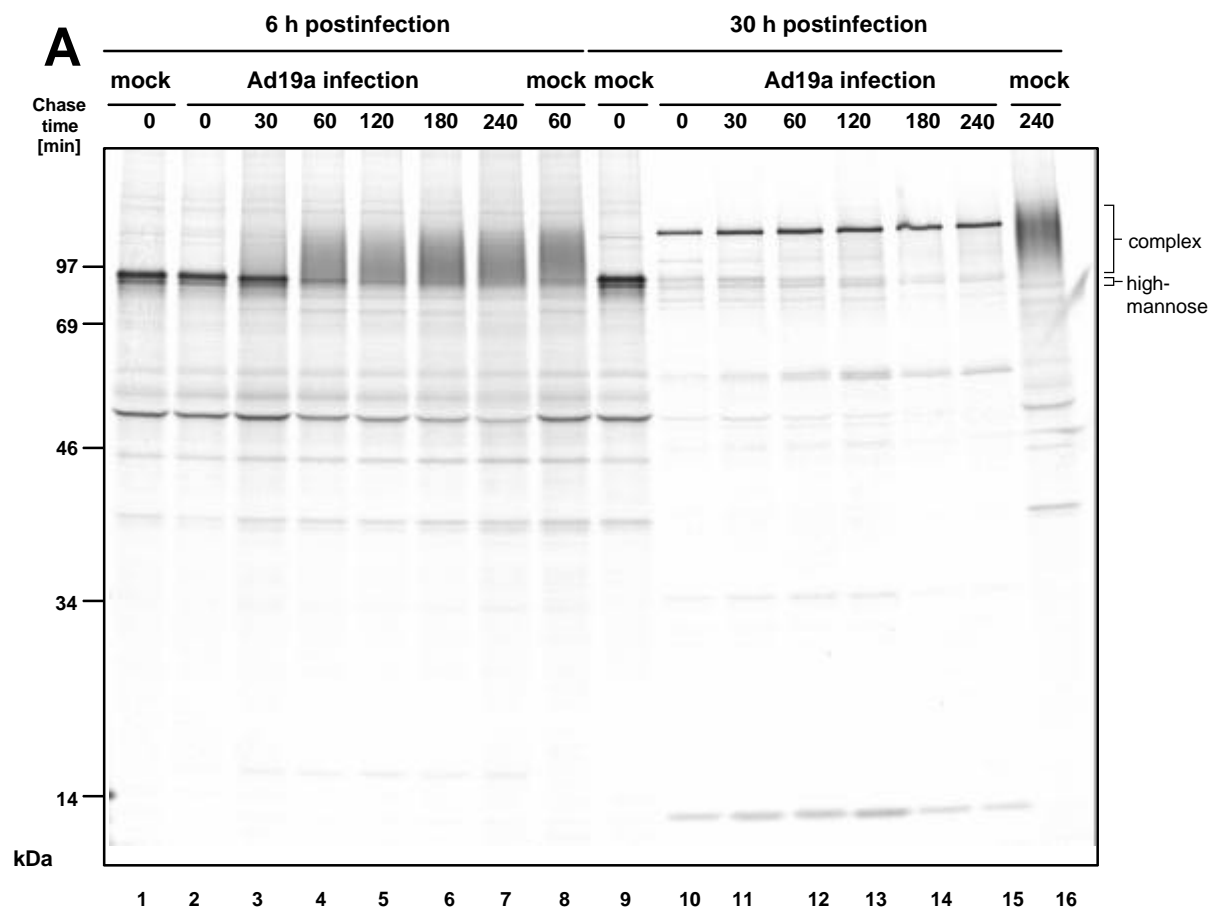


FIG. 9. Differential processing of E3/49K in the early and late phase of infection. A pulse/chase analysis was carried out 6 h p.i. (early) or 30 h p.i. (late). A549 cells were metabolically labeled for 20 min with 200 μ Ci/ml [35 S]-methionine/cysteine and subsequently chased with medium containing non-radioactive methionine/cysteine for the indicated periods of time. Ad19a E3/49K protein was immunoprecipitated (R25050) and analyzed by SDS-PAGE as in Fig. 8. Bands a-d represent different forms of E3/49K. In addition, during the chase low molecular weight fragments were detected (h).

Then it was examined whether the observed processing defect of E3/49K in the late phase of infection is common also to host proteins by monitoring the processing of lysosome-associated membrane protein 1, lamp-1 (Fig. 10A), and the transferrin receptor (Fig. 10B). The interpretation of these data is complicated by the decreased expression of cellular proteins late during infection due to the host shutoff (Fig. 10C, compare lanes 10-15, 30 h p.i., with lanes 2-7, 6 h p.i.). Nevertheless, it is obvious that lamp-1 exhibited also an impaired processing during the late phase of infection (Fig. 10A, compare lanes 10-15 with lanes 2-7). Early during infection high-mannose lamp-1 proteins were completely processed within 120 min chase (Fig. 10A, lanes 2-5), whereas late during infection high-mannose lamp-1 forms were detected up to 240 min chase. Transferrin receptor on the other hand was not significantly affected (Fig. 10B, compare lanes 10-15 to lanes 2-7). Therefore, the inhibition of glycan processing was not a general phenomenon but rather seemed to affect a selective set of glycoproteins.



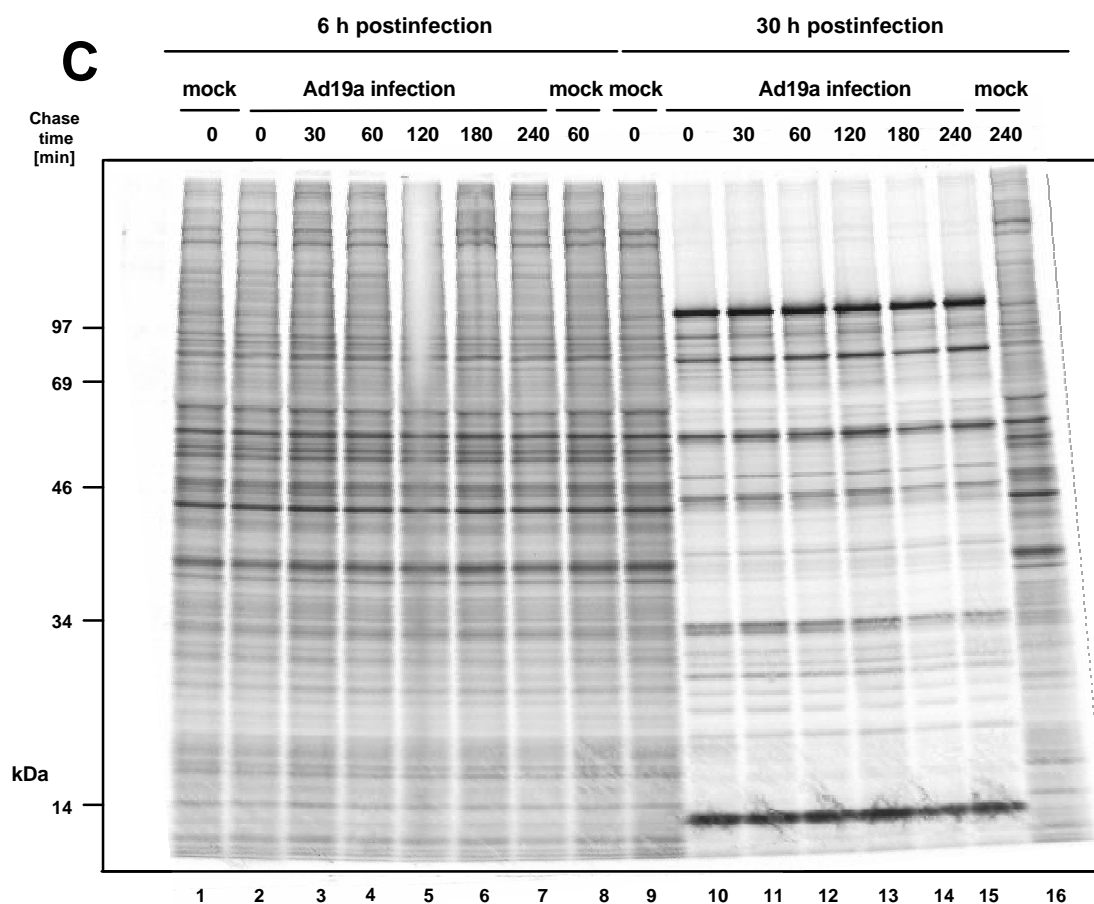


FIG. 10. Inhibition of glycan processing late during Ad19a infection is neither a 49K specific nor a general phenomenon. In a pulse/chase experiment as described in Fig. 9 the processing of cellular proteins lamp-1 (A) and transferrin receptor (B) was investigated by immunoprecipitation using antibodies described in Materials and Methods. High-mannose and complex glycan containing protein species are indicated. 30 h postinfection synthesis of cellular proteins was dramatically decreased, also shown by analysis of 5 μ l of total cell lysate (C).

3.3 E3/49K expression in 293 and A549 cell lines

To investigate 49K independently of the viral context, e.g. glycan or proteolytic processing and localization, cell lines stably expressing 49K were established (Fig. 11). A549 and 293 cells were transfected with a pSG5 vector (Stratagene) containing the Ad19a gene under control of the early SV40 promoter with the intron II of the rabbit β -globin gene located at the 5'-end of the 49K gene. Clones stably expressing 49K were isolated as described in Materials and Methods. Most 293 clones exhibited in addition to the 49K-specific bands detected in infection two bands representing protein(s) with a molecular mass of approximately 47 and 57 kDa (e.g. K62). Only few 293 clones reproduced the pattern seen in infection (e.g. K35). Data from pulse/chase experiments and Western blotting analysis indicated that the 57 kDa protein is a degradation product of 49K, whereas the 47 kDa protein coprecipitates with 49K (data not shown). These bands were not detected in A549 cell lines expressing 49K. Interestingly, the low molecular

weight fragments (h) observed in infection (Fig. 9) were also detected in 293 as well as in A549 clones expressing 49K. Thus, the carbohydrate and proteolytic processing of 49K seen in infection could be reproduced in A549 and partly in 293 cell lines stably expressing 49K. In the following, A549 cell lines were used as a model system to investigate biochemical and functional features of 49K.

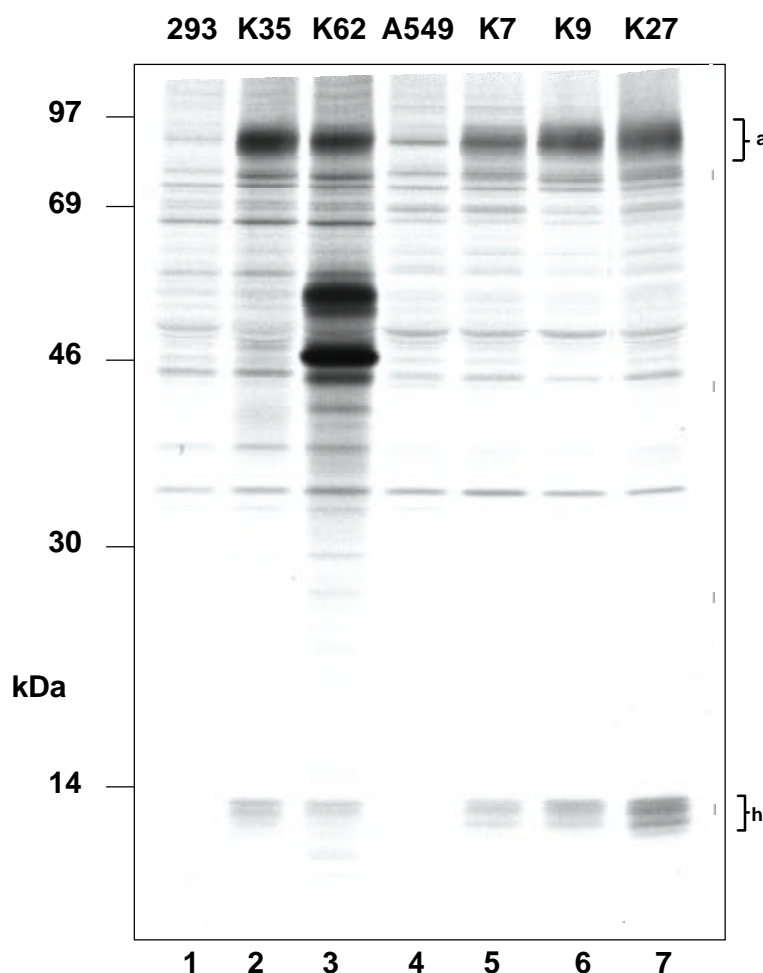


FIG. 11. Expression of E3/49K in A549 and 293 cell lines. A549 and 293 cell lines stably expressing the 49K protein were established using a pSG5-49K construct as described in Materials and Methods. After 2 h metabolic labeling 49K cells were lysed and immunoprecipitation (R25050) was followed by SDS-PAGE analysis.

3.4 Expression of the N-terminal ectodomain of Ad19a E3/49K as a HisTag-fusion protein in *E.coli*

The low molecular weight fragments detected in Ad19a-infected and 49K-transfected cells indicated that 49K is proteolytically processed. The antibodies utilized in these experiments recognized the C-terminus of 49K. Therefore, a proteolytic cleavage was postulated which separated the short C-terminal part that was detected in immunoprecipitation from the N-terminal part of 49K. The fate of the large N-terminal part of the protein remained elusive. Two

possibilities were envisaged: Proteolytic degradation or release of the ectodomain to an intracellular compartment or to the extracellular space, i.e. secretion.

To address this question the N-terminal part of the protein was expressed as a HisTag-fusion protein in *E. coli* (Fig. 12). Upon induction, a significant part of the bacterial proteins was constituted by the 49K-HisTag-fusion protein (Fig. 12A, compare lanes 1 and 2). The protein was found mainly in inclusion bodies (Fig. 12A, lanes 3 and 4) but could be purified after solubilization with guanidinium hydrochloride.

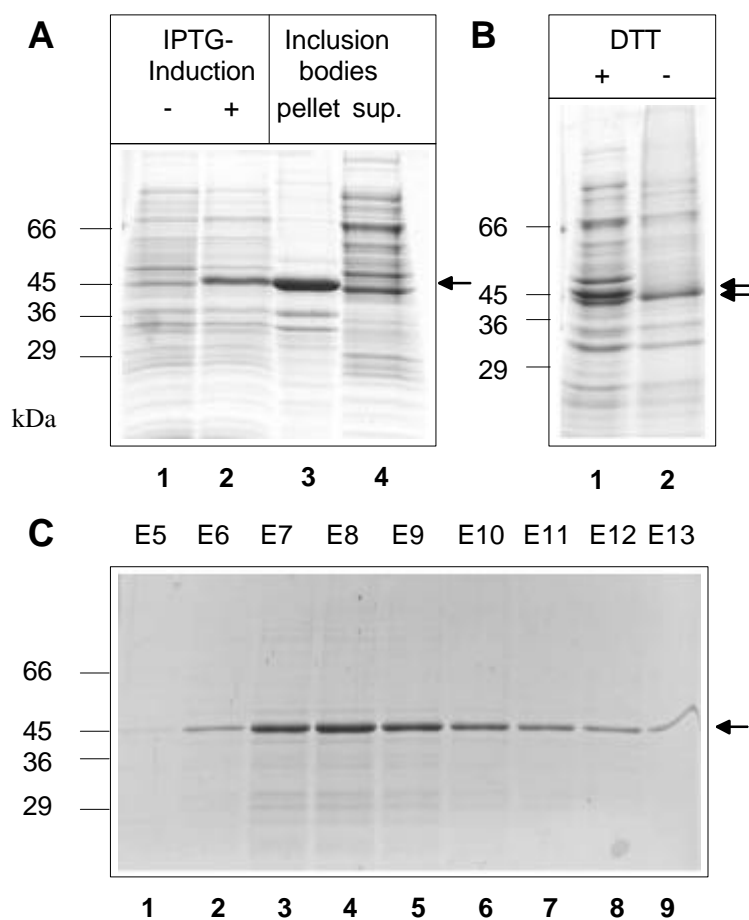


FIG. 12. Purification of the N-terminal ectodomain of 49K expressed as a HisTag-fusion protein. A) Expression of the 49K-HisTag-fusion protein encompassing residues 20-382 of 49K (Fig. 6) in *E. coli*. The DNA encoding the N-terminal part of 49K was PCR amplified using the primers 49K5'NCO and 49K3'BAM as described in Materials and Methods. This fragment was cloned into the pQE-60 expression vector (Qiagen) after restriction endonuclease digestion with NcoI and BamHI. The sequence was confirmed by sequencing. The 49K-HisTag-fusion protein was expressed as described in Materials and Methods. *E. coli* cell lysates from IPTG induced (A, lane 2) or uninduced cultures (lane 1, 100 μ l out of 200 ml culture) were analyzed by SDS-PAGE as well as samples from supernatant (lane 4, 5 μ l out of 5 ml) or the resuspended pellet including inclusion bodies (IBs) (lane 3, 1 μ l out of 2 ml) obtained after sonication. From 200 ml culture 15-20 mg of HisTag-fusion protein were obtained that was exclusively found in inclusion bodies. 49K-specific bands are indicated by arrows. B) Presence of disulfide bonds in the 49K-HisTag-fusion protein expressed in *E. coli*. The 49K-HisTag-fusion protein contained disulfide bonds in *E. coli* as indicated by the observed shift upon reduction with DTT (compare lanes 1 and 2, *E. coli* cell lysates). C) Elution of refolded 49K-HisTag-fusion protein. After refolding on the Ni-agarose column, 49K-HisTag-fusion protein was eluted as described in Materials and Methods. 500 μ l fractions were recovered (designated E1-E15) which contained protein in a max. concentration of about 300-500 μ g/ml, as measured by OD_{280nm}. 10 μ l per fraction were analyzed by SDS-PAGE (C, lanes 1-9).

Interestingly, the 49K-HisTag-fusion protein contained intramolecular disulfide bonds as indicated by the faster migration of 49K-HisTag-fusion protein in the absence of the reducing agent dithiothreitol (DTT) (Fig. 12B, compare lanes 1 and 2). These disulfide bonds could not be resolved by addition of β -mercaptoethanol to the solubilization buffer (data not shown). In order to generate a 49K-HisTag-fusion protein that adopts a rather native structure, it was attempted to refold 49K, while bound to the Ni-agarose column used for the purification of the HisTag-fusion protein, and to elute the refolded protein (Fig. 12C). The eluted proteins contained disulfide bonds (data not shown). The molecular weight difference (ca. 1.2 kDa) between 49K-HisTag-fusion protein with or without disulfide bonds observed in SDS-PAGE analysis is very similar to that seen in WT E3/49K expressed during infection (ca. 1.1 kDa, Fig. 20).

3.5 Production of polyclonal and monoclonal antibodies directed against the N-terminal domain of E3/49K

Recombinant E3/49K was utilized to generate polyclonal rabbit antibodies and monoclonal rat antibodies (the latter in cooperation with Elisabeth Kremmer, GSF, Munich, Germany). With antisera derived from immunized rabbits, 49K could be immunoprecipitated from lysates of Ad19a-infected A549 cells (Fig. 13).

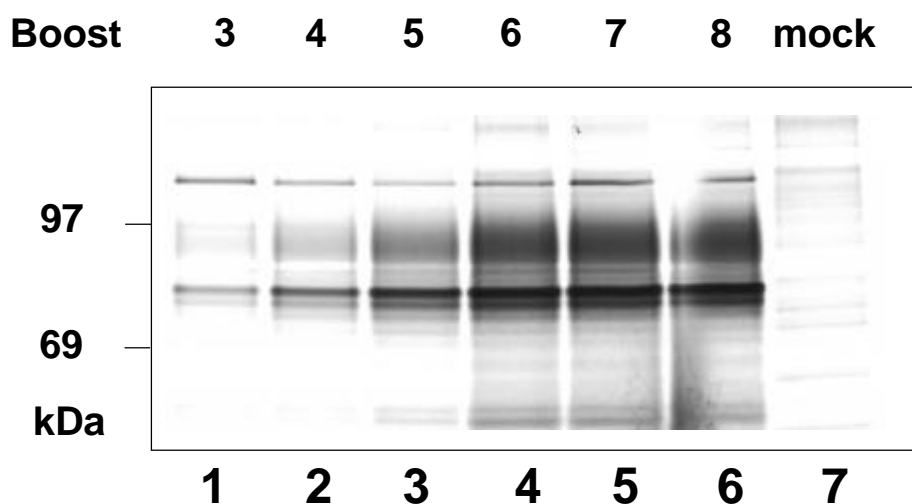


Fig. 13. Production of polyclonal rabbit antiserum against 49K. Two rabbits were immunized with approximately 250 μ g of refolded 49K-HisTag-fusion-protein (rabbit and derived sera named R48) or 250 μ g inclusion bodies (rabbit and derived sera named R47) and boosted several times with the same amount of protein. 5 μ l rabbit antiserum (from R48), prepared as described in Materials and Methods, were tested in immunoprecipitation using lysates of Ad19a- (lanes 1-6) or mock- (lane 7) infected A549 cells after 1 h metabolic labeling. After eight (ten) boosts no further increase in the activity of the antibodies obtained from R48 (R47) in immunoprecipitation was detected and the rabbit was sacrificed. The antiserum obtained from rabbit R48 showed higher specific activity in immunoprecipitation and was used in the following studies.

These antisera detected 49K also in Western blots (Fig. 14, lane 2). As expected, antibodies directed against the N-terminus of E3/49K recognized only the high molecular weight forms of E3/49K, whereas antibodies directed against the C-terminus recognized in addition the low molecular weight fragments (Fig. 14, compare lane 2 with lane 4). These fragments appear in this experiment as one band due to limited separation in the minigel. This also demonstrated clearly that the low molecular weight fragments detected in the immunoprecipitation are 49K-derived and do not represent coprecipitated proteins.

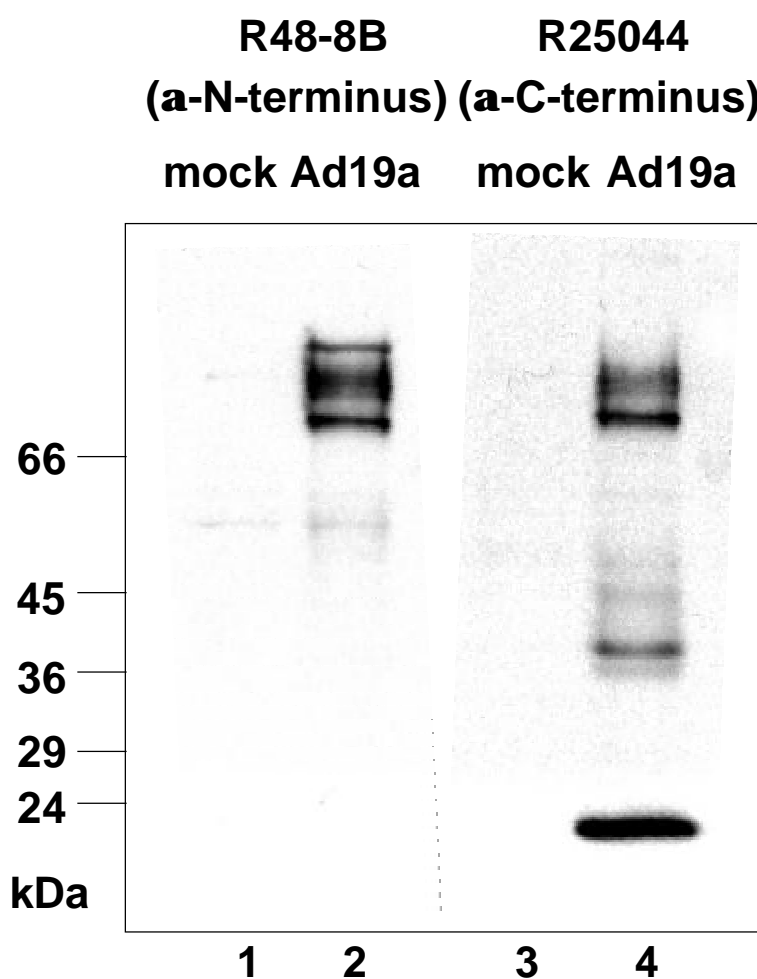


FIG. 14. Western blotting with antibodies directed against the N- and the C-terminus of 49K. Full-length 49K could be detected after SDS-PAGE analysis of lysates of Ad19a- (lanes 2, 4) or mock- (lanes 1, 3) infected A549 cells 24 h p.i. (10 μ g total protein/lane) with antibodies directed against the N- (R48-8B) and the C-terminus (R25044) in Western blotting (lanes 2, 4). Low molecular weight fragments could be detected only with antibodies directed against the C-terminus (lane 4).

Hybridoma cell supernatants containing rat monoclonal antibodies showed differential activities in different immunoassays (Tab. 4, data not shown). Differences are, if not caused by different antibody concentrations, most likely based on the differences in the recognition of epitopes between the 49K-HisTag-fusion protein expressed in *E. coli* and the WT 49K protein expressed

upon Ad19a infection in eukaryotic cells. In particular, misfolding and the lack of glycosylation in the 49K-HisTag-fusion protein might lead to the generation of antibodies recognizing 49K-HisTag-fusion protein epitopes that are not accessible in the WT 49K protein. As antibodies from clone 4D1 recognized 49K in immunofluorescence, immunoprecipitation, Western blotting and flow cytometry, in the following experiments these antibodies were utilized. The isotypes of antibodies from clone 4D1 and 1E6 were determined to be both isotype IgG_{2a}.

Tab. 4: Activity of ELISA-positive supernatants of hybridoma cell lines containing rat monoclonal antibodies in different immunoassays

Supernatants (mAb) from hybridoma clones	IF	IP	Western	Flow cytometry (fixed, internal)	Flow cytometry (surface)
1E6	+	+	+	-	+
1F4	-	-	+	-	-
1H8	-	+/-	++	-	-
4D1	+++	++	+++	+	++
5A7	-	-	-	-	-
5D3	-	-	++	-	-
6C9	-	-	-	-	-
6C12	-	-	-	-	-
7H10	-	-	-	-	-
10A11	-	-	-	-	-

-: No activity; +/-: Poor activity; +: Low activity; ++: Medium activity; +++: High activity

3.6 Proteolytic processing and secretion of E3/49K

The antibodies directed against the N-terminal part of protein made it possible to address the fate of the N-terminal portion of 49K. 49K was immunoprecipitated from lysates and supernatants of Ad19a-infected A549 cells (Fig. 15A, B) and 49K-transfected cells (Fig. 15C, D) in a pulse/chase experiment with antibodies directed against the C-terminal or the N-terminal part of 49K. With antibodies directed against the C-terminus, 49K could be precipitated from lysates but not from the supernatants (Fig. 15A, C). Strikingly, with antibodies against the N-terminus, 49K could be precipitated from lysates as well as from the supernatants demonstrating that the N-terminal portion of the protein is secreted (Fig. 15B, D). Low molecular weight fragments were detected in the chased samples intracellularly only with antibodies directed against the C-terminus (A, C) not with antibodies against the N-terminus (B, D). This finding confirmed that these fragments were derived from the C-terminus of 49K. The proteolytic processing was observed in Ad19a-infected and 49K-transfected cells in the absence of additional viral gene products demonstrating that the proteolytic processing of 49K is independent of the viral context. Therefore, the proteolytic cleavage of 49K is executed by cellular proteases.

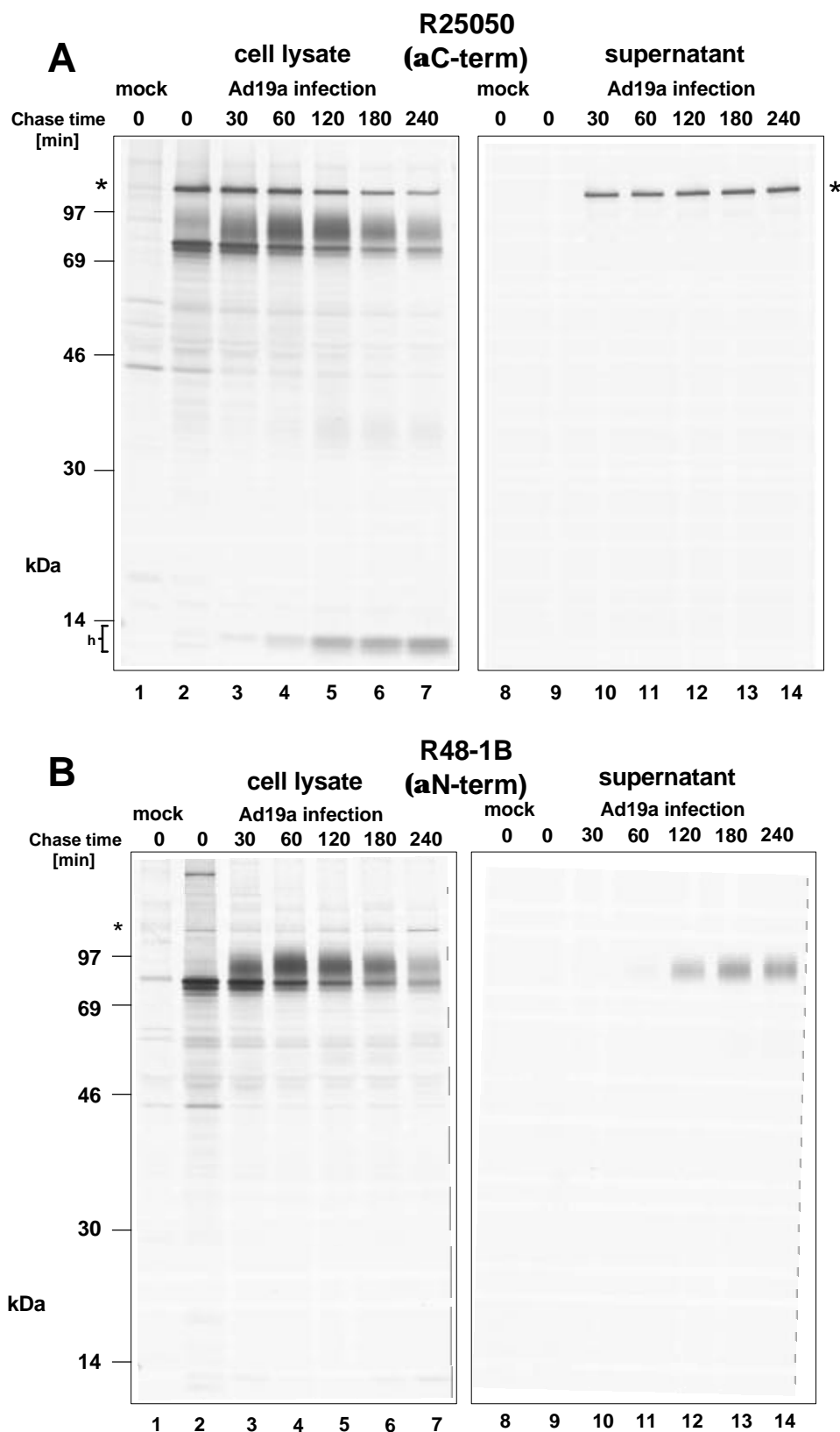
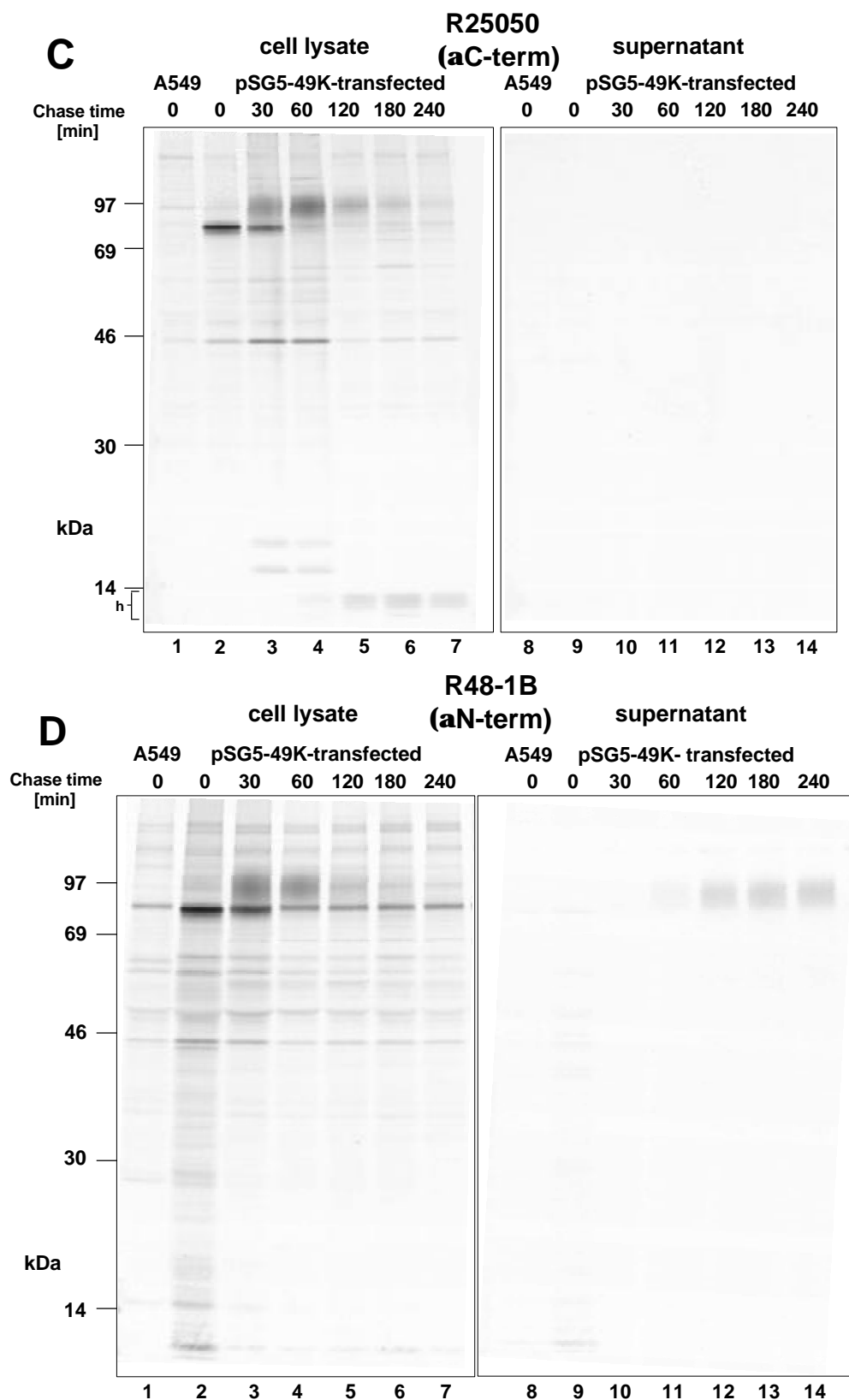


FIG. 15. Proteolytic processing and secretion of E3/49K. Ad19a-infected A549 (A, B, 16 h p.i.) and 49K-transfected A549 cells (C, D, A549 clone K27S) were metabolically labeled for 30 min with [35 S]-methionine and chased with medium containing non-radioactive methionine for the indicated times. Subsequently, E3/49K was precipitated from cell lysates and from supernatants with antibodies directed against the C-terminus (R25050, A, C) or N-terminus (R48-1B, B, D).



In the lysate and in the supernatant of infected cells the abundant hexon protein is detected (designated with a star) which unspecifically coprecipitates with several antibodies.

3.7 Fully processed E3/49K proteins contain high-mannose and/or hybrid in addition to complex N-glycans

The difference between the apparent molecular mass of 80-100 kDa in SDS-PAGE and the calculated molecular mass of the protein backbone of 46,915 kDa (without signal sequence) indicated that E3/49K is highly glycosylated. The appearance of the three E3/49K species b-d in the pulse labeled sample (Fig. 9, lane 1) indicated that they represent the high-mannose forms of the protein that are further processed to the protein species represented by the diffuse upper band a (Fig. 9), supposedly containing complex glycans.

To verify this idea, a pulse/chase experiment was performed and immunoprecipitated E3/49K from lysates and supernatants was treated with endoglycosidase H (Endo H, Fig. 16A, B). Endo H cleaves high-mannose and hybrid, but not complex carbohydrates. Endo H treatment of the pulsed lysate sample (Fig. 16A, lane 2) resulted in a decrease of the apparent molecular mass and the appearance of two prominent protein species of about 50 and 53 kDa (f and g), respectively (Fig. 16A, lane 10), demonstrating that only high-mannose and/or hybrid N-glycans were present. The 53 kDa species represents E3/49K with one N-linked glycan. Its appearance is due to incomplete Endo H digestion and was not observed after Endo H treatment under denaturing conditions (data not shown), Endo F treatment (Blusch et al., 2002) or PNGase F treatment (Fig. 18A, lane 11). In parallel to the appearance of the diffuse upper band in the mock treated lysate samples (20'-240' chase, Fig. 16A, lanes 3-8), E3/49K forms of 67-92 kDa were visualized in the Endo H treated samples (e, Fig. 16A, lanes 11-16). As these forms migrated faster than the heterogenous species of 87-100 kDa appearing in the untreated samples, the processed form of E3/49K was obviously not completely resistant to Endo H. Therefore, the processed E3/49K contained complex N-glycans and/or O-glycans not cleavable by Endo H but also high-mannose and/or hybrid N-linked sugars cleavable by Endo H. While the 87-100 kDa band of E3/49K disappeared gradually during the chase, small fragments of 12-13 kDa (h) were precipitated in increasing amounts. These fragments were not sensitive to Endo H digestion indicating that they are either not glycosylated or that the attached glycan(s) are Endo H resistant. Endo H treatment of secreted 77-90 kDa 49K species in the supernatant, which seemed to correspond to the heterogenous species of 87-100 kDa in the lysate, were partially Endo H sensitive indicated by the shift to an apparent molecular mass of 62-86 kDa (Fig. 16B). In addition, a weak 49K-related band corresponding to protein species of approximately 50-60 kDa was detected in the supernatant during the chase (Fig. 16B, lanes 6-8).

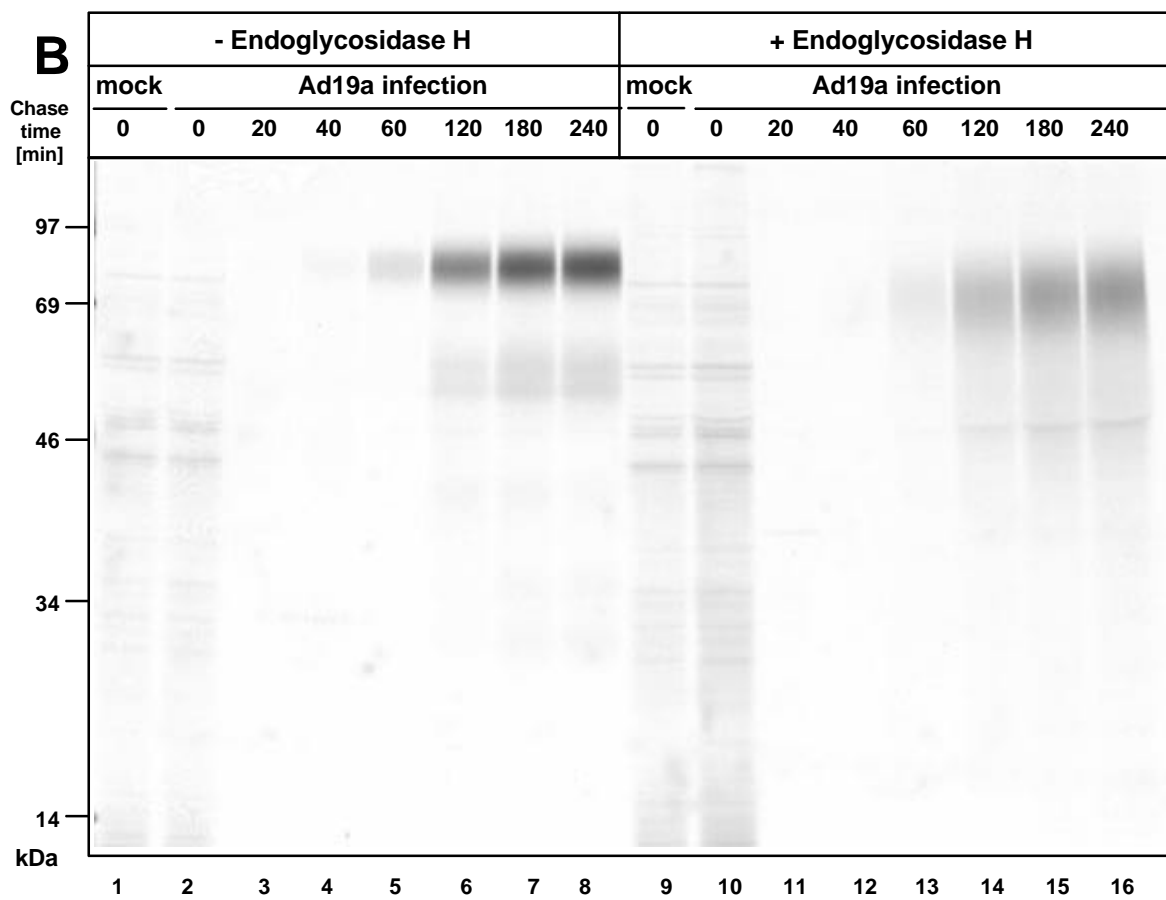
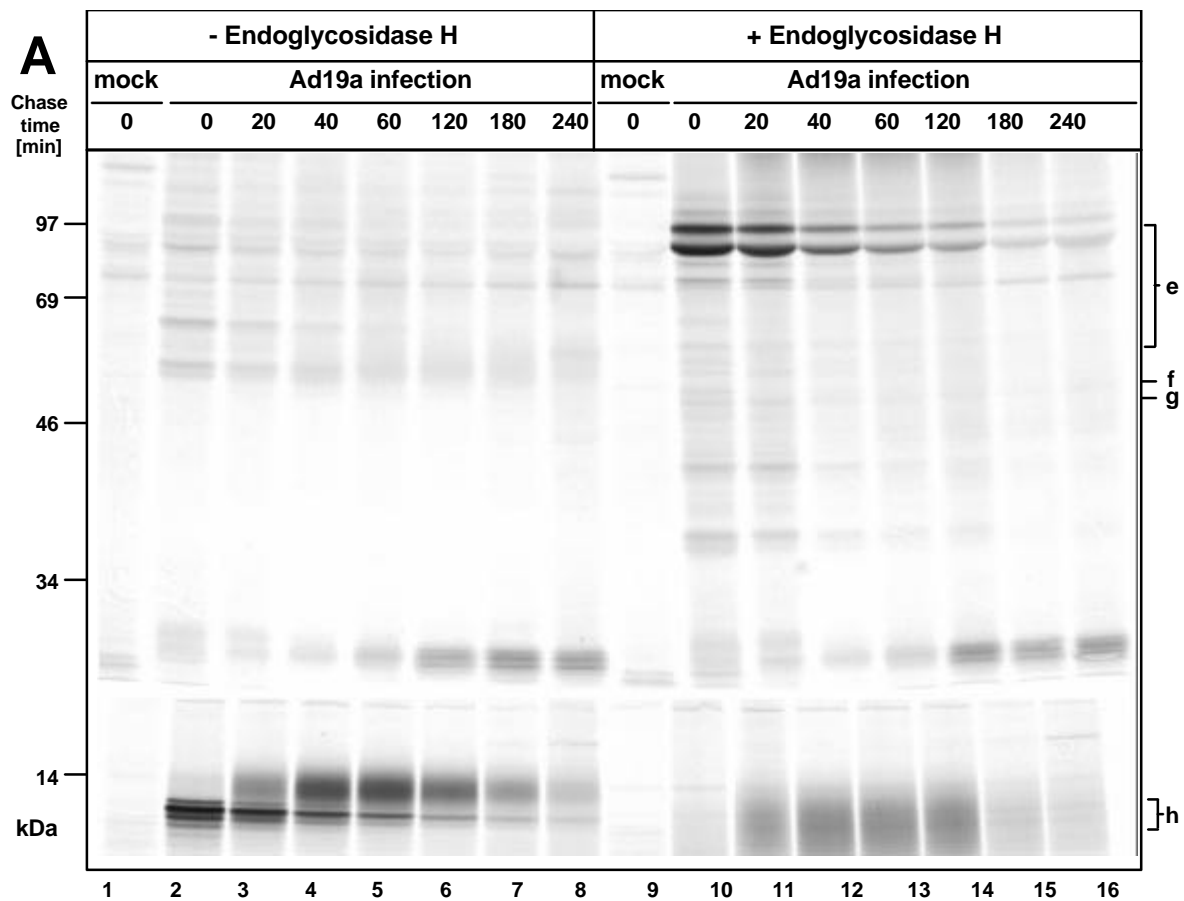


FIG. 16. Mature E3/49K protein remains partially Endo H sensitive. A549 cells were infected with Ad19a. At 6 h p.i. cells were labeled for 20 min with [³⁵S]-methionine and then chased for the time periods indicated. Two culture dishes were mock-infected (lanes 1 and 9). Lysates (A) and supernatants (B) were collected. For each time point, two culture dishes were lysed, the lysates (supernatants) were pooled and then split into two aliquots for E3/49K immunoprecipitation: one sample was treated with Endo H for 24 h (lanes 9-16), the other one was mock-treated (lanes 1-8). A) Endo H treatment of 49K immunoprecipitated from lysates generated the protein species e-g. Band f corresponds to 49K molecules containing a residual oligosaccharide chain (53 kDa) that is not efficiently removed under the non-denaturing conditions used. When 49K immunoprecipitates were denatured prior to Endo H treatment or incubated with Endo F (data not shown), only the 50 kDa form with all N-linked glycans removed (g) and the heterogeneous species of 67-92 kDa, designated e, is visualized. B) The secreted form of 49K is still Endo H sensitive in a similar fashion as the mature intracellular 49K species of 87-100 kDa.

3.8 Only 12-13 of the 14 predicted N-glycosylation sites of E3/49K are utilized

To investigate how many of the 14 predicted N-glycosylation sites are actually utilized, E3/49K was immunoprecipitated from Ad19a-infected A549 cells after metabolic labeling for 20 min. During this labeling period E3/49K is supposed to contain exclusively high-mannose N-glycans. By incubation with Endo H for different time periods and subsequent analysis of the samples by SDS-PAGE, partially deglycosylated forms of E3/49K could be differentiated that differ by one glycan each (Fig. 17). By counting the various forms it is obvious that the E3/49K form with the highest apparent molecular mass contained 13 N-linked glycans, but the great majority of E3/49K proteins had only 12 carbohydrates attached. Therefore, not all of the 14 predicted N-glycosylation sites were utilized.

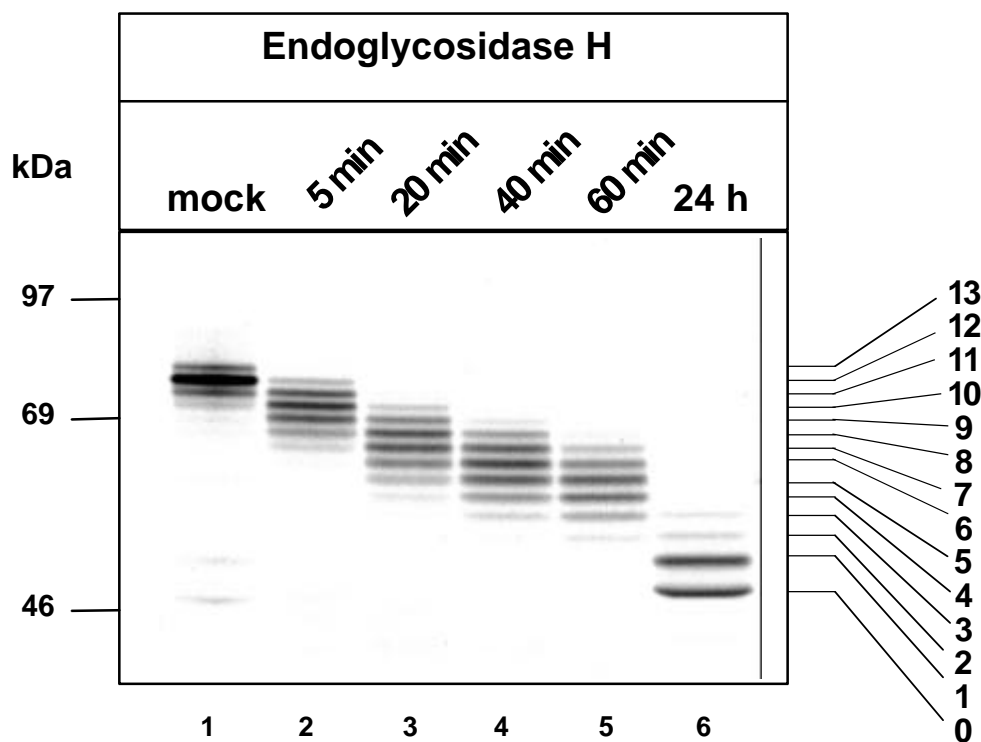


FIG. 17. Not all of the predicted N-glycosylation sites are utilized. E3/49K was immunoprecipitated after 20 min metabolic labeling of Ad19a-infected A549 cells 6 h p.i. and incubated with Endo H for the times indicated on top of the figure. Digested material was analyzed by SDS-PAGE, resulting in a series of 49K molecules differing by one oligosaccharide chain. The number of attached N-glycans for each 49K species is indicated on the right.

3.9 Evidence for O-glycosylation of E3/49K

The pulse/chase analysis of E3/49K (Fig. 16) demonstrated that the protein became partially Endo H resistant indicating the presence of complex N-glycans and/or O-glycans. E3/49K is predicted to contain three O-glycosylation sites (Hansen et al., 1998) (Fig. 6). To experimentally substantiate this prediction, Ad19a-infected A549 cells were pulse labeled for 1 h and chased for 1 h to generate fully processed potentially O-glycosylated E3/49K molecules. To compare the glycosylation of 49K in infected and 49K-transfected cells, in addition, 49K-transfected A549 cells were labeled 2 h. Subsequently, the protein was immunoprecipitated and treated with various glycosidases (Fig. 18A, B). To facilitate the detection of O-linked carbohydrates, all N-linked sugars were removed by treating immunoprecipitated E3/49K with PNGase F (Fig. 18A, lane 7-11; B, lane 4-7). By cleaving N-linked glycans this enzyme converts glycan-linked asparagine residues into aspartic acid residues, which changed the migration behavior of the protein due to the added negative charges (data not shown). As a reference for potential modifications occurring during the chase, E3/49K was immunoprecipitated from pulse labeled cells (A, 20 min; B, 30 min) and treated with PNGase F. This generated an E3/49K molecule (k) without glycan structures, but containing aspartates instead of asparagines (Fig. 18A, lane 11; B, lane 7). Two E3/49K species (i) with an apparent molecular mass of ~53-54 kDa could be differentiated after PNGase F treatment of the chased protein (Fig. 18A, lane 7; B, lane 4), that migrated slower than the pulsed PNGase F treated form (k) with about 50 kDa (Fig. 18A, lane 11; B, lane 7). This indicates the presence of a posttranslational modification in addition to N-glycosylation. The reduction of the apparent molecular mass of the PNGase F treated form upon neuraminidase treatment (j) to ~52 kDa (Fig. 18A, lane 9; B, lane 5) clearly demonstrates the presence of glycan structures containing sialic acid even after PNGase F treatment and indicates O-glycosylation. However, the utilized O-glycosidase from *Diplococcus pneumoniae* had no effect either used alone (Fig. 18A, lanes 3 and 8 (+PNGase F)) or in combination with neuraminidase that removes attached sialic acid groups potentially inhibiting O-glycosidase activity (Fig. 18A, lanes 4 and 10 (+PNGase F); B, lanes 1 and 6 (+PNGase F)). But the O-glycosidase decreased the apparent molecular mass of CD46, a highly O-glycosylated protein (Liszewski et al., 1991) (Fig. 18B, lanes 8 and 13, compare with lanes 9 and 12, respectively), which was used as a positive control for the O-glycosidase activity. Interestingly, in an experiment with a high MOI of ~10, in which most cells were infected with Ad19a (6 h p.i.), CD46 synthesis was decreased to undetectable levels (data not shown). Thus, this phenomenon seems to be Ad-induced and may have implications for Ad immune evasion and replication. The O-glycosidase used in these experiments removes the disaccharide core Gal β (1-3) GalNAc of O-glycans only if no other carbohydrate groups, e.g. sialic acid, are attached to the core. The finding that neuraminidase

treatment caused a shift after all N-glycans were removed can only be explained by the presence of O-glycans that contained sialic acids. Thus, the lack of sensitivity for the O-glycosidase was either due to the presence of O-glycan core structures, which cannot be cleaved by the O-glycosidase used, or the inaccessibility of the disaccharide core Gal β (1-3)GalNAc. Interestingly, the low molecular weight fragments (h) were not sensitive to any of the treatments suggesting that they are not glycosylated (Fig. 18A, lanes 2-10, B, lanes 1-6).

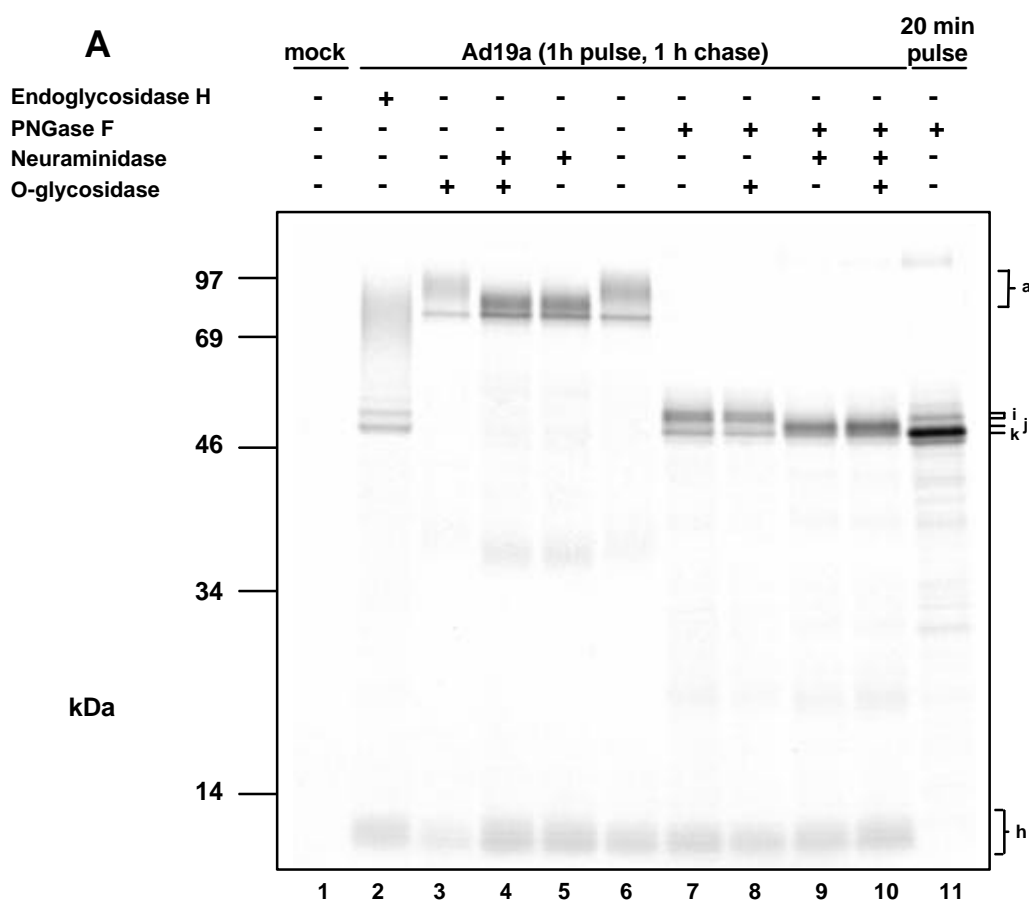
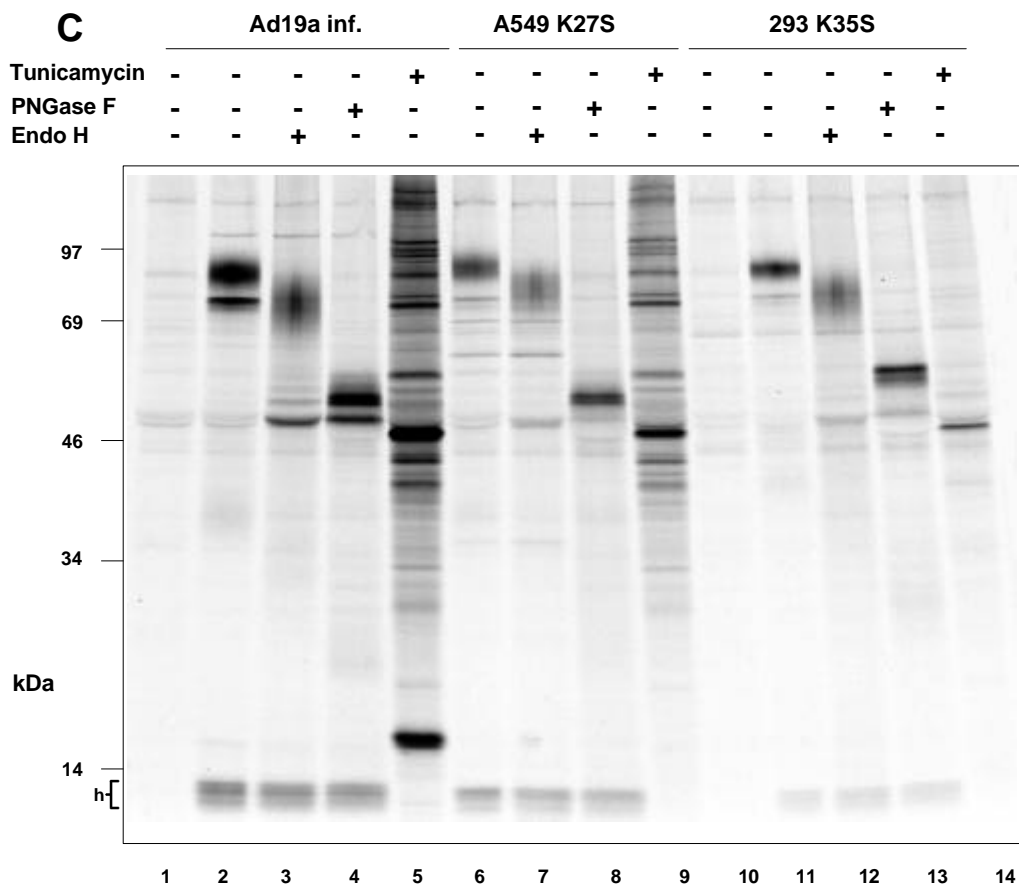
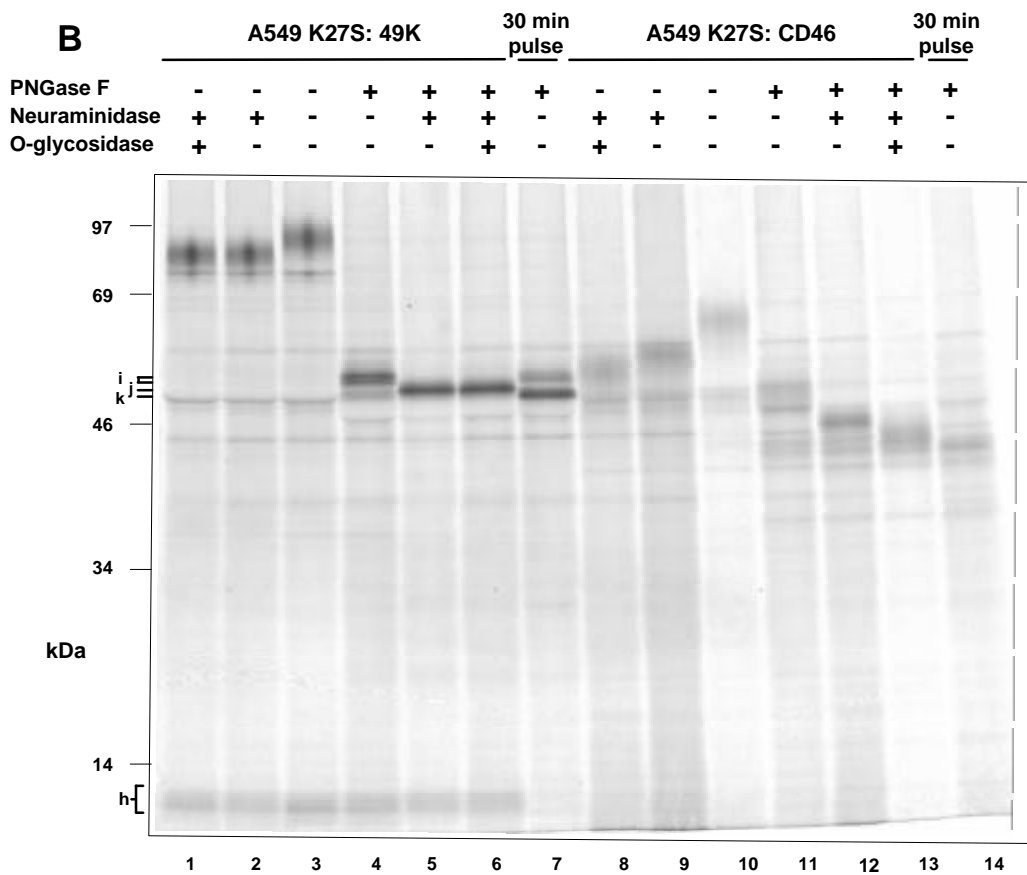


FIG. 18. Evidence for O-glycosylation of E3/49K. Ad19a-infected (6 h p.i., A) and 49K-transfected A549 cells (K27S, B) were labeled for 1 h with [35 S]-methionine/cysteine and chased for an additional hour with medium containing unlabeled methionine/cysteine (A) or were labeled for 2 h (B). To obtain a source of unprocessed 49K, one culture dish of cells was labeled for 20 min (A) or 30 min (B) with [35 S]-methionine/cysteine (A, lane 11; B, lane 7, 14). E3/49K and CD46 were sequentially immunoprecipitated from the same lysates and were incubated with different glycosidases as indicated on top of the figure and analyzed by SDS-PAGE. Endoglycosidase H cleaves only high-mannose and hybrid N-linked glycan structures. PNGase F removes all N-linked glycans. The O-glycosidase from *Diplococcus pneumoniae* cleaves only the unmodified disaccharide Gal(β 1 \rightarrow 3)GalNAc, one of the core structures of O-glycans bound to Ser/Thr. (C) To compare glycosylation of 49K in A549 and 293 cells, Ad19a-infected (lane 2-5), 49K-transfected A549 cells (lane 6-9) and 49K-transfected 293 cells (11-14) were metabolically labeled for 2 h. 49K was immunoprecipitated and digested with glycosidases as indicated. For tunicamycin treatment 10 μ g/ml tunicamycin were included in the starvation medium and were present during labeling.



The N- and O-glycosylation patterns of E3/49K in Ad19a-infected and 49K-transfected cells are very similar (compare Fig. 18A and 18B). Only the molecular mass of processed 49K seems to be slightly higher in transfected cells (Fig. 18C, compare lane 2 with lane 6). Thus, the viral context has no major effect on carbohydrate processing of Ad19a E3/49K, proteolytic processing and secretion (Fig. 15). Therefore, the intracellular processing is an intrinsic property of the E3/49K protein.

Interestingly, the glycan processing of 49K in 293 cells seems to differ partly from that in A549 cells indicated by the higher molecular weight of the PNGase F treated 49K forms (Fig. 18C, compare lanes 4 and 8 with lane 13). Therefore, 49K might be more extensively O-glycosylated or O-glycans may contain more sugar groups in 293 cells. Another explanation would be the presence of additional posttranslational modifications, e.g. phosphorylation.

3.10 Kinetics of E3/49K processing

The overall processing kinetics of 49K in Ad19a-infected cells (Fig. 19A) and a 49K-transfected cell line (Fig. 19B) are very similar. In general, the processing in the cell line is slightly faster. The high-mannose forms of 49K, which are produced cotranslationally, are the main 49K species present after the pulse (0 h). They are converted to 49K proteins containing hybrid and complex N-glycans as well as O-glycans. The half-life of the high-mannose forms was 30-35 min in infected cells, 20-25 min in 49K-transfected cells. The quantity of complex and hybrid sugar containing mature 49K proteins reaches a maximum at ~60 min chase. This is also the first time point at which C-terminal low molecular weight fragments are detected intracellularly and the secreted N-terminal ectodomain is detected in the supernatant. Most likely only the terminally processed 49K proteins are proteolytically processed. During the following chase time their quantity decreases constantly. The half-life of the mature 49K species was 40-60 min in infected cells and 30-50 min in 49K transfected cells assuming a first order rate law for the elimination of mature 49K. The amounts of low molecular weight C-terminal fragments intracellularly and secreted 49K in the supernatant increase during the chase. However, after 240 min only ca. 10% of the initial labeling is recovered in the cytoplasmic tail fragments and only 10-15 % in the secreted 49K in the supernatant. The overall half-life was 120 min in infected cells, 80-100 min in 49K-transfected cells.

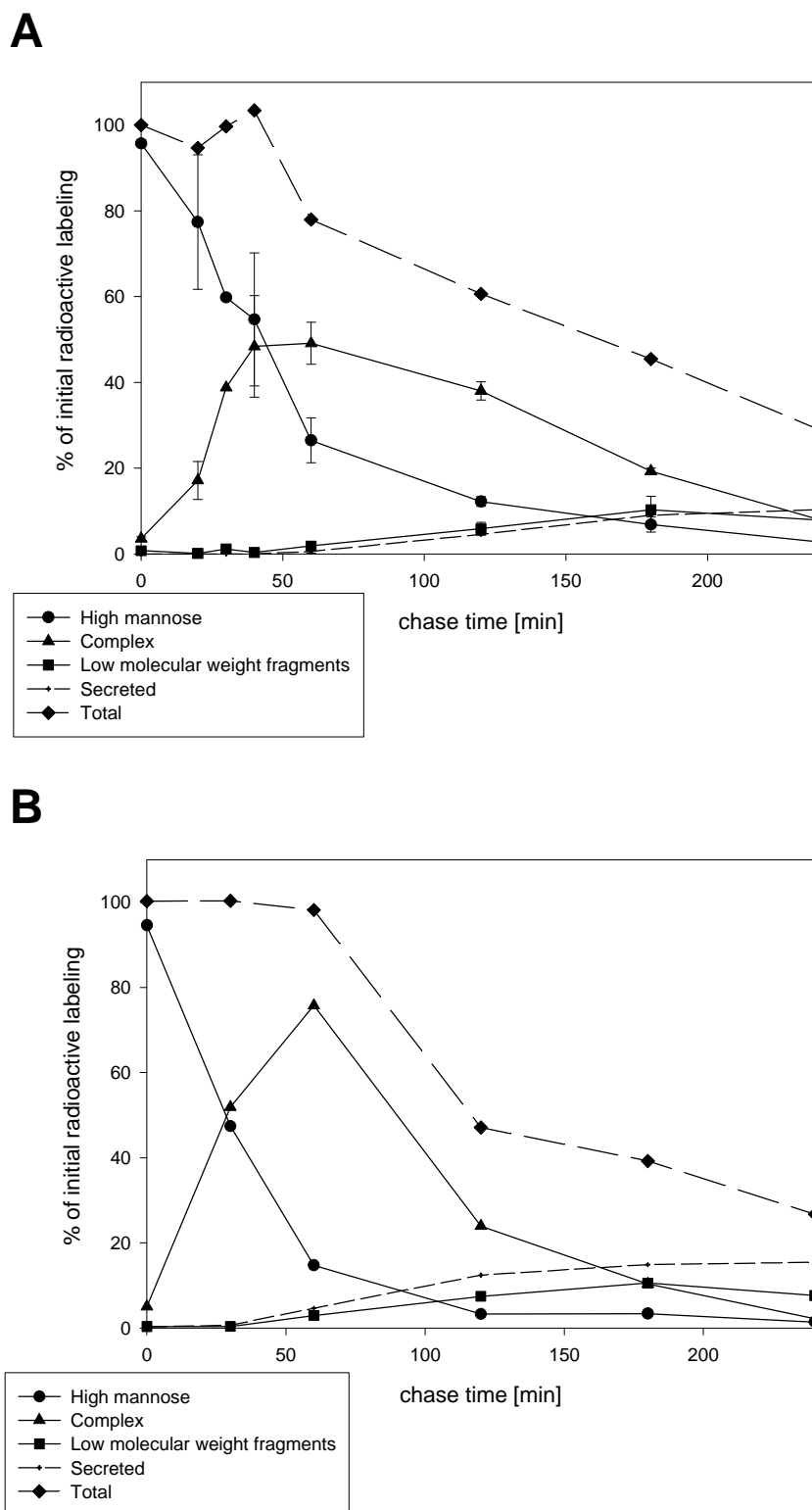


FIG. 19. Processing kinetics of 49K in Ad19a-infected (A) and 49K-transfected (K27S, B) A549 cells. For the data of 49K processing in Ad19a-infected cells results of four independent experiments were analyzed, for the 49K processing in transfected cell lines the result of a single experiment is shown. The initial labeling after the pulse (20 min in infection, 30 min in the 49K transfectant) was used as a reference (100%). The high-mannose forms are represented by the bands b-d (e.g. in Fig. 9), the complex form by the band a (e.g. in Fig. 9) and the low molecular weight fragments by the band h (e.g. in Fig. 9). Immunoprecipitation was performed with the antibodies directed against the C-terminus from cell lysates and with antibodies directed against the N-terminus from supernatants. Data were analyzed with SigmaPlot for Windows Version 5.00.

3.11 E3/49K contains intramolecular disulfide bonds

There are six cysteine residues in the luminal domain of E3/49K capable to form intramolecular disulfide bonds or S-S mediated E3/49K multimers (Fig. 6A, B). To investigate the presence of disulfide bonds in E3/49K, the protein was immunoprecipitated and analyzed by SDS-PAGE in the presence and absence of the reducing agent dithiothreitol (Fig. 20). To evaluate the potential apparent molecular mass changes more easily, the experiment was also performed in the presence of tunicamycin, an inhibitor of N-glycosylation (Duksin and Mahoney, 1982) (Fig. 20, lanes 1, 2). In both cases E3/49K migrated faster without dithiothreitol demonstrating the presence of intramolecular disulfide bonds. The difference in the migration behavior corresponded to ~1.1 kDa. Compared to the altered migration of the major histocompatibility complex (MHC) class I heavy chain containing two loops of ~60 amino acids that corresponded to about 1.2 kDa (data not shown), this rather small shift suggests that no large disulfide bonded loops are formed. Thus, it is likely that the six cysteine residues in the luminal domain form three disulfide bonds, in which neighboring cysteines are linked, creating loops of 13 and 9 amino acids respectively (Fig. 6B).

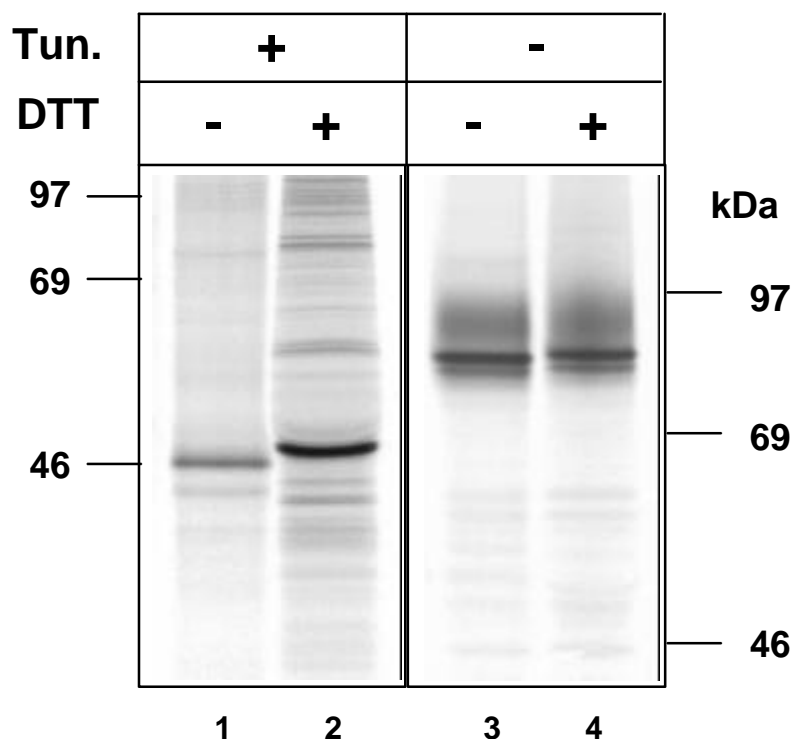


FIG. 20. E3/49K contains intramolecular disulfide bonds. Ad19a-infected A549 cells were preincubated in methionine/cysteine free medium containing (lanes 1 and 2) or not containing 10 $\mu\text{g}/\text{ml}$ tunicamycin (lanes 3 and 4). After 1 h metabolic labeling with [^{35}S]-methionine/cysteine in the presence (lanes 1 and 2) or absence (lanes 3 and 4) of 10 $\mu\text{g}/\text{ml}$ tunicamycin, E3/49K was immunoprecipitated. Immunoprecipitates were heated for 5 min to 95°C in the presence (lanes 2 and 4) or absence (lanes 1 and 3) of the reducing agent dithiothreitol (DTT) prior to SDS-PAGE analysis.

3.12 Intracellular staining patterns detected with antibodies directed against the N- and the C-terminus of E3/49K early during infection are indistinguishable

In order to find out how the intracellular trafficking of 49K may be connected to the proteolytic processing and to gain insight into a potential function of 49K, immunofluorescence studies were performed. Primary foreskin fibroblasts (SeBu) were utilized because intracellular compartments can be more readily differentiated in these cells than in immortal cell lines, e.g. A549, with a more condensed cytoplasm. Since 49K is proteolytically cleaved resulting in the separation of C- and N-terminus, it was first examined whether C- and N-terminus of 49K colocalize or may follow partly different trafficking pathways in Ad19a-infected SeBu cells 12-15 h p.i. This time point corresponds to the early phase of infection in SeBu cells. The intracellular staining patterns of 49K detected with C- and N-terminal antibodies were indistinguishable (Fig. 21). Therefore, full-length proteins and the C-terminal fragments generated by the proteolytic processing seem to follow very similar intracellular trafficking pathways. With both antibodies a perinuclear, vesicular and tubular compartment and numerous vesicles in the periphery of the cell were stained.

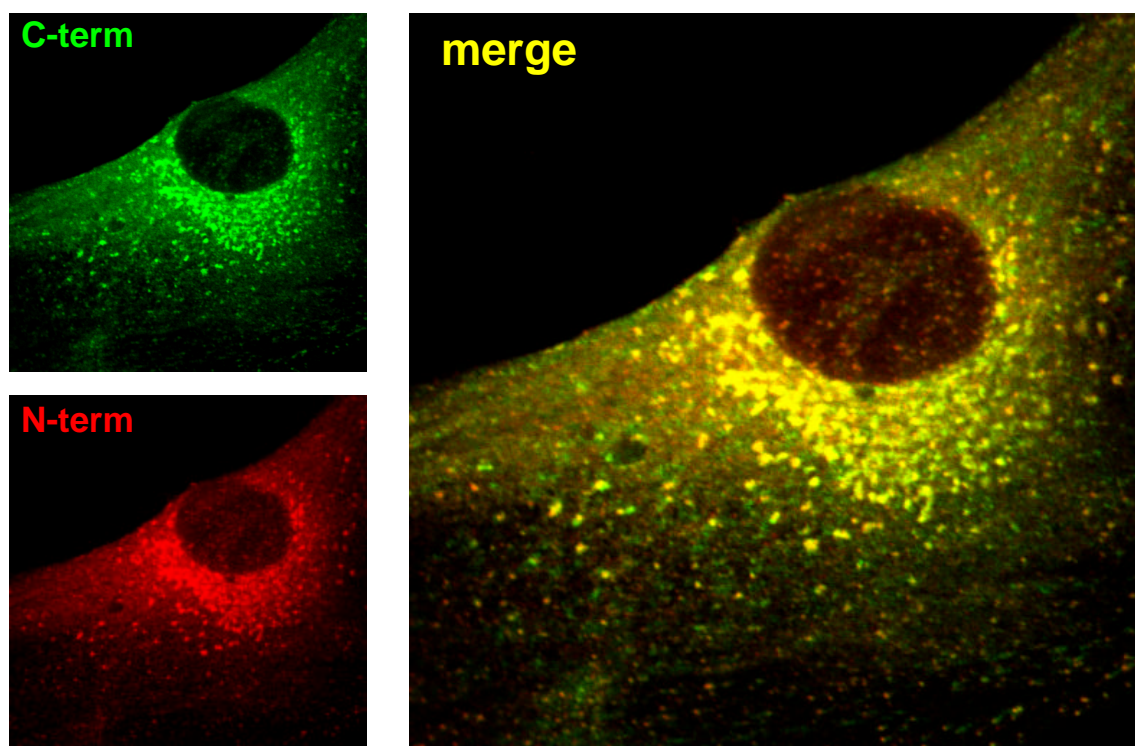


FIG. 21. Intracellular colocalization of the C- and the N-terminus of 49K. Primary fibroblasts (SeBu) were infected with Ad19a and processed for confocal laser microscopy 12-15 h p.i. as described in Materials and Methods. The localization of the C-terminus of 49K was analyzed with a polyclonal rabbit antiserum (R25050, green) and that of the N-terminus with a monoclonal rat antibody (4D1, red).

3.13 E3/49K localizes to the Golgi/*trans*-Golgi-network (TGN) and early endosomal vesicles early during infection

In colocalization studies with various cellular marker proteins it was analyzed, in which intracellular compartments E3/49K is localized. Hardly any colocalization with the ER marker calnexin was found (Fig. 22A). The perinuclear structure could be identified as the Golgi/*trans*-Golgi network (TGN) by colocalization with GM130, a marker for the *cis*-Golgi cisternae (Nakamura et al., 1995) (Fig. 22B), β 1 \rightarrow 4-Galactosyltransferase, a marker for *trans*-Golgi cisternae and the TGN (Nilsson et al., 1993) (Fig. 22C), AP-1 (Fig. 22D) and TGN46 (Fig. 26B), both markers for the TGN (Ahle et al., 1988; Ponnambalam et al., 1996). To distinguish between the Golgi complex and the TGN, brefeldin A (BFA) was used (data not shown), a drug reported to have differential effects on proteins of the Golgi complex and the TGN (Klausner et al., 1992). Whereas proteins of the Golgi complex redistribute to the ER, the TGN collapses onto the microtubule-organizing center (MTOC) (Ladinsky and Howell, 1992; Reaves and Banting, 1992). Upon BFA treatment, E3/49K staining of the perinuclear region disappeared almost completely and a slightly increased ER staining was detected in Ad19a-infected SeBu cells (data not shown). However, like TGN46, E3/49K was also detected in a perinuclear spot. This suggests that at steady-state E3/49K was present in the TGN as well as in the Golgi complex. Interestingly, the integrity of the Golgi/TGN was disturbed by the Ad19a infection. In uninfected cells the Golgi/TGN was represented by a number of tubules (Fig. 26A), whereas in infected cells the Golgi/TGN exhibited a rather vesicular appearance (Fig. 26B). Since this effect was already observed 12-15 h p.i., it seems to be mediated by early Ad gene products and is not related to late phenomena like host shutoff. Currently it is unknown whether this phenomenon is related to the inhibition of 49K and lamp-1 processing late during infection (Fig. 9, 10A).

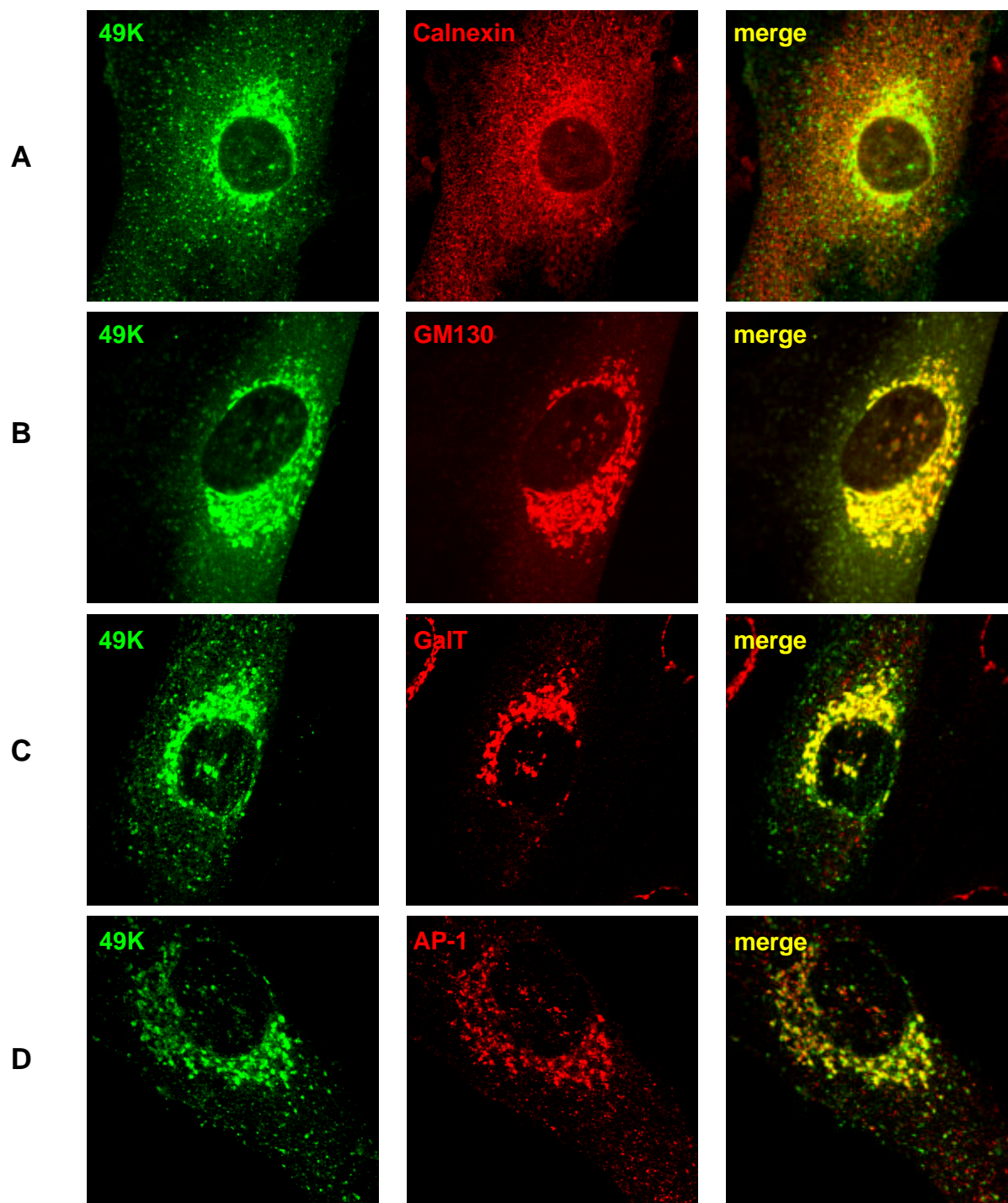


FIG. 22. E3/49K localizes to the Golgi/*trans*-Golgi network. Primary fibroblasts (SeBu) were infected with Ad19a and processed for confocal laser microscopy 12-15 h p.i. Intracellular localization of E3/49K (green, R25050) was compared to that of marker proteins (red) for different cellular compartments: A) calnexin (endoplasmic reticulum); B) GM130 (cis-Golgi); C) GalT (trans-Golgi/TGN); D) AP-1 (TGN). The antibodies used are given in Materials and Methods.

In studies to determine the identity of the E3/49K-positive peripheral vesicles, colocalization of 49K was observed neither with the late endosomal marker lysobisphosphatidic acid, LBPA (Kobayashi et al., 1998) (Fig. 23B) nor with the lysosomal marker lamp-2 (Hunziker and Geuze, 1996) (Fig. 23C). In contrast, a substantial number of E3/49K-positive vesicles did colocalize with EEA1 (Fig. 23A), an early endosomal marker (Mu et al., 1995). These data suggest that E3/49K is targeted to early endosomal but not to late endosomal and lysosomal compartments early during infection.

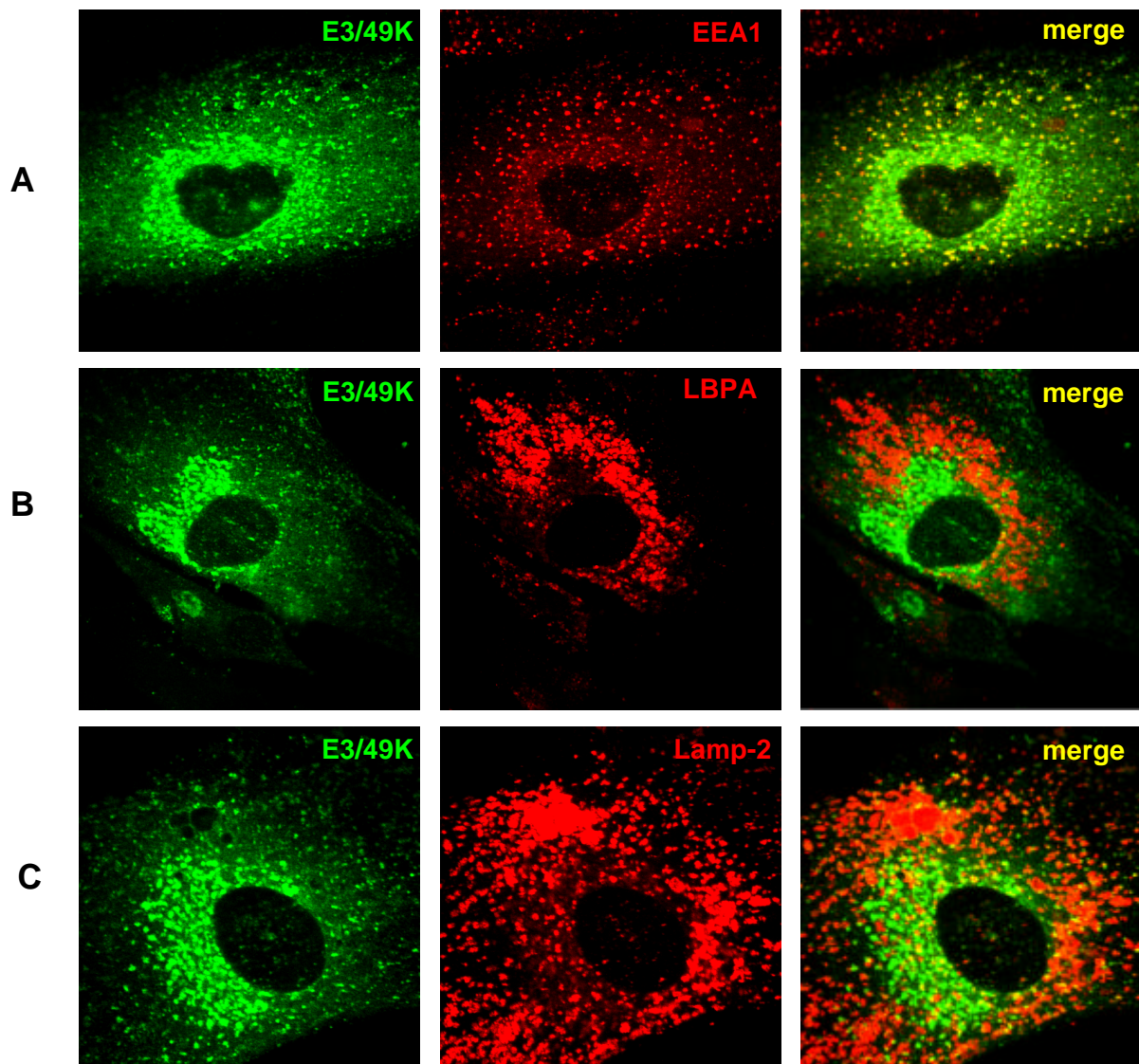


FIG. 23. E3/49K localizes to early endosomes but not late endosomes or lysosomes. Primary fibroblasts (SeBu) were infected with Ad19a and processed for confocal laser microscopy 12-15 h p.i. Intracellular localization of E3/49K (green, R25050) was compared to that of marker proteins (red) for different endosomal/lysosomal compartments: EEA-1 (early endosomes, A), lysobisphosphatidic acid (LBPA, late endosomes, B), lamp-2 (late endosomes and lysosomes, C). The antibodies used are given in Materials and Methods.

In cells expressing very high amounts of 49K, cell surface expression of 49K was detected in immunofluorescence (data not shown). Cell surface expression of 49K was subsequently confirmed by flow cytometry analysis of cell lines stably expressing 49K (Fig. 24) and in infected cells (data not shown).

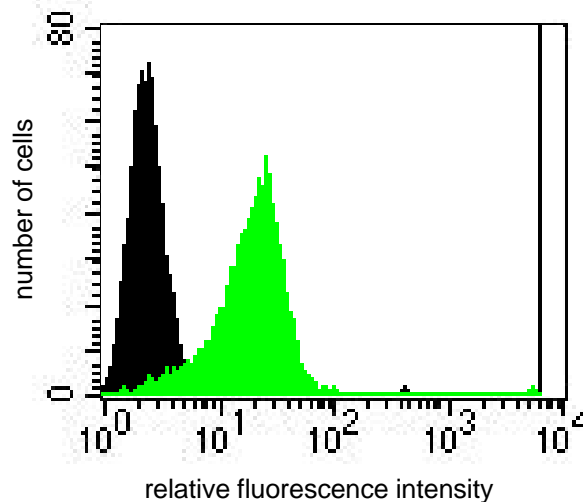


FIG. 24. E3/49K is expressed on the cell surface. Rat monoclonal antibody (4D1) directed against the N-terminus of 49K was used to detect 49K on the cell surface of 49K-transfected A549 cells (grey) using flow cytometry shown in comparison to the mock-transfected parental cell line (black).

3.14 Cytoplasmic tail fragments of E3/49K accumulate in late endosomes/lysosomes during the course of Ad19a infection

No striking difference in the intracellular localization of E3/49K was found in A549 cell lines stably expressing E3/49K or after transient transfections (data not shown). In contrast to 49K localization in the early phase of infection in SeBu cells, in some cases a limited colocalization of 49K with lamp-2 staining in peripheral vesicles was observed. Interestingly, in the late phase of Ad19a infection of SeBu cells, colocalization of E3/49K with lamp-2 was observed (Fig. 25). In general, at around 18 h p.i., E3/49K was found in few peripheral vesicles that were only weakly lamp-2-positive, whereas the major fraction of the lamp-2-positive vesicles remained E3/49K-negative. At later time points (24-48 h p.i.) a major fraction of lamp-2-positive vesicles exhibited a profound E3/49K staining. Notably, this phenomenon was only observed with the C-terminal antibodies, but not with the N-terminal antibodies (36 h p.i., Fig. 25).

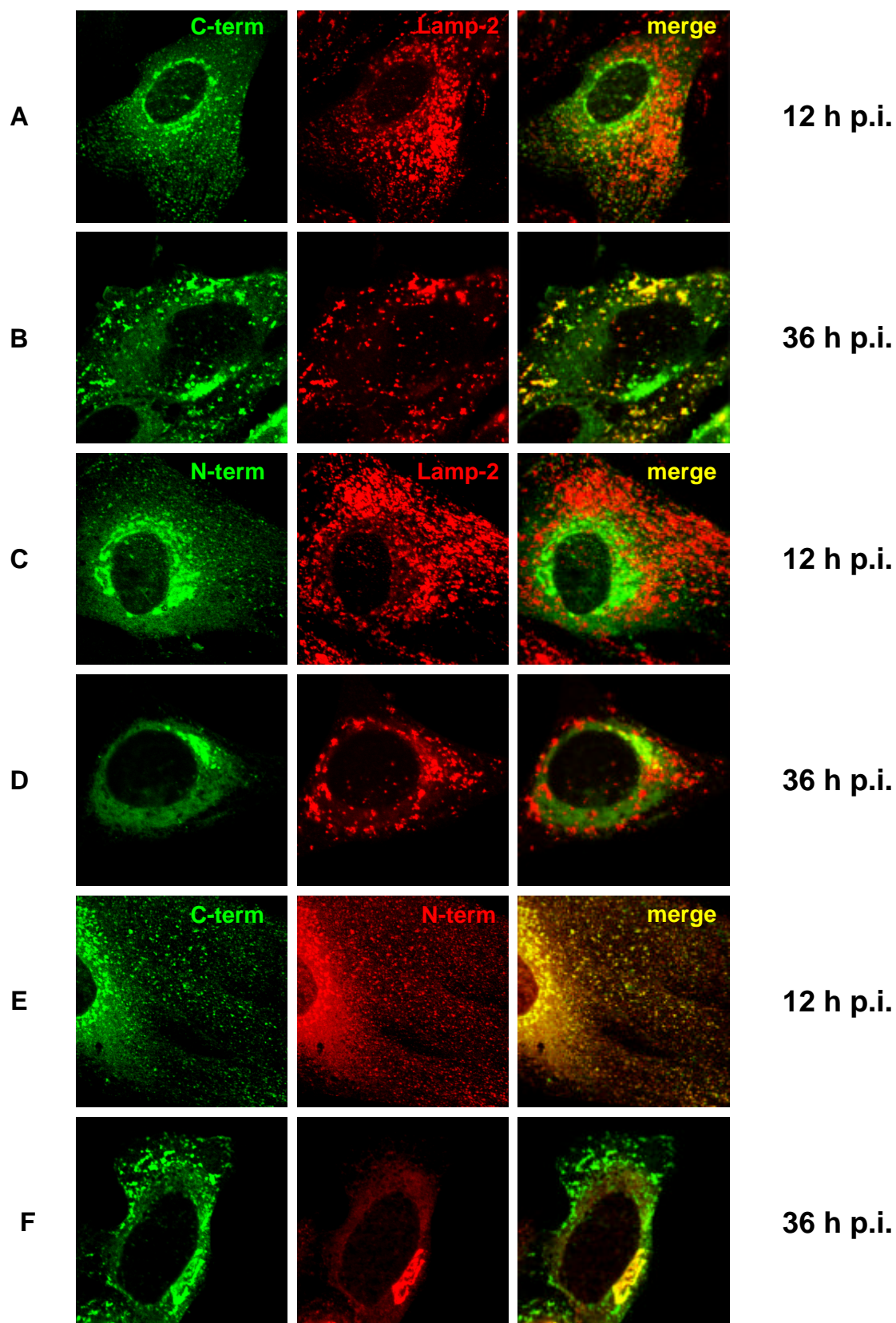


FIG. 25. Cytoplasmic tail fragments of 49K localize to the Golgi/TGN and late endosomes/lysosomes late during infection. Primary fibroblasts (SeBu) were infected with Ad19a and processed for confocal laser microscopy 12 or 36 h p.i. Intracellular localization of 49K was analyzed with antibodies directed against the C- (polyclonal rabbit (R25050), A, B, E, F) and the N-terminus (polyclonal rabbit (R48-7B), C, D; rat mAb (4D1), E, F) and was compared to the localization of lamp-2 (mouse mAb, 2D5), a late endosomal/lysosomal marker.

Early during infection (12 h p.i.) with neither antibody a colocalization of 49K with lamp-2 was found (Fig. 25A, C). Late during infection (36 h p.i.) 49K was detected in lamp-2-positive vesicles with antibodies directed against the C-terminus (Fig. 25B) but not with antibodies directed against the N-terminus (Fig. 25D). Both antibodies stained a lamp-2-negative perinuclear structure, presumably the Golgi/TGN (Fig. 25F) that seemed to contain full-length 49K proteins. In addition, a more pronounced ER staining was visible late during infection (Fig. 25B, D, F). Only rarely vesicles were stained late during infection with antibodies directed against the N-terminus of 49K. This result indicates that the impaired processing observed in Ad19a-infected A549 cells in the late phase of infection (Fig. 9) is accompanied by a transport block in the ER/Golgi/TGN.

3.15 Intracellular localization of E3/49K is influenced by acidotropic agents

One possible explanation for the finding that 49K could not be detected in late endosomal/lysosomal structures early during infection is that 49K localizes only transiently to these compartments, e.g. due to rapid degradation. Therefore, it was tested whether treatment with acidotropic/lysosomotropic agents, like bafilomycin A1 and chloroquine, that block trafficking at an early or late endosomal state, increase the pH of endosomal compartments and inhibit lysosomal degradation (de Duve, 1983) would allow the detection of 49K in late endosomes or lysosomes. These compounds were also shown to block recycling of TGN38/46 to the TGN (Banting and Ponnambalam, 1997; Ponnambalam et al., 1996). Unexpectedly, overnight treatment of SeBu cells with 100 μ M chloroquine resulted in changes in the ER morphology and in an accumulation of 49K in the ER, which was not observed in transiently or stably transfected A549 cells or after 3 h treatment of Ad19a-infected SeBu cells. After 3 h treatment no significant increase in colocalization of 49K and lamp-2 was detected (data not shown). However, the tubular TGN46 staining of the Golgi/TGN that was mostly perinuclear in untreated cells shifted dramatically to a vesicular staining in the periphery of chloroquine treated cells (Fig. 26B, C). Interestingly, these peripheral TGN46-positive vesicles contained also 49K. TGN46 is known to recycle from the cell surface to the TGN via early endosomal vesicles (Ghosh et al., 1998; Mallet and Maxfield, 1999). These findings indicate that the trafficking pathways of 49K and TGN46 overlap in early endosomal vesicles and may suggest that these proteins utilize similar trafficking pathways.

Overnight treatment with acidotropic agents like chloroquine was feasible with E3/49K transfected A549 cells without deleterious effects on the ER. Upon treatment with chloroquine, 49K could be detected in large swollen vesicles (Fig. 33B). These were partially lamp-2 positive (data not shown). Since it is a matter of debate whether acidotropic agents block trafficking at an

early or late endosomal state (Bayer et al., 1998; Clague et al., 1994; van Deurs et al., 1996; van Weert et al., 1995), it is questionable if this colocalization truly reflects targeting to and stabilization of 49K in a late endosomal/lysosomal compartment. Colocalization may be rather caused by a redistribution of lamp-2 to an early endosomal compartment. The colocalization of 49K with TGN46 after treatment with chloroquine supports the latter interpretation.

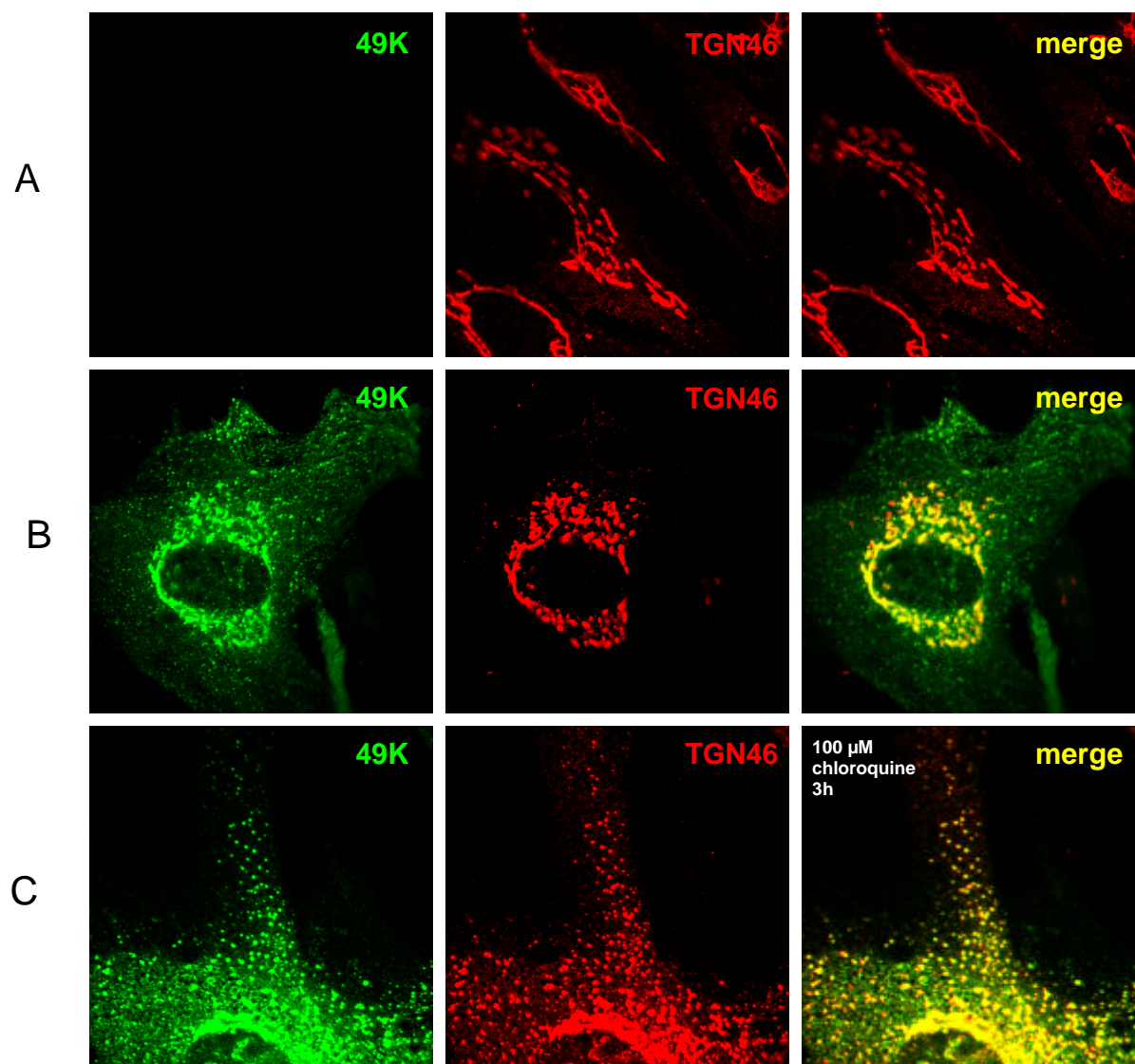


FIG. 26. Colocalization of E3/49K with TGN46 in peripheral vesicles upon chloroquine treatment. Primary fibroblasts (SeBu) were Ad19a- (B, C) or mock- (A) infected and processed for confocal laser microscopy 12-15 h p.i. Intracellular structures were stained with antibodies against TGN46 and E3/49K (R25050) in mock-infected cells (A), mock-treated Ad19a-infected cells (B) or Ad19a-infected cells treated for 3 h with 100 μ M chloroquine (C).

3.16 Evidence for E3/49K recycling to the TGN

To answer the question whether the prominent Golgi/TGN staining of 49K at steady-state represents newly synthesized protein or 49K molecules recycled from the cell surface via early endosomes as demonstrated for TGN46, Ad19a-infected SeBu cells were treated for 6 h with cycloheximide to inhibit protein synthesis. Subsequently, the localization of 49K was determined using antibodies directed against the C- and the N-terminus and was compared to TGN46 localization (Fig. 27). After 6 h cycloheximide treatment the perinuclear labeling of 49K detected with the antibody against the N-terminus diminished drastically (Fig. 27D, F, compare with C and E, respectively) and frequently disappeared entirely (data not shown), whereas the labeling with the antibody against the C-terminus was still present (Fig. 27B, F, compare with A and E, respectively), although the intensity of the staining decreased. The TGN46 staining was essentially unchanged (Fig. 27B, D, compare with A and C, respectively). Thus, C-terminal fragments of 49K were recycled to the Golgi/TGN suggesting that full-length proteins presumably also utilize this pathway. Therefore, the steady-state localization of 49K in the Golgi/TGN represents newly synthesized proteins as well as proteins recycled from the cell surface. At the moment it is unknown how much each fraction contributes to the Golgi/TGN staining of 49K.

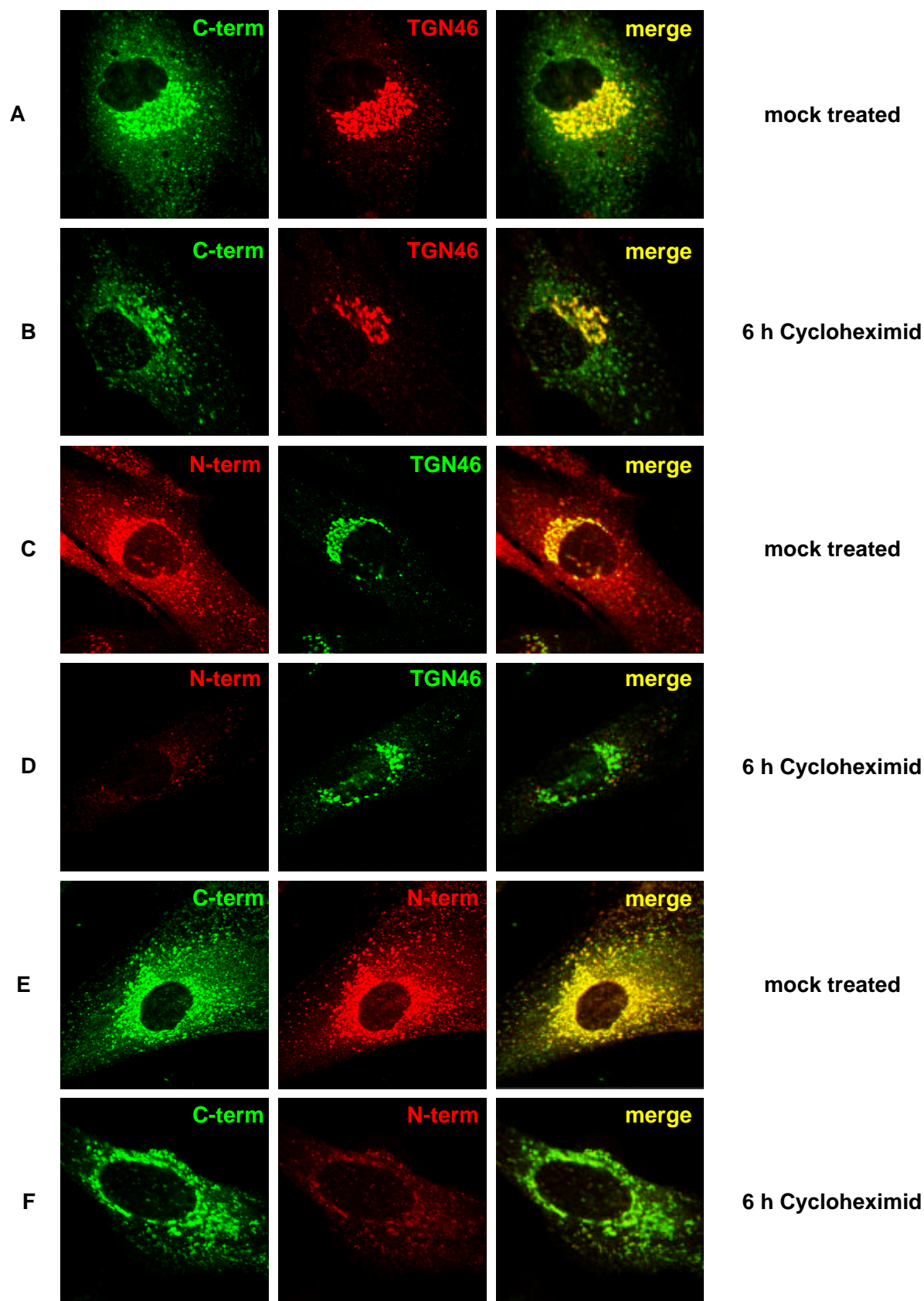


FIG. 27. Newly synthesized as well as recycled 49K proteins localize to the Golgi/TGN. Primary fibroblasts (SeBu) were infected with Ad19a. 12 h p.i. cells were treated 6 h with 50 $\mu\text{g}/\text{ml}$ cycloheximide. Subsequently, cells were processed for confocal laser microscopy. 49K was stained using antibodies directed against the C- (rabbit polyclonal Ab (R25050), A, B, E, F) and against the N-terminus (rat mAb, 4D1), C, D, E, F). To evaluate the Golgi/TGN localization, the TGN marker TGN46 was detected as well (sheep polyclonal Ab, A, B; rabbit polyclonal Ab, C, D).

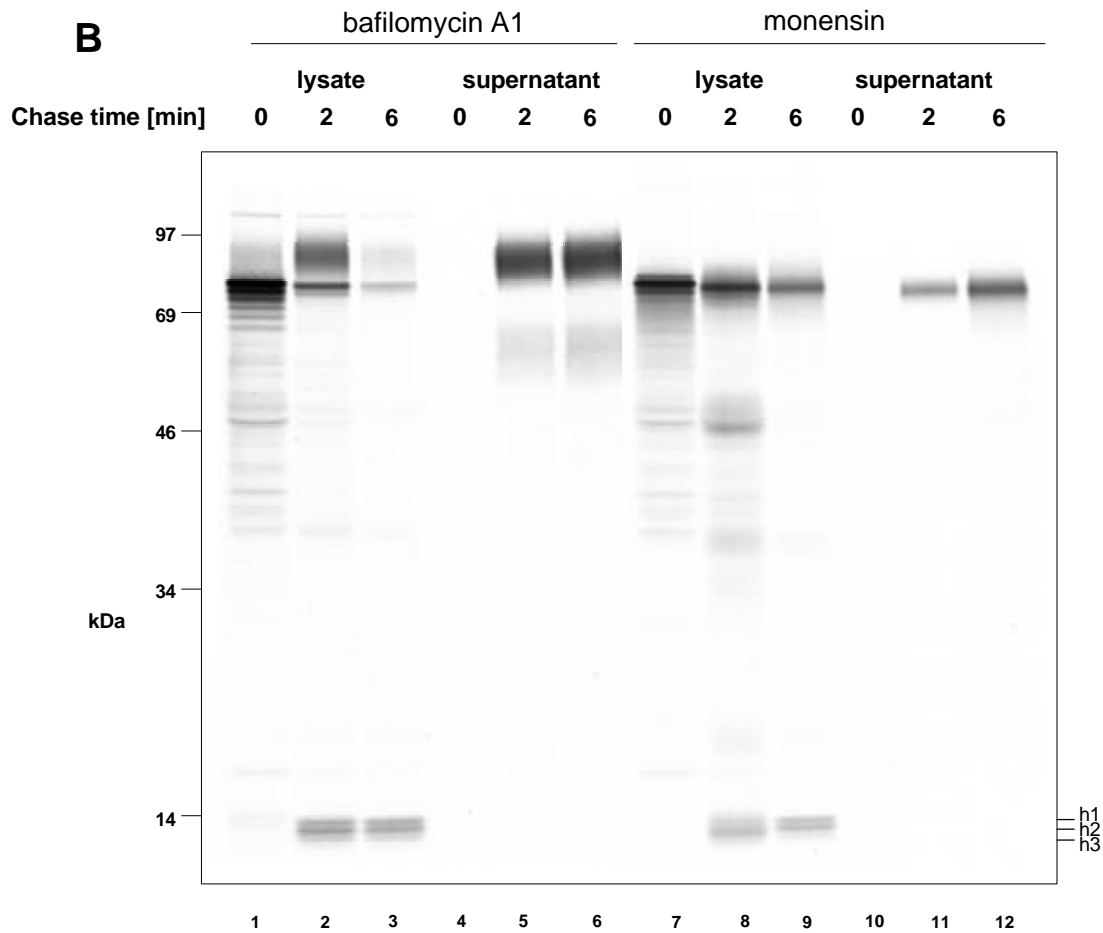
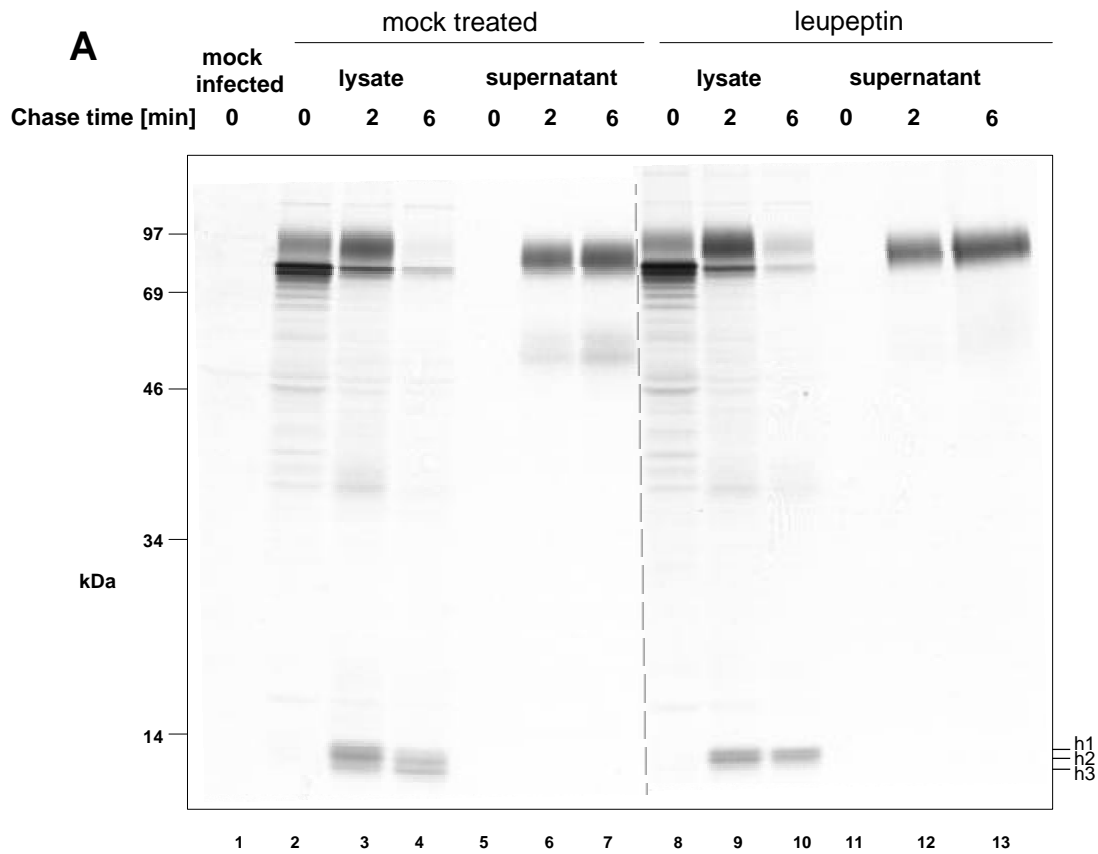
3.17 Processing of E3/49K is influenced by agents affecting glycosylation, acidification, lysosomal proteases and intracellular trafficking

The immunofluorescence studies indicated that acidotropic agents affect the intracellular trafficking of 49K. In order to find out how this may affect the proteolytic processing of 49K and to identify the compartments, where the processing of 49K occurs, Ad19a-infected A549 cells were treated with chloroquine, ammonium chloride, bafilomycin A1 and the Na⁺ ionophore monensin, which increase the pH of acidic compartments (Fig. 28B, C). In addition, leupeptin, an inhibitor of lysosomal cysteine and serine proteases, tunicamycin, an inhibitor of N-glycosylation, and brefeldin A, an inhibitor of guanine nucleotide exchange factors (GEFs) for Arfs, which induces the collapse of the Golgi onto the ER and blocks transport to the cell surface, were applied (Fig. 28A, D). In a pulse/chase experiment the intracellular processing of 49K was followed with the C-terminal antibody, whereas the secretion of 49K was monitored with the N-terminal antibody.

In mock-treated cells the known processing was visualized (Fig. 28A, lanes 2-7). Notably, a distinct low molecular weight band is detected after 6 h chase (h3), indicating that C-terminal fragments are further trimmed after the initial cleavage(s) releasing the N-terminal ectodomain. This seems to occur in a different compartment than the initial cleavage, since the fragment h3 appeared in general later during the chase (2-3 h) than the other fragments, h1 and h2 (~1 h). Interestingly, upon treatment with leupeptin (Fig. 28A, lanes 8-13) fragment h3 was not detected (compare lane 10 with lane 4). This suggests that a lysosomal cysteine or serine protease generates this fragment. On the other hand, the secretion of the N-terminal ectodomain is not significantly affected by leupeptin. Fragment h3 was also not detected after treatment with agents that elevate the pH of intracellular, particularly endosomal/lysosomal, compartments, like bafilomycin A1 (Fig. 28B lanes 1-6), monensin (Fig. 28B, lanes 7-12) and chloroquine (Fig. 28C, lanes 1-6), substantiating the hypothesis that the cleavage producing the fragment with the lowest apparent molecular weight (h3) takes place in late endosomes/lysosomes in a pH-dependent manner. After treatment with ammonium chloride reduced amounts of the C-terminal fragment h3 were detected (Fig. 28C, lanes 7-12). Interestingly, the acidotropic compounds also changed the glycan processing of 49K: Chloroquine and to a lesser extent bafilomycin A1 prolonged the processing time. Ammonium chloride and monensin impaired modifications in the glycan structures indicated by a different molecular weight of the processed 49K. This effect was even more dramatic at a higher concentration (50 mM) of ammonium chloride (data not shown).

In order to investigate the influence of these agents on the proteolytic cleavage and secretion, the secretion rate was determined as follows: secretion rate [%] = (radioactive label of the secreted 49K in the supernatant after 6 h chase / ((radioactive label of intracellular high molecular weight

forms of 49K after the pulse; 0 h chase) – (radioactive label of intracellular high molecular weight forms of 49K after 6 h chase)) x 100. This procedure was required, since due to the influence of some agents on the glycan processing after 6 h chase still significant amounts of 49K could be detected, e.g. with chloroquine, whereas, e.g. in mock-treated cells, only very low amounts of 49K remained after 6 h chase intracellularly. Therefore, the radioactive label of 49K in the supernatant after 6 h chase itself was not conclusive in order to evaluate the influence of the tested agents on proteolytic cleavage and secretion. Labeling was performed with [³⁵S]-methionine. 49K without the signal peptide contains five methionine residues, one in the cytoplasmic tail, four in the N-terminal ectodomain (Fig. 6). Therefore, 20% of total labeling is expected to end up in cytoplasmic tail fragments and 80% in the N-terminal ectodomain. In these calculations potential differences in the affinities of the antibodies directed against the N- (supernatant) and the C-terminus (lysate) were ignored. Other experiments indicated that slight differences exist. Surprisingly, chloroquine and bafilomycin A1 treatment increased the secretion rate from 25-30% in untreated cells to ~66% and 56%, respectively. In contrast, ammonium chloride had no significant effect on the secretion rate. Monensin, which has been reported to inhibit secretion of several proteins (Mollenhauer et al., 1990), decreased secretion only slightly to about 20% of total labeling. Treatment with the inhibitor of N-glycosylation, tunicamycin, and the inhibitor of ER to Golgi transport, brefeldin A, totally blocked the proteolytic processing of 49K as indicated by the absence of low molecular weight fragments in the lysates and secreted 49K in the supernatants (Fig. 28D). In immunofluorescence studies after treatment with tunicamycin, 49K was detected in the ER, which was probably due to misfolding (data not shown). This also explains the coprecipitation of the ER resident Ad19a E3/19K protein. Brefeldin A causes the redistribution of the Golgi complex into the ER. The marginal molecular weight shift indicative of limited glycan processing of 49K during the chase upon brefeldin A treatment is most likely caused by the residual activity of Golgi glycosyltransferases in the fused Golgi-ER-complex (Fig. 28D, lane 7-9). Also after BFA treatment coprecipitation of low amounts of Ad19a E3/19K was observed.



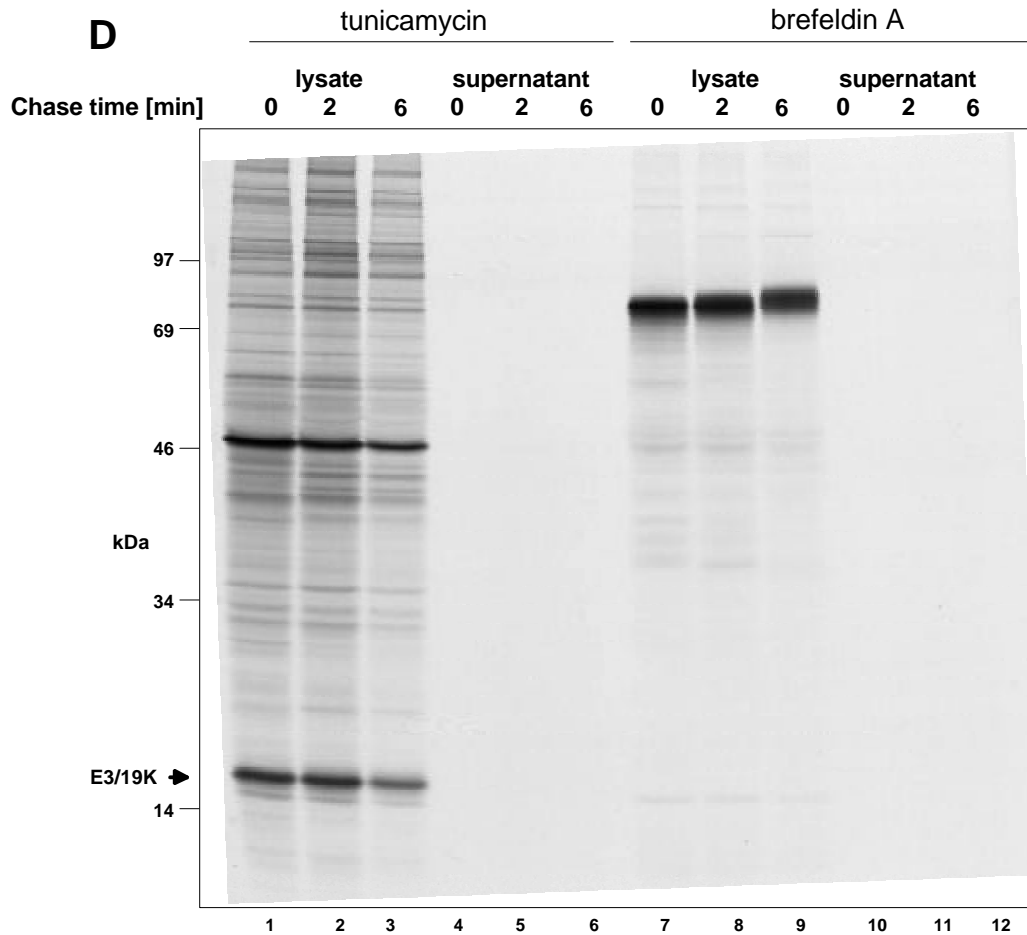
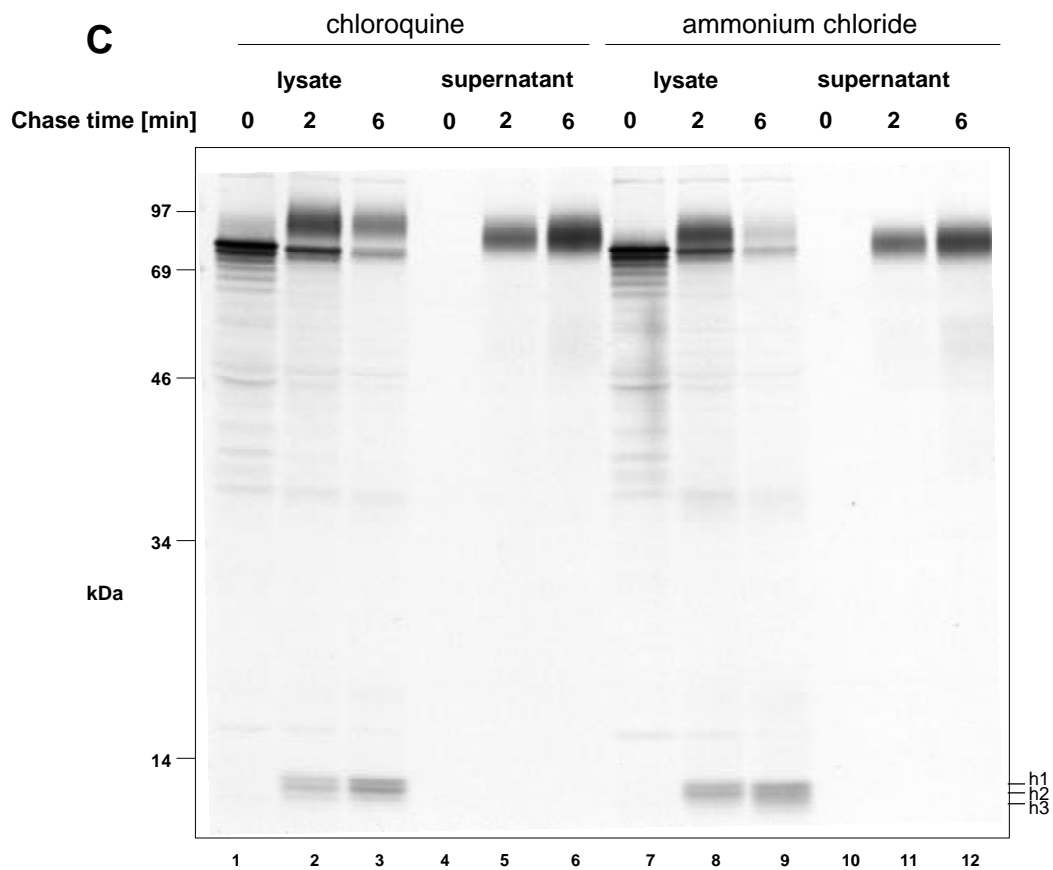


FIG. 28. 49K processing in the presence of agents affecting glycosylation, intracellular trafficking or protease activities. Ad19a-infected cells were pulsed with [³⁵S]-methionine for 30 min and chased with medium containing non-radioactive methionine for 2 h and 6 h. Several different agents were included in the starvation medium and were present in all other incubations: A) mock (lanes 2-7) and leupeptin (200 μM, lanes 8-13); B) bafilomycin A1 (0.1 μM, lanes 1-6) and monensin (10 μM, lanes 7-12); C) chloroquine (100 μM, lanes 1-6) and ammonium chloride (10 mM, lanes 7-12); D) tunicamycin (10 μg/ml, lanes 1-6) and brefeldin A (5 μg/ml, lanes 7-12).

3.18 Function of the potential endosomal/lysosomal sorting motifs in the cytoplasmic tail of E3/49K

3.18.1 Surface plasmon resonance analysis

The data presented so far demonstrated that 49K localizes mainly to the Golgi/TGN, the plasma membrane and early endosomes. In addition, a minor trafficking pathway to late endosomes and lysosomes seems to exist. The cytoplasmic tail of 49K contains potential endosomal/lysosomal sorting motifs, YXXΦ and LL, which are possibly implicated in the regulation of the intracellular trafficking of 49K. These motifs are known to interact with the clathrin adaptor complexes AP-1 to AP-4 (chapter 1.8.3). At first, it was therefore examined whether peptides representing the cytoplasmic tail of 49K bind *in vitro* to purified clathrin adaptor complexes AP-1 and AP-2 (in collaboration with Stefan Höning, University of Göttingen, Germany). Interestingly, an interaction with both AP-1 and AP-2 was detected (Fig. 29). Mutating either of the putative sorting motifs decreased the interaction with the adaptor complexes, mutating both motifs abolished binding entirely. These data indicated that both motifs contribute to the binding to AP-1 and AP-2 *in vitro* and may be functional *in vivo*.

Peptides	K _D (M)	
	AP-1	AP-2
CRKRPRAYNHMVDP LL SFSY (WT)	2.4 × 10 ⁻⁷	3.2 × 10 ⁻⁷
CRKRPRAA N HMVDP LL SFSY (YA)	6.4 × 10 ⁻⁷	5 × 10 ⁻⁷
CRKRPRAYNHMVDP AA SFSY (LLAA)	20 × 10 ⁻⁷	8 × 10 ⁻⁷
CRKRPRAA N HMVDP AA SFSY (YA/LLAA)	no binding detectable	no binding detectable

FIG. 29. Peptides representing the cytoplasmic tail of 49K interact with AP-1 and AP-2 *in vitro* via the YXXF and LL motifs. The interaction of purified adaptor complexes AP-1 and AP-2 with peptides representing the cytoplasmic tail of 49K as indicated was examined by surface plasmon resonance analysis as described in Materials and Methods. In addition, peptides with the YXXΦ and LL motif mutated to AXXΦ and AA respectively were tested and the equilibrium constants (K_D) were determined.

3.18.2 Increased cell surface expression of E3/49K proteins with mutated cytoplasmic tails

To test the function of the putative sorting motifs *in vivo*, cell lines were established that expressed 49K proteins with mutated motifs. The tyrosine of the YXX Φ and the leucines of the LL were replaced by alanine individually creating the YA and the LLAA mutant respectively or both generating the YA/LLAA double mutant. To examine the influence of the entire cytoplasmic tail, in addition a 49K mutant lacking the entire cytoplasmic tail was generated (Δ CT). The cell surface expression and the intracellular levels of WT and mutated 49K in the cell lines were determined by flow cytometry. The cell surface expression of the mutated proteins was not directly utilized to evaluate effects of the mutations, since the different clones exhibited different synthesis rates. Therefore, the ratio of 49K detected on the cell surface to intracellular 49K was used, which was independent of the expression rate (Fig. 30).

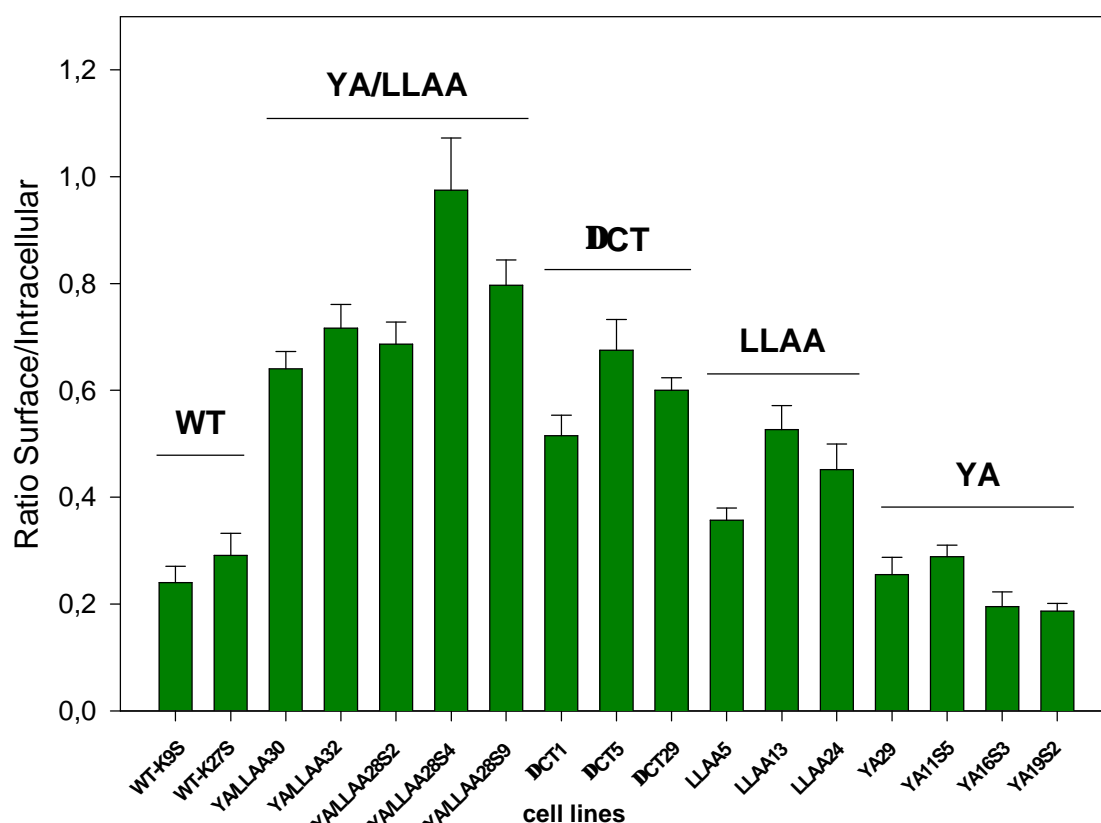


FIG. 30. Internalization of 49K from the cell surface is mainly directed by the LL motif in the cytoplasmic tail. Constructs for the expression of mutant proteins were based on the pSG5-49K plasmid. DNA sequences containing mutations were generated by PCR (sense: 49KUSER546; antisense: 49KdelCT, 49KYLLAAA, 49KYA, 49KLLAA) and cloned into pSG5-49K using BglII restriction sites. The mutated sequences were confirmed by sequencing. A549 cell lines stably expressing 49K WT and mutant proteins with one or both of the YXX Φ and LL motifs in the cytoplasmic tail mutated to AXX Φ and AA or with the entire cytoplasmic tail deleted (Δ CT) were generated as described in Materials and Methods and analyzed by flow cytometry. Cell surface and internal 49K levels were measured and the ratio of the mean fluorescence values of cell surface and internal expression was determined for several isolated clones of 49K WT and mutants as indicated. Mean values were calculated from 4-6 independent experiments. Error bars indicate the standard error determined with SigmaPlot for Windows Version 5.00.

The ratio was determined for 2-5 clones of WT and mutant 49K proteins to exclude clonal differences. For WT 49K this ratio was 0.24-0.29. The YA/LLAA and Δ CT mutants showed clearly enlarged ratios of 0.64-0.97 and 0.51-0.68 respectively. In the LLAA mutants the ratio was slightly increased to 0.36-0.53. The YA mutants exhibited ratios of 0.19-0.28, which was comparable to WT. Thus, YA/LLAA and Δ CT, and to a lesser extent also the LLAA mutant 49K proteins were expressed in higher amounts on the cell surface than WT and YA mutant 49K proteins indicating impaired internalization.

The immunoprecipitation data demonstrated that 49K is proteolytically processed. The site of that cleavage was unknown but it had to be considered that the cleavage might occur at the cell surface. In that case the proteolytic cleavage would limit the accumulation of 49K mutants deficient in endocytosis on the cell surface. Consistent with this hypothesis, WT and mutated 49K proteins were rapidly lost from the cell surface, when cells were treated with brefeldin A to inhibit the transport of newly synthesized protein to the cell surface (Fig. 31).

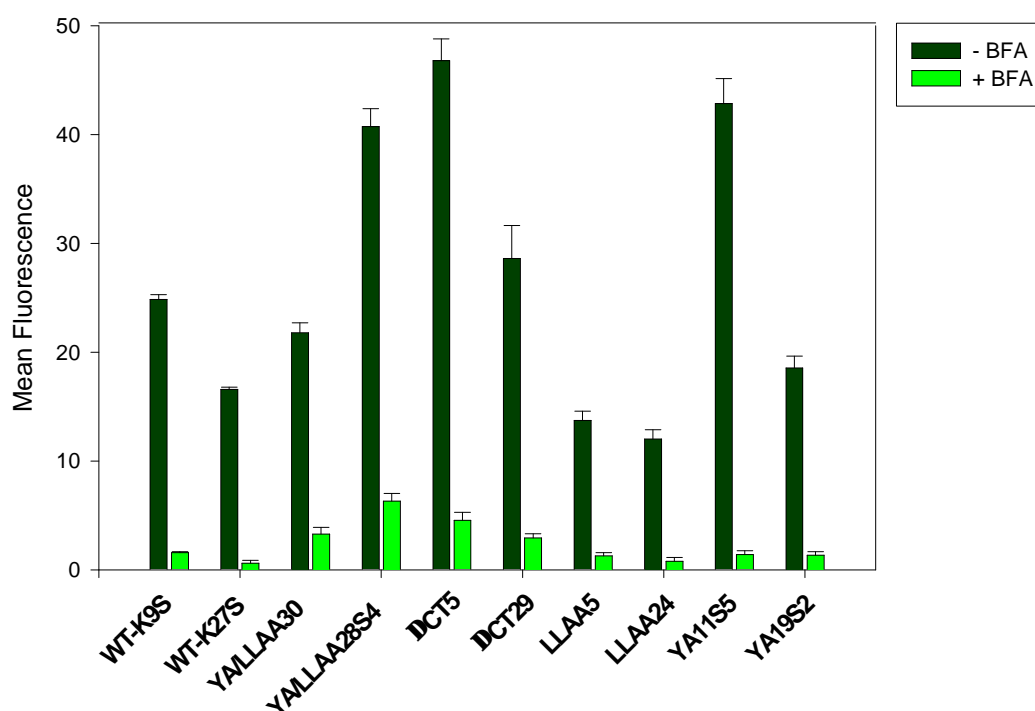


FIG. 31. Rapid decrease of cell surface expression of 49K in cell lines expressing WT and mutated 49K proteins after brefeldin A treatment. Mean fluorescence of cell surface expression of 49K was determined by flow cytometry after mock (black bars) or 4 h brefeldin A treatment (5 μ g/ml, grey bars) of cell lines expressing WT and mutant 49K proteins as indicated. Mean values were calculated from 4-6 independent experiments. Error bars indicate the standard error determined with SigmaPlot for Windows Version 5.00.

After 4 h BFA treatment only 4-6% WT, 3-7% YA mutant, 6-9% LLAA mutant, 15% YA/LLAA mutant and 9-10% Δ CT mutant 49K proteins remained at the cell surface. The cell surface expression of some cellular proteins in comparison was only slightly decreased to about 80% of the levels of untreated cells (HLA: ca. 75%, Fas: ca. 86%, EGFR: ca. 80%). Thus, although the internalization of mutated 49K proteins was impaired, 49K staining at the cell surface is still rapidly lost during BFA treatment. One explanation for that finding is that two mechanisms exist that are able to remove WT 49K from the cell surface: Endocytosis and proteolytic cleavage. In case of the mutant 49K proteins, a deficit in endocytosis may result only in a limited accumulation at the cell surface (Fig. 30), since 49K can also be removed from the cell surface by the proteolytic processing.

3.18.3 Increased secretion of E3/49K proteins with mutated cytoplasmic tails

The results from the brefeldin A experiment (Fig. 31) indicated that mutations of the cytoplasmic tail of E3/49K do not prevent proteolytic processing. Therefore, cleavage may occur on the way to and/or at the cell surface. In immunoprecipitation, 49K was detected in cell lines expressing WT and mutant 49K proteins after 2 h labeling (Fig. 32A). Low molecular weight fragments (h) were detected in lysates from cell lines stably expressing mutated E3/49K proteins using antibodies directed against the C-terminus (except for the mutants lacking the cytoplasmic tail which could only be detected with antibodies against the N-terminus). This finding confirmed that the mutant 49K proteins were still proteolytically processed. Notably, the mutations affected the recognition of the cytoplasmic tail of mutated 49K proteins. The YA/LLAA32 clone for example expressed three- to fourfold higher levels of 49K than WT K27S as determined by immunoprecipitation with N-terminal antibody after pulse labeling (Fig. 32B, compare lanes 2 and 15) but is less well precipitated by the antibody against the C-terminus (Fig. 32A, compare lanes 3 and 5). In addition, synthesis rates were measured by quantification of intracellular 49K after brefeldin A treatment by flow cytometry with similar results (data not shown). Interestingly, every mutation changes the migration behavior of the low molecular weight fragments in the polyacrylamide gel (Fig. 32A).

To investigate the processing kinetics of WT and mutated 49K, a pulse/chase experiment (30 min pulse, 45 and 180 min chase) with individual clones with similar synthesis rates was performed. No significant differences in the processing kinetics between WT and mutant 49K proteins were observed (Fig. 32C, data not shown). Particularly, the intracellular processing of WT (lane 3-5) and Δ CT (lane 15 -17) 49K proteins was almost identical. The YA/LLAA mutant 49K protein was difficult to precipitate intracellularly (lane 9-11) because of the already described decreased recognition of the mutated cytoplasmic tail with the C-terminal antibody.

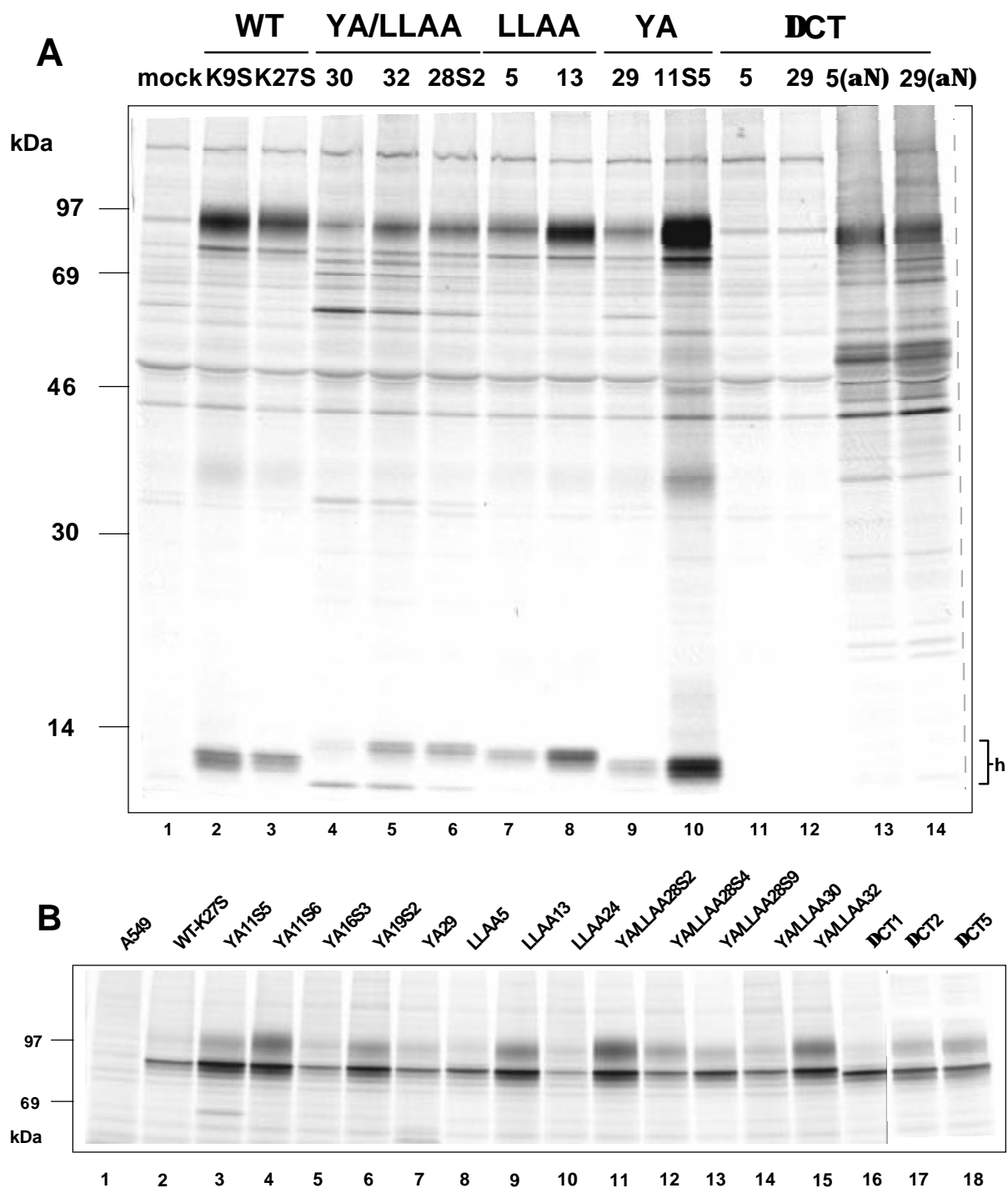
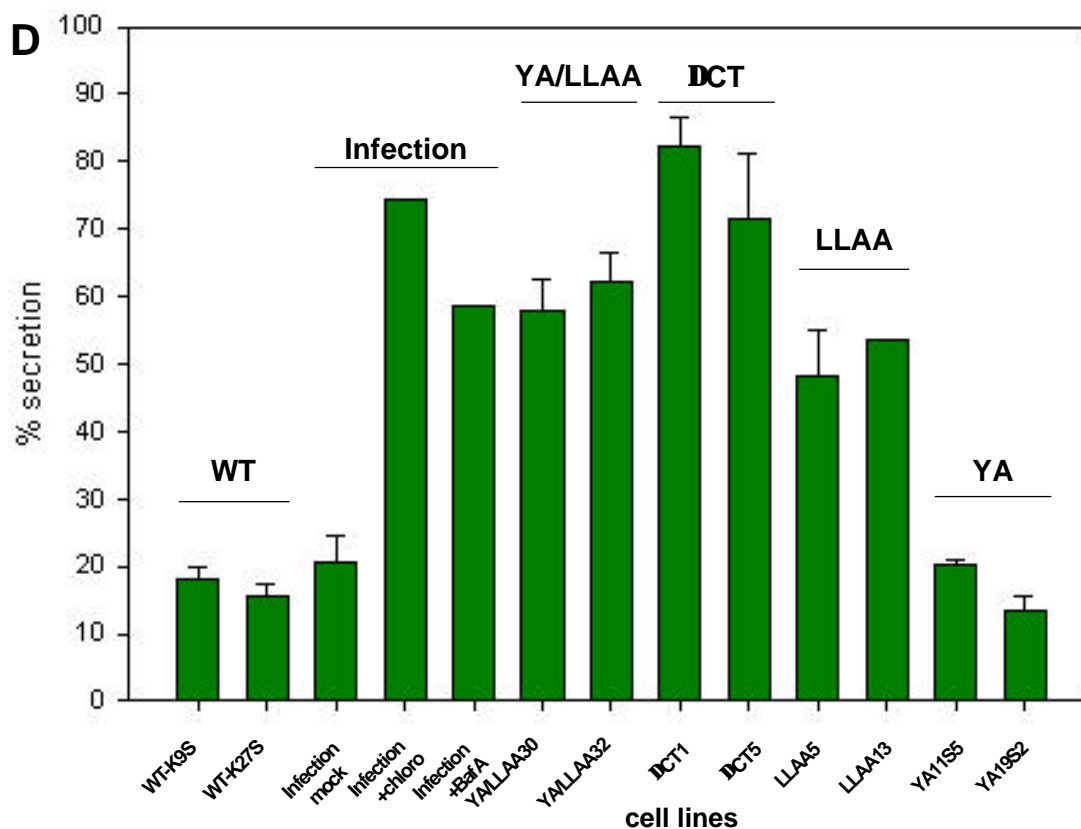
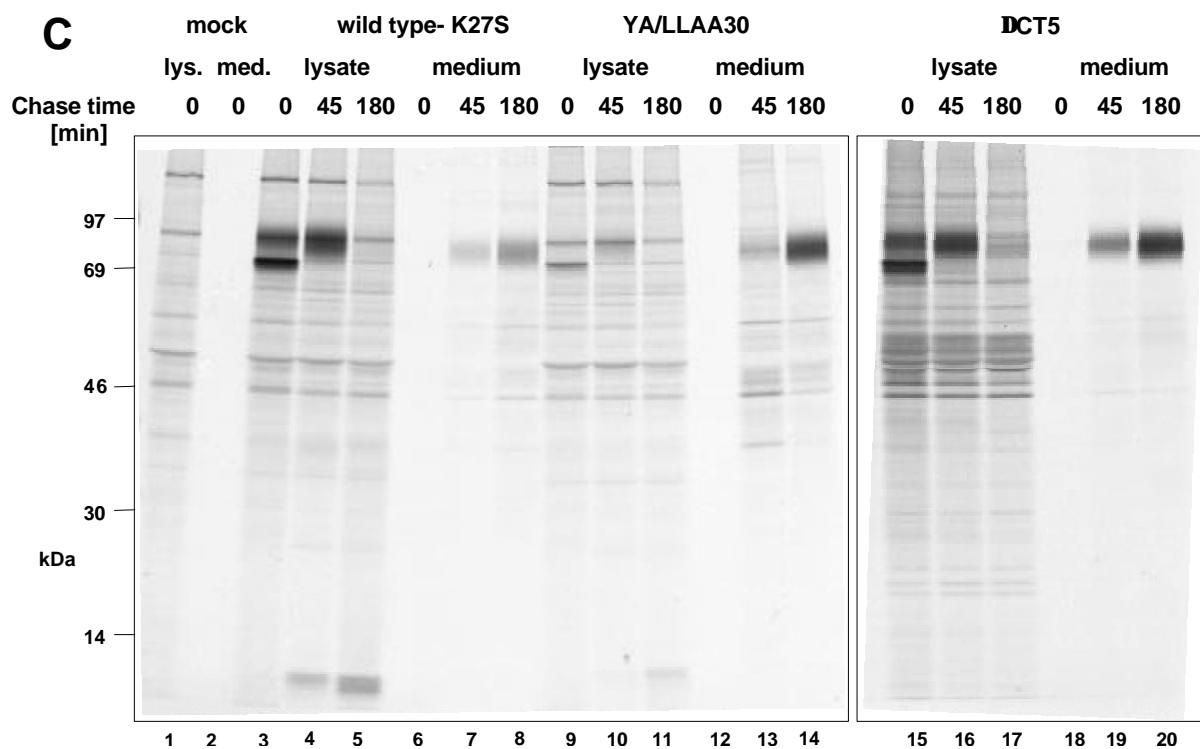


FIG. 32. Decreased internalization of mutated 49K proteins correlates with increased secretion. A) Different clones expressing 49K WT and mutant proteins were metabolically labeled for 2 h and 49K was precipitated with antibodies directed against the C-terminus (R25050, lanes 1-12) and with antibodies directed against the N-terminus (R48-7B, lanes 13, 14). B) Different clones expressing 49K WT and mutant proteins were pulse labeled 30 min and 49K was precipitated with antibodies directed against the N-terminus to determine the synthesis rate of each clone. C) The processing kinetics of WT and mutated 49K proteins were determined in a pulse (30 min)/ chase (45 and 180 min) experiment, in which 49K was precipitated from WT and YA/LLAA mutant cell lysates with antibodies directed against the C-terminus (lanes 3-5, 9-11) and from Δ CT mutant cell lysates (lane 15-17) and all supernatants (lanes 6-8, 12-14, 18-20) with antibodies directed against the N-terminus of 49K. D) The secretion rate of 49K was determined in a pulse (0.5 h)/chase (4 h) experiment followed by immunoprecipitation with antibodies directed against the N-terminus (48-7B) and SDS-PAGE. Bands corresponding to 49K were quantified by phosphorimager analysis.



The radioactive labeling of 49K after the pulse was defined as 100%. The cytoplasmic tail contains 20% of total [35 S]-methionine labeling. Therefore, the maximum value for secretion is expected to be 80% of total 49K labeling. Mean values were calculated from two independent experiments (except for values of chloroquine and bafilomycin A1 treatment which represent results of single experiments). Error bars indicate the standard error determined with SigmaPlot for Windows Version 5.00.

Also the kinetics of the secretion of 49K seemed unchanged in the mutant 49K proteins (compare YA/LLAA, lanes 12-14, and Δ CT, lanes 18-20, with WT, lanes 6-8). However, the quantity of the secreted 49K seemed to be increased in the YA/LLAA and in the Δ CT mutant (compare lanes 14 and 20 with lane 8). Therefore, the secretion rate of two individual clones of each mutant was determined in a pulse (0.5 h)/chase (4 h) experiment and compared to WT clones and infection (Fig. 32D). Strikingly, the secretion of the YA/LLAA and the Δ CT mutants was increased to 58-62% and 71-82%, respectively, of total labeling compared to about 16-18% for WT clones and 20% in infection. The secretion rate of the LLAA mutant was also clearly increased to 48-54%, whereas the secretion of the YA mutant was not (14-20%). Interestingly, the increased secretion of mutant 49K proteins correlated with the increased cell surface expression substantiating the hypothesis that proteolytic cleavage can occur at the cell surface (Fig. 30). As shown before, acidotropic agents increased the secretion rate (Fig. 22C). In this experimental setting secretion rates of 75% of total 49K labeling during chloroquine and of 59% during bafilomycin A1 treatment were measured after Ad19a infection.

3.18.4 Decreased internalization of mutated E3/49K proteins and accumulation of mutated cytoplasmic tail fragments at the cell surface

Proteolytic cleavage, occurring most likely at the cell surface, was observed with all 49K mutants. Some of the mutants exhibited an increased cell surface expression suggesting a deficiency in endocytosis. Therefore, the proteolytic processing and secretion at the cell surface may limit the accumulation of endocytosis deficient 49K mutants at the cell surface if 49K is detected with antibodies directed against the N-terminus. On the other hand mutant cytoplasmic fragments are supposed to remain at the cell surface after proteolytic cleavage and secretion of the N-terminal ectodomain if motifs required for endocytosis have been eliminated. However, the detection of mutated cytoplasmic tails with antibodies directed against the WT C-terminus is decreased compared to WT. Despite this limitation, immunofluorescence demonstrated that the cytoplasmic tail fragments of the YA/LLAA mutant accumulated at the cell surface (Fig. 33A, left panel). The LLAA mutant exhibited only very slightly increased surface levels, whereas in the YA mutant no difference to WT was detectable. With antibodies directed against the N-terminus only a slight accumulation of full-length Δ CT and YA/LLAA but not of YA and LLAA mutant 49K proteins at the cell surface could be detected (Fig. 33A, middle panel).

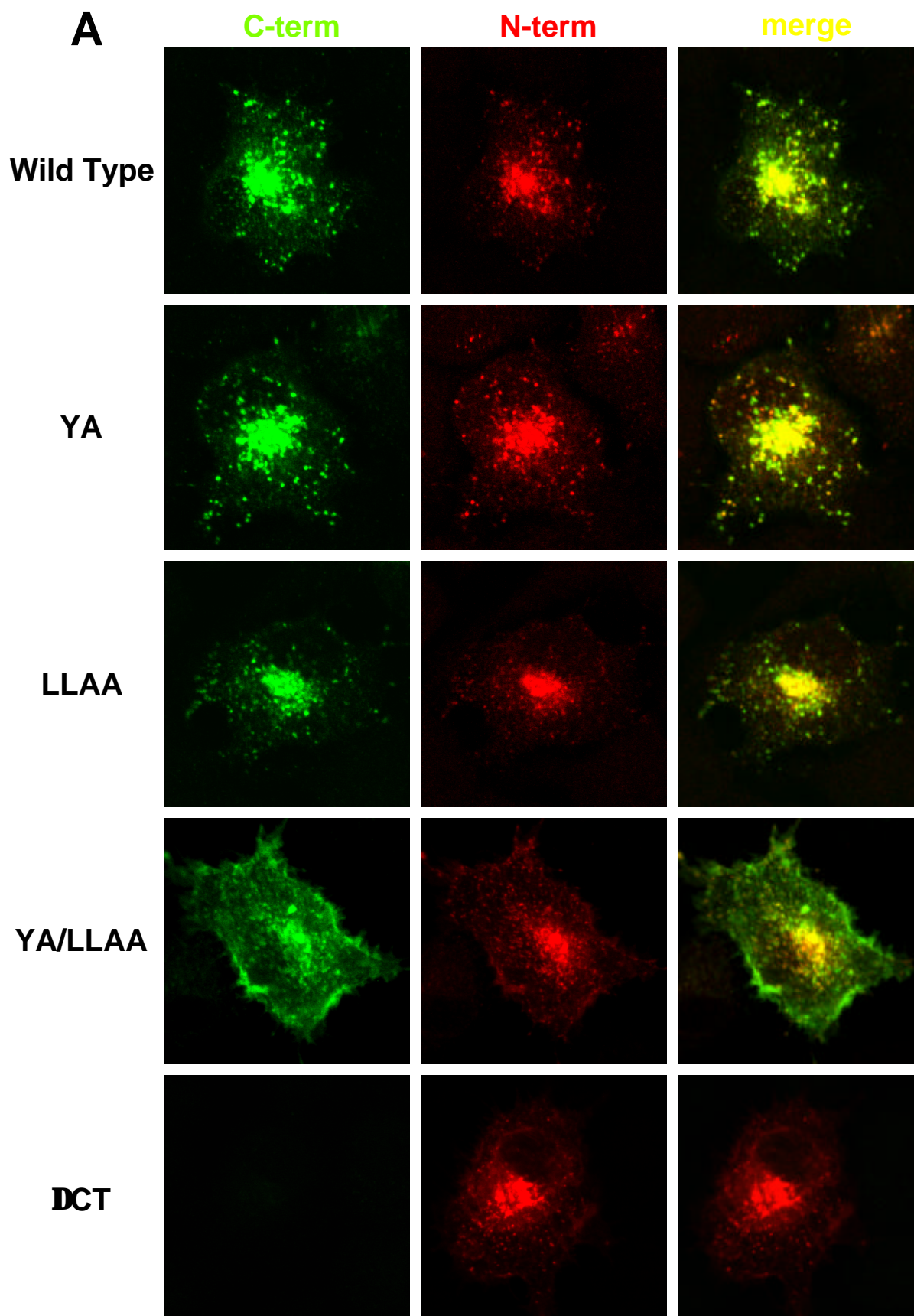
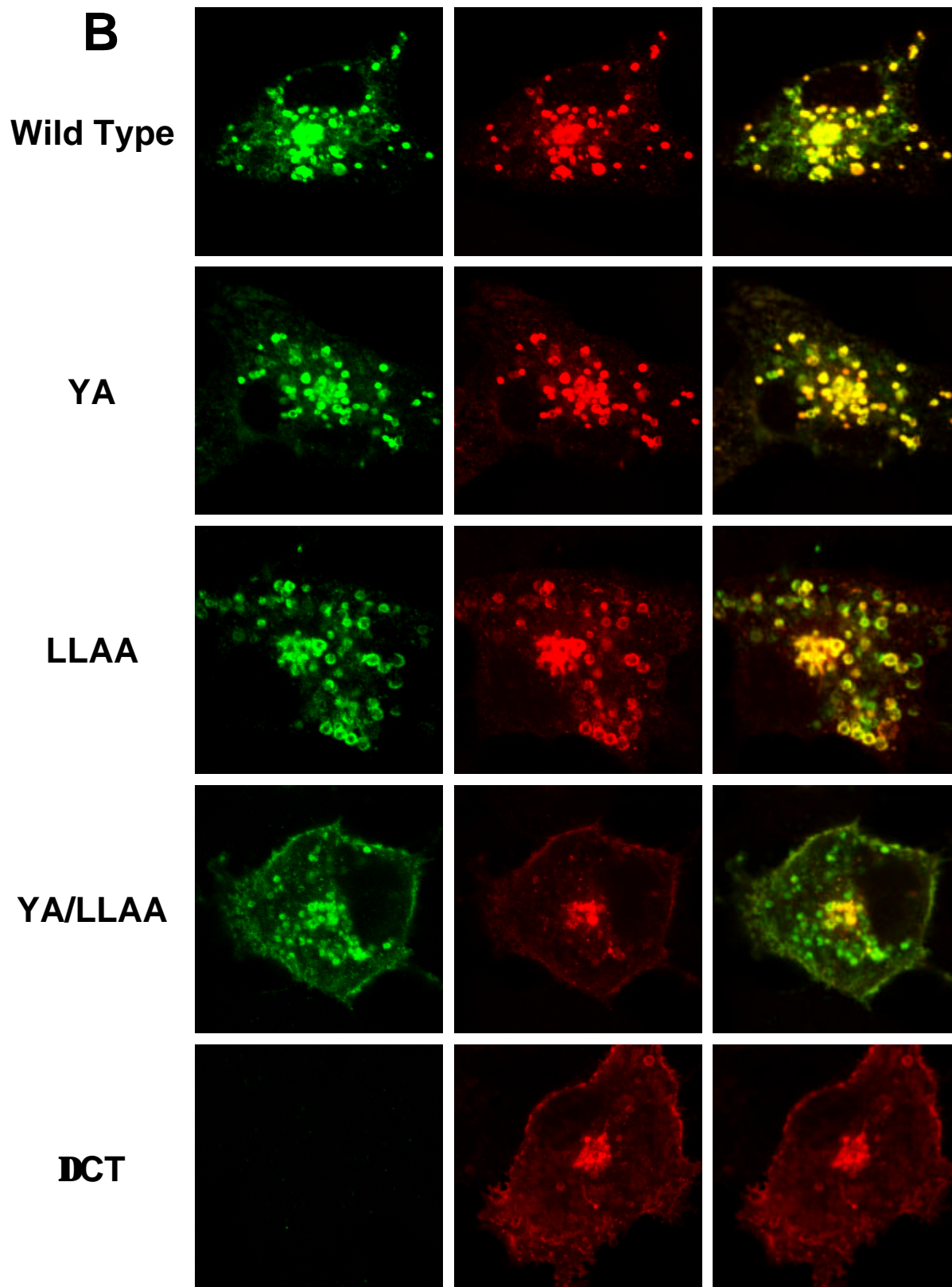


FIG. 33. Decreased internalization of mutated 49K proteins results in accumulation of the cytoplasmic tail at the cell surface and reduced intracellular accumulation in swollen endosomal vesicles during chloroquine treatment. A549 cells were transiently transfected with pSG5 plasmids encoding WT and mutant 49K proteins as described in Materials and Methods.

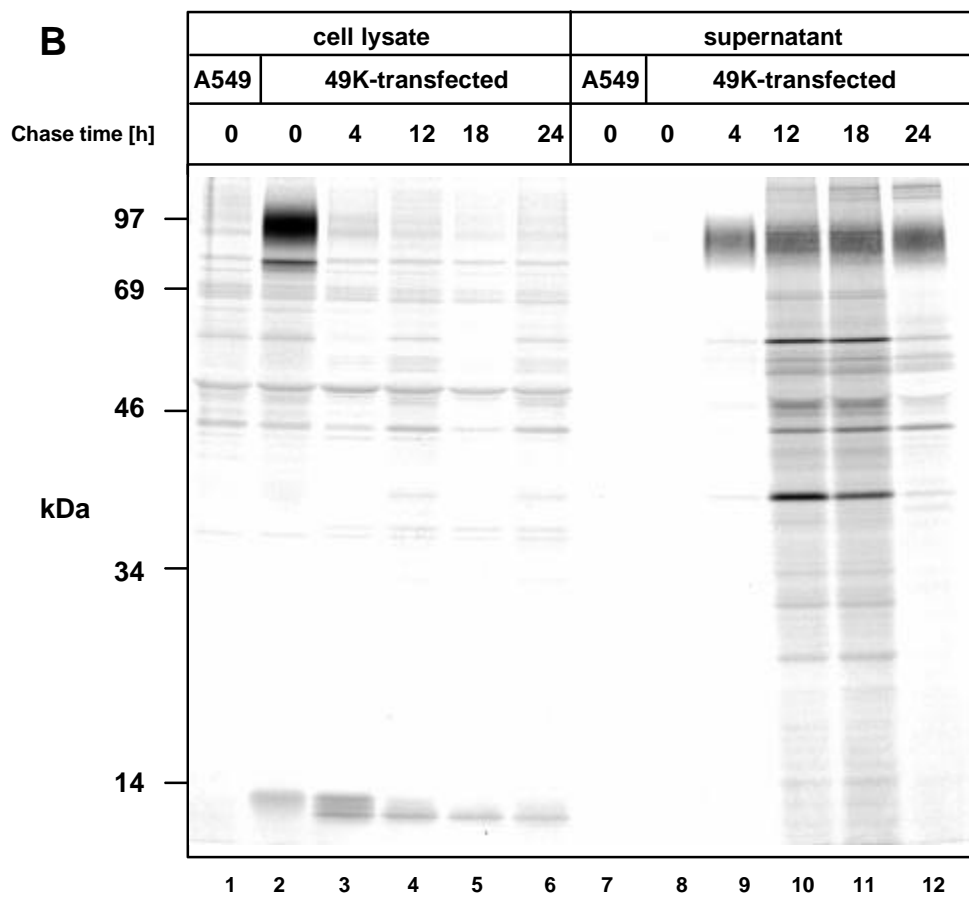
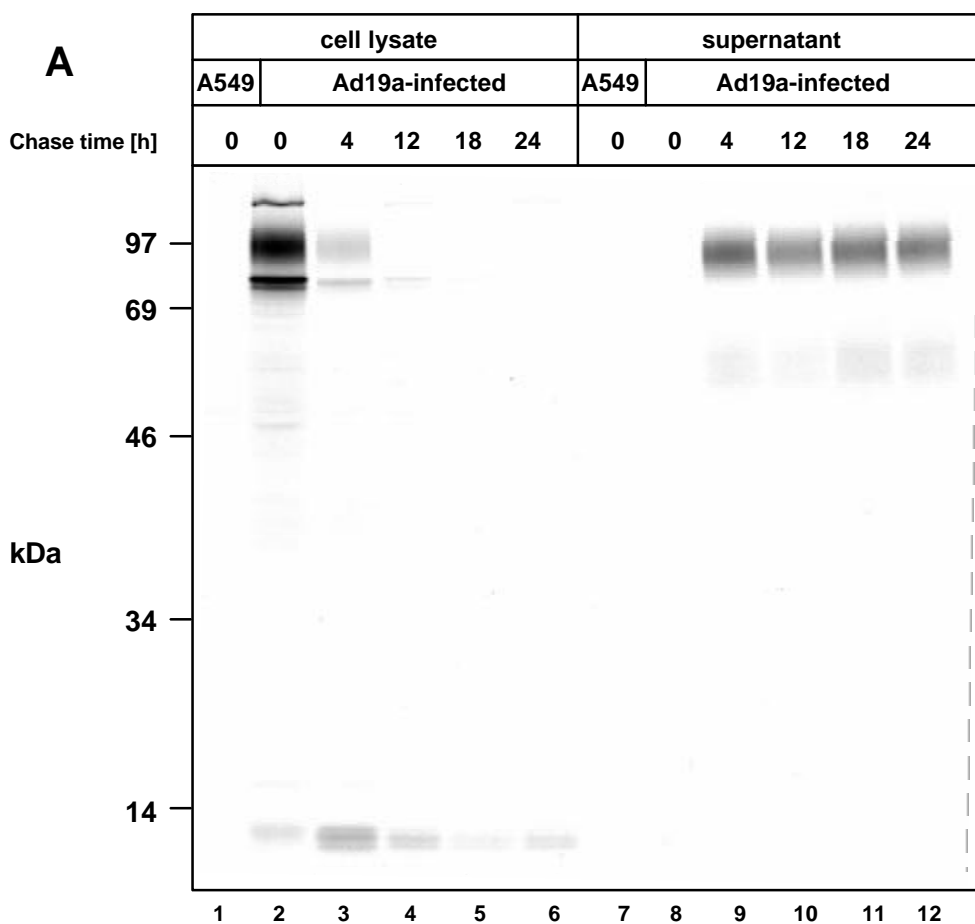


After 36 h cells were processed for confocal laser microscopy. Staining was performed with antibodies directed against the N- (rat monoclonal, 4D1) and the C-terminus (rabbit polyclonal, R25050) of 49K. Cells were mock-treated (A) or treated with 100 μ M chloroquine for 12 h (B).

Treatment with acidotropic agents like chloroquine blocks intracellular transport at an early or late endosomal state. Transport of proteins internalized from the cell surface to the Golgi/TGN or lysosomes can be inhibited resulting in an accumulation of proteins in early or late endosomal vesicles. This has been shown to be the case for WT 49K (Fig. 26, 33B). Therefore, it was tested how the trafficking of 49K mutants is affected by this treatment. A549 cells were transiently transfected with pSG5 constructs encoding WT and mutant 49K proteins to exclude clonal differences of stable transfectants. WT 49K accumulated in swollen vesicles after chloroquine treatment (Fig. 33B) and could be detected with antibodies directed against the C- as well as the N-terminus. In the YA mutant no difference was evident, in the LLAA mutant the accumulation was still clearly detectable, although it seemed to be slightly reduced. Some swollen vesicles were detected with antibodies against the C-terminus of 49K in the YA/LLAA mutant, although the staining was much weaker than in case of WT 49K. Hardly any stained swollen vesicles were detected with antibodies against the N-terminus of 49K. The same result was obtained for the Δ CT mutant. These findings are consistent with the view that internalization of the YA/LLAA and the Δ CT mutant 49K proteins is indeed strongly impaired. This is particularly evident for the full-length 49K proteins detected with the antibodies directed against the N-terminus.

3.19 High stability of E3/49K in the supernatant of Ad19a-infected and E3/49K-transfected cells

In order to address the function of 49K, it was attempted to purify the secreted form of 49K. Initially, the stability of the protein in the supernatant of Ad19a-infected cells (Fig. 34A) and 49K-transfected cells (Fig. 34B) was tested in a pulse/chase experiment with chase times up to 24 h. The levels of 49K detected in the supernatant remained constant from 4 h to 24 h chase. Thus, it could be concluded that the 49K protein is stably maintained in the supernatant after its secretion. This was confirmed by Western blotting analysis of soluble 49K in the supernatant of the stable transfectant (Fig. 34C), in which 49K accumulated during 9 days of incubation.



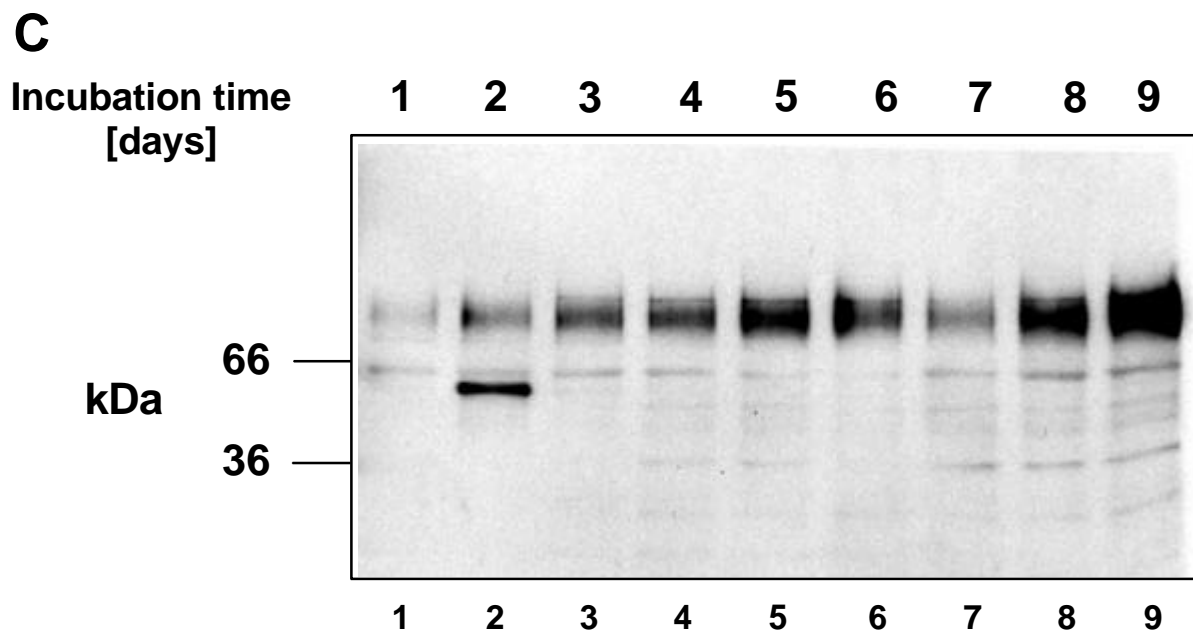


FIG. 34. High stability of secreted 49K. 49K was precipitated from lysates with anti-C-terminus (R25050) and from supernatants with anti-N-terminus (48-7B) antibodies from Ad19a-infected (A) and 49K-transfected (K27S, B) A549 cells after metabolic labeling with [³⁵S]-methionine for 1 h (9 h p.i.) and a chase with medium containing unlabeled methionine for 4, 12, 18 and 24 h. (C) Supernatants of 49K transfected cells were collected after 1-9 days and 15 μ l were directly analyzed by SDS-PAGE and Western blotting using antibodies directed against the N-terminus (R48-7B).

3.20 Purification of secreted E3/49K

To purify the secreted form of 49K, rat monoclonal antibodies directed against the N-terminal domain of 49K (4D1) were coupled to a protein G-Sepharose column as described in Materials and Methods. Supernatant from a cell line stably expressing 49K was collected after 8-9 days of incubation. The supernatant was precleared with a protein G-Sepharose column to remove antibodies and proteins present in the supernatant that bind to protein G-Sepharose. Then, the precleared supernatant was transferred to the affinity column. Finally, 49K was eluted with glycine buffer (pH 3.0). The eluted fractions were analyzed by silver staining and Western blotting (Fig. 35). The fractions contained very pure soluble 49K, represented by the major large (77-90 kDa) and a minor species (50-60 kDa) which was also detected in immunoprecipitation experiments, e.g. Fig. 16B.

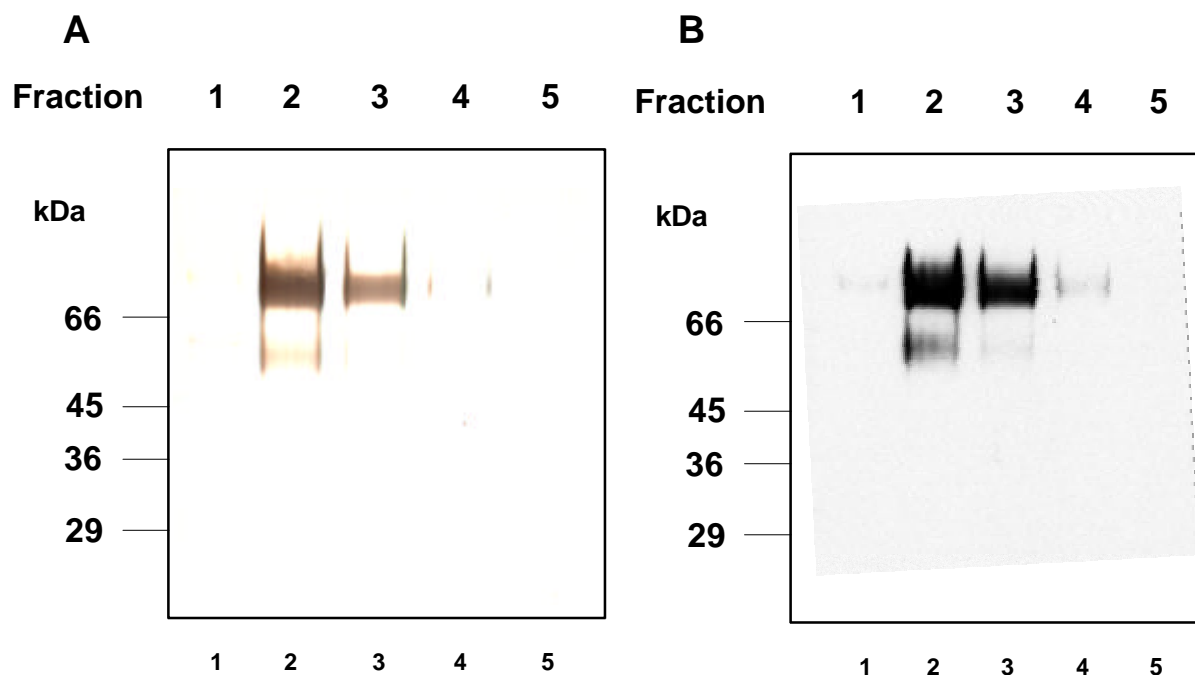


FIG. 35. Purification of E3/49K. Purification was performed as described in Materials and Methods. E3/49K was eluted from an anti-49K affinity column, in which the rat monoclonal antibody (4D1) directed against the N-terminus was coupled to protein G-Sepharose beads. 500 μ l fractions were collected. 15 μ l of each fraction was analyzed by SDS-PAGE, silver staining (A) and Western blotting (B) with antibodies directed against the N-terminus of 49K (R48-7B).

3.21 E3/49K is a lymphocyte binding factor

Proteins encoded by the early transcription unit 3 of human adenoviruses are involved in immune evasion (chapter 1.7). Cell surface expression and secretion of 49K led to the hypothesis that 49K does not affect the infected cell as other E3 gene products but rather influences surrounding cells, most likely cells of the immune system. In this scenario, binding of 49K to a receptor on immune cells was postulated. Therefore, the binding of purified, secreted 49K to lymphocyte and other cell lines was tested (Fig. 36). Cells were incubated for 1 h with purified 49K at 4°C prior to flow cytometry analysis using a rat monoclonal antibody directed against 49K. In these experiments the specific binding of 49K to several human lymphocyte cell lines, derived from NK cells, T lymphocytes and B lymphocytes, but not to primary human fibroblasts (SeBu) or to other human cell lines, e.g. A549 (lung epithelial carcinoma), 293 (embryonal kidney), HeLa (cervix carcinoma) or K562 (erythroleukemia) cells, could be shown. Thus, 49K seems to bind specifically to protein(s) expressed on lymphocytes leading to the hypothesis that this binding affects functions of these immune cells in the antiviral immune response.

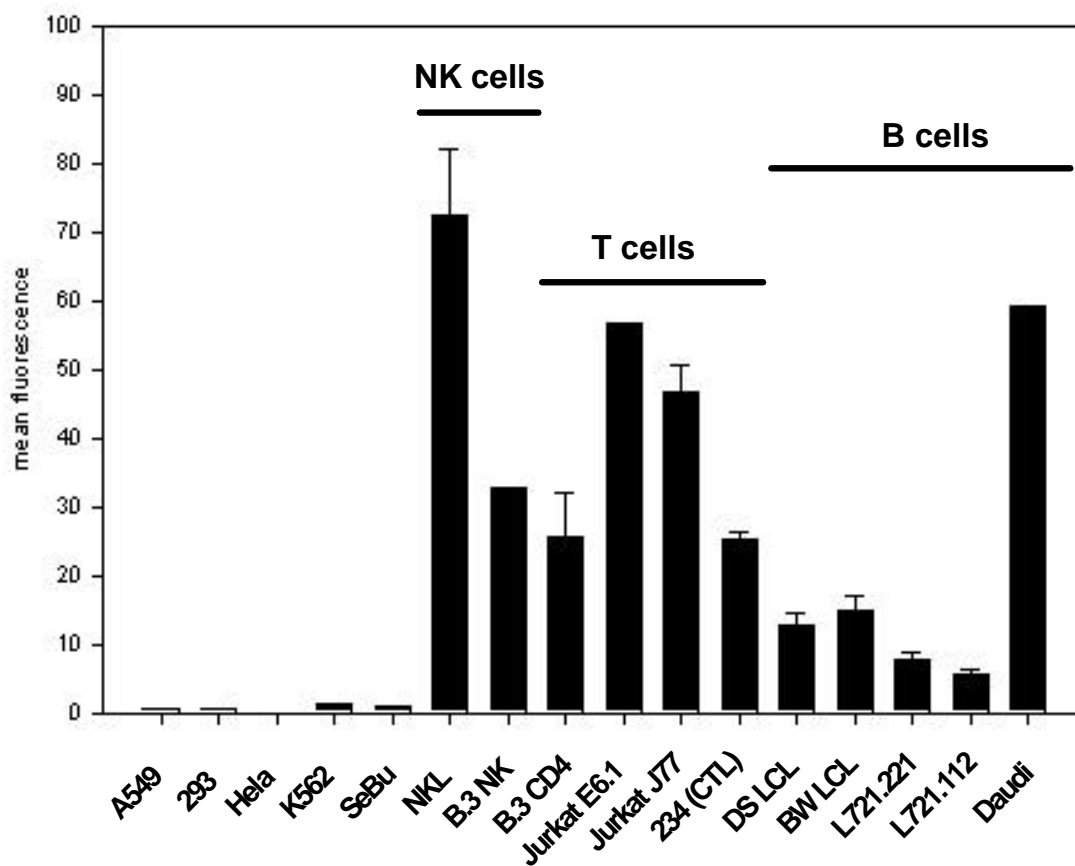


FIG. 36. Secreted E3/49K binds specifically to lymphocyte cell lines. Binding of secreted 49K to different cell lines and primary fibroblasts (SeBu) was tested in a modified flow cytometry protocol, in which secreted 49K (~200 ng) was incubated with cells in multiwell plates for 1 h at 4°C followed by incubation with anti-N-terminus (monoclonal rat, 4D1) antibodies and anti-rat FITC-labeled antibodies as described in the standard protocol for flow cytometry analysis in Materials and Methods.

3.22 Jurkat specific 49K-binding proteins coprecipitate with E3/49K

In order to identify proteins interacting with 49K, it was attempted to coprecipitate proteins from Jurkat (T cell leukemia) cells, which were shown to bind 49K in flow cytometry analysis (Jurkat J77 derived clone SVT35 (Ting et al., 1996)). A549 cells, which did not bind 49K as determined by flow cytometry, were used as a negative control. A549 and Jurkat cells were infected with Ad19a or Ad19a-49K(-), a 49K-deficient Ad19a virus, or mock-infected. A549 (6 h p.i.) and Jurkat (18 h p.i.) cells were labeled with [³⁵S]-methionine for 1.5 h. 49K was precipitated from the lysates (Fig. 37) of A549 (lanes 1-3) or Jurkat cells (lanes 7-9). Since adenoviruses do not infect lymphocytes very efficiently (Korner and Burgert, 1994), it was attempted to identify coprecipitating proteins by two different approaches. First, lysates of Ad- or mock-infected A549 cells were mixed with lysates of mock-infected Jurkat cells (lanes 4-6). Second, purified 49K was used to precipitate potential interaction partners from lysates of mock-infected A549 and Jurkat cells (lanes 10-13).

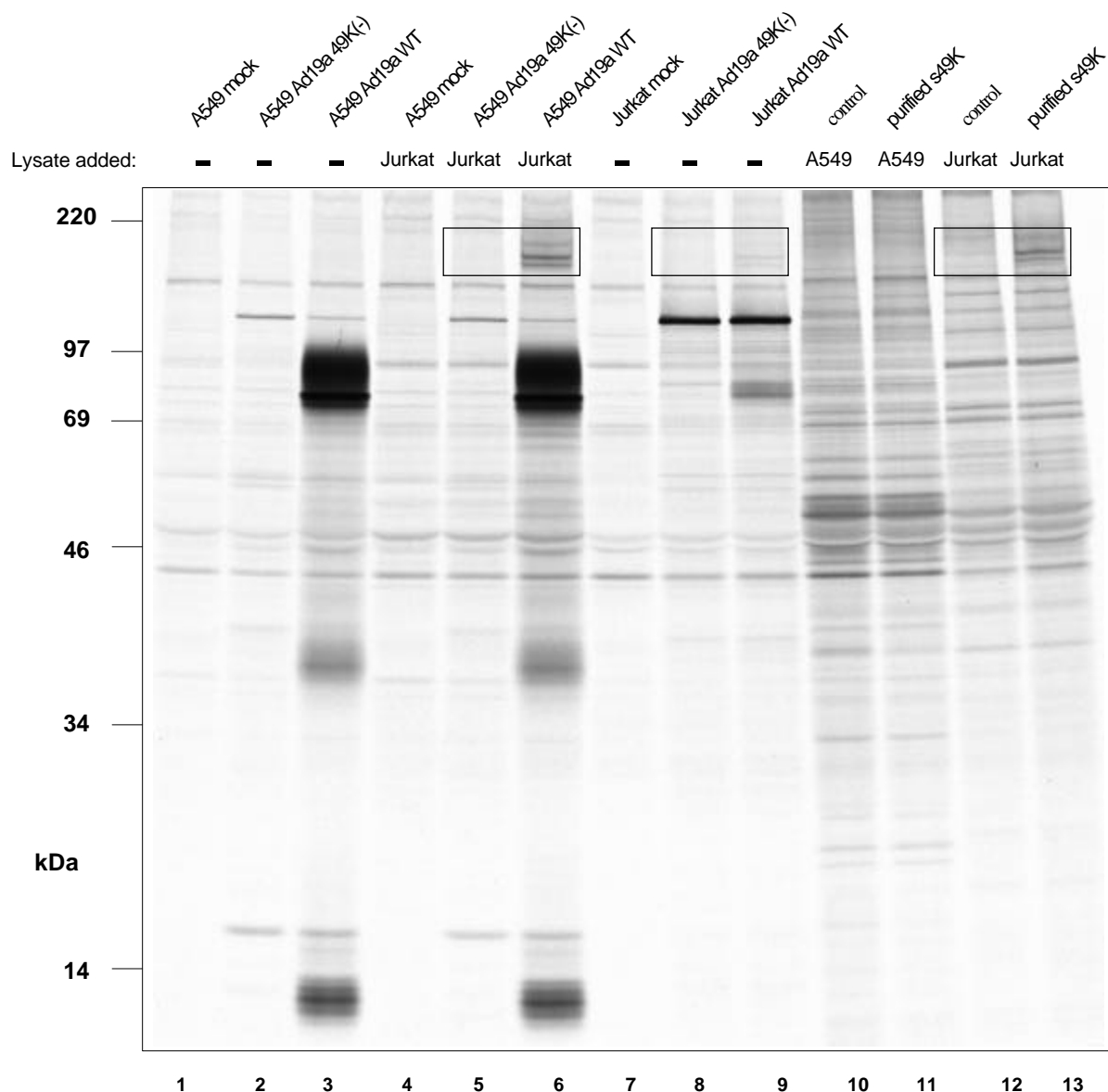


FIG. 37. Specific coprecipitation of high molecular weight protein species from Jurkat cells with E3/49K. 2×10^6 A549 cells were infected with Ad19a or Ad19a-49K(-), in which a frameshift mutation abolished 49K expression, or mock-infected, labeled 6 h p.i. for 1.5 h and lysed in 1 ml IP-lysis buffer. 4×10^6 Jurkat J77 (clone SVT35 (Ting et al., 1996)) cells were Ad19a- or Ad19a-49K(-)- or mock-infected, labeled 18 h p.i. for 1.5 h and lysed in 0.5 ml IP-lysis buffer. 500 μ l of the different lysates were mixed with 500 μ l of other lysates as indicated or with 500 μ l IP-lysis buffer. For precipitation with purified 49K, 600 ng protein was added and incubated for 1 h at 4°C prior to immunoprecipitation. Immunoprecipitation was performed with antibodies directed against the C-terminus (R25050, lanes 1-9) or with antibodies directed against the N-terminus (R48-7B, lanes 10-13) as described in Materials and Methods. Infections with Ad19a and Ad19a-49K(-) were performed both with an MOI of 10. Equal amounts of E3/19K were precipitated from cells infected with the different Ads (data not shown) suggesting no differences in early gene expression between Ad19a- and Ad19a-49K(-)-infected cells in addition to the abolished 49K expression. The areas with the bands of the coprecipitated proteins are highlighted by boxes.

Strikingly, high molecular weight protein species with an apparent molecular mass of approximately 172, 181 and 196 kDa coprecipitated specifically with 49K using Jurkat cell lysates (lanes 6, 9, 13). In the absence of 49K the corresponding bands were not detected (lanes 4, 5, 7, 8, 12). In addition, from A549 cell lysates these proteins were not precipitated, neither in the

presence (lanes 3, 11) nor in the absence of 49K (lanes 1, 2, 10). These proteins seem to be of cellular origin, because the additional bands were not detected after infection with Ad19a-49K(-) not expressing the 49K protein (lanes 5, 8). Furthermore, purified 49K alone was sufficient to precipitate the high molecular weight protein species from Jurkat lysates (lane 13).

3.23 E3/49K inhibits NK cell-mediated lysis

In the 49K binding assays, the NK cell line NKL exhibited the highest mean value of fluorescence suggesting high expression of potential 49K-binding proteins. To test whether the binding of 49K might interfere with NK cell functions, NK cell-mediated lysis was measured in the presence and in the absence of purified 49K (in collaboration with Christine Falk, GSF, Munich, Germany). NKL cells induce lysis of MHC class I negative K562 (erythroleukemia) cells. E3/49K was able to inhibit the NKL-cell mediated lysis in a dose-dependent manner and reduced lysis from 56% to 28% (Fig. 38). NKL cell-mediated lysis of K562 cells can be inhibited by transfecting these cells with expression vectors encoding for HLA-E and the signal peptide of HLA-A2. Binding of the HLA-E/HLA signal peptide on the cell surface of the K562 cells to its receptor CD94/NKG2A on NKL cells inhibits the lysis of the target cells. This mechanism was able to reduce NKL cell-mediated lysis of target cells to 29%, which is comparable to the reduction achieved with secreted 49K. In addition, the NKL mediated lysis of Daudi cells could be reduced from about 16% to 6% (data not shown). Preliminary data from experiments with the CD4⁺ CTL clone 234 indicate that the lysis of target cells mediated by these cells is not affected by 49K (data not shown). On one hand this finding makes it rather unlikely that the 49K-mediated inhibition of NKL cell-mediated lysis was due to an unspecific effect, on the other hand it raises the question what effects 49K binding to the CTL cells, revealed by flow cytometry, may have. 49K-mediated disturbance of other aspects of lymphocyte cell biology are conceivable. However, in case of the NKL cells, the 49K binding to NKL cells as determined by flow cytometry analysis seems to result in an inhibition of NKL cell-mediated killing of target cells indicating an immunomodulatory function of E3/49K.

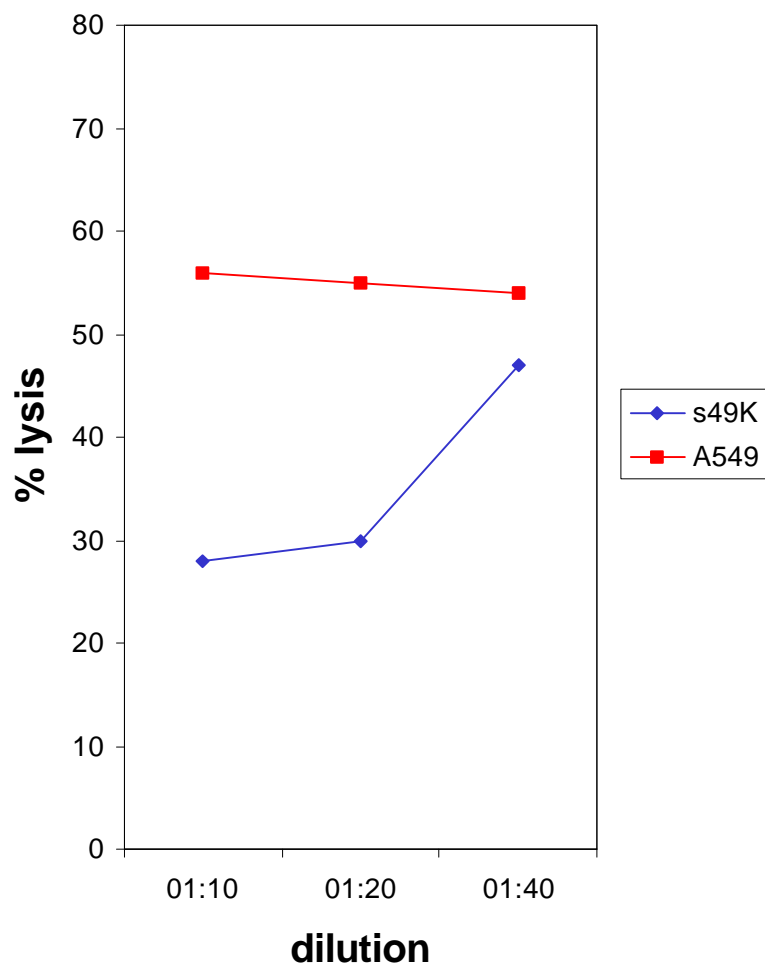


FIG. 38. Purified, secreted 49K inhibits NK cell-mediated target cell lysis. NKL cell-mediated lysis of K562 cells was determined in a standard chromium-51 assay as described in Materials and Methods. Purified secreted 49K and controls (A549) were diluted as indicated. 60, 30 or 15 ng purified 49K were added to the lysis reaction in a total volume of 100 μ l. The killer/target ratio was 20:1 (40000 NKL cells: 2000 K562 target cells).

4 DISCUSSION

The E3/49K protein is encoded by the early transcription unit 3 (E3) of Ad19a, an adenovirus causing epidemic keratoconjunctivitis (EKC). The characterization of the Ad19a E3/49K protein is the first study about an E3 protein specific to subgenus D adenoviruses. E3/49K may be implicated in subgenus-specific diseases or serotype-specific functions of the Ad19a E3/49K may play a role in causing EKC.

4.1 Ad19a E3/49K expression during the time course of infection

As expected from its position in the early transcription unit 3, expression of E3/49K was initiated in the early phase of infection and reached a maximum at 6 h p.i. (Fig. 8). Unlike E3/19K, E3/49K was also synthesized in significant amounts in the late phase of infection (30 h p.i.). Whereas E3/19K synthesis decreased dramatically to ~1-2% of the maximal value, E3/49K was still produced at a level of ~25-30% at 30 h p.i. Similar to E3/49K, the synthesis rate of 20.5K of Ad3 (subgenus B) was also shown to be high early during infection and continued at lower levels throughout the infection cycle (Hawkins and Wold, 1995a). Remarkably, the synthesis of E3/49K seemed to reach a minimum at 18 h p.i. and increased again slightly at later time points. The mechanism of this regulation is unknown at present. Some E3 proteins such as 11.6K of Ad2 (subgenus C) and 30K of Ad4 (subgenus E) were shown to be synthesized at higher rates late during infection (Li and Wold, 2000; Tollefson et al., 1992). In contrast to 49K, 11.6K is scarcely synthesized during the first 12 h of infection and synthesis is greatly amplified (~400 fold) in the late phase (>24 h p.i. (Tollefson et al., 1992)). In the late phase of infection, Ad gene transcription is driven by the major late promoter (MLP) and 11.6K mRNA is spliced to the y leader located within the E3 region and the major late tripartite leader (Wold et al., 1995). Little is known about splicing of E3 transcripts of Ads other than subgenus C. However, splicing of the E3 RNAs of Ad35 and Ad3 (subgenus B) differs substantially (Basler and Horwitz, 1996; Signas et al., 1986). The presence of a typical splice acceptor site in front of the 49K gene suggests that 49K mRNA can be synthesized independently of E3/19K.

4.2 Posttranslational modifications of Ad19a E3/49K: N- and O-glycosylation, disulfide bonds

The sequence of the 49K protein encoded by the E3 region of Ad19a predicts a type I transmembrane protein with a short cytoplasmic tail containing two motifs, YXXΦ and LL, that have been implicated in endosomal/lysosomal targeting (chapter 1.8.3.2) (Heilker et al., 1999). Remarkably, the E3/49K sequence contains 14 potential N-glycosylation sites and three potential O-glycosylation sites (Fig. 6). Experimental evidence was provided that E3/49K is indeed highly

N-glycosylated and presumably contains also O-glycans. The abundant glycosylation resulted in an apparent molecular mass of ~80-100 kDa (e.g. Fig. 8, 9, 16-18). No major differences between 49K synthesized in the early phase of Ad19a infection or in 49K-transfected A549 cells were detected (Fig. 18). The E3/49K protein was initially synthesized with Endo H cleavable high-mannose oligosaccharides, migrating with an apparent molecular mass of 77-83 kDa. Subsequently, these 49K forms were processed to the 87-100 kDa protein species (Fig. 16). Endo H treatment shifted the processed E3/49K species to an apparent molecular mass of 67-92 kDa (Fig. 16, band e) demonstrating the presence of a mixture of high-mannose, hybrid and complex N- and/or O-glycans. Limiting Endo H treatment of pulsed E3/49K revealed that the majority of the E3/49K proteins (~65 %) contained 12, a small fraction (~17% each) 13 and 11 N-linked oligosaccharides (Fig. 17). Based on the molecular weight difference the average molecular mass of a high-mannose N-glycan of 49K was estimated to be approximately ~2.7 kDa. The glycans of the 49K protein species represented by the lower border of the 87-100 kDa band are most likely processed to a lower degree to complex glycans than 49K protein species represented by the upper border. Therefore, the latter are supposed to contain more Endo H resistant carbohydrates and the 49K protein species represented by the upper border of the 87-100 kDa band without treatment are most likely represented by the upper border of the 67-92 kDa band after Endo H treatment, 49K protein species represented by the lower border of the 87-100 kDa band are represented by the lower border of the 67-92 kDa band. By calculating the shift in the molecular weight the number of Endo H sensitive N-glycans could be estimated: Mature 49K protein species contain still between three and seven high-mannose and/or hybrid N-glycans. The majority of mature 49K proteins had still five high-mannose and/or hybrid N-glycans attached. In the largest fraction of E3/49K proteins one or two N-glycosylation sites are not utilized (Fig. 17). Three rules are known to govern the usage of potential N-glycosylation sites. Firstly, NxS/Tx sites are rarely glycosylated if x is a proline residue (Gavel and von Heijne, 1990). This does not explain the incomplete glycosylation of E3/49K, since none of the potential N-glycosylation sites of E3/49K contains proline residues in these positions (Fig. 6). Secondly, steric hindrance may prevent glycosylation if the potential acceptor sites are too close to each other. There are indeed two positions, where potential glycosylation sites are in close proximity (N25 and N31, and N312 and N317), which might cross-inhibit the glycosylation of the adjacent acceptor sites. However, it has been shown that two NxS/T acceptor sites separated by a single amino acid (distance between the Ns 3 aa) can still be glycosylated at both sites (Gavel and von Heijne, 1990). Thirdly, unglycosylated acceptor sites tend to be found more frequently towards the C-termini of glycoproteins (Gavel and von Heijne, 1990). Thus, it is possible that the site closest to the transmembrane segment (N343) may not be utilized. This is supported by the

observation, that the C-terminally derived fragments (h, Fig. 9, 16, 18), generated by the proteolytic processing discussed below (chapter 4.3), are not glycosylated (Fig. 18). Considering their apparent molecular mass of 12-13 kDa, the cleavage site is predicted to be N-terminal of the predicted N-glycosylation site at position 343. Thus, it is likely that the E3/49K form with 13 oligosaccharides lacks a glycan at position 343 and that with 12 glycans might in addition be devoid of carbohydrates at position 312 or 317 (Fig. 6). It is noteworthy, that incomplete glycosylation was also observed for E3/19K molecules of Ad19a (Deryckere and Burgert, 1996). Thus, the cleavage site for the proteolytic processing is proposed to be between N317 and N343. Although the presence of O-glycans could not be directly demonstrated with the O-glycosidase from *Diplococcus pneumoniae* that hydrolyzes only the unmodified disaccharide core Gal β (1 \rightarrow 3)GalNAc from serine or threonine, the presence of O-glycans was indicated by a shift in the apparent molecular mass upon neuraminidase treatment of E3/49K lacking all N-glycans (Fig. 18). Presumably, other O-glycan core structures or modifications not cleavable by the used O-glycosidase were present. The apparent molecular mass difference potentially originating from O-glycans accounts for \sim 3.5 kDa (Fig. 18A). This is consistent with the proposed three O-glycosylation sites, assuming core structures of 4-5 sugar groups each. Interestingly, two bands appeared after PNGase F treatment (i, Fig. 18A, lane 7, Fig. 18B, lane 4) suggesting that E3/49K forms exist that differ either in the number of the utilized O-glycosylation sites or in the sugar side chains attached to these core units. In summary, the terminally processed form of E3/49K contains high-mannose/hybrid as well as complex N-glycans and O-linked oligosaccharides. Unexpectedly, the glycosylation pattern changed in the late phase of infection, in which E3/49K forms with high-mannose carbohydrates represented by the defined bands of 77-83 kDa were the major species (b-d, Fig. 8). A pulse/chase experiment (Fig. 9) demonstrated that late during infection the processing of the high-mannose to the complex glycans was severely impaired. Presumably, the exit of 49K out of the ER is prevented or at least delayed, and the prolonged residence time in the ER favors the generation of 49K molecules with 13 N-linked glycans (b). This was neither a 49K-specific nor a generalized processing defect induced by Ad infection, e.g. caused by host shutoff late during infection, since the processing of the transferrin receptor was not significantly changed, whereas lamp-1 processing was also affected (Fig. 10A, B). This result suggests that only a selective set of glycoproteins seems to be affected. Lamp-1 and E3/49K are both heavily N-glycosylated with 18 (Hunziker and Geuze, 1996) and 11-13 (Fig. 17) N-glycans, respectively, whereas the transferrin receptor contains only three N-glycosylation sites (Schneider et al., 1982). The reason for the differential sensitivity of the glycoproteins is unclear, but they may utilize different transport pathways (Karlsson and Carlsson, 1998), which might be differentially affected late during Ad infection. Interestingly, the Golgi/TGN appeared more

vesicular in infected than in uninfected cells (Fig. 26). At present, it is not known whether these two phenotypic changes, the altered processing late during infection and the altered morphology of the Golgi, which is visible already in the early phase, are related. However, it is unlikely that E3/49K plays a direct role in these phenomena: First, transfectants stably expressing E3/49K exhibited a similar processing as observed in the early phase of infection (Fig. 15) and no obvious changes in Golgi morphology were observed. Second, the processing deficiency is established only late during infection, when E3/49K synthesis is already significantly decreased. Interestingly, full-length 49K proteins were detected late during Ad19a infection in SeBu cells mainly in the ER/Golgi/TGN and only rarely in peripheral vesicles as early during infection (Fig. 25). This finding substantiates the hypothesis that the impaired glycan processing late during infection is accompanied by a severely delayed transport through the ER/Golgi/TGN. Notably, a slower carbohydrate processing was also observed for the 20.5K protein of Ad3 (subgenus B) in the late phase of infection (Hawkins and Wold, 1995a), suggesting that this phenomenon is not restricted to subgenus D Ads.

As another post- or co-translational modification, 49K contains intramolecular disulfide bonds (Fig. 20). Since only a shift of 1.1 kDa in the apparent molecular mass was determined upon reduction, disulfide bonds are most likely formed by adjacent cysteine residues (Fig. 6). It cannot be excluded that additional posttranslational modifications are present in the mature 49K protein, e.g. palmitoylation. The 11.6K protein of subgenus C Ads was shown to be palmitoylated at cysteine residues close to the transmembrane region (ICCLKR) (Hausmann et al., 1998). A similar sequence (ICCRKR) is found in the 49K protein. Palmitoylation of 49K may play a role in 49K trafficking (Tab. 3).

4.3 Posttranslational modifications of Ad19 a E3/49K: Proteolytic processing and secretion

A striking observation from the initial pulse/chase experiments was the appearance of E3/49K derived fragments with apparent molecular masses of about 12-13 kDa starting at about 60 min of chase (h, Fig. 9). Similar fragments were also observed in the cell lines stably expressing Ad19a E3/49K (h, Fig. 11). A low molecular weight band was also detected in Western blotting analysis (Fig. 14, lane 4) excluding the possibility that these bands represent coprecipitated proteins. This suggested that E3/49K is proteolytically cleaved. In order to elucidate the fate of the N-terminal ectodomain of 49K, rabbit polyclonal and rat monoclonal antibodies were generated against the N-terminal part of 49K expressed as a HisTag-fusion protein (Fig. 12). These antibodies recognized 49K in all assays tested (Fig. 13, 14, 21, 24), although different activities were observed with different rat monoclonal antibodies (Tab. 4). With these antibodies directed

against the N-terminus of 49K, it could be demonstrated that the N-terminal ectodomain is secreted from Ad19a-infected as well as from 49K-transfected A549 (Fig. 15) and 293 cells (data not shown). The proteolytic processing of 49K in 49K-transfected cells demonstrates that no viral protein is required for the cleavage but a cellular protease.

As four of the five methionine residues in the 49K sequence (without signal peptide) are present in the N-terminal ectodomain (Fig. 6), 80% of the total labeling is expected to be contained in that part of 49K. The labeling of the cytoplasmic tail is expected to contain 20% of total labeling (one methionine). Notably, only a fraction of about 20% of total initial labeling with [³⁵S]-methionine was secreted (Fig. 32). 20% of total labeling corresponds to 25% of the labeling of the N-terminal ectodomain of 49K. Thus, 75% of the initially labeled N-terminal part of 49K appears to be eliminated by a so far unknown degradation system. Several agents influencing trafficking, glycosylation, acidification of intracellular compartments (chloroquine, bafilomycin A1, ammonium chloride, monensin, brefeldin A, tunicamycin) and an inhibitor lysosomal cysteine and serine proteases (leupeptin) were applied in order to define their influence on the processing, secretion and intracellular degradation of 49K (Fig. 28). Tunicamycin inhibits N-glycosylation and retained 49K in the ER, most likely due to misfolding based on the requirement of N-glycosylation for proper folding (Parodi, 2000). Low molecular weight fragments were not detected under these conditions (Fig. 28D) suggesting that their generation requires export from the ER. Brefeldin A induces the collapse of Golgi but not of TGN membranes onto the ER. This was associated with an impaired glycan and an inhibition of proteolytic processing of 49K (Fig. 28D). This implies that the protease cleaving 49K does not localize to the Golgi and that the proteolytic processing of 49K occurs in a post-Golgi compartment. 49K was detected in swollen endosomal vesicles during chloroquine treatment (Fig. 33B). Acidotropic agents (chloroquine, bafilomycin A1, ammonium chloride, monensin) and the lysosomal cysteine and serine protease inhibitor leupeptin did not inhibit proteolytic processing and secretion but influenced to a different degree the glycan processing (Fig. 28 A-C). Chloroquine and bafilomycin A1 even increased the secretion rate up to 75% of initially labeled 49K, which corresponds to more than 90% of the labeled N-terminal part of 49K (Fig. 32D). Acidotropic agents disturb the acidification of intracellular compartments, e.g. endosomes, which can inhibit proteases if their activity depends on an acidic pH. On the other hand, intracellular trafficking is affected by acidotropic compounds. However, it is still controversial whether they block trafficking at an early or late endosomal state (Bayer et al., 1998; Clague et al., 1994; van Deurs et al., 1996; van Weert et al., 1995). The result that leupeptin, an inhibitor of lysosomal cysteine and serine proteases did not significantly increase the secretion rate supports the view that rather the influence of acidotropic agents on trafficking than the inhibition of lysosomal proteases by an

increased pH was responsible for the increased secretion. Acidotropic agents efficiently block transport from early or late endosomes to lysosomes and to the TGN, but they only delay and do not inhibit recycling to the cell surface (Presley et al., 1997). Blocking transport in early or late endosomes by acidotropic agents, allowing a slow recycling to the cell surface, increased the 49K secretion rate. This supports the idea that proteolytic processing leading to secretion of 49K can occur at the cell surface (or less likely in a pH-insensitive way in endosomes) and that degradation of 49K intracellularly occurs in a compartment that is reached after passing early or late endosomes or in a pH-sensitive way in early or late endosomes. Proteolytic processing at the cell surface is further supported by the analysis of 49K proteins with mutated sorting motifs in the cytoplasmic tail discussed below (chapter 4.4). In this scenario, 49K is internalized from the cell surface and targeted to early or late endosomes. The treatment with acidotropic agents blocks further transport to the TGN or to late endosomes and lysosomes, which most likely is required for the intracellular degradation of 49K. Instead, 49K is slowly recycled to the cell surface, where proteolytic processing resulting in secretion of the N-terminal ectodomain occurs. In sum, these processes induced by acidotropic agents result in an increased secretion rate. A major contribution of lysosomal degradation to the intracellular degradation of 49K seems unlikely because no stabilization is observed during leupeptin treatment, although 49K degradation by lysosomal proteases not sensitive to leupeptin cannot be excluded. Preliminary data suggest that 49K processing and degradation is also not affected by the proteasome inhibitor lactacystine (data not shown) arguing against a major contribution of the proteasome in 49K processing or degradation.

Another interesting observation from the experiments with leupeptin and acidotropic agents was that the proteolytic processing of the low molecular fragments was affected by these compounds. The generation of the fragment with the lowest molecular weight (h3), which appeared later in the chase (2-3 h) than the other fragments (~1 h), was inhibited by acidotropic agents and remarkably also by leupeptin (Fig. 28). This strongly favors the idea that the initial cleavage occurs in a different compartment than the subsequent processing generating the fragment with the lowest molecular weight (h3). The result that leupeptin inhibits the production of this fragment implies that this processing step is mediated by cysteine and serine proteases in late endosomes or lysosomes, whereas the initial cleavage seems to occur in the TGN/secretory vesicles and/or at the cell surface (Fig. 39).

Proteolytic processing of precursor proteins in the secretory pathway is frequently mediated by members of a family of calcium-dependent serine endoproteases related to subtilisin and the yeast processing protease Kex2p that are called subtilisin-like proprotein convertases (SPCs) (Zhou et al., 1999). These proteins are either localized in dense core vesicles of the regulated

secretory pathway (PC2, PC1/3) or in the TGN and secretory vesicles of the constitutive secretory pathway (furin, PACE4, PC5/PC6, PC7/8/LPC), where they mediate proteolytic processing. Among their substrates are growth and blood clotting factors, prohormones but also viral proteins, e.g. the Ebola glycoprotein, the influenza virus hemagglutinin and the HIV envelope glycoprotein. These SPCs cleave proproteins usually after KR or RR sequences, but also amino acids in position -4 and -6 seem to be important for the cleavage. Because of similar cleavage sites, different SPCs may have redundant activities (Lissitzky et al., 2000). It was postulated that in addition to the R in position -1 at least two basic residues, K or R, in positions -2, -4 or -6 are required for cleavage, although the efficiency of different target sequences can differ significantly (Watanabe et al., 1993). In the Ad19a E3/49K sequence a weak potential SPC recognition site (KDEGKR) is found at position 332 in the region where 49K is assumed to be cleaved, i.e. N-terminal of the predicted N-glycosylation site at position 343 which is most likely not utilized and C-terminal of the predicted N-glycosylation site at position 317 which is presumably partially used. This sequence is also found in Ad37 49K that is identical to Ad19a 49K. In Ad15 49K the K in position -6 is substituted by R, in Ad8 and Ad9 49K the R in position -2 is replaced by N, but instead in position -4 a K is found which would still represent a potential cleavage site according to the rules described above. This might indicate that an evolutionary advantage exists to retain a weak recognition site for SPCs.

LoVo cells are deficient in furin and PC5/6 expression, but synthesize PACE4 and PC7 (Seidah et al., 1994; Seidah et al., 1996; Takahashi et al., 1995). After Ad19a infection of LoVo cells, secretion of 49K was clearly reduced compared to A549 cells. After 3 h metabolic labeling 49K was precipitated from the lysate and the supernatant, and 49K labeling was quantified. In A549 cells ~70% of the 49K label was detected intracellularly whereas ~30% were detected in the supernatant. In case of the LoVo cells ~97% of the 49K labeling was intracellular and only ~3% in the supernatant (data not shown). This supported the view that furin or another SPC deficient in this cell line may play a role in 49K cleavage. The residual proteolytic cleavage may be explained by a redundant activity of SPCs expressed in LoVo cells or the activities of other cellular proteases. However, preliminary results with the furin inhibitor decanoyl-R-V-K-R revealed only slightly decreased secretion levels (data not shown). These results have to be confirmed in further experiments. In addition, the effect of the inhibitor on other SPCs than furin remains to be clarified. Nevertheless, based on the results from the LoVo cells a role for SPCs in the processing of 49K may be proposed.

SPCs are mainly active in the TGN and secretory vesicles either of the regulated or the constitutive secretory pathway. But SPCs might be transported to the cell surface from which they are retrieved to the TGN via endosomal compartments (Molloy et al., 1999). SPCs may

exhibit some residual activity at the cell surface (Wolfgang Garten, Philipps-University Marburg, Germany, personal communication) leaving the possibility that they also participate in proteolytic processing at the cell surface. The cell surface is proposed to be the site where 49K is at least partly proteolytically processed. The process of proteolytic processing of proteins at the cell surface and subsequent secretion of the ectodomain is called “protein shedding”. Protein ectodomain shedding is a widely used mechanism to modulate the surface of eukaryotic cells (Blobel, 2000; Kiessling and Gordon, 1998). Proteins released by this process include EGFR ligands, such as heparin-binding EGF-like growth factor (HB-EGF) and transforming growth factor α (TGF α), cytokines, such as TNF α , cytokine receptors, adhesion molecules and other proteins, e.g. the amyloid precursor protein (APP). Many of these shedding processes have been linked to metalloproteases. Therefore, metalloproteases may be involved in the cleavage of 49K at the cell surface. No consensus sequence for metalloprotease-mediated cleavage at the cell surface has emerged so far. Preliminary results obtained with the metalloprotease inhibitor marimastat (BB-2516) revealed only a slight decrease in 49K secretion (data not shown). Further experiments and utilization of other metalloprotease inhibitors with different specificities should clarify their involvement in 49K processing.

At present, the possibility that several proteases are able to cleave 49K cannot be excluded, e.g. SPCs in the TGN/secretory vesicles and metalloproteases at the cell surface. This may complicate inhibitor studies and would be consistent with the fact that a number of low molecular weight fragments are detected that might be generated by cleavage of 49K at different positions mediated by different proteases. Thus, the protease or the proteases involved in the proteolytic processing of Ad19a E3/49K remain to be identified.

4.4 Intracellular trafficking and secretion of Ad19a E3/49K directed by sorting motifs in the cytoplasmic tail

Several structural features of E3/49K, such as the abundant N-glycosylation, the presence of O-linked glycans, intramolecular disulfide bonds and the short cytoplasmic tail with endosomal/lysosomal targeting signals, are reminiscent of the lysosome-associated membrane proteins (lamps) (Hunziker and Geuze, 1996). Despite these striking similarities, the intracellular localization of E3/49K and lamp-2 differed considerably in primary foreskin fibroblasts (SeBu) in the early phase of infection (12-15 h p.i., Fig. 23). At this time point the intracellular staining patterns revealed with antibodies directed against the C- and the N-terminus of 49K were indistinguishable. Thus, the trafficking pathways of full-length 49K proteins and cytoplasmic tail fragments seem to be very similar, and it may be proposed that the trafficking of full-length 49K is directed by its C-terminal cytoplasmic portion. E3/49K was localized primarily in a perinuclear

compartment that was identified as the Golgi/TGN 12-15 h p.i. (Fig. 22). In immunofluorescence studies the Golgi complex and the TGN could not be differentiated due to limited resolution. TGN staining was demonstrated by brefeldin A treatment that induces the collapse of the Golgi onto the ER, whereas TGN membranes are relocated to the MTOC (Klausner et al., 1992). Most of the Golgi/TGN staining in untreated cells seemed to merge into the ER. Nevertheless, a TGN46-positive structure was still weakly 49K-positive suggesting that at steady-state the Golgi as well as the TGN contain 49K (data not shown). The 49K fraction detected in the Golgi/TGN included newly synthesized 49K and most likely recycled full-length 49K and C-tails from the cell surface as indicated by the finding that after 6 h treatment with cycloheximide cytoplasmic tail fragments but not full-length 49K proteins could be detected in the Golgi/TGN (Fig. 27). Nevertheless, since the intracellular trafficking pathways of full-length 49K and C-tails seem to be very similar, both are most likely recycled to the TGN. At present, it is unknown whether the prominent Golgi/TGN staining can be mainly attributed to newly synthesized or recycled 49K proteins. The TMD of 49K encompasses approximately 22 aa, which is much longer than that of typical Golgi resident proteins (chapter 1.8.2). Therefore, it is unlikely that the TMD of 49K directs the Golgi/TGN localization. In addition to the perinuclear Golgi/TGN staining, numerous E3/49K-positive vesicles were detected in the perinuclear region and in the periphery. A significant proportion of these vesicles were shown to be early endosomes by colocalization with the early endosomal marker EEA-1 (Fig. 23A). In the early phase no colocalization with the late endosomal marker lysobisphosphatidic acid (LBPA, Fig. 23B) and the late endosomal/lysosomal marker lamp-2 (Fig. 23C) was found. This changed in the late phase of infection, when colocalization of E3/49K and lamp-2 was observed (Fig. 25). Strikingly, only cytoplasmic tail fragments colocalized with lamp-2 in vesicular structures but not full-length proteins. The cytoplasmic tail fragments of E3/49K seem to accumulate in late endosomes/lysosomes during the course of infection resulting in the colocalization with lamp-2 in the late phase of infection. This concept is supported by the finding that the small E3/49K derived fragments exhibit a longer half-life than full-length E3/49K (5-6 h vs. ~2 h; Fig. 34A/B). The existence of a minor trafficking pathway to late endosomes and lysosomes is also supported by experiments with acidotropic/lysosomotropic agents and leupeptin. Treatment of Ad19a-infected or 49K-transfected A549 cells with various acidotropic/lysosomotropic agents, e.g. chloroquine, stabilized 49K in swollen endosomal vesicles in immunofluorescence studies, whereas the serine and cysteine protease inhibitor leupeptin exhibited no significant effect (Fig. 33B, data not shown). The increased secretion rates obtained with some acidotropic agents are also indicative of 49K stabilization (Fig. 28, 32D). This stabilization may rather originate from a disturbed trafficking than from an inhibition of proteases dependent on low pH, since leupeptin

did not significantly stabilize full-length 49K proteins. Thus, lysosomal degradation of E3/49K most likely plays only a minor role. On the other hand, leupeptin affected the processing of the cytoplasmic tail fragments. It inhibited the generation of a low molecular weight fragment (h3), which appeared late in the chase (Fig. 28A). This leupeptin sensitive proteolytic cleavage therefore seems to occur in late endosomes or lysosomes (Fig. 39). Strikingly, after long chase times mainly the cytoplasmic tail fragment h3 is detected (Fig. 28A, Fig. 34A, B). Thus, predominantly h3 may be detected late during infection in immunofluorescence studies in late endosomes and lysosomes (Fig. 25).

In Ad19a-infected cells expressing E3/49K at high levels a significant staining of the cell surface was observed with antibodies against the C-terminus in immunofluorescence studies indicating that E3/49K may reach the plasma membrane. Cell surface expression was unequivocally demonstrated by flow cytometry using an antibody directed against the N-terminal portion of the 49K protein (Fig. 24). No significant differences in the 49K localization in 49K-transfected cells compared to Ad19a-infected cells were observed (data not shown).

Thus, at steady-state E3/49K localizes to the Golgi/TGN, early endosomes and the cell surface in the early phase of infection. Some unidentified vesicular structures might represent secretory vesicles. From early endosomes 49K is recycled to the TGN and a minor pathway also leads to late endosomes and lysosomes. The putative sorting motifs, YXX Φ and LL, in the cytoplasmic tail of 49K may direct the intracellular localization and trafficking of 49K. These motifs are involved in trafficking between the TGN, the endosomal/lysosomal system and the plasma membrane (chapter 1.8.3.2). The finding that peptides representing the sequence of the cytoplasmic tail of E3/49K bind to the clathrin adaptor protein complexes AP-1 and AP-2 *in vitro* supported a functional role *in vivo* (Fig. 29). This was confirmed by the examination of cell lines stably expressing E3/49K proteins with mutations in the putative sorting motifs. In these mutants, 49K expression on the cell surface was increased as shown by an increased ratio of cell surface to intracellular 49K staining in flow cytometry analysis (Fig. 30). In addition, an accumulation of YA/LLAA mutant cytoplasmic tail fragments at the cell surface was detected by immunofluorescence (Fig. 33A), even though the mutated tails are not as well recognized as WT C-tails by the relevant antibodies. Therefore, accumulation of 49K C-tails with the YA/LLAA mutation at the cell surface is expected to be even more dramatic. Moreover, accumulation of 49K proteins in swollen endosomal vesicles after chloroquine treatment is dramatically decreased in YA/LLAA and Δ CT mutants and slightly in LLAA mutants but not in YA mutants compared to WT (Fig. 33B). Since the accumulation in swollen endosomal vesicles most likely occurred after internalization, these results imply that endocytosis from the cell surface is impaired in YA/LLAA and Δ CT and to a lesser extent in LLAA mutants. No full-length YA/LLAA and

Δ CT mutant 49K proteins were detected in swollen endosomal vesicles after chloroquine treatment with antibodies directed against the N-terminus (Fig. 33B). This finding is consistent with the view that the proteolytic processing of these mutant 49K proteins at the cell surface is faster than their internalization. Proteolytic cleavage at the cell surface is also supported by flow cytometry analysis after brefeldin A treatment, inhibiting transport of newly synthesized 49K to the cell surface (Fig. 31). Despite the presumed deficiency in endocytosis, 49K staining on the cell surface is still rapidly lost in transfected cells expressing mutated 49K proteins most likely due to proteolytic processing. The mutations do not inhibit proteolytic processing and secretion and do not significantly change the processing kinetics (Fig. 32C) but affect the secretion rate (Fig. 32D). Interestingly, increased cell surface expression correlates with increased secretion rates (Fig. 30, Fig. 32D). The Δ CT mutants even reached secretion rates of \sim 80% of total labeling, which corresponds to about 100% of the labeling of the N-terminal ectodomain. These results suggest that the intracellular degradation of WT 49K that limits the secretion rate occurs after endocytosis. Thus, the decreased internalization rate of the YA/LLAA and the Δ CT mutant allows a highly efficient proteolytic processing of full-length 49K proteins at the cell surface and disfavors internalization and subsequent intracellular degradation. Interestingly, two different approaches to disturb 49K trafficking, treatment with acidotropic agents as well as mutations of the cytoplasmic tail, increase the secretion rate, most likely by increasing the overall residence time of 49K proteins at the cell surface.

An interesting cellular protein, that is cleaved and secreted similar to 49K, is the β -amyloid precursor protein (APP). Proteolytic processing of APP involves three proteases, α -, β -, and γ -secretases (Esler and Wolfe, 2001). The large N-terminal ectodomain of APP (APP_s) can be secreted after α - and β -secretase cleavage. The cytoplasmic tail of APP contains two YXX Φ motifs that direct the intracellular traffic of APP. One motif (YENP) seems to mediate mainly endocytosis, whereas the other (YTSI) regulates basolateral targeting (Haass et al., 1995; Perez et al., 1999). Interestingly, as shown for 49K, mutation of the YXX Φ motif mediating endocytosis resulted in an increased secretion of APP_s (Perez et al., 1999). However, in case of the Ad19a E3/49K protein the LL motif seems to be decisive for endocytosis, whereas the YXX Φ motif plays only a minor role. Mutation of the LL motif to AA significantly disturbed the intracellular trafficking of 49K resulting in an increased cell surface expression and secretion rate, whereas 49K proteins with a mutation of the Y of the YXX Φ motif to A behaved like WT. However, a significant effect was observed after mutation of the Y of the YXX Φ motif in addition to the elimination of the LL motif (YA/LLAA compared to LLAA). This suggests that the LL motif dominates the YXX Φ motif in the WT cytoplasmic tail of 49K. Interestingly, according to a

statistical analysis of residues surrounding functional YXX Φ and LL motifs, the YXX Φ motif of 49K is not flanked by particularly favored amino acids, whereas a proline in position -1 of the LL motif, as found in the 49K sequence, was present in 23% of functional LL motifs (Windheim et al., 2002). This finding supports the view that the LL motif in the cytoplasmic tail of 49K is functional *in vivo*. At present it cannot be excluded that the YXX Φ motif plays a role in processes following internalization, e.g. basolateral targeting. The possibility that the 49K sorting motifs may mediate targeting to the basolateral membrane in polarized cells has not been addressed so far (chapter 1.8.3.2).

49K trafficking is reminiscent of that of TGN46, a protein that also localizes to the TGN at steady-state and is targeted to the basolateral membrane in polarized cells (Banting and Ponnambalam, 1997). TGN46 also contains a YXX Φ motif but no LL motif and is continuously recycled from the cell surface via early endosomes to the TGN (Tab. 3, Ghosh et al., 1998; Mallet and Maxfield, 1999). The trafficking pathways of E3/49K and TGN46 were shown to overlap in endosomes (Fig. 26). Another cellular protein with similar trafficking pathways is the protein encoded by the Menkes disease gene. The Menkes disease protein, a copper transporting ATPase, is localized in the Golgi/TGN and cycles between the TGN and the plasma membrane. For Menkes disease protein an LL motif was shown to be important for the steady-state Golgi/TGN localization (Tab. 3). Interestingly, this motif seems to be critical for internalization from the cell surface but it may not be sufficient for retrieval to the Golgi/TGN, because it was unable to target chimeric CD8 proteins to that compartment (Francis et al., 1999). It is possible that the LL motif of 49K is the dominant endocytosis motif, but another sorting motif, e.g. the YXX Φ motif, may direct retrieval to the TGN from endosomes or basolateral targeting. Combinations of LL and YXX Φ motifs are found in a number of proteins. These motifs can be additive in their activities. The cystic fibrosis transmembrane conductance regulator contains an LL and a YXX Φ motif in its cytoplasmic tail which both contribute to internalization (Hu et al., 2001). But LL and YXX Φ motifs may also have different activities. The sequence YQGV at the C-terminus of CD1d contains a tyrosine-based internalization motif (YQGV) that also directs basolateral sorting. This YXX Φ motif overlaps with a leucine-based (VL) sorting motif that is also sufficient for basolateral sorting, but is not active in internalization (Rodionov et al., 2000). The interleukin-6 (IL-6) receptor is composed of two different subunits, gp80 and gp130. The gp130 subunit contains an LL motif in its cytoplasmic tail that mediates endocytosis (Dittrich et al., 1996), whereas in the C-tail of the gp80 subunit two motifs, an LL and a YXX Φ motif, are found that direct basolateral sorting (Martens et al., 2000). Interestingly, in both LL motifs of the IL-6 receptor a proline is present in position -1, as in the LL motif of 49K.

LL and YXX Φ motifs are also found in other viral transmembrane proteins. Endocytosis and AP-1 and AP-2 interaction of simian as well as human immunodeficiency virus envelope glycoproteins seems to be controlled by LL and YXX Φ motifs (Bowers et al., 2000; Wyss et al., 2001). Herpes simplex virus (HSV) and varicella zoster virus (VZV) are enveloped viruses that have been proposed to acquire their envelope in the *trans*-Golgi-network. That is the reason why the viral envelope glycoproteins VZV-gE and HSV-gE are targeted to that compartment. Interestingly, this is achieved by the utilization of YXX Φ motifs and other signals that also direct the TGN localization of cellular proteins like TGN46 and furin (Alconada et al., 1996; Alconada et al., 1999). In analogy to the cellular TGN proteins, the viral envelope glycoproteins cycle between the TGN and the plasma membrane, a trafficking pathway also 49K seems to utilize. The Ad2/5 10.4K and 14.5K proteins, like 49K encoded by the early transcription unit 3, form a complex and down-regulate Fas and EGFR (chapter 1.7). Both proteins contain sorting motifs in their cytoplasmic tails. The YXX Φ motif of 14.5K mediates internalization, whereas the LL motif of 10.4K seems to be required for recycling of the complex from endosomes to avoid lysosomal degradation (Hilgendorf et al., in preparation). Thus, in this case the two motifs appear to function sequentially. For the E3/49K protein the function of the LL motif in internalization was demonstrated. A role for the YXX Φ motif in recycling, e.g. to the TGN, seems unlikely. In that case an increased intracellular degradation and a decreased secretion rate would be expected, but was not detected (Fig. 32D). Basolateral targeting remains a potential function of the YXX Φ motif of 49K, but the LL motif also may be functional in both internalization and basolateral sorting, as shown for the invariant chain (Simonsen et al., 1998) and the Fc receptor II (Hunziker and Fumey, 1994). Thus, a potential basolateral targeting of 49K and a potential function of the YXX Φ or the LL motif in such a sorting event remains to be clarified.

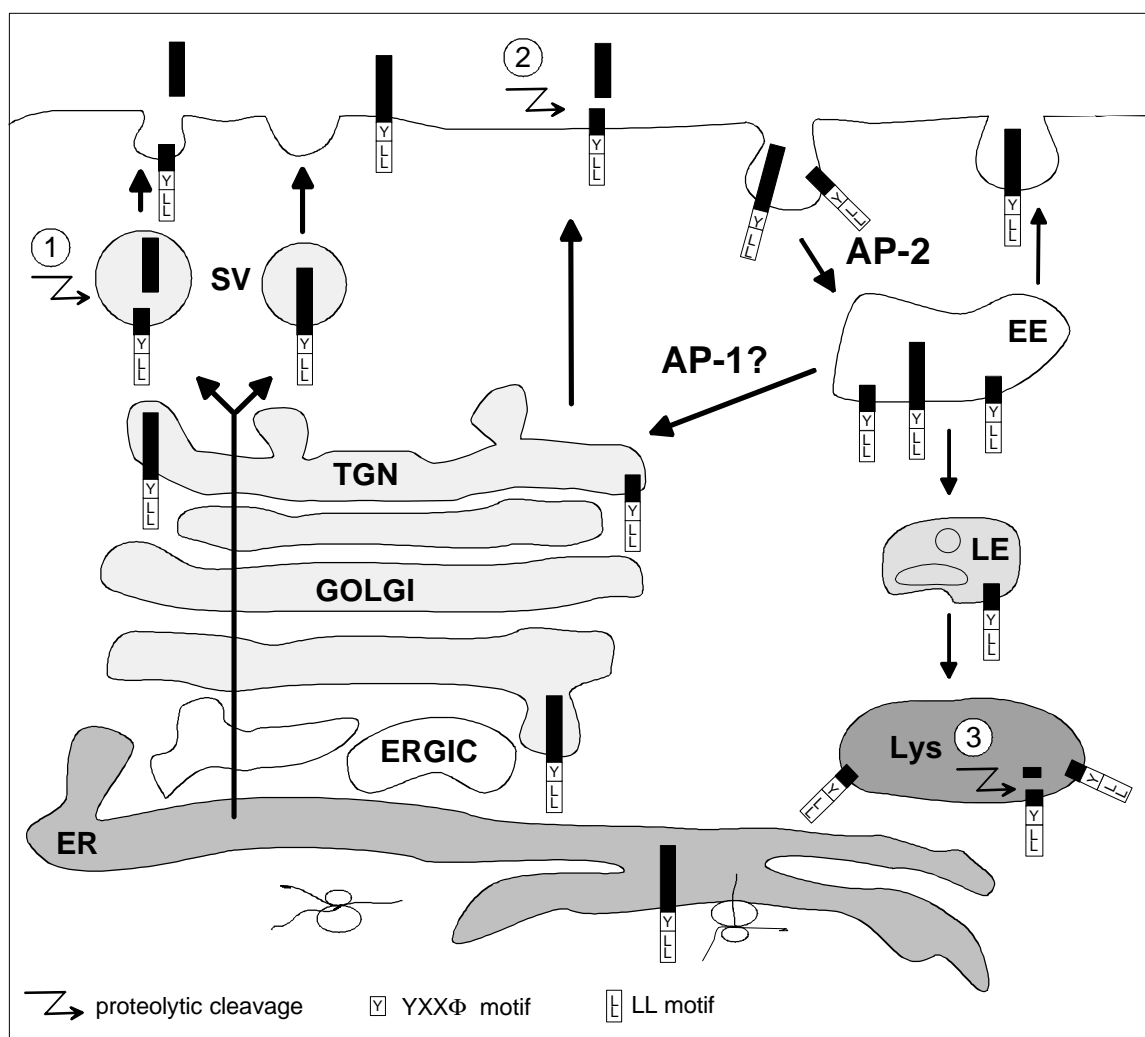


FIG. 39. Model of E3/49K trafficking and proteolytic processing. At steady-state, E3/49K is found in the Golgi/TGN, at the plasma membrane and in early endosomes. After synthesis E3/49K passes the secretory pathway and is extensively posttranslationally modified obtaining N- and O-glycans and intramolecular disulfide bonds. At the TGN, E3/49K is packaged into secretory vesicles. Proteolytic cleavage releasing the N-terminal ectodomain most likely occurs at the cell surface (“shedding”) (2), but cleavage in secretory vesicles (1) and/or in the TGN cannot be excluded at present. The cytoplasmic tail and uncleaved full-length E3/49K proteins can be endocytosed from the cell surface mainly by virtue of the LL motif in the C-tail involving AP-2 interaction. From early endosomes (EE) E3/49K can be recycled to the TGN possibly regulated by the interaction of the sorting motifs in the cytoplasmic tail with AP-1. Recycling from early endosomes may also occur to the cell surface. A minor pathway directs E3/49K and cytoplasmic tail fragments to late endosomes (LE) and finally to lysosomes (Lys), where an additional proteolytic processing takes place (3). For details and references see text.

4.5 Binding of secreted 49K to lymphocyte cell lines and coprecipitation of 49K-binding protein(s)

Based on the assumption that 49K has an immunomodulatory function, it was hypothesized that the secreted 49K may affect effector cells of the immune system. Interestingly, a SMART search for homologies to common domain families (Schultz et al., 2000) revealed a similarity of R3 (Fig. 7C) with the consensus sequence for immunoglobulin (Ig) -like domains. In addition, secondary structure prediction suggests that the N-terminal ectodomain of 49K contains mainly β -strands

(Cuff et al., 1998). Notably, in R3 as well as in R1 and R2 (Fig. 6), several β -strand regions were predicted, which is consistent with the 7-10 β -strands characteristically found in Ig-like domains. Recently, the structure of the HCMV US2 protein bound to the class I molecule HLA-A2 was resolved (Gewurz et al., 2001b). US2 functions in HCMV immune evasion and targets MHC class I molecules to the proteasome for degradation. US2 shows no sequence homology to host proteins. Nevertheless, the crystal structure revealed that US2 adopts an Ig-like fold. US2 binds a structure on MHC class I molecules that is not recognized by known host proteins interacting with MHC class I, e.g. CD8 or T cell receptor. Thus, it seems that HCMV has evolved a novel protein for this purpose. However, the scaffold for the recognition, the Ig-like fold, is widely used by viral and host proteins. Interestingly, it was suggested that also the Ad E3/19K adopts an Ig-like fold (Gewurz et al., 2001a). Thus, like HCMV US2, Ad E3/19K and E3/49K proteins may use the scaffold of the Ig-fold to bind to their target structures on host proteins. Ig-folds are frequently found in proteins with functions in the immune system. Strikingly, about 54% of all leukocyte membrane proteins contain at least one domain with an Ig-like fold, which is mostly involved in protein-protein interactions (Barclay et al., 1997). Therefore, it was reasonable to assume that E3/49K may bind to cell surface protein(s) of leukocytes. Indeed, purified, secreted 49K binds specifically to lymphocyte cell lines of different origin, NK, T and B cells, but not to a number of other cell lines of non-lymphocytic origin, like primary fibroblasts (SeBu), lung epithelial cells (A549) or erythroleukemia cells (K562) (Fig. 36). This supports the hypothesis that 49K may have an immunomodulatory function and indicates the presence of lymphocyte-specific 49K-binding protein(s). As a first attempt to identify such proteins, 49K was precipitated from lysates of labeled Jurkat cells (Fig. 37). Strikingly, three high molecular weight protein species of 172-196 kDa could be coprecipitated with 49K specifically from Jurkat cell lysates. A strong interaction of 49K with these proteins can be postulated, since the interaction was not disrupted by 1% Triton-X 100 present during immunoprecipitation.

Interestingly, a database search for similarities to the 49K repeat regions 1-3 (R1-3, Fig. 6), revealed homologies with HIV/SIV gp120 proteins (Fig. 40). The HIV/SIV envelope glycoprotein gp120 binds to the receptor CD4 and coreceptors on lymphocytes, mainly chemokine receptors (Loetscher et al., 2000). Interestingly, two regions implicated in gp120 coreceptor binding, V3 and V1/V2, show similarities to 49K (Fig. 40) (Loetscher et al., 2000; Poignard et al., 2001). Like Ad19a 49K, HIV/SIV gp120 is also highly glycosylated and N-glycosylation in the V3 and V1/V2 regions affects coreceptor utilization (Pollakis et al., 2001). Homologous sequences of 49K and HIV/SIV gp120 include potential N-glycosylation sites (two in C2/V3 and V1/V2, Fig. 40A, D; one in C4/V4/C5, Fig. 40C). However, the molecular masses of gp120 coreceptors are much lower than the 172-196 kDa of the 49K-binding proteins in

Jurkat cells. Gp120 is non-covalently associated with gp41 at the cell surface and can be shed into the supernatant of infected cells. The biological significance of soluble gp120 is largely unknown. The envelope glycoproteins have pleiotropic effects on various cell types of the immune system, directly or indirectly (Chirmule and Pahwa, 1996). Thus, it might be worthwhile to examine whether 49K has similar effects.

A	49K 46-94	D T Q . G L W F . C N G S R V K N P Q I R H T C N D Q N L T	28
	HIV-2 gp120	E T Q T S T W F G F N G T R A E N R T Y I Y W H G R D N R T	30
	49K 46-94	L I H V N K T Y E R T Y M G Y N R Q G T K	49
	HIV-2 gp120	I I S L N K Y Y N L T . M H C K R P G N K	50
B	49K 129-156	L E G P P G T P V T W F N Q D G K K F C E G E K V L H P	28
	HIV-1 gp120	L F N S T W N N S T W N N T E G S K N T E G N T I T H P	28
C	49K 131-166	G P P G T P V T W F N Q D G K K F C E G E K V L H P E F N H T C D K Q N	36
	SIV gp120	G D P E I T N M M F N C G E F F Y C N T T P L F N K F N Y T C D N Q N	36
D	49K 308-342	C N N Q N L T L I N V T K D Y E G T Y Y G . T N D K D E G K R Y R V K V	35
	HIV-1 gp120	C I N V N V T S V N T T E D R E G L K N C S F N M T T E L R D K R K K V	36

FIG. 40: Homologies between Ad19a 49K and HIV/SIV gp120 proteins. Different regions of the 49K sequence exhibit similarities to HIV/SIV gp120 proteins: A) 49K sequence 46-94 (R1) with the HIV-2 gp120 C2/V3 region (TrEMBL entry: Q9E8H3); B) 49K sequence 129-156 (R2) with the HIV-1 gp120 C4/V4/C5 (Q97740); C) 49K sequence 131-166 (R2) with SIV gp120 (Q9Q069); D) 49K sequence 308-342 (R3) with the HIV-1 gp120 V1/V2 region (O71468). Database similarity search was performed with BLAST on <http://www.ncbi.nih.gov/BLAST>.

A number of secreted, viral proteins have been identified that may serve immunomodulatory functions (Alcami and Koszinowski, 2000; Tortorella et al., 2000). Most of these proteins exhibit sequence homologies to known host proteins. It is commonly believed that the corresponding genes have been captured from the host. Viral homologs of host genes involved in immune defense are mainly encoded by large DNA viruses (herpes- and poxviruses). These include homologs of proteins involved in complement activation, soluble receptors for interferon- α and - β , soluble cytokine receptors (viroceptors) and cytokines (virokines). Only a few secreted viral proteins without homology to host proteins like 49K have been identified so far. Several poxviruses, e.g. myxoma virus and rabbitpox virus, encode chemokine-binding proteins (vCkBPs) that have no cellular counterparts and interact with a broad spectrum of chemokines (Lalani et al., 2000). In analogy, a potential function of 49K in chemokine binding could be proposed. Therefore, binding of 49K to cytokines/chemokines, e.g. MIP-1 α , TNF- α and IL-8, was tested (in collaboration with Antonio Alcami, University of Cambridge, United Kingdom),

but so far no interaction has been detected. In addition, no influence of 49K on the chemotaxis of leukocytes was found (in collaboration with Alberto Mantovani, University of Brescia, Italy). Similar to Ad19a E3/49K, the Ebola virus glycoprotein is found in two forms, a secreted (50-70 kDa) and a transmembrane (120-150 kDa) form, which is incorporated into the virion. Production of both forms from the same gene is regulated by RNA editing introducing a frame shift. The first 295 aa of both proteins are identical, but the secreted glycoprotein contains additional 69 and the transmembrane glycoprotein another 381 aa. The secreted form seems to bind to CD16b, the neutrophil-specific form of the Fc γ receptor III (Yang et al., 1998), whereas the transmembrane protein binds not to neutrophils but to endothelial cells. 49K may also function in the secreted as well as in the membrane-associated form. The relatively slow proteolytic processing of 49K allows the expression of significant amounts of 49K on the cell surface. However, in case of 49K it is unlikely that secreted and membrane-associated forms have different binding properties, since essentially the entire N-terminal ectodomain of 49K is released.

In sum, the 49K-binding proteins seem to be expressed specifically by lymphocyte cell lines. 49K-binding proteins were neither detected on the cell surface of A549 (lung epithelial carcinoma) cells by flow cytometry, nor intracellularly in A549 cells by coprecipitation, but in Jurkat J77 (T cell leukemia) cells. Although the possibility cannot be excluded that E3/49K affects functions of the infected cell like other Ad E3 proteins, these findings suggest that 49K targets infiltrating immune cells.

Since Ad E3 proteins may be involved in subgenus-specific pathogenesis (chapter 1.1, 1.7), the Ad19a E3/49K protein may play a role in diseases characteristically caused by subgenus D Ads, particularly diseases of the eye. In addition, even though all Ads of subgenus D tested express a 49K homolog, 49K may still contribute to the pathological features of the epidemic keratoconjunctivitis, in that 49K proteins of different subgenus D Ads bind to a different set of receptors on lymphocytes and possibly to different sets of leukocytes, which may be crucial for causing EKC or conjunctivitis or other diseases. Thus, potential differential activities of different subgenus D Ad 49K proteins remain to be addressed in future studies.

4.6 Inhibition of NK cell-mediated target cell lysis

49K binding to a number of lymphocyte cell lines raised the question whether the binding has any functional consequences. Indeed, purified, secreted 49K inhibited target cell lysis mediated by the NK cell line NKL (Fig. 38). Thus, in this case binding, as measured by flow cytometry (Fig. 36), correlated with interference with NKL function. However, the mechanism as to how 49K affects NK cell lysis remains unknown.

The regulation of NK cell-mediated lysis seems to be controlled by a delicate balance between activating and inhibitory receptors. Consequently, 49K may trigger inhibitory NK receptors or suppress activating receptors. Inhibitory receptors bind to MHC class I molecules on target cells. In virus-infected or tumor cells the expression of MHC on the cell surface is frequently reduced sensitizing these cells to NK cell-mediated lysis. Three families of inhibitory MHC-specific receptors have been discovered, the Ly49 receptors in rodents, the killer cell immunoglobulin-like receptors (KIR) in primates and the CD94/NKG2 heterodimers in both primates and rodents (Raulet et al., 2001). Some of the activating receptors may recognize MHC class I molecules and belong to the same families as the inhibitory MHC-specific receptors, whereas others bind to non-MHC ligands, which in many cases have not been characterized yet (Moretta et al., 2001; Raulet et al., 2001).

The role of NK cells in Ad infection is still elusive. Upon Ad infection an NK cell response is elicited, and, in case of recombinant Ads, they seem to play an important role in virus elimination (chapter 1.5). In addition, results were obtained indicating that Ads are able to suppress NK cell-mediated killing of infected cells by a so far unknown mechanism (Routes and Cook, 1989; Routes and Cook, 1995). Some viruses express MHC class I homologs, e.g. MCMV m144, HCMV UL18, which have been implicated in the inhibition of NK cell-mediated lysis. The HCMV UL40 protein provides a peptide required for the maturation of the HLA-E molecule that can inhibit NK cell-mediated lysis *in vitro* via interaction with CD94/NKG2A on NK cells (Alcami and Koszinowski, 2000).

The inhibition of NK cell-mediated lysis by 49K seems to utilize a different mechanism. Few cell surface markers with potential relevance for NK cell function on NKL cells are known. The heterodimer CD94/NKG2A is found on the cell surface of NKL cells and triggers an inhibitory signal upon ligation to HLA-E molecules presenting an HLA signal peptide by the target cell. In contrast, NKG2D is an activating receptor. NKG2D binds to the closely related MICA and MICB molecules (Moretta et al., 2001). In addition, 2B4 is expressed on NKL cells, which seems to function as a coreceptor in NK-cell mediated cytotoxicity and binds to CD48 (Moretta et al., 2001). Interestingly, CD56, a marker for primary NK cells, is expressed only in very low amounts on NKL cells. In some experiments, 49K suppressed NK cell-mediated lysis even when lysis was

already reduced by the expression of the HLA-E/HLA signal peptide complex on the target cell (data not shown). This may suggest that 49K-mediated inhibition is independent of CD94/NKG2A. In addition, none of the proteins involved in NK cell-mediated natural cytotoxicity, including CD94, NKG2A, NKG2D and 2B4, displays a molecular mass of 172-196 kDa as found for the 49K-binding proteins in Jurkat cells. The expression of a potential 49K receptor in different lymphocyte cell lines argues against a NK cell-specific factor. Thus, the 49K-binding proteins involved in 49K-mediated inhibition of NK cell-mediated lysis remain to be identified.

4.7 Conclusion and outlook

In this work the Ad19a E3/49K protein was identified as a secreted lymphocyte binding factor. Preliminary data show that 49K has an immunomodulatory function: 49K inhibited NKL mediated target cell lysis *in vitro*. Other E3 proteins investigated so far exclusively affect the infected cell. Therefore, 49K seems to be the first Ad protein that directly influences lymphocytes, presumably in the membrane bound as well as in the secreted form. 49K biochemistry and cell biology is characterized by an extensive posttranslational processing including proteolytic cleavage and a complex intracellular trafficking. The biochemical and functional characterization revealed that in many ways Ad19a E3/49K exhibits unique properties indicating that 49K function in adenoviral immune evasion represents a novel principle.

5 SUMMARY

Human adenoviruses (Ads) cause a variety of acute diseases but also establish persistent infections. Ads have evolved a number of mechanisms to evade the host immune response that seem to facilitate virus replication and transmission *in vivo*. Interestingly, one Ad transcription unit, the early transcription unit 3 (E3), appears to encode exclusively proteins with immunomodulatory functions. Recently, a novel open reading frame, E3/49K, was identified in the E3 region of the epidemic keratoconjunctivitis causing serotype Ad19a. The sequence predicts a type I transmembrane protein with a large N-terminal domain and a short cytoplasmic tail of 19 amino acids (aa). The N-terminal part contains three repeat regions (R1-3) of about 80 aa each with R3 exhibiting a significant homology to immunoglobulin-like domains.

This study shows that 49K is a highly glycosylated protein with an apparent molecular mass of 80-100 kDa. 12-13 out of 14 predicted N-glycosylation sites are utilized, and there is also evidence for O-glycosylation. 49K contains intramolecular disulfide bonds and is proteolytically processed. As a result of the cleavage the N-terminal ectodomain is secreted: Ad19a E3/49K is the first Ad protein known to be secreted.

At steady-state, E3/49K is detected in the Golgi/TGN, early endosomes and at the cell surface of Ad19a-infected as well as 49K-transfected cells. The cytoplasmic tail, which contains two potential endosomal/lysosomal targeting motifs, YXX Φ and LL, plays a major role in the 49K trafficking. The proteolytic processing may occur in the TGN or secretory vesicles and/or at the cell surface. The finding that an increased cell surface expression of 49K correlates with an increased secretion rate indicates proteolytic processing of 49K at the cell surface. The C-terminal fragments and also unprocessed 49K proteins are internalized possibly by the interaction of the LL motif in the cytoplasmic tail with the clathrin adaptor complex AP-2. From early endosomes 49K proteins and C-terminal fragments recycle to the TGN potentially involving the interaction of the cytoplasmic tail of 49K with the clathrin adaptor complex AP-1 or to the cell surface, whereas a fraction is delivered to late endosomes and lysosomes.

Remarkably, the secreted form of 49K specifically binds to various lymphocyte cell lines, including NK, B and T cell lines, but not to other cell types, e.g. fibroblasts, suggesting that the soluble and possibly also the membrane-bound 49K binds to receptor(s) on lymphocytes. Indeed, in Jurkat (T cell leukemia) cells, 49K-binding protein(s) with apparent molecular masses of 172-196 kDa were identified. Moreover, purified 49K inhibited the NK cell-mediated lysis of target cells. Thus, upon binding to cell surface receptors, 49K may trigger an inhibitory signal or inhibit an activating signal. While other Ad E3 proteins affect the infected cell, 49K seems to influence infiltrating cells of the immune system. Therefore, 49K function appears to represent an entirely novel Ad immune evasion mechanism.

6 REFERENCES

- Aguilar, R.C., Boehm, M., Gorshkova, I., Crouch, R.J., Tomita, K., Saito, T., Ohno, H., and Bonifacino, J.S. (2001). Signal-binding specificity of the mu4 subunit of the adaptor protein complex AP-4. *J. Biol. Chem.* *276*, 13145-13152.
- Ahle, S., Mann, A., Eichelsbacher, U., and Ungewickell, E. (1988). Structural relationships between clathrin assembly proteins from the Golgi and the plasma membrane. *EMBO J.* *7*, 919-929.
- Alcami, A. and Koszinowski, U.H. (2000). Viral mechanisms of immune evasion. *Mol. Med. Today* *6*, 365-372.
- Alconada, A., Bauer, U., and Hoflack, B. (1996). A tyrosine-based motif and a casein kinase II phosphorylation site regulate the intracellular trafficking of the varicella-zoster virus glycoprotein I, a protein localized in the trans-Golgi network. *EMBO J.* *15*, 6096-6110.
- Alconada, A., Bauer, U., Sodeik, B., and Hoflack, B. (1999). Intracellular traffic of herpes simplex virus glycoprotein gE: characterization of the sorting signals required for its trans-Golgi network localization. *J. Virol.* *73*, 377-387.
- Andrade, F., Bull, H.G., Thornberry, N.A., Ketner, G.W., Casciola-Rosen, L.A., and Rosen, A. (2001). Adenovirus L4-100K assembly protein is a granzyme B substrate that potently inhibits granzyme B-mediated cell death. *Immunity* *14*, 751-761.
- Arnberg, N., Edlund, K., Kidd, A.H., and Wadell, G. (2000a). Adenovirus type 37 uses sialic acid as a cellular receptor. *J. Virol.* *74*, 42-48.
- Arnberg, N., Kidd, A.H., Edlund, K., Olfat, F., and Wadell, G. (2000b). Initial interactions of subgenus D adenoviruses with A549 cellular receptors: sialic acid versus alpha(v) integrins. *J. Virol.* *74*, 7691-7693.
- Arnberg, N., Mei, Y., and Wadell, G. (1997). Fiber genes of adenoviruses with tropism for the eye and the genital tract. *Virology* *227*, 239-244.
- Bailey, A. and Mautner, V. (1994). Phylogenetic relationships among adenovirus serotypes. *Virology* *205*, 438-452.
- Banting, G. and Ponnambalam, S. (1997). TGN38 and its orthologues: roles in post-TGN vesicle formation and maintenance of TGN morphology. *Biochim. Biophys. Acta* *1355*, 209-217.
- Barclay, A.N., Brown, M.H., Law, S.K.A., McNight, A.J., Tomlinson, M.G., and van der Merwe, P.A. (1997). *The Leukocyte Antigen Factsbook*. Academic Press, San Diego, CA, USA.
- Basler, C.F. and Horwitz, M.S. (1996). Subgroup B adenovirus type 35 early region 3 mRNAs differ from those of the subgroup C adenoviruses. *Virology* *215*, 165-177.
- Bayer, N., Schober, D., Prchla, E., Murphy, R.F., Blaas, D., and Fuchs, R. (1998). Effect of bafilomycin A1 and nocodazole on endocytic transport in HeLa cells: implications for viral uncoating and infection. *J. Virol.* *72*, 9645-9655.
- Benedict, C.A., Norris, P.S., Prigozy, T.I., Bodmer, J.L., Mahr, J.A., Garnett, C.T., Martinon, F., Tschopp, J., Gooding, L.R., and Ware, C.F. (2001). Three adenovirus E3 proteins cooperate to evade apoptosis by tumor necrosis factor-related apoptosis-inducing ligand receptor-1 and -2. *J. Biol. Chem.* *276*, 3270-3278.
- Benkö, M., Harrach, B., and Russel, W.C. (1999). Adenoviridae. In *Virus Taxonomy*. Seventh Report of the International Committee on Taxonomy of Viruses. M.H.V. van Regenmortel, C.M. Fauquet, and D.H.L. Bishop, eds. Academic Press, San Diego, USA, pp. 227-238.

- Bergelson, J.M., Krithivas, A., Celi, L., Droguett, G., Horwitz, M.S., Wickham, T., Crowell, R.L., and Finberg, R.W. (1998). The murine CAR homolog is a receptor for coxsackie B viruses and adenoviruses. *J. Virol.* *72*, 415-419.
- Besser, M. and Wank, R. (1999). Cutting edge: clonally restricted production of the neurotrophins brain-derived neurotrophic factor and neurotrophin-3 mRNA by human immune cells and Th1/Th2-polarized expression of their receptors. *J. Immunol.* *162*, 6303-6306.
- Bewley, M.C., Springer, K., Zhang, Y.B., Freimuth, P., and Flanagan, J.M. (1999). Structural analysis of the mechanism of adenovirus binding to its human cellular receptor, CAR. *Science* *286*, 1579-1583.
- Biron, C.A., Nguyen, K.B., Pien, G.C., Cousens, L.P., and Salazar-Mather, T.P. (1999). Natural killer cells in antiviral defense: function and regulation by innate cytokines. *Annu. Rev. Immunol.* *17*, 189-220.
- Black, M.W. and Pelham, H.R. (2001). Membrane traffic: How do GGAs fit in with the adaptors? *Curr. Biol.* *11*, R460-R462.
- Blobel, C.P. (2000). Remarkable roles of proteolysis on and beyond the cell surface. *Curr. Opin. Cell Biol.* *12*, 606-612.
- Blum, H., Beier, H., and Gross, H.J. (1987). Improved silver staining of plant proteins, RNA and DNA in polyacrylamide gels. *Electrophoresis* *8*, 93-99.
- Blusch, J., Deryckere, F., Windheim, M., Ruzsics, Z., Arnberg, N., Adrian, T., and Burgert, H.-G. (2002). E3/49K: A novel early region 3 protein specifically expressed by adenoviruses of subgenus D. *Virology*. *in press*.
- Boehm, M. and Bonifacino, J.S. (2001). Adaptins: the final recount. *Mol. Biol. Cell* *12*, 2907-2920.
- Boll, W., Ohno, H., Songyang, Z., Rapoport, I., Cantley, L.C., Bonifacino, J.S., and Kirchhausen, T. (1996). Sequence requirements for the recognition of tyrosine-based endocytic signals by clathrin AP-2 complexes. *EMBO J.* *15*, 5789-5795.
- Bowers, K., Pelchen-Matthews, A., Honing, S., Vance, P.J., Creary, L., Haggarty, B.S., Romano, J., Ballensiefen, W., Hoxie, J.A., and Marsh, M. (2000). The simian immunodeficiency virus envelope glycoprotein contains multiple signals that regulate its cell surface expression and endocytosis. *Traffic* *1*, 661-674.
- Bradshaw, J.D., Lu, P., Leytze, G., Rodgers, J., Schieven, G.L., Bennett, K.L., Linsley, P.S., and Kurtz, S.E. (1997). Interaction of the cytoplasmic tail of CTLA-4 (CD152) with a clathrin-associated protein is negatively regulated by tyrosine phosphorylation. *Biochemistry* *36*, 15975-15982.
- Branton, P.E. and Roopchand, D.E. (2001). The role of adenovirus E4orf4 protein in viral replication and cell killing. *Oncogene* *20*, 7855-7865.
- Bremnes, T., Lauvrak, V., Lindqvist, B., and Bakke, O. (1998). A region from the medium chain adaptor subunit (μ) recognizes leucine- and tyrosine-based sorting signals. *J. Biol. Chem.* *273*, 8638-8645.
- Burgert, H.-G. (1996). Subversion of the MHC class I antigen-presentation pathway by adenoviruses and herpes simplex viruses. *Trends Microbiol.* *4*, 107-112.
- Burgert, H.-G. and Kvist, S. (1985). An adenovirus type 2 glycoprotein blocks cell surface expression of human histocompatibility class I antigens. *Cell* *41*, 987-997.
- Burgert, H.-G., Ruzsics, Z., Obermeier, S., Hilgendorf, A., Windheim, M., and Elsing, A. (2002). Subversion of host defense mechanisms by adenoviruses. *Curr. Top. Microbiol. Immunol.* *269*. *in press*.

- Burgert, H.G. and Blusch, J.H. (2000). Immunomodulatory functions encoded by the E3 transcription unit of adenoviruses. *Virus Genes* 21, 13-25.
- Carroll, K.S., Hanna, J., Simon, I., Krise, J., Barbero, P., and Pfeffer, S.R. (2001). Role of Rab9 GTPase in facilitating receptor recruitment by TIP47. *Science* 292, 1373-1376.
- Chen, P., Tian, J., Kovesdi, I., and Bruder, J.T. (1998). Interaction of the adenovirus 14.7-kDa protein with FLICE inhibits Fas ligand-induced apoptosis. *J. Biol. Chem.* 273, 5815-5820.
- Chen, Y.A. and Scheller, R.H. (2001). SNARE-mediated membrane fusion. *Nat. Rev. Mol. Cell Biol.* 2, 98-106.
- Chillon, M., Bosch, A., Zabner, J., Law, L., Armentano, D., Welsh, M.J., and Davidson, B.L. (1999). Group D adenoviruses infect primary central nervous system cells more efficiently than those from group C. *J. Virol.* 73, 2537-2540.
- Chirmule, N. and Pahwa, S. (1996). Envelope glycoproteins of human immunodeficiency virus type 1: profound influences on immune functions. *Microbiol. Rev.* 60, 386-406.
- Chirmule, N., Propert, K., Magosin, S., Qian, Y., Qian, R., and Wilson, J. (1999). Immune responses to adenovirus and adeno-associated virus in humans. *Gene Ther.* 6, 1574-1583.
- Clague, M.J., Urbe, S., Aniento, F., and Gruenberg, J. (1994). Vacuolar ATPase activity is required for endosomal carrier vesicle formation. *J. Biol. Chem.* 269, 21-24.
- Collawn, J.F., Stangel, M., Kuhn, L.A., Esekogwu, V., Jing, S.Q., Trowbridge, I.S., and Tainer, J.A. (1990). Transferrin receptor internalization sequence YXRF implicates a tight turn as the structural recognition motif for endocytosis. *Cell* 63, 1061-1072.
- Cook, J.L., May, D.L., Lewis, A.M., Jr., and Walker, T.A. (1987). Adenovirus E1A gene induction of susceptibility to lysis by natural killer cells and activated macrophages in infected rodent cells. *J. Virol.* 61, 3510-3520.
- Cook, J.L., Routes, B.A., Walker, T.A., Colvin, K.L., and Routes, J.M. (1999). E1A oncogene induction of cellular susceptibility to killing by cytolytic lymphocytes through target cell sensitization to apoptotic injury. *Exp. Cell Res.* 251, 414-423.
- Corsi, A.K. and Schekman, R. (1996). Mechanism of polypeptide translocation into the endoplasmic reticulum. *J. Biol. Chem.* 271, 30299-30302.
- Crump, C.M., Xiang, Y., Thomas, L., Gu, F., Austin, C., Tooze, S.A., and Thomas, G. (2001). PACS-1 binding to adaptors is required for acidic cluster motif-mediated protein traffic. *EMBO J.* 20, 2191-2201.
- Cuff, J.A., Clamp, M.E., Siddiqui, A.S., Finlay, M., and Barton, G.J. (1998). JPred: a consensus secondary structure prediction server. *Bioinformatics* 14, 892-893.
- Davison, E., Kirby, I., Elliott, T., and Santis, G. (1999). The human HLA-A*0201 allele, expressed in hamster cells, is not a high-affinity receptor for adenovirus type 5 fiber. *J. Virol.* 73, 4513-4517.
- de Duve, C. (1983). Lysosomes revisited. *Eur. J. Biochem.* 137, 391-397.
- De Jong, J.C., Wermenbol, A.G., Verweij-Uijterwaal, M.W., Slaterus, K.W., Wertheim-Van, D.P., Van Doornum, G.J., Khoo, S.H., and Hierholzer, J.C. (1999). Adenoviruses from human immunodeficiency virus-infected individuals, including two strains that represent new candidate serotypes Ad50 and Ad51 of species B1 and D, respectively. *J. Clin. Microbiol.* 37, 3940-3945.
- Dell'Angelica, E.C., Puertollano, R., Mullins, C., Aguilar, R.C., Vargas, J.D., Hartnell, L.M., and Bonifacino, J.S. (2000). GGAs: a family of ADP ribosylation factor-binding proteins related to adaptors and associated with the Golgi complex. *J. Cell Biol.* 149, 81-94.

- Dell'Angelica, E.C., Shotelersuk, V., Aguilar, R.C., Gahl, W.A., and Bonifacino, J.S. (1999). Altered trafficking of lysosomal proteins in Hermansky-Pudlak syndrome due to mutations in the beta 3A subunit of the AP-3 adaptor. *Mol. Cell* *3*, 11-21.
- Deryckere, F. and Burgert, H.-G. (1996). Early region 3 of adenovirus type 19 (subgroup D) encodes an HLA-binding protein distinct from that of subgroups B and C. *J. Virol.* *70*, 2832-2841.
- Deryckere, F., Ebenau-Jehle, C., Wold, W.S., and Burgert, H.-G. (1995). Tumor necrosis factor alpha increases expression of adenovirus E3 proteins. *Immunobiology* *193*, 186-192.
- Dietrich, J., Hou, X., Wegener, A.M., and Geisler, C. (1994). CD3 gamma contains a phosphoserine-dependent di-leucine motif involved in down-regulation of the T cell receptor. *EMBO J.* *13*, 2156-2166.
- Dietrich, O., Gallert, F., and Hasilik, A. (1996). Purification of lysosomal membrane proteins from human placenta. *Eur. J. Cell Biol.* *69*, 99-106.
- Dittie, A.S., Hajibagheri, N., and Tooze, S.A. (1996). The AP-1 adaptor complex binds to immature secretory granules from PC12 cells, and is regulated by ADP-ribosylation factor. *J. Cell Biol.* *132*, 523-536.
- Dittrich, E., Haft, C.R., Muys, L., Heinrich, P.C., and Graeve, L. (1996). A di-leucine motif and an upstream serine in the interleukin-6 (IL-6) signal transducer gp130 mediate ligand-induced endocytosis and down-regulation of the IL-6 receptor. *J. Biol. Chem.* *271*, 5487-5494.
- Duksin, D. and Mahoney, W.C. (1982). Relationship of the structure and biological activity of the natural homologues of tunicamycin. *J. Biol. Chem.* *257*, 3105-3109.
- Ellgaard, L., Molinari, M., and Helenius, A. (1999). Setting the standards: quality control in the secretory pathway. *Science* *286*, 1882-1888.
- Elsing, A. and Burgert, H.-G. (1998). The adenovirus E3/10.4K-14.5K proteins down-modulate the apoptosis receptor Fas/Apo-1 by inducing its internalization. *Proc. Natl. Acad. Sci. USA* *95*, 10072-10077.
- Esler, W.P. and Wolfe, M.S. (2001). A portrait of Alzheimer secretases-new features and familiar faces. *Science* *293*, 1449-1454.
- Falk, C.S., Nossner, E., Frankenberger, B., and Schendel, D.J. (2000). Non-MHC-restricted CD4+ T lymphocytes are regulated by HLA-Cw7-mediated inhibition. *Hum. Immunol.* *61*, 1219-1232.
- Faundez, V., Horng, J.T., and Kelly, R.B. (1998). A function for the AP3 coat complex in synaptic vesicle formation from endosomes. *Cell* *93*, 423-432.
- Folsch, H., Ohno, H., Bonifacino, J.S., and Mellman, I. (1999). A novel clathrin adaptor complex mediates basolateral targeting in polarized epithelial cells. *Cell* *99*, 189-198.
- Francis, M.J., Jones, E.E., Levy, E.R., Martin, R.L., Ponnambalam, S., and Monaco, A.P. (1999). Identification of a di-leucine motif within the C terminus domain of the Menkes disease protein that mediates endocytosis from the plasma membrane. *J. Cell Sci.* *112 (Pt 11)*, 1721-1732.
- Futter, C.E., Gibson, A., Allchin, E.H., Maxwell, S., Ruddock, L.J., Odorizzi, G., Domingo, D., Trowbridge, I.S., and Hopkins, C.R. (1998). In polarized MDCK cells basolateral vesicles arise from clathrin-gamma-adaptin-coated domains on endosomal tubules. *J. Cell Biol.* *141*, 611-623.
- Gallimore, P.H. and Turnell, A.S. (2001). Adenovirus E1A: remodelling the host cell, a life or death experience. *Oncogene* *20*, 7824-7835.

- Gavel, Y. and von Heijne, G. (1990). Sequence differences between glycosylated and non-glycosylated Asn-X-Thr/Ser acceptor sites: implications for protein engineering. *Protein Eng.* 3, 433-442.
- Geisler, C., Dietrich, J., Nielsen, B.L., Kastrop, J., Lauritsen, J.P., Odum, N., and Christensen, M.D. (1998). Leucine-based receptor sorting motifs are dependent on the spacing relative to the plasma membrane. *J. Biol. Chem.* 273, 21316-21323.
- Gewurz, B.E., Gaudet, R., Tortorella, D., Wang, E.W., and Ploegh, H.L. (2001a). Virus subversion of immunity: a structural perspective. *Curr. Opin. Immunol.* 13, 442-450.
- Gewurz, B.E., Gaudet, R., Tortorella, D., Wang, E.W., Ploegh, H.L., and Wiley, D.C. (2001b). Antigen presentation subverted: Structure of the human cytomegalovirus protein US2 bound to the class I molecule HLA-A2. *Proc. Natl. Acad. Sci. USA* 98, 6794-6799.
- Ghosh, R.N., Mallet, W.G., Soe, T.T., McGraw, T.E., and Maxfield, F.R. (1998). An endocytosed TGN38 chimeric protein is delivered to the TGN after trafficking through the endocytic recycling compartment in CHO cells. *J. Cell Biol.* 142, 923-936.
- Girones, N., Alvarez, E., Seth, A., Lin, I.M., Latour, D.A., and Davis, R.J. (1991). Mutational analysis of the cytoplasmic tail of the human transferrin receptor. Identification of a sub-domain that is required for rapid endocytosis. *J. Biol. Chem.* 266, 19006-19012.
- Goodbourn, S., Didcock, L., and Randall, R.E. (2000). Interferons: cell signalling, immune modulation, antiviral response and virus countermeasures. *J. Gen. Virol.* 81, 2341-2364.
- Gorelick, F.S. and Shugrue, C. (2001). Exiting the endoplasmic reticulum. *Mol. Cell Endocrinol.* 177, 13-18.
- Greenway, A.L., Holloway, G., and McPhee, D.A. (2000). HIV-1 Nef: a critical factor in viral-induced pathogenesis. *Adv. Pharmacol.* 48, 299-343.
- Gropp, R., Frye, M., Wagner, T.O., and Bargon, J. (1999). Epithelial defensins impair adenoviral infection: implication for adenovirus-mediated gene therapy. *Hum. Gene Ther.* 10, 957-964.
- Gu, F. and Gruenberg, J. (1999). Biogenesis of transport intermediates in the endocytic pathway. *FEBS Lett.* 452, 61-66.
- Guidotti, L.G. and Chisari, F.V. (2001). Noncytolytic control of viral infections by the innate and adaptive immune response. *Annu. Rev. Immunol.* 19, 65-91.
- Haass, C., Koo, E.H., Capell, A., Teplow, D.B., and Selkoe, D.J. (1995). Polarized sorting of beta-amyloid precursor protein and its proteolytic products in MDCK cells is regulated by two independent signals. *J. Cell Biol.* 128, 537-547.
- Hansen, J.E., Lund, O., Tolstrup, N., Gooley, A.A., Williams, K.L., and Brunak, S. (1998). NetOglyc: prediction of mucin type O-glycosylation sites based on sequence context and surface accessibility. *Glycoconj. J.* 15, 115-130.
- Harty, J.T., Tvinnereim, A.R., and White, D.W. (2000). CD8+ T cell effector mechanisms in resistance to infection. *Annu. Rev. Immunol.* 18, 275-308.
- Hauri, H.P., Kappeler, F., Andersson, H., and Appenzeller, C. (2000). ERGIC-53 and traffic in the secretory pathway. *J. Cell Sci.* 113 (Pt 4), 587-596.
- Hausmann, J., Ortmann, D., Witt, E., Veit, M., and Seidel, W. (1998). Adenovirus death protein, a transmembrane protein encoded in the E3 region, is palmitoylated at the cytoplasmic tail. *Virology* 244, 343-351.
- Hawkins, L.K., Wilson-Rawls, J., and Wold, W.S. (1995). Region E3 of subgroup B human adenoviruses encodes a 16-kilodalton membrane protein that may be a distant analog of the E3-6.7K protein of subgroup C adenoviruses. *J. Virol.* 69, 4292-4298.

- Hawkins, L.K. and Wold, W.S. (1995a). A 20,500-Dalton protein is coded by region E3 of subgroup B but not subgroup C human adenoviruses. *Virology* 208, 226-233.
- Hawkins, L.K. and Wold, W.S. (1995b). The E3-20.5K membrane protein of subgroup B human adenoviruses contains O-linked and complex N-linked oligosaccharides. *Virology* 210, 335-344.
- Heilker, R., Spiess, M., and Crottet, P. (1999). Recognition of sorting signals by clathrin adaptors. *Bioessays* 21, 558-567.
- Hicke, L. (1999). Gettin' down with ubiquitin: turning off cell-surface receptors, transporters and channels. *Trends Cell Biol.* 9, 107-112.
- Hierholzer, J.C., Wigand, R., Anderson, L.J., Adrian, T., and Gold, J.W. (1988). Adenoviruses from patients with AIDS: a plethora of serotypes and a description of five new serotypes of subgenus D (types 43-47). *J. Infect. Dis.* 158, 804-813.
- Hillemann, M.R. and Werner, J.R. (1954). Recovery of a new agent from patients with acute respiratory illness. *Proceedings of the Society for Experimental Biology and Medicine* 85, 183-188.
- Hinshaw, J.E. (2000). Dynamin and its role in membrane fission. *Annu. Rev. Cell Dev. Biol.* 16, 483-519.
- Hirst, J., Bright, N.A., Rous, B., and Robinson, M.S. (1999). Characterization of a fourth adaptor-related protein complex. *Mol. Biol. Cell* 10, 2787-2802.
- Hong, S.S., Karayan, L., Tournier, J., Curiel, D.T., and Boulanger, P.A. (1997). Adenovirus type 5 fiber knob binds to MHC class I alpha2 domain at the surface of human epithelial and B lymphoblastoid cells. *EMBO J.* 16, 2294-2306.
- Hong, W. (1998). Protein transport from the endoplasmic reticulum to the Golgi apparatus. *J. Cell Sci.* 111 (Pt 19), 2831-2839.
- Honing, S., Sandoval, I.V., and von Figura, K. (1998). A di-leucine-based motif in the cytoplasmic tail of LIMP-II and tyrosinase mediates selective binding of AP-3. *EMBO J.* 17, 1304-1314.
- Honing, S., Sosa, M., Hille-Rehfeld, A., and von Figura, K. (1997). The 46-kDa mannose 6-phosphate receptor contains multiple binding sites for clathrin adaptors. *J. Biol. Chem.* 272, 19884-19890.
- Horwitz, M.S. (1996). Adenoviruses. In *Fields Virology*. Fields, B.N., Knipe, D.M, and Howley, P.M., eds. Lippincott-Raven Publishers, Philadelphia, New York, pp. 2149-2171.
- Horwitz, M.S. (2001). Adenovirus immunoregulatory genes and their cellular targets. *Virology* 279, 1-8.
- Hu, W., Howard, M., and Lukacs, G.L. (2001). Multiple endocytic signals in the C-terminal tail of the cystic fibrosis transmembrane conductance regulator. *Biochem. J.* 354, 561-572.
- Hunziker, W. and Fumey, C. (1994). A di-leucine motif mediates endocytosis and basolateral sorting of macrophage IgG Fc receptors in MDCK cells. *EMBO J.* 13, 2963-2967.
- Hunziker, W. and Geuze, H.J. (1996). Intracellular trafficking of lysosomal membrane proteins. *Bioessays* 18, 379-389.
- Janeway, C.A., Travers, P., Walport, M., and Shlomchik, M. (2001). Appendices II-V. In *Immunobiology*. Garland Publishing, New York, USA, pp. 561-581.
- Kafri, T., Morgan, D., Krahl, T., Sarvetnick, N., Sherman, L., and Verma, I. (1998). Cellular immune response to adenoviral vector infected cells does not require de novo viral gene expression: implications for gene therapy. *Proc. Natl. Acad. Sci. USA* 95, 11377-11382.

- Kaplan, J.M., Armentano, D., Scaria, A., Woodworth, L.A., Pennington, S.E., Wadsworth, S.C., Smith, A.E., and Gregory, R.J. (1999). Novel role for E4 region genes in protection of adenovirus vectors from lysis by cytotoxic T lymphocytes. *J. Virol.* *73*, 4489-4492.
- Karlsson, K. and Carlsson, S.R. (1998). Sorting of lysosomal membrane glycoproteins lamp-1 and lamp-2 into vesicles distinct from mannose 6-phosphate receptor/gamma-adaptin vesicles at the trans-Golgi network. *J. Biol. Chem.* *273*, 18966-18973.
- Kawano, J., Ide, S., Oinuma, T., and Suganuma, T. (1994). A protein-specific monoclonal antibody to rat liver beta 1->4 galactosyltransferase and its application to immunohistochemistry. *J. Histochem. Cytochem.* *42*, 363-369.
- Keller, P., Toomre, D., Diaz, E., White, J., and Simons, K. (2001). Multicolour imaging of post-Golgi sorting and trafficking in live cells. *Nat. Cell Biol.* *3*, 140-149.
- Kiessling, L.L. and Gordon, E.J. (1998). Transforming the cell surface through proteolysis. *Chem. Biol.* *5*, R49-R62.
- Kirchhausen, T. (1999). Adaptors for clathrin-mediated traffic. *Annu. Rev. Cell Dev. Biol.* *15*, 705-732.
- Kirchhausen, T. (2000a). Clathrin. *Annu. Rev. Biochem.* *69*, 699-727.
- Kirchhausen, T. (2000b). Three ways to make a vesicle. *Nat. Rev. Mol. Cell Biol.* *1*, 187-198.
- Klausner, R.D., Donaldson, J.G., and Lippincott-Schwartz, J. (1992). Brefeldin A: insights into the control of membrane traffic and organelle structure. *J. Cell Biol.* *116*, 1071-1080.
- Kobayashi, T., Stang, E., Fang, K.S., de Moerloose, P., Parton, R.G., and Gruenberg, J. (1998). A lipid associated with the antiphospholipid syndrome regulates endosome structure and function. *Nature* *392*, 193-197.
- Koerner, H., Fritzsche, U., and Burgert, H.-G. (1992). Tumor necrosis factor alpha stimulates expression of adenovirus early region 3 proteins: implications for viral persistence. *Proc. Natl. Acad. Sci. USA* *89*, 11857-11861.
- Koerner, H. and Burgert, H.-G. (1994). Down-regulation of HLA antigens by the adenovirus type 2 E3/19K protein in a T-lymphoma cell line. *J. Virol.* *68*, 1442-1448.
- Kohler, G. and Milstein, C. (1992). Continuous cultures of fused cells secreting antibody of predefined specificity. 1975. *Biotechnology* *24*, 524-526.
- Kremmer, E., Kranz, B.R., Hille, A., Klein, K., Eulitz, M., Hoffmann-Fezer, G., Feiden, W., Herrmann, K., Delecluse, H.J., Delsol, G., Bornkamm, G.W., Mueller-Lantsch, N., and Grassert, F.A. (1995). Rat monoclonal antibodies differentiating between the Epstein-Barr virus nuclear antigens 2A (EBNA2A) and 2B (EBNA2B). *Virology* *208*, 336-342.
- Ktiskakis, N.T. and Roth, M.G. (1996). Protein sorting during endocytosis. In *Protein Targeting*. S.M. Hurlley, ed. IRL Press, Oxford, New York, Tokyo, pp. 176-212.
- Ktistakis, N.T., Thomas, D., and Roth, M.G. (1990). Characteristics of the tyrosine recognition signal for internalization of transmembrane surface glycoproteins. *J. Cell Biol.* *111*, 1393-1407.
- Kuivinen, E., Hoffman, B.L., Hoffman, P.A., and Carlin, C.R. (1993). Structurally related class I and class II receptor protein tyrosine kinases are down-regulated by the same E3 protein coded for by human group C adenoviruses. *J. Cell Biol.* *120*, 1271-1279.
- Ladinsky, M.S. and Howell, K.E. (1992). The trans-Golgi network can be dissected structurally and functionally from the cisternae of the Golgi complex by brefeldin A. *Eur. J. Cell Biol.* *59*, 92-105.

- Laemmli, U.K. (1970). Cleavage of structural proteins during the assembly of the head of bacteriophage T4. *Nature* 227, 680-685.
- Laird, V. and Spiess, M. (2000). A novel assay to demonstrate an intersection of the exocytic and endocytic pathways at early endosomes. *Exp. Cell Res.* 260, 340-345.
- Lalani, A.S., Barrett, J.W., and McFadden, G. (2000). Modulating chemokines: more lessons from viruses. *Immunol. Today* 21, 100-106.
- Lazarovits, J. and Roth, M. (1988). A single amino acid change in the cytoplasmic domain allows the influenza virus hemagglutinin to be endocytosed through coated pits. *Cell* 53, 743-752.
- Le Borgne, R., Alconada, A., Bauer, U., and Hoflack, B. (1998). The mammalian AP-3 adaptor-like complex mediates the intracellular transport of lysosomal membrane glycoproteins. *J. Biol. Chem.* 273, 29451-29461.
- Leopold, P.L., Kreitzer, G., Miyazawa, N., Rempel, S., Pfister, K.K., Rodriguez-Boulan, E., and Crystal, R.G. (2000). Dynein- and microtubule-mediated translocation of adenovirus serotype 5 occurs after endosomal lysis. *Hum. Gene Ther.* 11, 151-165.
- Leppard, K.N. (1997). E4 gene function in adenovirus, adenovirus vector and adeno-associated virus infections. *J. Gen. Virol.* 78 (Pt 9), 2131-2138.
- Li, Y. and Wold, W.S. (2000). Identification and characterization of a 30K protein (Ad4E3-30K) encoded by the E3 region of human adenovirus type 4. *Virology* 273, 127-138.
- Lin, S., Naim, H.Y., and Roth, M.G. (1997). Tyrosine-dependent basolateral sorting signals are distinct from tyrosine-dependent internalization signals. *J. Biol. Chem.* 272, 26300-26305.
- Lissitzky, J.C., Luis, J., Munzer, J.S., Benjannet, S., Parat, F., Chretien, M., Marvaldi, J., and Seidah, N.G. (2000). Endoproteolytic processing of integrin pro-alpha subunits involves the redundant function of furin and proprotein convertase (PC) 5A, but not paired basic amino acid converting enzyme (PACE) 4, PC5B or PC7. *Biochem. J.* 346 Pt 1, 133-138.
- Liszewski, M.K., Post, T.W., and Atkinson, J.P. (1991). Membrane cofactor protein (MCP or CD46): newest member of the regulators of complement activation gene cluster. *Annu. Rev. Immunol.* 9:431-55., 431-455.
- Loetscher, P., Moser, B., and Baggiolini, M. (2000). Chemokines and their receptors in lymphocyte traffic and HIV infection. *Adv. Immunol.* 74, 127-180.
- Lukashok, S.A. and Horwitz, M.S. (1998). New perspectives in adenoviruses. *Curr. Clin. Top. Infect. Dis.* 18, 286-305.
- Mahr, J.A. and Gooding, L.R. (1999). Immune evasion by adenoviruses. *Immunol. Rev.* 168, 121-130.
- Mallet, W.G. and Maxfield, F.R. (1999). Chimeric forms of furin and TGN38 are transported with the plasma membrane in the trans-Golgi network via distinct endosomal pathways. *J. Cell Biol.* 146, 345-359.
- Martens, A.S., Bode, J.G., Heinrich, P.C., and Graeve, L. (2000). The cytoplasmic domain of the interleukin-6 receptor gp80 mediates its basolateral sorting in polarized madin-darby canine kidney cells. *J. Cell Sci.* 113 (Pt 20), 3593-3602.
- Martinez-Menarguez, J.A., Geuze, H.J., Slot, J.W., and Klumperman, J. (1999). Vesicular tubular clusters between the ER and Golgi mediate concentration of soluble secretory proteins by exclusion from COPI- coated vesicles. *Cell* 98, 81-90.
- Matter, K., Yamamoto, E.M., and Mellman, I. (1994). Structural requirements and sequence motifs for polarized sorting and endocytosis of LDL and Fc receptors in MDCK cells. *J. Cell Biol.* 126, 991-1004.

- Mellman, I. and Warren, G. (2000). The road taken: past and future foundations of membrane traffic. *Cell* 100, 99-112.
- Meyer, C., Zizioli, D., Lausmann, S., Eskelinen, E.L., Hamann, J., Saftig, P., von Figura, K., and Schu, P. (2000). mu1A-adaptin-deficient mice: lethality, loss of AP-1 binding and rerouting of mannose 6-phosphate receptors. *EMBO J.* 19, 2193-2203.
- Mittereder, N., March, K.L., and Trapnell, B.C. (1996). Evaluation of the concentration and bioactivity of adenovirus vectors for gene therapy. *J. Virol.* 70, 7498-7509.
- Mollenhauer, H.H., Morre, D.J., and Rowe, L.D. (1990). Alteration of intracellular traffic by monensin; mechanism, specificity and relationship to toxicity. *Biochim. Biophys. Acta* 1031, 225-246.
- Molloy, S.S., Anderson, E.D., Jean, F., and Thomas, G. (1999). Bi-cycling the furin pathway: from TGN localization to pathogen activation and embryogenesis. *Trends Cell Biol.* 9, 28-35.
- Molnar-Kimber, K.L., Serman, D.H., Chang, M., Kang, E.H., ElBash, M., Lanuti, M., Elshami, A., Gelfand, K., Wilson, J.M., Kaiser, L.R., and Albelda, S.M. (1998). Impact of preexisting and induced humoral and cellular immune responses in an adenovirus-based gene therapy phase I clinical trial for localized mesothelioma. *Hum. Gene Ther.* 9, 2121-2133.
- Moretta, A., Bottino, C., Vitale, M., Pende, D., Cantoni, C., Mingari, M.C., Biassoni, R., and Moretta, L. (2001). Activating receptors and coreceptors involved in human natural killer cell-mediated cytotoxicity. *Annu. Rev. Immunol.* 19, 197-223.
- Mu, F.T., Callaghan, J.M., Steele-Mortimer, O., Stenmark, H., Parton, R.G., Campbell, P.L., McCluskey, J., Yeo, J.P., Tock, E.P., and Toh, B.H. (1995). EEA1, an early endosome-associated protein. EEA1 is a conserved alpha-helical peripheral membrane protein flanked by cysteine "fingers" and contains a calmodulin-binding IQ motif. *J. Biol. Chem.* 270, 13503-13511.
- Munro, S. (1998). Localization of proteins to the Golgi apparatus. *Trends Cell Biol.* 8, 11-15.
- Muruve, D.A., Barnes, M.J., Stillman, I.E., and Libermann, T.A. (1999). Adenoviral gene therapy leads to rapid induction of multiple chemokines and acute neutrophil-dependent hepatic injury in vivo. *Hum. Gene Ther.* 10, 965-976.
- Nakamura, N., Rabouille, C., Watson, R., Nilsson, T., Hui, N., Slusarewicz, P., Kreis, T.E., and Warren, G. (1995). Characterization of a cis-Golgi matrix protein, GM130. *J. Cell Biol.* 131, 1715-1726.
- Nemerow, G.R. (2000). Cell receptors involved in adenovirus entry. *Virology* 274, 1-4.
- Nielsen, M.S., Madsen, P., Christensen, E.I., Nykjaer, A., Gliemann, J., Kasper, D., Pohlmann, R., and Petersen, C.M. (2001). The sortilin cytoplasmic tail conveys Golgi-endosome transport and binds the VHS domain of the GGA2 sorting protein. *EMBO J.* 20, 2180-2190.
- Nilsson, T., Pypaert, M., Hoe, M.H., Slusarewicz, P., Berger, E.G., and Warren, G. (1993). Overlapping distribution of two glycosyltransferases in the Golgi apparatus of HeLa cells. *J. Cell Biol.* 120, 5-13.
- O'Connor, R.J. and Hearing, P. (2000). The E4-6/7 protein functionally compensates for the loss of E1A expression in adenovirus infection. *J. Virol.* 74, 5819-5824.
- Odorizzi, G. and Trowbridge, I.S. (1997). Structural requirements for major histocompatibility complex class II invariant chain trafficking in polarized Madin-Darby canine kidney cells. *J. Biol. Chem.* 272, 11757-11762.
- Ohno, H., Aguilar, R.C., Yeh, D., Taura, D., Saito, T., and Bonifacino, J.S. (1998). The medium subunits of adaptor complexes recognize distinct but overlapping sets of tyrosine-based sorting signals. *J. Biol. Chem.* 273, 25915-25921.

- Ohno, H., Fournier, M.C., Poy, G., and Bonifacino, J.S. (1996). Structural determinants of interaction of tyrosine-based sorting signals with the adaptor medium chains. *J. Biol. Chem.* *271*, 29009-29015.
- Ohno, H., Stewart, J., Fournier, M.C., Bosshart, H., Rhee, I., Miyatake, S., Saito, T., Gallusser, A., Kirchhausen, T., and Bonifacino, J.S. (1995). Interaction of tyrosine-based sorting signals with clathrin-associated proteins. *Science* *269*, 1872-1875.
- Ooi, C.E., Dell'Angelica, E.C., and Bonifacino, J.S. (1998). ADP-Ribosylation factor 1 (ARF1) regulates recruitment of the AP-3 adaptor complex to membranes. *J. Cell Biol.* *142*, 391-402.
- Owen, D.J. and Evans, P.R. (1998). A structural explanation for the recognition of tyrosine-based endocytotic signals. *Science* *282*, 1327-1332.
- Parodi, A.J. (2000). Role of N-oligosaccharide endoplasmic reticulum processing reactions in glycoprotein folding and degradation. *Biochem. J.* *348 Pt 1*, 1-13.
- Perez, R.G., Soriano, S., Hayes, J.D., Ostaszewski, B., Xia, W., Selkoe, D.J., Chen, X., Stokin, G.B., and Koo, E.H. (1999). Mutagenesis identifies new signals for beta-amyloid precursor protein endocytosis, turnover, and the generation of secreted fragments, including Abeta42. *J. Biol. Chem.* *274*, 18851-18856.
- Petris, M.J., Camakaris, J., Greenough, M., LaFontaine, S., and Mercer, J.F. (1998). A C-terminal di-leucine is required for localization of the Menkes protein in the trans-Golgi network. *Hum. Mol. Genet.* *7*, 2063-2071.
- Pfeffer, S.R. (1999). Transport-vesicle targeting: tethers before SNAREs. *Nat. Cell Biol.* *1*, E17-E22.
- Piguet, V., Wan, L., Borel, C., Mangasarian, A., Demaurex, N., Thomas, G., and Trono, D. (2000). HIV-1 Nef protein binds to the cellular protein PACS-1 to downregulate class I major histocompatibility complexes. *Nat. Cell Biol.* *2*, 163-167.
- Poignard, P., Saphire, E.O., Parren, P.W., and Burton, D.R. (2001). gp120: Biologic aspects of structural features. *Annu. Rev. Immunol.* *19*, 253-274.
- Pollakis, G., Kang, S., Kliphuis, A., Chalaby, M.I., Goudsmit, J., and Paxton, W.A. (2001). N-linked glycosylation of the HIV type-1 gp120 envelope glycoprotein as a major determinant of CCR5 and CXCR4 coreceptor utilization. *J. Biol. Chem.* *276*, 13433-13441.
- Ponnambalam, S., Girotti, M., Yaspo, M.L., Owen, C.E., Perry, A.C., Sukanuma, T., Nilsson, T., Fried, M., Banting, G., and Warren, G. (1996). Primate homologues of rat TGN38: primary structure, expression and functional implications. *J. Cell Sci.* *109*, 675-685.
- Presley, J.F., Mayor, S., McGraw, T.E., Dunn, K.W., and Maxfield, F.R. (1997). Bafilomycin A1 treatment retards transferrin receptor recycling more than bulk membrane recycling. *J. Biol. Chem.* *272*, 13929-13936.
- Puertollano, R., Aguilar, R.C., Gorshkova, I., Crouch, R.J., and Bonifacino, J.S. (2001a). Sorting of mannose 6-phosphate receptors mediated by the GGAs. *Science* *292*, 1712-1716.
- Puertollano, R., Randazzo, P.A., Presley, J.F., Hartnell, L.M., and Bonifacino, J.S. (2001b). The GGAs promote ARF-dependent recruitment of clathrin to the TGN. *Cell* *105*, 93-102.
- Putzer, B.M., Stiewe, T., Parssanedjad, K., Rega, S., and Esche, H. (2000). E1A is sufficient by itself to induce apoptosis independent of p53 and other adenoviral gene products. *Cell Death Differ.* *7*, 177-188.
- Rapoport, I., Chen, Y.C., Cupers, P., Shoelson, S.E., and Kirchhausen, T. (1998). Dileucine-based sorting signals bind to the beta chain of AP-1 at a site distinct and regulated differently from the tyrosine-based motif-binding site. *EMBO J.* *17*, 2148-2155.

- Raulet, D.H., Vance, R.E., and McMahon, C.W. (2001). Regulation of the natural killer cell receptor repertoire. *Annu. Rev. Immunol.* *19*, 291-330.
- Reaves, B. and Banting, G. (1992). Perturbation of the morphology of the trans-Golgi network following Brefeldin A treatment: redistribution of a TGN-specific integral membrane protein, TGN38. *J. Cell Biol.* *116*, 85-94.
- Reich, N., Pine, R., Levy, D., and Darnell, J.E., Jr. (1988). Transcription of interferon-stimulated genes is induced by adenovirus particles but is suppressed by E1A gene products. *J. Virol.* *62*, 114-119.
- Reusch, U., Muranyi, W., Lucin, P., Burgert, H.-G., Hengel, H., and Koszinowski, U.H. (1999). A cytomegalovirus glycoprotein re-routes MHC class I complexes to lysosomes for degradation. *EMBO J.* *18*, 1081-1091.
- Roberts, D.L., Weix, D.J., Dahms, N.M., and Kim, J.J. (1998). Molecular basis of lysosomal enzyme recognition: three-dimensional structure of the cation-dependent mannose 6-phosphate receptor. *Cell* *93*, 639-648.
- Robertson, M.J., Cochran, K.J., Cameron, C., Le, J.M., Tantravahi, R., and Ritz, J. (1996). Characterization of a cell line, NKL, derived from an aggressive human natural killer cell leukemia. *Exp. Hematol.* *24*, 406-415.
- Robinson, M.S. and Bonifacino, J.S. (2001). Adaptor-related proteins. *Curr. Opin. Cell Biol.* *13*, 444-453.
- Rodionov, D.G. and Bakke, O. (1998). Medium chains of adaptor complexes AP-1 and AP-2 recognize leucine- based sorting signals from the invariant chain. *J. Biol. Chem.* *273*, 6005-6008.
- Rodionov, D.G., Nordeng, T.W., Kongsvik, T.L., and Bakke, O. (2000). The cytoplasmic tail of CD1d contains two overlapping basolateral sorting signals. *J. Biol. Chem.* *275*, 8279-8282.
- Roelvink, P.W., Lizonova, A., Lee, J.G., Li, Y., Bergelson, J.M., Finberg, R.W., Brough, D.E., Kovesdi, I., and Wickham, T.J. (1998). The coxsackievirus-adenovirus receptor protein can function as a cellular attachment protein for adenovirus serotypes from subgroups A, C, D, E, and F. *J. Virol.* *72*, 7909-7915.
- Roelvink, P.W., Mi, L.G., Einfeld, D.A., Kovesdi, I., and Wickham, T.J. (1999). Identification of a conserved receptor-binding site on the fiber proteins of CAR-recognizing adenoviridae. *Science* *286*, 1568-1571.
- Rohn, W.M., Rouille, Y., Waguri, S., and Hoflack, B. (2000). Bi-directional trafficking between the trans-Golgi network and the endosomal/lysosomal system. *J. Cell Sci.* *113 (Pt 12)*, 2093-2101.
- Rohrer, J., Schweizer, A., Russell, D., and Kornfeld, S. (1996). The targeting of Lamp1 to lysosomes is dependent on the spacing of its cytoplasmic tail tyrosine sorting motif relative to the membrane. *J. Cell Biol.* *132*, 565-576.
- Rothman, J.E. and Wieland, F.T. (1996). Protein sorting by transport vesicles. *Science* *272*, 227-234.
- Routes, J.M. and Cook, J.L. (1989). Adenovirus persistence in man. Defective E1A gene product targeting of infected cells for elimination by natural killer cells. *J. Immunol.* *142*, 4022-4026.
- Routes, J.M. and Cook, J.L. (1995). E1A gene expression induces susceptibility to killing by NK cells following immortalization but not adenovirus infection of human cells. *Virology* *210*, 421-428.

- Rowe, W.P., Huebner, R.J., Gilmore, L.K., Parrot, R.H., and Ward, T.G. (1953). Isolation of a cytopathic agent from human adenoids undergoing spontaneous degradation in tissue culture. *Proceedings of the Society for Experimental Biology and Medicine* 84, 570-573.
- Russell, W.C. (2000). Update on adenovirus and its vectors. *J. Gen. Virol.* 81, 2573-2604.
- Schendel, D.J., Wank, R., and Dupont, B. (1979). Standardization of the human in vitro cell-mediated lympholysis technique. *Tissue Antigens* 13, 112.
- Schmitz, H., Wigand, R., and Heinrich, W. (1983). Worldwide epidemiology of human adenovirus infections. *Am. J. Epidemiol.* 117, 455-466.
- Schneider, C., Sutherland, R., Newman, R., and Greaves, M. (1982). Structural features of the cell surface receptor for transferrin that is recognized by the monoclonal antibody OKT9. *J. Biol. Chem.* 257, 8516-8522.
- Schnurr, D. and Dondero, M.E. (1993). Two new candidate adenovirus serotypes. *Intervirology* 36, 79-83.
- Schultz, J., Copley, R.R., Doerks, T., Ponting, C.P., and Bork, P. (2000). SMART: a web-based tool for the study of genetically mobile domains. *Nucleic Acids Res.* 28, 231-234.
- Schweizer, A., Kornfeld, S., and Rohrer, J. (1996). Cysteine³⁴ of the cytoplasmic tail of the cation-dependent mannose 6-phosphate receptor is reversibly palmitoylated and required for normal trafficking and lysosomal enzyme sorting. *J. Cell Biol.* 132, 577-584.
- Seidah, N.G., Chretien, M., and Day, R. (1994). The family of subtilisin/kexin like pro-protein and pro-hormone convertases: divergent or shared functions. *Biochimie* 76, 197-209.
- Seidah, N.G., Hamelin, J., Mamarbachi, M., Dong, W., Tardos, H., Mbikay, M., Chretien, M., and Day, R. (1996). cDNA structure, tissue distribution, and chromosomal localization of rat PC7, a novel mammalian proprotein convertase closest to yeast kexin-like proteinases. *Proc. Natl. Acad. Sci. USA* 93, 3388-3393.
- Shao, R., Hu, M.C., Zhou, B.P., Lin, S.Y., Chiao, P.J., von Lindern, R.H., Spohn, B., and Hung, M.C. (1999). E1A sensitizes cells to tumor necrosis factor-induced apoptosis through inhibition of I κ B kinases and nuclear factor κ B activities. *J. Biol. Chem.* 274, 21495-21498.
- Shao, R., Karunakaran, D., Zhou, B.P., Li, K., Lo, S.S., Deng, J., Chiao, P., and Hung, M.C. (1997). Inhibition of nuclear factor- κ B activity is involved in E1A-mediated sensitization of radiation-induced apoptosis. *J. Biol. Chem.* 272, 32739-32742.
- Shenk, T. (1996). Adenoviridae: The Viruses and Their Replication. In *Fields Virology*. Fields, B.N., Knipe, D.M., and Howley, P.M., eds. Lippincott-Raven Publishers, Philadelphia, New York, pp. 2111-2148.
- Shimizu, Y. and DeMars, R. (1989). Production of human cells expressing individual transferred HLA-A,-B,-C genes using an HLA-A,-B,-C null human cell line. *J. Immunol.* 142, 3320-3328.
- Shin, J., Dunbrack, R.L., Jr., Lee, S., and Strominger, J.L. (1991). Phosphorylation-dependent down-modulation of CD4 requires a specific structure within the cytoplasmic domain of CD4. *J. Biol. Chem.* 266, 10658-10665.
- Shiratori, T., Miyatake, S., Ohno, H., Nakaseko, C., Isono, K., Bonifacio, J.S., and Saito, T. (1997). Tyrosine phosphorylation controls internalization of CTLA-4 by regulating its interaction with clathrin-associated adaptor complex AP-2. *Immunity* 6, 583-589.
- Shisler, J., Yang, C., Walter, B., Ware, C.F., and Gooding, L.R. (1997). The adenovirus E3-10.4K/14.5K complex mediates loss of cell surface Fas (CD95) and resistance to Fas-induced apoptosis. *J. Virol.* 71, 8299-8306.

- Signas, C., Akusjarvi, G., and Pettersson, U. (1986). Region E3 of human adenoviruses; differences between the oncogenic adenovirus-3 and the non-oncogenic adenovirus-2. *Gene* 50, 173-184.
- Simonsen, A., Bremnes, B., Nordeng, T.W., and Bakke, O. (1998). The leucine-based motif DDQxxLI is recognized both for internalization and basolateral sorting of invariant chain in MDCK cells. *Eur. J. Cell Biol.* 76, 25-32.
- Stephens, D.J. and Banting, G. (1997). Insulin dependent tyrosine phosphorylation of the tyrosine internalisation motif of TGN38 creates a specific SH2 domain binding site. *FEBS Lett.* 416, 27-29.
- Stewart, P.L., Burnett, R.M., Cyrklaff, M., and Fuller, S.D. (1991). Image reconstruction reveals the complex molecular organization of adenovirus. *Cell* 67, 145-154.
- Suomalainen, M., Nakano, M.Y., Keller, S., Boucke, K., Stidwill, R.P., and Greber, U.F. (1999). Microtubule-dependent plus- and minus end-directed motilities are competing processes for nuclear targeting of adenovirus. *J. Cell Biol.* 144, 657-672.
- Takahashi, S., Nakagawa, T., Kasai, K., Banno, T., Duguay, S.J., Van de Ven, W.J., Murakami, K., and Nakayama, K. (1995). A second mutant allele of furin in the processing-incompetent cell line, LoVo. Evidence for involvement of the homo B domain in autocatalytic activation. *J. Biol. Chem.* 270, 265-269.
- Takai, Y., Sasaki, T., and Matozaki, T. (2001). Small GTP-binding proteins. *Physiol. Rev.* 81, 153-208.
- Tauber, B. and Dobner, T. (2001). Adenovirus early E4 genes in viral oncogenesis. *Oncogene* 20, 7847-7854.
- Teasdale, R.D. and Jackson, M.R. (1996). Signal-mediated sorting of membrane proteins between the endoplasmic reticulum and the golgi apparatus. *Annu. Rev. Cell Dev. Biol.* 12, 27-54.
- Ting, A.T., Pimentel-Muinos, F.X., and Seed, B. (1996). RIP mediates tumor necrosis factor receptor 1 activation of NF-kappaB but not Fas/APO-1-initiated apoptosis. *EMBO J.* 15, 6189-6196.
- Tollefson, A.E., Hermiston, T.W., Lichtenstein, D.L., Colle, C.F., Tripp, R.A., Dimitrov, T., Toth, K., Wells, C.E., Doherty, P.C., and Wold, W.S. (1998). Forced degradation of Fas inhibits apoptosis in adenovirus-infected cells. *Nature* 392, 726-730.
- Tollefson, A.E., Scaria, A., Saha, S.K., and Wold, W.S. (1992). The 11,600-MW protein encoded by region E3 of adenovirus is expressed early but is greatly amplified at late stages of infection. *J. Virol.* 66, 3633-3642.
- Tollefson, A.E., Toth, K., Doronin, K., Kuppuswamy, M., Doronina, O.A., Lichtenstein, D.L., Hermiston, T.W., Smith, C.A., and Wold, W.S. (2001). Inhibition of trail-induced apoptosis and forced internalization of trail receptor 1 by adenovirus proteins. *J. Virol.* 75, 8875-8887.
- Tomko, R.P., Xu, R., and Philipson, L. (1997). HCAR and MCAR: the human and mouse cellular receptors for subgroup C adenoviruses and group B coxsackieviruses. *Proc. Natl. Acad. Sci. USA* 94, 3352-3356.
- Tortorella, D., Gewurz, B.E., Furman, M.H., Schust, D.J., and Ploegh, H.L. (2000). Viral subversion of the immune system. *Annu. Rev. Immunol.* 18, 861-926.
- Trapani, J.A., Davis, J., Sutton, V.R., and Smyth, M.J. (2000). Proapoptotic functions of cytotoxic lymphocyte granule constituents in vitro and in vivo. *Curr. Opin. Immunol.* 12, 323-329.
- Traub, L.M., Bannykh, S.I., Rodel, J.E., Aridor, M., Balch, W.E., and Kornfeld, S. (1996). AP-2-containing clathrin coats assemble on mature lysosomes. *J. Cell Biol.* 135, 1801-1814.

- Traub, L.M. and Kornfeld, S. (1997). The trans-Golgi network: a late secretory sorting station. *Curr. Opin. Cell Biol.* 9, 527-533.
- Trotman, L.C., Mosberger, N., Fornerod, M., Stidwill, R.P., and Greber, U.F. (2001). Import of adenovirus DNA involves the nuclear pore complex receptor CAN/Nup214 and histone H1. *Nat. Cell Biol.* 3, 1092-1100.
- Van Deurs, B., Holm, P.K., and Sandvig, K. (1996). Inhibition of the vacuolar H(+)-ATPase with bafilomycin reduces delivery of internalized molecules from mature multivesicular endosomes to lysosomes in HEp-2 cells. *Eur. J. Cell Biol.* 69, 343-350.
- Van Weert, A.W., Dunn, K.W., Geuze, H.J., Maxfield, F.R., and Stoorvogel, W. (1995). Transport from late endosomes to lysosomes, but not sorting of integral membrane proteins in endosomes, depends on the vacuolar proton pump. *J. Cell Biol.* 130, 821-834.
- Voorhees, P., Deignan, E., van Donselaar, E., Humphrey, J., Marks, M.S., Peters, P.J., and Bonifacino, J.S. (1995). An acidic sequence within the cytoplasmic domain of furin functions as a determinant of trans-Golgi network localization and internalization from the cell surface. *EMBO J.* 14, 4961-4975.
- Wadell, G. (1984). Molecular epidemiology of human adenoviruses. *Curr. Top. Microbiol. Immunol.* 110, 191-220.
- Watanabe, T., Murakami, K., and Nakayama, K. (1993). Positional and additive effects of basic amino acids on processing of precursor proteins within the constitutive secretory pathway. *FEBS Lett.* 320, 215-218.
- White, E. (2001). Regulation of the cell cycle and apoptosis by the oncogenes of adenovirus. *Oncogene* 20, 7836-7846.
- Windheim, M., Hilgendorf, A., and Burgert, H.-G. (2002). Immune evasion by adenovirus E3 proteins: Exploitation of intracellular trafficking pathways. *Curr. Top. Microbiol. Immunol.* *in press*.
- Wold, W.S., Doronin, K., Toth, K., Kuppuswamy, M., Lichtenstein, D.L., and Tollefson, A.E. (1999). Immune responses to adenoviruses: viral evasion mechanisms and their implications for the clinic. *Curr. Opin. Immunol.* 11, 380-386.
- Wold, W.S., Tollefson, A.E., and Hermiston, T.W. (1995). E3 transcription unit of adenovirus. *Curr. Top. Microbiol. Immunol.* 199 (Pt 1), 237-274.
- Worgall, S., Wolff, G., Falck-Pedersen, E., and Crystal, R.G. (1997). Innate immune mechanisms dominate elimination of adenoviral vectors following in vivo administration. *Hum. Gene Ther.* 8, 37-44.
- Wyss, S., Berlioz-Torrent, C., Boge, M., Blot, G., Honing, S., Benarous, R., and Thali, M. (2001). The highly conserved C-terminal dileucine motif in the cytosolic domain of the human immunodeficiency virus type 1 envelope glycoprotein is critical for its association with the AP-1 clathrin adapter. *J. Virol.* 75, 2982-2992.
- Yamano, S., Tokino, T., Yasuda, M., Kaneuchi, M., Takahashi, M., Niitsu, Y., Fujinaga, K., and Yamashita, T. (1999). Induction of transformation and p53-dependent apoptosis by adenovirus type 5 E4orf6/7 cDNA. *J. Virol.* 73, 10095-10103.
- Yang, Z., Delgado, R., Xu, L., Todd, R.F., Nabel, E.G., Sanchez, A., and Nabel, G.J. (1998). Distinct cellular interactions of secreted and transmembrane Ebola virus glycoproteins. *Science* 279, 1034-1037.
- Zabner, J., Chillon, M., Grunst, T., Moninger, T.O., Davidson, B.L., Gregory, R., and Armentano, D. (1999). A chimeric type 2 adenovirus vector with a type 17 fiber enhances gene transfer to human airway epithelia. *J. Virol.* 73, 8689-8695.

-
- Zerial, M. and McBride, H. (2001). Rab proteins as membrane organizers. *Nat. Rev. Mol. Cell Biol.* *2*, 107-117.
- Zhou, A., Webb, G., Zhu, X., and Steiner, D.F. (1999). Proteolytic processing in the secretory pathway. *J. Biol. Chem.* *274*, 20745-20748.
- Zhu, Y., Doray, B., Poussu, A., Lehto, V.P., and Kornfeld, S. (2001). Binding of GGA2 to the lysosomal enzyme sorting motif of the mannose 6- phosphate receptor. *Science* *292*, 1716-1718.
- Ziegler, H., Muranyi, W., Burgert, H.-G., Kremmer, E., and Koszinowski, U.H. (2000). The luminal part of the murine cytomegalovirus glycoprotein gp40 catalyzes the retention of MHC class I molecules. *EMBO J.* *19*, 870-881.
- Zwart, D.E., Brewer, C.B., Lazarovits, J., Henis, Y.I., and Roth, M.G. (1996). Degradation of mutant influenza virus hemagglutinins is influenced by cytoplasmic sequences independent of internalization signals. *J. Biol. Chem.* *271*, 907-917.

7 ABBREVIATIONS

For amino acids the one-letter code was used.

a	adenine
aa	amino acid
Ab	antibody
Ad	adenovirus
Arf	ADP-ribosylation factor
AIDS	acquired immune deficiency syndrome
AP	adaptor protein complex
APP	β -amyloid precursor protein
APP _s	secreted form of the β -amyloid precursor protein
APS	ammonium persulfate
ATCC	American Type Culture Collection
ATP	adenosine triphosphate
B	basolateral
bp	base pair
c	cytosine
°C	degree Celsius
CAR	coxsackie adenovirus receptor
Ci	Curie
CD	cluster of differentiation
CD-MPR	cation-dependent mannose-6-phosphate receptor
CI-MPR	cation-independent mannose-6-phosphate receptor
conc.	concentration
cpm	counts per minute
CPE	cytopathic effect
CT	cytoplasmic tail
C-tail	cytoplasmic tail
CTL	cytotoxic T lymphocytes
d	deoxy
DBP	DNA bending protein
DMEM	Dulbecco's modified Eagle medium
DNA	deoxyribonucleic acid
dNTP	deoxynucleoside triphosphate
DTT	dithiothreitol
E	early
E	endocytosis
EE	early endosomes
E3	early transcription unit 3
E. coli	Escherichia coli
EDTA	ethylenediamine tetraacetic acid
EGF	epidermal growth factor
EKC	epidemic keratoconjunctivitis
ELISA	enzyme-linked immunosorbent assay
Endo H	endoglycosidase H
ER	endoplasmatic reticulum
ERGIC	ER- Golgi intermediate compartment
EtOH	ethanol
FACS	fluorescence activated cell sorter
FasL	Fas ligand

FCS	fetal calf serum
FIG.	figure
Fig.	figure
FITC	fluorescein-isocyanat
g	gram
g	gravitation constant
g	guanine
G	golgi
GGA	Golgi associated γ ear containing Arf binding protein
gp	glycoprotein
H	hour(s)
HAc	acetic acid
HCMV	human cytomegalovirus
HEPES	2-[4-(2-Hydroxyethyl)-1-piperazinyl]-ethane sulfonic acid
HIV	human immunodeficiency virus
HSV	herpes simplex virus
IF	immunofluorescence
IFN	interferon
IgG	immunglobulin G
i.p.	intraperitoneal
IPTG	isopropylthiogalactoside
ISRE	IFN-stimulated response element
Jak	Janus kinase
kb	kilo base pair
kDa	kilodaltons
KLH	keyhole limpet hemocyanin
l	liter
L	late
lamp	lysosome-associated membran protein
LB	Luria-Bertani
LE	late endosomes
limp	lysosomal integral membrane protein
Lys	lysosomes
μ	micro (10^{-6})
m	milli (10^{-3})
m	meter
M	mol/liter
M	mitochondrium
MIIC	MHC class II compartment
mAb	monoclonal antibody
MCMV	murine cytomegalovirus
MeOH	methanol
mdm2	murine double minute 2
MHC	major histocompatibility complex
min	minute(s)
MLP	major late promoter
MPR	mannose-6-phosphate receptor
MOI	multiplicity of infection
MOPS	3- (N-Morpholino)propanesulfonic acid
mRNA	messenger RNA
MTOC	microtubule organizing center
n	nano (10^{-9})

NFκB	nuclear factor κB
NK	natural killer
o/n	overnight
OD	optical density
ORF	open reading frame
p	pico (10 ⁻¹²)
p.i.	postinfection
PAGE	polyacrylamide gel electrophoresis
PBS	phosphate buffered saline
PCR	polymerase chain reaction
PFU	plaque forming units
PKR	double stranded RNA-dependent protein kinase R
PM	plasma membrane
PNGase F	peptide- <i>N</i> -glycosidase F
Pwo	<i>Pyrococcus woesei</i>
R	receptor
RNA	ribonucleic acid
rpm	revolutions per minute
RT	room temperature
s	second(s)
s.c.	subcutaneous
SDS	sodium dodecylsulfate
SIV	simian immunodeficiency virus
SPC	subtilisin-like proprotein convertase
SRP	signal recognition particle
STAT	signal transducer and activator of transcription
t	thymine
Tab.	table
TAP	Transporter associated with antigen processing
TEMED	N, N, N', N'-tetramethylethylenediamine
TGN	<i>trans</i> -Golgi network
TMD	transmembrane domain
TNF	tumor necrosis factor
TP	terminal protein
TRAIL	tumor necrosis factor-related apoptosis-inducing ligand
Tris	Tris(hydroxymethyl)aminomethane
VA	virus-associated
w/o	without
U	Unit, enzyme activity
UV	ultraviolet
V	Volt
vCkBP	viral chemokine binding protein
VSV G	vesicular stomatitis virus glycoprotein
VZV	varicella zoster virus
v/v	volumen/volumen
w/v	weight/volumen
wt	wild type

8 PUBLICATIONS

Parts of this work have been published:

Original publications:

Mark Windheim and Hans-Gerhard Burgert. 2002. Characterization of E3/49K, a novel highly glycosylated E3 protein of the epidemic keratoconjunctivitis-causing adenovirus type 19a. *Journal of Virology* 76. 755-766.

Jürgen H. Blusch, Francois Deryckere, Mark Windheim, Zsolt Ruzsics, Niklas Arnberg, Thomas Adrian and Hans-Gerhard Burgert. 2002. The novel early region 3 protein E3/49K is specifically expressed by adenoviruses of subgenus D: Implications for epidemic keratoconjunctivitis and adenovirus evolution. *Virology*. 2002. *In press*.

Reviews:

Hans-Gerhard Burgert, Zsolt Ruzsics, Susanne Obermeier, Annette Hilgendorf, Mark Windheim and Andreas Elsing. 2002. Subversion of host defense mechanisms by adenoviruses. *Current Topics in Microbiology and Immunology* 269. *In press*.

Mark Windheim, Annette Hilgendorf and Hans-Gerhard Burgert. 2002. Immune evasion by adenovirus E3 proteins: Exploitation of intracellular trafficking pathways. *Current Topics in Microbiology and Immunology*. *In press*.

9 CURRICULUM VITAE

Persönliche Daten:

Name	Mark Windheim
Anschrift	Danklstr. 32 81371 München
Geburtsdatum	28. September 1970
Geburtsort	Stadthagen, Kreis Schaumburg-Lippe
Staatsangehörigkeit	deutsch
Familienstand	verheiratet

Schulbildung:

1977-1981	Grundschule in Münchehagen
1981-1983	Orientierungsstufe in Loccum
1983-1988	Gymnasium in Stolzenau
1988-1990	Ratsgymnasium in Stadthagen
Mai 1990	Allgemeine Hochschulreife

Zivildienst:

1990-1991	Zivildienst in Bad Rehburg / Lebenshilfe Nienburg gGmbH
-----------	--

Hochschulausbildung:

1991-1997	Studium der Biochemie (Diplom) an der Eberhard-Karls-Universität Tübingen
1994-1995	Studium der Biochemie an der "University of North Carolina at Chapel Hill", Chapel Hill, USA
1997	Diplomarbeit unter Anleitung von PD Dr. Eberhard Pfaff an der Bundesforschungsanstalt für Viruskrankheiten der Tiere in Tübingen Thema: Etablierung von Zelllinien zur regulierbaren Expression der für die RNA- abhängige RNA Polymerase und den Nichtstrukturbereich von Hepatitis C Virus kodierenden Genfragmente
November 1997	Abschluß: Diplom
1998-2002	Dissertation am Max-von-Pettenkofer-Institut, Genzentrum der Ludwig-Maximilians- Universität München unter der Betreuung von Prof. Dr. Ernst-Ludwig Winnacker und der Anleitung von PD Dr. Hans-Gerhard Burgert